Refinements and practical implementation of a power based loss of grid detection algorithm for embedded generators

Barrett, James

Award date:
1994

Awarding institution:
University of Bath

Refinements and Practical Implementation of a Power Based Loss of Grid Detection Algorithm for Embedded Generators.

Submitted by James Barrett,

for the degree of Ph.D.

of the University of Bath

1994

ProQuest LLC
789 East Eisenhower Parkway
P.O. Box 1346
Ann Arbor, MI 48106-1346

Synopsis

The incorporation of small, privately owned generation operating in parallel with, and supplying power to, the distribution network is becoming more widespread. This method of operation does however have problems associated with it. In particular, a loss of the connection to the main utility supply which leaves a portion of the utility load connected to the embedded generator will result in a power island. This situation presents possible dangers to utility personnel and the public, complications for smooth system operation and probable plant damage should the two systems be reconnected out-of-synchronism.

Loss of Grid (or Islanding), as this situation is known, is the subject of this thesis. The work begins by detailing the requirements for operation of generation embedded in the utility supply with particular attention drawn to the requirements for a loss of grid protection scheme. The mathematical basis for a new loss of grid protection algorithm is developed and the inclusion of the algorithm in an integrated generator protection scheme described. A detailed description is given on the implementation of the new algorithm in a microprocessor based relay hardware to allow practical tests on small embedded generation facilities, including an in-house multiple generator test facility. The results obtained from the practical tests are compared with those obtained from simulation studies carried out in previous work and the differences are discussed.

The performance of the algorithm is enhanced from the theoretical algorithm developed using the simulation results with simple filtering together with pattern recognition techniques. This provides stability during severe load fluctuations under parallel operation and system fault conditions and improved performance under normal operating conditions and for loss of grid detection.

In addition to operating for a loss of grid connection, the algorithm will respond to load fluctuations which occur within a power island should the embedded generator be left connected to part of the utility load following an undetected loss of grid. Finally, if the loss of grid still remains undetected, a subsequent out-of-step reclosure will be detected leading to removal of the generator from the system before serious damage can occur.

Acknowledgements

The author would like to acknowledge with thanks:

Dr M A Redfern without whom none of this would have happened.

The School of Electrical and Electronic Engineering (at least that was what it was called when I started my course) at The University of Bath for providing the laboratory resources and equipment needed to carry out most of the work.

GEC Alsthom T & D Protection and Control Ltd. in Stafford for providing financial and technical support throughout the project. The assistance of Tony Yip, Dave Banham, Richard Price, Peggy Ling, Geoff Weller, Paul Hindle and Adrian Newbould requires particular thanks.

Neil Deacon for always being available to turn it on for me whenever I needed it, (the laboratory power supply that is).

All the technical staff at the University of Bath who have assisted me during this work.

Ömer Usta for his assistance during the early part of my work.

Jerzy Grzjewski for always providing that long and detailed explanation to even the simplest of questions.

Allexon Chiwaya for always being there, day and night!

Matt Checksfield for having a more pessimistic outlook on life than even I could manage.

A final thank-you has to go to Michelle for all the encouragement and support which she has offered throughout the duration of this work and without whom my life in Bath would have been incomplete.

Contents

Chapter 3

Chapter 4

List of Symbols and Abbreviations

Symbols used in Main Text:

P	-	Power
P_g	-	Embedded Generator Output Power
P_L	-	Local Load Input Power
F	-	Frequency
H	-	Inertia Constant of a Machine or System
S	-	Rated Capacity
S_g	-	Embedded Generator Rated Capacity
S_m	-	Utility Mains Rated Capacity
v	-	Instantaneous Voltage
V	-	R.M.S. Voltage
i	-	Instantaneous Current
I	-	R.M.S. Current

Abbreviations used in Thesis:

C.H.P.	-	Combined Heat and Power
C.E.G.B.	-	Central Electricity Generating Board
E.H.V.	-	Extra High Voltage
C.C.G.T.	-	Combined Cycle Gas Turbine
N.F.F.O.	-	Non Fossil Fuel Obligation
P.U.R.P.A.	-	Public Utility Regulatory Policies Act
D.S.G.	-	Dispersed Storage and Generation
L.O.G.	-	Loss of Grid
R.E.C.	-	Regional Electricity Company
Z.P.S.	-	Zero Phase Sequence
N.P.S.	-	Negative Phase Sequence
I.D.M.T.	-	Inverse Definite Minimum Time
A.V.R.	-	Automatic Voltage Regulator
S.C.A.D.A.	-	Supervisory Control and Data Acquisition
R.O.C.O.F.	-	Rate of Change of Frequency
R.E.E.D.	-	Reactive Export Error Detector
M.P.R.	-	Microprocessor Relay
P.C.	-	Personal Computer
A to D	-	Analogue to Digital
C.T.	-	Current Transformer
V.T.	-	Voltage Transformer
I./O.	-	Input/Output
P.C.B.	-	Printed Circuit Board
P.L.L.	-	Phase Locked Loop
R.A.M.	-	Random Access Memory
E.P.R.O.M.	-	Erasable Programmable Read Only Memory
E^2.P.R.O.M.	-	Electrically Erasable Programmable Read Only Memory
B.A.S.I.C.	-	Beginners All-purpose Symbolic Instruction Code
B.I.O.S.	-	Basic Input Output System
M.T.E.	-	Multi-Tasking Executive
R.M.S.	-	Root Mean Square

Chapter 1

Introduction

1.1 Background to Embedded Generation.

Over the past two decades there have been increased economic, political and environmental pressures on the production of electricity that have greatly increased interest in incorporating embedded generation into public utility networks.

Moves towards the more efficient use of primary fuels and changes in the electricity market have encouraged the use of Combined Heat and Power (C.H.P.) plants which recover what would otherwise be waste heat. This requires that the power stations are situated near to industry or areas of dense population which can utilise the heat generated. Public pressure and the cost of fuel transportation means that these stations are in general smaller than current power stations.

For years the trend was towards increasingly large generation plants and centralised electricity generation, particularly in the U.K. under the C.E.G.B. This was justified by the economies of scale, and the cost of transmission of electricity (especially at E.H.V.) compared to the cost of fuel transportation. This lead to centralisation of generation plant near coal fields, oil refineries and deep water berths.

However, centralisation is only competitive for a reasonably high load factor such as base load power stations. For low load factors the cost of electrical transmission outweighs that of fuel transportation, leading to increased numbers of small electricity generating units being employed close to the load.

The following factors are also hastening the move towards increased numbers of small and medium sized embedded generation units:

- Large power stations employing condensing turbines result in only 35% of the fuel's calorific value being converted into electrical energy. With C.H.P. units, overall efficiencies of 90% are possible.

- The uncertain future for conventional coal, oil and nuclear power stations due to increased pressure to reduce emissions, erratic oil prices and high decommissioning costs.

- The availability of natural gas and the efficiency and cleanliness of gas turbines. With the lifting of the moratorium in the U.K. on the use of natural gas for large scale generation, there has been a big 'dash for gas' and licences have been granted for the building of over 950MW of Combined Cycle Gas Turbine (C.C.G.T.) stations.

- Increased awareness of environmental issues and energy savings has lead to encouragement of generation from renewable sources.

Small scale generation includes alternative energy sources such as landfill gas, waste incineration and especially renewables like wind, tidal, solar, mini-hydro and bio-fuel schemes. The Non Fossil Fuel Obligation (N.F.F.O.) entitles alternative energy schemes to receive premium price for their electricity.

Alternative energy sources are by their very nature dispersed over large areas and the cost of building a transmission system just to collect and manage this power is not economically practical. The only feasible method of exploiting this power is by embedded connection of the separate schemes directly into the local utility's distribution network.

In the U.S.A. and the U.K., interest in embedded generation has been further encouraged by government legislation, the P.U.R.P.A. (1978) in the U.S.A., the 1983 U.K. Energy Act and the 1989 U.K. Electricity Act which have allowed these local systems to operate in parallel with the utility networks and export power. This new legislation makes it more attractive for consumers and private investors to purchase their own generation devices and sell their power to electric utilities.

1.2 What is Embedded Generation?

Embedded generation (or Dispersed Storage and Generation, D.S.G.) is the operation of generation connected to and often supplying power in parallel with a utility's distribution network. This is in contrast to the conventional tiered system of electricity supply where generation is connected to a transmission network and through that to the distribution system. Embedded generation encompasses the increasingly popular use of small power producing facilities in addition to the well developed industrial practice of cogeneration.

Cogeneration has been used in certain industrial sectors for many years as an economical means of producing electrical power in parallel with the heat or pressurised steam used by the industrial process. However, the recent changes in legislation have granted permission for local embedded generation to supply surplus power to the utility's distribution network.

Electricity utilities have long operated small scale generation, such as small gas turbine stations and internal combustion engines, embedded into their distribution networks to either reduce overall demand or support weak parts of their system during maximum loading (Peak lopping). Localised generation can be used to prevent large power flows and the associated system losses.

1.3 Problems Associated with Embedded Generation.

Unfortunately, when an embedded generator is connected to the utility network distribution system, difficulties arise with both the operation and the protection of the power system. The parallel operation of an embedded generator creates difficulties for reliable and safe operation which arise from the embedded generator's capacity to supply power to the network from a source which is not under the utility's direct control. Special precautions are therefore required to prevent the embedded generator supplying low quality electricity to other utility customers and to ensure that it is disconnected from the network whenever there are faults on either system.

Generally, because of the lack of control, utilities have resisted the introduction of privately owned generation connected to their systems. Several large utilities have produced guidelines defining their technical requirements before they will agree to allow an embedded generator to operate in parallel with their networks.[1-7] In addition, the regulating authorities require the utilities to ensure that the embedded generators will not detract from the quality of supply to other customers and these guidelines define the general protection requirements for protection against all types of faults and abnormal operating conditions.

A major consideration in these guidelines is to provide equipment that will detect a loss of grid (or islanding) condition. This is when an embedded generator is disconnected from the main source of power due to a random opening of a utility circuit breaker. Depending on the amount of connected load, a synchronous generator, or an induction generator with sufficient capacitance connected to it for self-excitation, can continue to supply the local load and some utility load when the connection to the main source of supply is broken. The loss of the utility grid supply may cause dramatic changes in the electrical operation of the power island, particularly if there is a mis-match in the available generation and connected load. Excess generation in the power island will cause an increase in system frequency and voltage leading to over-excitation of the transformers. Insufficient generation, however, will drag the generator's voltage and frequency down affecting industrial process loads and possibly leading to a complete system outage. With closely matched generation and load the disconnection may cause insufficient system disturbance to operate the over/under voltage or over/under frequency protection resulting in the independent power island continuing to operate undetected. A schematic representation of the loss of grid situation can be seen in figure 1.1. This shows the embedded generator supplying some of the utility load following the loss of connection to the grid when the 'loss of grid' circuit breaker is opened. The 'loss of grid' circuit breaker could potentially be any circuit breaker, switch or isolator in the main utility system which connects the main source of supply to the embedded generator.

Protection against loss of grid is therefore essential to protect both the embedded generator and the utility system against accidental isolation of the two systems. Isolated operation is not a problem in itself provided that the voltage and frequency remain within

statutory limits. The main concerns are for safety of utility personnel and the potentially disastrous scenario of restoration of the utility supply when the two systems are out of synchronism. The loss of grid protection must therefore immediately detect the isolation of the two systems and disconnect the utility part of the power island by tripping the intertie breaker between the embedded generation busbar and the utility system before an auto-recloser can reconnect the two systems.

It is the responsibility of the operator of the embedded generator to supply the necessary level of protection and control equipment for the embedded generator scheme, however the economics of small embedded generation is such that once the desired level of protection is defined, the costs to protect the interconnection do not vary with generation capacity.[8] There is a widespread complaint from potential operators of embedded generation that the utility grade relays are too expensive. For a small scheme, the protection costs can be comparable to that of the generator itself. To make any relatively small generation scheme economically viable there is obviously a need for low cost, high quality protection packages for the protection of the embedded generator system. The use of a single microprocessor based protection relay with multiple functions is one solution to this requirement.[8-11]

1.4 Objectives and Previous Work.

Quoting from a recent I.E.E.E. paper on the subject of embedded generation[12], "Providing protection against islanding probably is the single most challenging aspect of designing the electrical power system involving cogeneration."

The work detailed in this thesis is concerned with the detection of a loss of grid (or islanding) situation, leading to a subsequent isolation of the embedded generator from the remaining utility system. The proposed technique is based upon a measurement of the power at the terminals of the generator. This can be carried out using a microprocessor based relay system which will also allow a number of other protection functions for embedded generation to be implemented in a single piece of hardware.[9,10]

The main objective of the research was the modification of the theoretical change in power loss of grid algorithm, which was conceived in previous work[1], to operate in the 'real world' environment. This involves implementing the theoretical algorithm in a digital environment and determining the refinements required to allow the algorithm to correctly operate in the practical system. The final aim of the research project is for a field tested algorithm to be included in a microprocessor based protection relay along with the other protection functions to provide complete protection for an embedded generation scheme.

1.5 Scope of this Thesis.

A brief summary of the information provided in each chapter of this thesis is given below:

Chapter 2: The thesis begins by detailing the requirements for an embedded generation scheme and highlights areas of concern and interest. This includes information on the legal, technical and operational requirements of an embedded generation scheme along with the required protection equipment and system configuration.

Chapter 3: The current methods employed to detect a loss of grid situation are the subject of the first part of this chapter. Information about the various techniques and their method of operation is given, but above all this section shows the limitations of the present protection techniques in detecting the occurrence of a loss of grid. After reviewing these methods, the chapter details the mathematical basis for a new method of detecting the loss of grid condition and gives the theory behind its operation. The algorithm is then developed and the process of its implementation in a digital environment outlined.

Chapter 4: In order to test the basic operation of the new algorithm, simulation studies were carried out using a simulation program written specifically for this purpose. Details of the simulation package and its method of operation are given in the first part of the chapter. Further to the simulation tests, practical real-time laboratory studies were carried

[1] Work undertaken by Dr Ömer Usta

out using a laboratory research system which includes a microprocessor relay and a personal computer. The construction and operation of this research bench along with the software required to carry out the tests is fully documented in this chapter. The final part of the chapter outlines the setup required for the field trials of the algorithm using the microprocessor relay. These tests were carried out on a diesel driven embedded generator operating on an industrial site.

Chapter 5: The results of the practical tests highlight the challenges of implementation of the theoretical algorithm in a practical environment. The presence of distortions in the measured practical data from the laboratory system requires refinements to the basic operation of the theoretical algorithm. The differences between the simulated system results and the laboratory results are presented and the reasons for the refinements demonstrated. The work is presented in a progressive manner which takes the algorithm from its basic theoretical form to the final practical implementation of the algorithm in a digital environment. Test results obtained from the field trials are also included in this chapter.

Chapter 6: Once the final form of the practical algorithm has been developed its operation for all the system studies is demonstrated with further test results. These results show the final practical response of the algorithm to a number of different system conditions as well as its operating limitations.

Chapter 7: This chapter contains the final conclusions and discussions about the work undertaken in the project and presented in this thesis. Areas of further interest for the project and suggestions for future work in this area are also discussed.

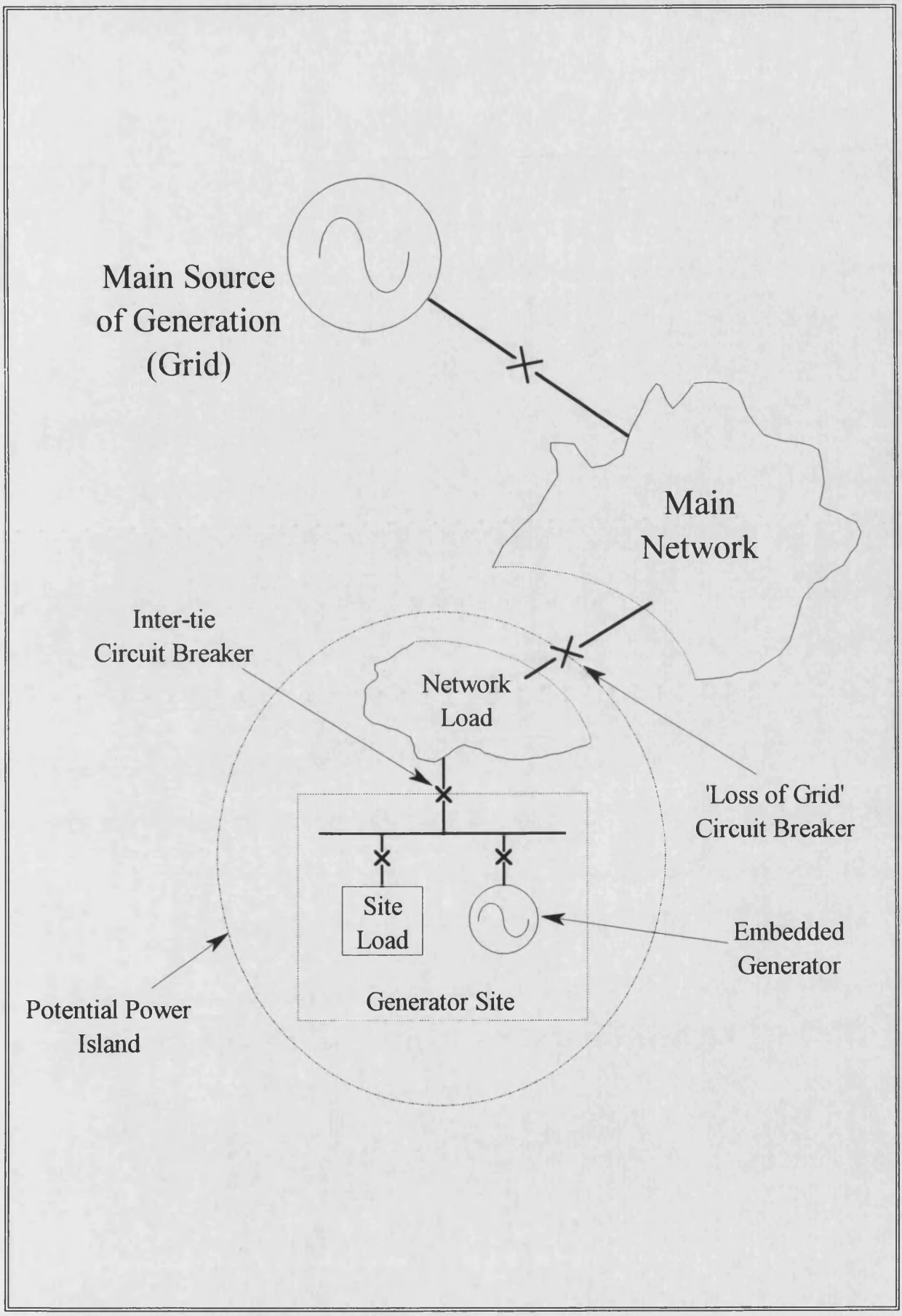

Figure 1.1 : Schematic Diagram Showing Loss of Grid Situation.

Chapter 2

Requirements for Embedded Generation

There are four main reasons for employing electricity generation close to the load[13]:

- Energy conservation using C.H.P. units to recover waste heat.
- Where a renewable source of energy can be harnessed and controlled economically.
- 'Peak lopping' such that the peak demand on the supplier's network is restrained by encouraging consumers to supply load from their own generation at times defined as 'contracted consumer load periods'.
- Improvement in supply security and minimisation of electricity supply interruptions particularly where industrial process plant loads are concerned.

However, before achieving the advantages offered by including embedded generation into a system, there are a number of requirements that must be satisfied.

2.1 Legislative Requirements.

2.1.1 The Energy Act.[14]

The Energy Act 1983, section 5(2), states: 'Where a private generator or supplier requests an Electricity Board

a) to give and continue to give a supply of electricity to premises where he generates electricity, or from which he supplies electricity to others, or
b) to purchase electricity generated by him, or
c) to permit him to use the Board's transmission and distribution system for the purpose of giving a supply of electricity to any premises.

the board shall offer to comply with the request unless on technical grounds it would not be reasonably practical to do so.'

This obliges any Regional Electricity Company (R.E.C.) to buy or transport energy from any generator who wishes to be connected to the R.E.C.'s distribution network. It is, however, standard practice for the R.E.C. to charge the private generator for any alterations to their system required to safely connect the plant.

In addition, Section 19(1) requires that 'It shall be the duty of every Electricity Board to adopt and support schemes-

a) for the combined production of heat and electricity, and
b) for the use of heat produced in combination with electricity, or incidental from its generation, for the heating of buildings or for other useful purposes.'

This is intended to increase the use of C.H.P. units to improve overall efficiencies.

2.1.2 Health and Safety.

Every private generator has a duty under section 3 of the Health and Safety at Work Act 1974 [15] 'to conduct his undertaking in such a way as to ensure, so far as is reasonably practicable, that persons not in his employment are not exposed to risks to their health or safety.' This obligation covers members of the public and includes any regional electricity company employees working on the company network to which the private generator is connected. This is particularly true when the network is supposedly isolated from all electrical supply points to allow for work on the system.

2.1.3 Safety and Quality of Supplies.

Electricity companies have a statutory obligation under The Electricity Supply Regulations 1937 [16] to ensure the safety and quality of the electricity supplies. This means that a private generator must not operate his plant in such a way that the electricity utility is unable to fulfil these obligations. The R.E.C.'s are only compelled to supply premises which they are reasonably satisfied that all equipment is in good condition. They are also able to disconnect supplies if the operation of any plant interferes with the efficient supply of electricity to any other user. These regulations apply equally to load or generation.

2.1.4 The Electricity Council Recommendations, G59.[1]

In the U.K., the technical requirements for connection of an embedded generator to a R.E.C.'s system are defined in the electricity council's engineering recommendations (G59). It is intended to provide guidelines for utilities where the connection is to be made at, or below 20kV and where the generator's output does not exceed 5MW.

The document applies to systems where the private generating plant may be paralleled with the Board's distribution system and where the private generating plant or the Electricity Board's system may be used to supply the same electrical load.

2.2 Connection and Operational Requirements.[1,5,6,17]

2.2.1 System Earthing.[1,18,19,20]

For high voltage (h.v.) systems, the Electricity Board may use direct, resistor, reactor or arc suppression coil methods for system neutral earthing. Where the Board's system is designed for single point earthing, no star point or earthing transformer should be connected by the private generator during parallel operation. However precautions must be taken to ensure that the private generator's h.v. system is earthed during isolated operation. Where the Board's system is designed for multiple earthing, during parallel operation, earthing may be achieved by the use of a busbar earthing transformer or the star point of the generator.

For low voltage (l.v.) systems, the Electricity Board's l.v. systems are directly earthed and the majority may now be multiple earthed. The neutral point of the embedded generator may therefore be connected directly to earth.

All customer generators should be isolated from utility-owned equipment by a power transformer connected so as to isolate the Zero Phase Sequence (Z.P.S.) circuit of the customer's generator from the Z.P.S. circuit of the utility.

2.2.2 Fault Infeed and Fuse Coordination.[1,17]

When proposing to install private generating plant, consideration must be given to the contribution of the private plant to the fault level on the Electricity Board's system. The extra fault current produced by connecting local generation can require the uprating of the existing network. Embedded generation can disrupt the expected pattern of currents flowing around a system under fault conditions and changes in the levels of fault currents, or fault currents flowing in the opposite direction to that predicted, will prevent fuses and protection relays from coordinating correctly.

The owner of the embedded generation system must provide, at his expense, whatever equipment is required to meet the functional requirements of the utility. The cost of any changes caused by increased fault current levels due to the customer's generation should also be considered as part of the parallel installation.

2.2.3 Synchronizing.[1]

In order to operate private generating plant, other than mains excited asynchronous machines, in parallel with a Regional Electricity Board's (R.E.C.) system it is necessary to synchronize the private generating plant with that of the R.E.C.'s system prior to making the parallel connection. To ensure that the machine is smoothly locked to the R.E.C. energy source, four conditions must be met[1,13]:

- The generator must be driven at a speed such that its frequency is acceptably close to 50Hz, and its phase sequence corresponds to that of the grid voltage.
- The generator voltage phasors must be matched in magnitude with the grid.
- The generator and grid voltage must be within 10° of equal phase.
- The voltage fluctuation on the Board's system during synchronizing should not exceed 3% at the point of common coupling.

Most utilities forbid manual synchronizing[12] because any difference between the instantaneous angle of the generator voltage and that of the utility will produce a momentary power swing (called a "bump") on the system. The utility is concerned that

the bump created will cause a voltage disturbance that will be experienced by other customers on their system. This bump can have a range of consequences from a momentary flicker of a light to a loss of production due to motor contactors dropping out unexpectedly.

To the embedded generator, the consequences of a bump may be more severe. Every time a transient torque is imposed on a generator shaft its life is reduced, leading to eventual premature failure. As a minimum, the embedded generator should have some relay supervision of manual synchronization where a protective relay is connected to prevent non-exact synchronization attempts. Ideally, the cogenerator would be equipped with automatic synchronizing.

For reasons of safety an embedded generator must not be permitted to pick up a dead utility circuit. Should a dead line be re-energised from the embedded generator end, there may be no way for the circuit breaker at the remote terminal to be synchronously closed.

2.2.4 Distortion and Interference.[1]

Where the generating plant input motive power may vary rapidly, causing corresponding changes in the output power, the voltage fluctuations at the common coupling point should not exceed 1%.

Harmonic voltages and currents produced within the private generator's system must not cause excessive harmonic voltage distortion on the Board's system.

The level of negative phase sequence voltage at the point of common coupling should not exceed 1.3% of the positive phase sequence voltage, assuming an initially symmetrical system. The utility should warn customers that certain conditions may cause Negative Phase Sequence (N.P.S.) currents to flow in the customer's generator and that it is the customer's responsibility to protect against N.P.S.

2.2.5 Engineering Planning.

To ensure that an embedded generation or cogeneration plant will operate safely, reliably and economically, power system studies are required during the planning and conceptual design stages of a project as well as periodically throughout the operating life of the plant.[21-24]

Areas that should be explored in discussions between cogenerators and utilities include[12]:

- Primary and back-up system protection practices,
- Automatic reclosing practices,
- Characteristics of major utility system loads,
- Transmission line surge protection practices,
- Transmission line routings near the embedded generation facility, and associated outage rates,
- Maintenance scheduling.

Every installation with private generating plant must be designed to be compatible with the Electricity Board's network to which it is to be connected. The utility may require that the details of the proposed protection scheme be submitted for approval and testing prior to commissioning. The utility may also require a lockable disconnect between the utility and the embedded generator which is accessible to utility personnel. The paralleling of customer generation with an electric utility requires that the customer and utility communicate and co-operate on the operating and protective relaying problems associated with the interconnection.[25] A utility point of view on the operating and protective relaying problems, together with some of the different interface schemes which a utility might provide for parallel operation with customer generation, can be found in references 12 and 25. In addition, the utility protection requirements for small wind turbine interconnection can be seen in reference 26.

2.3 General Protection Requirements.[27,28]

There are three main areas of concern:

1 The presence of embedded generation on a utility distribution system may contribute significant short-circuit current to faults and destroy the overcurrent protection coordination of reclosers and fuses.

2 Resonant conditions can develop on a section of distribution feeder with embedded generation that is isolated during single phase-to-ground faults resulting in an overvoltage condition on the unfaulted phases that can damage the embedded generator and feeder line equipment.

3 The operation of an embedded generator continuing to operate on a feeder that has been isolated from the substation by a recloser or other protection device ("Islanding"). The embedded generator can continue to supply power to the loads on the isolated feeder and become a safety hazard to repair personnel.

Reference 29 details the results of a simulation undertaken to highlight the problems associated with the interconnection of embedded generation.

2.3.1 Protective Equipment.[1]

The protection requirements of embedded generation depends on several factors:

- Generator capacity,
- Type of generator set,
- System voltage level,
- Method of system earthing,
- Point of connection,
- Mode of operation (i.e. parallel or independent).

The Electricity Council Recommendations G59 for the connection of embedded generation to a R.E.C.'s system requires that in addition to any generating plant protection

installed by the private generator for his own purposes, the Board requires protective equipment to be provided to achieve the following objectives:

- To inhibit connection of the generating equipment to the Board's supply unless all phases of the Board's supply are energised and operating within the protection settings.

- To disconnect the generator from the system when a system abnormality occurs that results in an unacceptable deviation of the voltage or frequency at the point of supply.

- To disconnect the generator from the Electricity Board's system in the event of loss of the Board's supply to the installation.

To achieve the objectives set out above, the protection must include the detection of:

- Over Voltage,
- Under Voltage,
- Over Frequency,
- Under Frequency,
- Loss of Grid.

Other protection could be required and may include the detection of:

- Neutral Voltage Displacement,
- Over Current,
- Earth Fault,
- Reverse Power,
- Stator Earth Fault,
- Rotor Earth Fault,
- Negative Phase Sequence,
- Loss of Excitation.

2.3.2 The Embedded Generator Protection Scheme.

The complete protection scheme for an embedded generator which could be incorporated in a digital multifunction protection relay is shown in figure 2.1. The individual relay elements are described below[6,8-11,27]:

- Over/Under Frequency (81O/U).[7,8]

Islanding is one of the major conditions for which protection is required. Should the cogenerator-utility intertie be opened, the generator will be expected to either accelerate or decelerate quickly, depending on the relative local load and generation conditions. Except for the case of an exact match of load and generation, the frequency will shift from 50Hz (60Hz in U.S.A.). The usual settings for these elements are 50.5Hz and 49.5Hz. The effectiveness of this technique for detecting loss of grid will be discussed in the next chapter. Over/Under frequency also provides a means of detecting abnormal frequency under normal conditions and removing the embedded generator.

- Over Voltage (59).[8]

Sensing the voltage is commonly suggested, along with frequency sensing, to protect against loss of grid. It is recommended that one overvoltage relay is connected between 106% and 110% voltage with a short time delay to prevent nuisance tripping. This protects the generator from a failure of the voltage regulator resulting in an increase in generator terminal voltage or an undesirable overvoltage condition on the utility system.

A second overvoltage protection function may be required which responds to the instantaneous value of the voltage under conditions of ferroresonance. Ferroresonance occurs when an embedded generator (synchronous or induction) becomes self-excited following separation from the utility source.[30] The high overvoltages and distorted waveshapes which occur means that the peak of the non-sinusoidal wave may be dangerously high while the R.M.S. value remains within an acceptable range. The second overvoltage function should therefore be set at 1.2 to 1.5 per unit with a minimum time delay.

The best solution to the ferroresonance problem is to remove the embedded generator itself from the island as soon as the isolation occurs and a study of the ability of certain relays to detect this condition is presented in reference 31.

- Under Voltage (27). [8]

The undervoltage element should be set at about 90% with a time delay of up to 60 cycles to prevent nuisance trips due to momentary dips in system voltage. This provides protection against closing the oncoming generator to a de-energised utility line. Under parallel operation the relay detects a reduction in system voltage due to a fault and removes the embedded generator from the system.

- Synchronizer (25). [32]

Check-Sync (25): Verifies proper frequency, voltage and phase relation between the oncoming generator and the utility system and provides permissive control for manual reclosure.

Automatic Synchronizer (25A): Monitors the phase relationships between the oncoming generator and utility bus and predicts the correct time to close the intertie breaker. The device provides speed and voltage correction signals for the generator. The conditions for paralleling are (deviation from nominal):

$$\text{Frequency} \leq 0.2 \text{ Hz}, \quad \text{Voltage} \leq 0.1 \text{ p.u}, \text{ Phase difference} \leq 5^{\circ}$$

- Negative Sequence Overcurrent (46N).

Protects the generator against damage caused by unbalanced currents resulting from a prolonged fault condition or abnormal load imbalance. The negative phase sequence currents induce eddy currents in the rotor at twice system frequency leading to severe rotor heating.

- Overcurrent (51) [32] and Stator Earth Fault (51N) [9,10].

Overcurrent relays provide three phase protection and disconnect on overcurrent and fault current flow in either direction. Their settings are coordinated with other elements in the power distribution circuit and their function is to achieve a cascaded circuit isolating system to isolate a faulted circuit as close to the fault location as possible.

The stator earth fault function is current operated and can be typically set to cover up to 95% of the stator windings. It is generally used for generators that are resistance earthed, but can be used to respond to current in the secondary circuit of an earthing transformer loaded with a resistor.

- Voltage Controlled/Restrained Overcurrent (51V).

There are two types of 51V relays. The voltage restrained relay is an overcurrent device in which the magnitude of the pick up current and operating time characteristics change as a function of system voltage.[12,27] With the voltage controlled overcurrent, the relay operates as an overcurrent relay only if the voltage on the system falls below a chosen minimum value. While the voltage is above this minimum the relay is disabled. In many applications, the choice between voltage restrained or voltage controlled overcurrent is a commercial decision, however there are significant application differences and these are discussed in reference 12.

- Field Failure (Loss-of-Excitation) Protection (40). [33]

When field failure occurs the generator will accelerate to a higher speed and operate as an induction generator at 40-60 percent of rated power with resultant high amortisseur currents in the rotor. In addition, exciting current (reactive power) will flow into the generator from the system. A generator is unlikely to be damaged by field failure provided the situation does not persist for more than 5-10 seconds. However, the heavy reactive load on the system can seriously reduce voltages, possibly causing collapse, instability, loss of load, tie tripping and related problems. Traditional field failure protection uses a distance type relay and operates from the apparent impedance viewed from the generator terminals.

- Directional Power (32R) [32] and Low Forward Power (32L). [9,10]

Directional power (Reverse power) relays protect against the generator motoring due to a loss of prime mover torque. The reverse power direction is power flow into the generator. The function should be time delayed since circulating (synchronising) power flow will occur upon initial connection of the generator to the bus.

Low forward power protection is sometimes applied to steam turbine generators where sequential shutdown is preferable under less urgent operation to avoid overspeeding.

- Generator Differential (87G).

Protects the generator against internal faults of the generator windings which can result in costly damage to the insulation, windings and core of the machine. This type of protection is not normally applied to machines below 1MVA.

- Directional Earth Fault (67N).[8,9]

When two or more generators are connected in parallel directly to a busbar, the directional earth fault function is used in conjunction with either stator earth fault or neutral displacement to discriminate between internal and external earth faults.

- Ground Fault Overvoltage or Neutral Displacement (59N).

This sensitive overvoltage device provides generator protection for ground faults where the generator neutral is grounded through a grounding transformer.

Additional protection functions which are not shown in figure 2.1 include:

- Temperature (49).

Protects against generator winding or bearing overheating.

- Phase Sequence Voltage Relay (47).[32]

This high speed relay separates the two power sources on undervoltage and excessive phase voltage unbalance. It also prevents synchronism of the generator with the utility until the utility is at nominal voltage on all phases and has the proper phase sequence.

- Directional Overcurrent (67).[32]

This is a high speed relay (3 cycles) which separates the local generator bus from the utility grid when the current flowing into the grid exceeds the full load current of the embedded generation plant.

- Out-of-Step Protection (78).[33]

Generators on distribution systems can be exposed to fault clearing times of 0.5-1 second or more and this can cause instability resulting in large power swings in generator power and potentially damaging shaft torque excursions. Generator currents during pole-slipping can be well above the current that the generator would deliver to a three phase fault and machine failure may occur after just a few events. Out-of-step relays respond to changes in 'apparent impedance' at the terminals of the generator as pole slipping occurs and limits exposure to one cycle of a pole-slip power swing.

2.3.3 Islanding of Embedded Generation.

A number of papers[7,8,12,13,17,26,29,31,33,34,35] have highlighted the problem that when an embedded generator is disconnected from the main source of power, a power island can result with a portion of the utility's network being isolated from the utility's supply, but still connected to the embedded generator. When considering the design of a protection system for embedded generation the most important design criterion is that 'The on-site generator(s) must be separated from the utility service grid immediately upon the occurrence of a power system disturbance that results in an unsafe, undesirable or objectionable operation.' For a system fitted with 12-cycle automatic reclosers, this means that the generator must be disconnected within eight or nine cycles maximum.[32]

The possible causes of isolated operation are [26]:

- Clearing of transient faults,
- Load shedding,
- Lines open for maintenance reasons,
- Possible equipment failures.

In a 'loss of grid' situation the voltage may collapse if the load is greater than the generation available, or the isolated system can continue to operate independently if the load on the isolated section of feeder closely matches the power output of the embedded generator connected to the feeder. The isolated operation of induction generators and line-commutated inverters is also possible with the proper combination of load and capacitor compensation.[29]

Analysis has suggested that if the ratio of local load to generator capacity is less than 3:1 then there is a significant possibility of a power island being formed.[31] This is dangerous for maintenance personnel because they may assume that the line has been de-energized since the substation breaker has been opened. In general, utility substations were designed to be the sole source of power on distribution networks so they may not be equipped with check synchronism relays. If a generator is left isolated from the main network, its speed and therefore frequency will be controlled independently by its own regulator and it is unlikely to stay in synchronism with the utility supply. There is therefore the danger that the two networks could be connected together out of phase, resulting in power surges and possible equipment damage particularly to the generator.

In general, if the rotating-type embedded generator output does not match the load exactly at the instant of isolation, there should be sufficient change in the generator speed for voltage and frequency relays to detect the islanding condition quickly enough to prevent damage to distribution equipment. However, there may be some cases where the load and generator capacity may be matched well enough where neither frequency nor voltage vary quickly enough for detection and therefore specific loss of grid protection will be required. It is recommended that utilities examine the possibility of isolated operation and satisfy themselves that it is adequately dealt with by the customer's protection.

Recloser settings should also be examined to determine if customer damage may result from high-speed reclosing. Winding and shaft damage can result from the currents and shaft torques caused by radial reclosing[33] and the potential for serious generator damage is so high that major investment to avoid it is warranted. Loss of grid protection is the subject of this thesis and a study into the effectiveness of current detection techniques together with a new method for its detection are detailed in the following chapter.

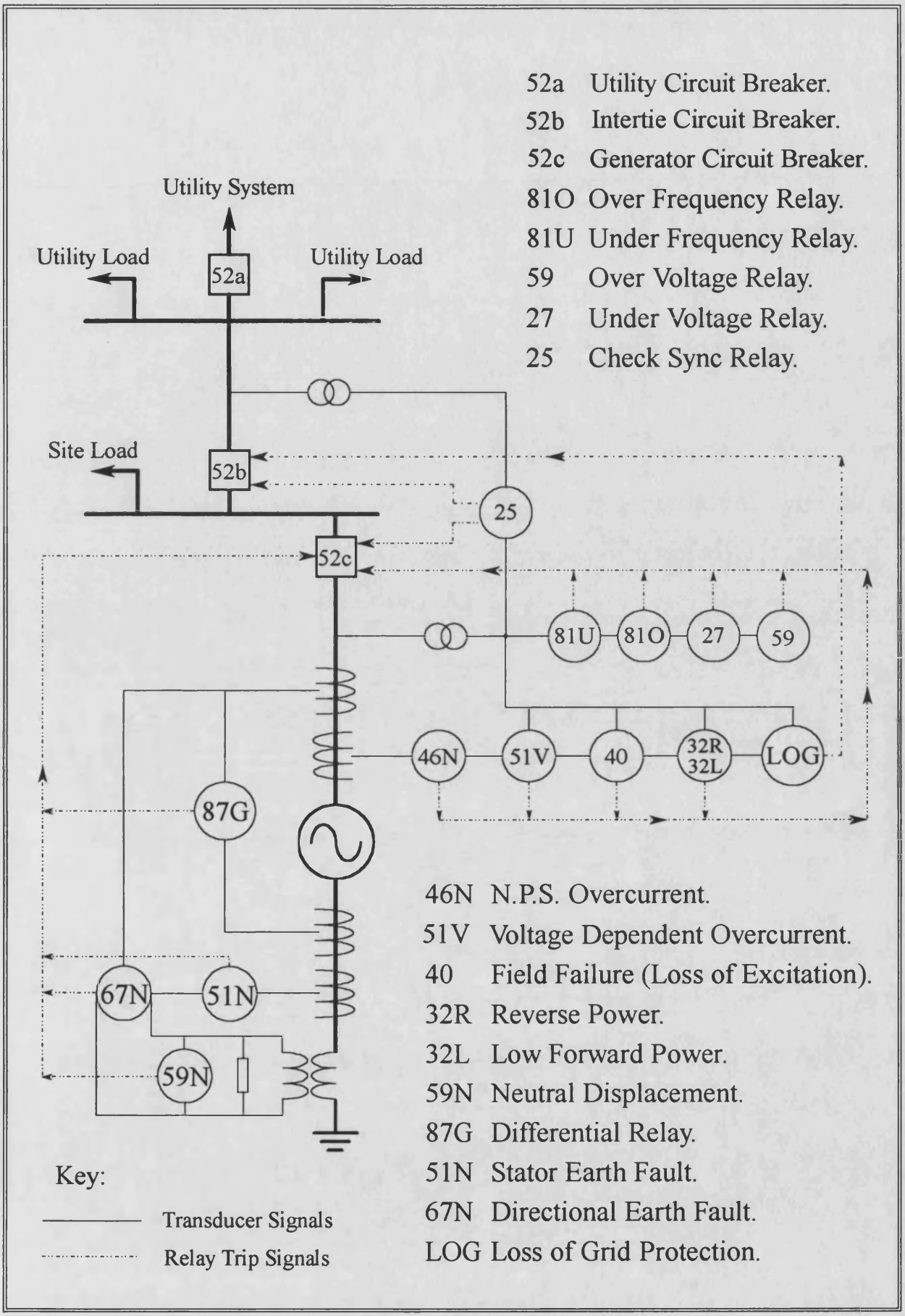

Figure 2.1 : Typical Protection Scheme Required for an Embedded Generator Operating in Parallel with the Utility Grid Network.

Chapter 3

Loss of Grid Protection

For a number of legal and technical reasons islanding is undesirable to the embedded generator because it is quite possible that the utility system load remaining in the island would be greater than the capability of the embedded generator with the result that it would be dragged down and carry with it the industrial process load, leading to a complete outage. The effect of an interruption to the utility supply depends on the power flow across the inter-tie just prior to the interruption.[34]

If power is being imported, then the industrial load exceeds the industrial generation. When the tie opens, the excess load is placed on the in-plant generation causing it to slow down. The rate of decay of generator speed (and hence frequency) is determined by the amount of overload and by the inertia of the generators.

If power is being exported, then the industrial generation exceeds the industrial load. When the tie opens, the excess generation will contribute to a rise in the industrial bus voltage leading to possible over-excitation of transformers and an increase in speed (frequency).

The principal objective for loss of grid protection is therefore to detect the condition where the embedded generation unit is left connected to a portion of the utility's load network, but disconnected from the main source of utility power following a switching operation. Typical requirements are that it should operate before the fastest automatic reclosure time of around twelve cycles. Fast detection of the loss of grid is also necessary to disconnect the two systems before the Automatic Voltage Regulator (A.V.R.) and Speed Governor can respond to try to restore a new power balance. Unfortunately, the loss of grid situation is further complicated since the circuit breaker that causes the loss of grid need not be a specific breaker in the system, but could be any breaker, switch or isolator which connects the main source of supply to the generator's site.

3.1 Present Techniques for Detecting Loss of Grid.

Difficulties arise because loss of grid is not a clearly defined fault condition, but is an undesirable and unsafe operating state. Several protection schemes have been developed to detect loss of grid and these can be split into two fundamental groups, passive or active. Passive techniques monitor system behaviour with no interaction with the power system and active techniques directly interact with the operation of the power system.

3.1.1 Transfer Trip from the Utility Substation.[5,6,12,17,33]

The most direct and effective method to detect a loss of grid connection is to take advantage of a Supervisory Control and Data Acquisition System (S.C.A.D.A.) to monitor the auxiliary contacts on all the circuit breakers, switches and isolators in the system between the embedded generator and the main utility supply. A transfer trip signal could then be provided to open the intertie circuit breaker. However most distribution systems, and the circuit breakers they employ, have not been fitted with a suitable supervisory system and the expense involved with a retro-fit is generally difficult to justify.

3.1.2 Over/Under Frequency and Over/Under Voltage.[12]

As previously mentioned, this is a widely accepted passive technique for detecting a loss of grid situation which monitors the variations in the system's frequency and voltage.[8,11] Any dramatic change in load on the embedded generator at the time of disconnection results in changes in the voltage and/or frequency of the system until a new energy balance is found. Over/Under frequency and Over/Under voltage relays are therefore able to provide a reasonable degree of protection. There are however, three considerations that may limit the effectiveness of these schemes:

1 If the load remaining in the island is close to the capability of the generator the voltage will neither increase nor decrease. Instead, a state of equilibrium will exist between load power and generated power and the island will continue to operate independently. Furthermore, large generators fitted with high speed automatic voltage regulators (A.V.R.s) may be able to match the subsequent island load after a short

time and it is therefore possible that the voltage and frequency can be maintained within prescribed limits and detection of the condition becomes more complex.

2 If separation leaves the island with an excess of generation, the theoretical response would be for voltage and frequency to rise. Most interconnected systems include many transformers and as voltage increases above normal the magnetic cores of these devices are over-excited. Over-excitation is essentially self limiting (i.e. over-exciting the core will cause an increase in excitation current drawn by the transformer which in turn limits the degree of overvoltage supplied to the transformer). When a core is over-excited, a significant degree of waveform distortion is imposed on the power system and many overvoltage and overfrequency relays commonly used to protect against islanding cannot properly respond in the presence of this distortion caused by the overvoltage.

3 Problems occur when the generation is far less than the total industrial plant demand, leading to very rapid frequency decay. Underfrequency relays must often shed the excess load in less than one second after the tie is opened. When relays are made faster, security may be sacrificed. Any disturbance which gives a change in system voltage also causes a transient disturbance in system frequency. Thus, if the frequency relays are set too high with very short time delays, they may mal-operate due to transient oscillations in frequency that follow the clearing of a fault within the industrial plant.

Under and over frequency relays will therefore do the job providing there is a measurable frequency excursion upon trip of the utility line but the frequency excursion is clearly difficult to predict and frequency based schemes cannot be 100 percent reliable. Voltage relays are similar to frequency relays in that it is difficult to ensure that reasonable voltage settings will reliably detect the loss of grid condition.

3.1.2 Rate of Change of Frequency (R.O.C.O.F.).[13,36]

This passive type of loss of grid relay can be used because for all practical purposes some difference between load and generating capacity will occur in the event of the 'islanding'

condition. The immediate effect of any change in the power being supplied by the generator is to change the kinetic energy of the machine and hence its speed. It can be shown from the swing equation that the initial rate of change of frequency is given by:

$$\frac{dF}{dT} = \frac{\Delta P\ F}{2HS} \qquad (3.1)$$

Where: ΔP is the change in power output,

F is the power system frequency,

H is the inertia constant of the machine and

S is the rated capacity of generation.[13]

The rate of change of frequency relay monitors the voltage waveform and trips if the rate of change of frequency exceeds the setting for longer than a set time delay. For small and medium sized embedded generation, an optimum operating time of 0.3 to 0.7 seconds is possible with a trip setting of 0.3 Hz/sec. The frequency is measured using a technique based upon zero crossings, using a high sampling rate and input signal filtering. A number of alternative methods are available for the calculation of the power system frequency.[37-40]

The biggest complaint about the R.O.C.O.F. relay is that it is difficult to determine the setting and as a consequence, mal-operation has occurred on a few occasions.

3.1.3 Phase Displacement Monitor.[35,41]

This passive relay detects phase displacements in the voltage waveform which are a result of changes in the loading of the embedded generator. Operating times of about 50 msec are possible for a loss of grid situation which results in a load change of greater than 5% of the generator rating. However, since sudden phase displacements occur mainly due to the changes in reactive power, the relay is less sensitive to the changes in real power due to a loss of grid.

3.1.4 Reactive Export Error Detector (R.E.E.D.).[36]

This is an active technique which involves exciting the generator so that it produces a level of reactive current at the relaying point which cannot occur if the protected generator is the only source of power to the system. The relay detects the loss of grid condition when the level of reactive current is not maintained at the setting value for longer than a preset time period. This time delay is chosen to be greater than the duration of any possible supply fluctuations.

Unfortunately, this technique requires direct control of the embedded generator as well as monitoring system operation. In addition, when a generator is operating in parallel it is usual for the excitation to be adjusted in order to minimise the MVAr demand charge by supplying the MVAr requirements of the local load. This is no longer possible when using this technique. Another possible drawback occurs if power factor correction capacitors remain connected in the power island and allow the reactive current level to be maintained at near the pre-loss value.

However, the technique is very effective, if somewhat slow (2 to 5 seconds), since it can detect a loss of grid when there is no load change due to the switching and it is often used as a back up to faster protection techniques.

3.1.5 System Fault Level Monitor.[42]

This is also an active technique which depends upon the measurement of the power system's source impedance close to the intertie. This is done by monitoring the magnitude of a short current pulse and voltage change which occurs when the current flow through a shunt inductor is controlled by a point-on-wave switch comprising anti-parallel thyristor pairs. By controlling the firing angle in order to keep the current pulse of constant magnitude the system fault level can be determined. The trip decision depends on a comparison of the measured system fault level with that corresponding to a network fed from utility generation.

Since there is a large difference between the fault levels of the utility's generation and that of the embedded generator the system need not be highly accurate. Fast operating times are also possible with a theoretical minimum of half a cycle. At present, there are no relays that adopt this technique, despite a similar technique being used to improve the performance of static voltage compensators.

3.1.6 Summary.

A comparative study of the effectiveness and speed of some of the above passive techniques in detecting a loss of grid can be seen in reference 43. These studies were carried out using a simulation that was developed specifically for loss of grid studies. The conclusions drawn in this paper show that a variety of different techniques are available for loss of grid protection. Active systems are usually more effective, but have the disadvantage of requiring a direct influence on system operation. Passive techniques however, cannot be guaranteed to operate under all conditions.

At present the only method of loss of grid protection that suffers no deficiencies is to monitor the auxiliary contacts on the utility circuit breakers and provide an intertrip signal, but for most power systems, this method is costly and unmanageable.[12]

3.2 The Change in Power Loss of Grid Algorithm.

The aim of this new algorithm is to provide a trip signal to open the intertie breaker between the embedded generation and the mains utility in the event of a loss of grid condition. The algorithm uses passive techniques to monitor the power measured at the terminals of the embedded generator. The development of the theoretical algorithm was based upon the following criteria:

- Loss of the main utility supply is a balanced three phase switching condition. Loss of only one or two phases is not considered to be a loss of grid since synchronism between the two systems is not lost, which allows subsequent unsupervised reconnection.

- Should a loss of grid occur undetected, any subsequent load change during isolated operation should produce a trip signal to open the intertie breaker and remove the 'islanded' utility load.

- If the loss of grid has not been detected before the utility supply is reconnected then the algorithm must produce a trip signal to remove the embedded generation from the system before serious damage can occur as a result of the unsupervised reclosure.

- The algorithm must remain stable for all load fluctuations during parallel operation.

- The operation of the algorithm must not be impaired or false operation occur due to the presence of unbalance or noise on the system.

- The algorithm must also remain stable and not mal-operate under local and remote power system fault conditions.

- The trip time should be fast enough to isolate the two systems before the A.V.R. and Speed Governor can correct the imbalance between available generation and connected load.

- The proposed technique must be fully compatible with the other protection functions associated with the embedded generator and be suitable for inclusion in a microprocessor based integrated generator protection package.

The key requirement for the Loss of Grid algorithm is to be able to detect whether the embedded generator is connected to the mains system. This is achieved by monitoring the response of the system to disturbances. The proposed algorithm uses changes in the power output from the generator to gain insight into the transfer function of the connected system. Under normal parallel operating conditions the characteristics are of both the mains supply and the embedded generator. However, following a loss of connection, the characteristics are of the embedded generator alone. There is sufficient difference between the relative capacities and inertia's of the two systems to provide for a method of immediate detection.

3.2.1 Mathematical Basis for Algorithm.

Consider a power system comprising n machines. An arbitrary load impact $\pm\Delta P_L$ on the system will cause each machine to accelerate/decelerate relative to its capacity and inertia constant. This occurs after an initial transient period detailed in appendix A.3. Under these conditions, the i^{th} machine will share the load impact according to:

$$\Delta P_i = \pm\Delta P_L \frac{H_i}{\sum_{J=1}^{n} H_j} \tag{3.2}$$

Where H is the inertia constant of the machine and is defined as the stored energy in the machine's rotating part per unit VA. In general it has units of MW.sec/MVA or seconds at unity power factor.

The mathematical theory behind the response of a synchronous generator to random power impacts, given by equation 3.2, is presented in Appendix A. In this appendix, the swing equation which governs the response of the generator is developed then a simple model of a single machine on an infinite busbar is produced. This model is then used to show the distribution of power impacts in a multi-machine network.

Equation 3.2, however, assumes a common base for H. Replacing H_i by $H_i(S_i/S_B)$ and H_j by $H_j(S_j/S_B)$ leads to the more general equation:

$$\Delta P_i = \pm\Delta P_L \frac{S_i H_i}{\sum_{J=1}^{n} S_j H_j} \tag{3.3}$$

Where S_i and S_j are the rated capacities in MVA.

When the generator is operating in parallel with the mains and both systems are modelled by idealised generators, as was shown in figure 1.1, the general equation (3.3) can be simplified to show the effect of the load impact $\pm\Delta P_L$ on the power output of the embedded generator:

$$\Delta P_g = \pm \Delta P_L \frac{H_g S_g}{H_g S_g + H_m S_m} \quad (3.4)$$

Where H_g and H_m are the inertia constants of the embedded generator and the utility supply respectively,

and S_g and S_m are the capacities of the embedded generator and utility supply.

Equation 3.4 therefore shows the response to a load change on the power system with the embedded generator operating in parallel with the main utility supply. It can be seen from this result that the effect of the load impact on the generator is greatly reduced by the presence of the product $H_m S_m$ in the denominator of the fraction. Typical values for H_m and S_m are 10 MW.sec/MVA and 250 MVA respectively, compared to around 1 MW.sec/MVA and 5 MVA for a typical embedded generator. After a loss of grid has occurred the effect of the main supply (i.e. $H_m S_m$) is removed and equation 3.4 becomes:

$$\Delta P_g = \pm \Delta P_L \quad (3.5)$$

Under these circumstances it is the change in the load $\pm\Delta P_L$, the embedded generator and the local network inertia constant that defines the system behaviour after the loss of grid. Since a loss of grid generally produces a change in the loading of the generator, monitoring the changes in the power output provides a method for detecting loss of grid.

It should be noted that following the loss of grid connection, the characteristics of the local generator determines the response to any changes in load. This may be the case when the local system is operating independently from the utility following an unseen loss of grid connection. In this situation the basis on which the new algorithm is proposed also provides a secondary means for detection should the first method fail due to insufficient change in generator loading. Thus a loss of grid connection can be detected due to a subsequent change in local load in the independent power island.

3.2.2 Structure of the Digital Protection Algorithm.

The theoretical algorithm consists of four main steps:

- The instantaneous power is calculated from the input data,
- The rate of change of power (i.e. derivative) is produced,
- The derivative signal is amplitude limited,
- The moving average of the clipped derivative is taken and compared with the trip setting.

Calculation of the Instantaneous Three Phase Power.

The input data required for this initial step of the algorithm consists of the instantaneous sampled values of the three line currents and the corresponding phase to ground voltages. Using these values, the instantaneous power can be calculated according to the formula:

$$P_g = v_a i_a + v_b i_b + v_c i_c \qquad (3.6)$$

Where v_a, v_b and v_c are the sampled phase voltages,
and i_a, i_b and i_c are the sampled line currents.

It is shown in appendix B that equation 3.6 for the instantaneous power measured on a three phase system, under balanced conditions, is equivalent to:

$$P_g = 3 V I \cos \phi \qquad (3.7)$$

Where V is the RMS line voltage, I is the RMS line current and $\cos\phi$ is the power factor.

Equation 3.7 shows that for a balanced system there are no sinusoidal components in the instantaneous power signal and it is therefore a 'd.c.' term. Unbalance present in the system produces a twice power system frequency term (i.e. 100Hz) in the power signal and the effect on the algorithm of any unbalance is shown in a later chapter.

The Rate of Change of Power.

The rate of change, or derivative, of a signal in a discrete environment can be found using the equation:

$$\frac{\Delta x}{\Delta t} = \frac{1}{\Delta t}\left(x_{j+1} - x_j \right) \tag{3.8}$$

For this application, the equation becomes:

$$\frac{\Delta P_{g\,(j+1)}}{\Delta t_s} = \frac{\left[P_{g\,(j+1)} - P_{g\,(j)} \right]}{\Delta t_s} \tag{3.9}$$

Where Δt_s is the sampling interval.

Providing the sampling interval is constant, the division by Δt_s is not required in the algorithm and can be included in a constant term in the trip setting. Equation 3.9 therefore reduces to:

$$\Delta P_{g\,(j+1)} = \left[P_{g\,(j+1)} - P_{g\,(j)} \right] \tag{3.10}$$

By reducing the calculation of the derivative to this simple subtraction, the required processing time in the microprocessor relay is greatly reduced.

Amplitude Limitation of the Rate of Change of Power Signal.

Mathematical analysis and simulation studies[43-45] have shown that at the instant of loss of grid, the instantaneous power changes very rapidly due to the stored electrical energy in the windings of the rotating machine. This is explained in greater detail in Appendix A as the response immediately following the load impact at time $t=0^+$. This fast change in turn produces a very large spike in the derivative term which leads to an almost instantaneous trip from the algorithm. To improve the stability of the algorithm by reducing the effect of this sub-transient response, it is necessary to limit the maximum value of the derivative spike to allow a minimum trip time to be set. This process of amplitude limiting the derivative is therefore included as a step in the algorithm to desensitize the algorithm to very fast initial changes in power which are due to stored electrical energy rather than stored inertial energy. In addition, clipping the signal

improves the stability of the algorithm under extremes of load imbalance and load fluctuations. The level to which the amplitude is clipped is shown in section 3.2.3.

The Moving Average of the Clipped Rate of Change of Power Signal.

The moving average filter is a technique used to smooth a signal and remove high frequency oscillations. Each smoothed value is calculated as the sum of the present value and each of the previous values in a predefined window size. The process can be mathematically expressed as:

$$y_{(n)} = \frac{1}{N} \sum_{r=0}^{N-1} x_{(n-r)} \tag{3.11}$$

Where: $y_{(n)}$ and $x_{(n)}$ are the present output and input respectively,
and N is the size of the moving average window.

The calculation speed of this equation can be greatly increased by maintaining a running total term throughout the calculation and simply subtracting from it the 'oldest' value and adding the 'latest' value. Equation 3.11 therefore becomes:

$$y_{(n)} = y_{(n-1)} + \frac{1}{N} [\, x_{(n)} - x_{(n-N)} \,] \tag{3.12}$$

Application of this moving average filter to the amplitude limited derivative signal results in an integration of the signal and provides a more stable algorithm output on which to base the trip decision. A trip occurs if the output of the moving average filter is greater than the predetermined trip level such that:

$$\left| \sum_{n=0}^{N-1} (\Delta P_g)_n \right| \geq K_s \tag{3.13}$$

Where K_s is the trip setting, ΔP_g is the rate of change of generator output power,
and N is the moving average window size which can be chosen to allow the maximum trip time to be set.

The final flow chart of the algorithm can be seen in figure 3.1.

3.2.3 Calculation of the Theoretical Trip Setting.[45]

When a loss of grid occurs it results in a load impact on the embedded generator. The acceleration or deceleration of the generator due to this load impact can be found using the machine's swing equation (Ignoring losses and the effect of damper windings).

$$a = \frac{d^2\delta}{dt^2} = \frac{\Delta P_L}{2\,S\,H} \qquad (p.u. / \text{sec}) \qquad (3.14)$$

Where: a is the acceleration or deceleration of the generator in p.u./sec,
S is the embedded generator rated capacity,
and H is the inertia constant of the generator in MW.sec/MVA.

The earlier analysis on the distribution of power impacts within a multi-machine network produced equation 3.3 which demonstrated the proportion of the load impact picked up by each machine. Equation 3.14 however shows the response of the individual machine following this load impact. The transient response of the generator and the subsequent changes in output power level are calculated using the machine's swing equation.

It can be shown [46] that the power of inertia of a rotating machine that is released at any speed variation is proportional to the acceleration/deceleration. The rate of change of power, from equation 3.14 is therefore:

$$\Delta P_i = K * \frac{\Delta P_L}{S\,H} \qquad (p.u. / \text{sec}) \qquad (3.15)$$

Where K is a constant coefficient.

This equation shows that the rate of change of power is proportional to the load impact and inversely proportional to the generator's rating and inertia constant. The trip setting of the algorithm is therefore dependent on the generator's capacity and inertia constant for a specified load change. The effect of the moving average window size and the sampling frequency are also included in the setting, but these are constant for all generator sizes.

Thus, if the algorithm is required to trip for a ΔP_S percentage change in the generators real power ($\Delta P_L = S.\Delta P_S$), the trip value in MW/sec will be:

$$K_s = \pm K S \frac{\Delta P_s}{H} N \qquad (MW / \sec) \tag{3.16}$$

Where: K_s is the trip setting in MW/sec at unity power factor for a generator which has inertia constant H and rated capacity S,

and N is the size of the moving average window.

($N = T_w/t_s$ with T_w = window size in msec and t_s = sampling interval in msec).

The level of the amplitude limitation of the derivative signal can be found for a minimum trip time of t_{min} as:

$$C_s = \frac{K_s t_s}{t_{min}} \tag{3.17}$$

3.2.4 Required Operation of the Power Based Loss of Grid Algorithm.

The development of the new loss of grid algorithm was based upon the criteria specified at the beginning of this section. Using the proposed algorithm specified above, the new loss of grid protection should therefore be able to:

- Detect a loss of grid connection resulting in an isolated power island being formed,
- Detect a subsequent change in loading within the power island whilst operating disconnected from the utility,
- Remain stable under severe system imbalance and in the presence of harmonics,
- Remain stable during large local load changes whilst operating in parallel with the main utility,
- Remain stable during local system and utility fault conditions,
- Operate before any subsequent auto-recloser action can re-connect the two separate power systems.

The ability of the new algorithm to provide this level of operation requires extensive testing and the systems used to carry out these performance assessment studies are detailed in the next chapter.

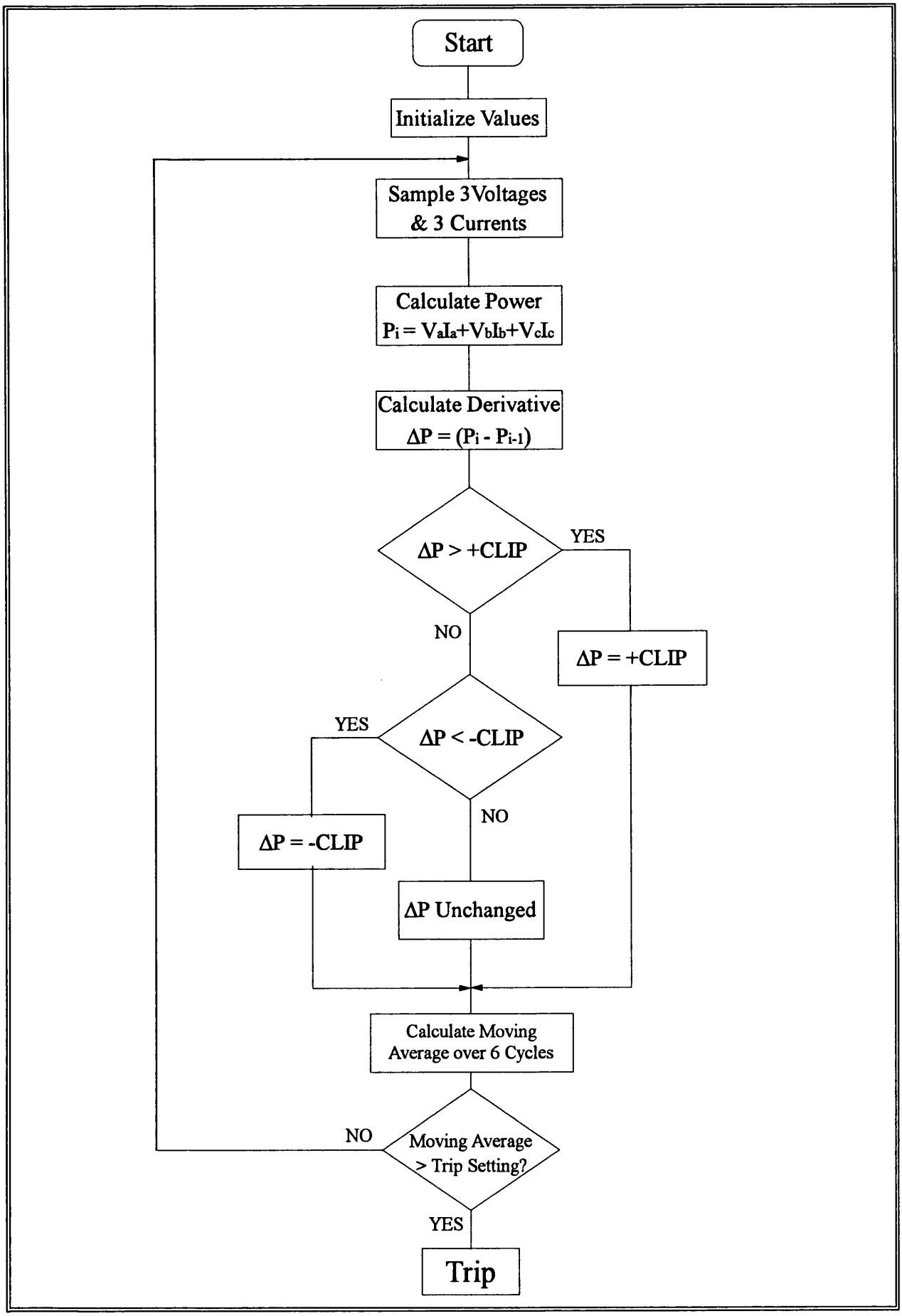

Figure 3.1 : Flow Chart for Theoretical Loss of Grid Algorithm.

Chapter 4

Algorithm Performance Studies

In order to test and develop the operation of the new loss of grid algorithm, a number of studies were required. This chapter explains the models used to evaluate the performance of the power based loss of grid algorithm. These are split into computer based simulation studies and practical real time system tests carried out in the laboratory and in the field.

The simulation studies were carried out using an in-house developed software simulation program which modelled the power system and allowed various system configurations and circuit breaker operations to simulate the event of a loss of grid connection along with certain other system events.

The practical laboratory tests required the construction of a suitable test facility[47,48] which consists of two small synchronous machines, a model power system for interconnection and a laboratory research bench. The research bench is made up of two main elements, a microprocessor based protection relay (M.P.R.) and a desktop personal computer (P.C.) with interface circuitry. These can both be used simultaneously to monitor the output of the synchronous machine using up to eight primary current transformers and three primary voltage transformers. A schematic diagram of the laboratory research bench and its interconnection to the model power system can be seen in figure 4.1.

The field trials were carried out on a diesel driven generator set which is one of three on an industrial site used for peak lopping and stand alone operation. The M.P.R. was attached via primary transducers to the terminals of this industrial generator and tests were carried out with an external load bank attached to the system. The resulting data files were downloaded following the test to the supervisory P.C.

The research facility can also be used as a teaching aid for undergraduates. In particular, it has been designed to provide a laboratory facility for the teaching of microprocessor based implementation of the biased differential technique for protecting the windings of

a synchronous machine. It has also provided the basis of a number of undergraduate research projects into microprocessor based protection of small synchronous generators.

4.1 Theoretical Simulation Studies.

Extensive simulation studies[1] have been carried out to determine the response of the proposed algorithm to a number of different disturbances including loss of grid. In addition, the performance of some of the present techniques for detecting loss of grid are tested for comparison.

A convenient model of the synchronous machine was selected and simulation software based on this model was written in FORTRAN to analyze the behaviour of the local generation unit for the following conditions:

- Loss of utility grid supply,
- Independent generator operation,
- Parallel operation with the utility,
- Out of step reconnection to the utility supply,
- System fault conditions.

The synchronous machine model was based upon the equations derived by R.H.Park which transforms the stator quantities (currents, fluxes and voltages) to a new synchronously rotating frame of reference. For the state space model of the synchronous machine, the machine currents were chosen as the state variables and the model used is therefore called "the current state space model." In the modelling of the utility power system, rather than using an infinite bus with infinite current capability at constant voltage and frequency, a synchronous generator model is used which represents the utility as a large synchronous generator with a reasonable inertia constant and rating.

The machine simulated is a 3.75 MVA salient pole synchronous generator with an inertia

[1] Work undertaken by Dr Ömer Usta.

constant of 0.91 MW.sec/MVA, connected to an 11kV network of capacity 250 MVA and inertia constant 10 MW.sec/MVA. The generator's control functions (i.e. A.V.R. and Speed Governor) were not included in the study since their response times were deemed too slow for the time frame under consideration.

The simulation software was designed according to the flow chart in figure 4.2. The operation can be considered in two parts:

- Calculation of the initial operating conditions using load flow analysis,
- Transient analysis of the proposed system under applied power system disturbances.

The test period generally used is one second of analysis with the required event occurring after 100 milliseconds of steady state. Using the simulation test system described, four out of the five modes of operation can be simulated (system fault conditions are considered separately). By adjusting the relative power levels of the generator and attached load, different conditions can be analysed to show the effect on the algorithm. (A complete description of the simulation studies can be found in reference 45).

The simulation system can also be used to evaluate the performance of the currently available loss of grid protection algorithms to allow for comparison. The trip levels used for these conventional passive relays are:

Under/over voltage	-	± 6% of nominal
Under/over frequency	-	± 1% of nominal
R.O.C.O.F.	-	0.3 Hz/sec

(Values taken from G59[1] and ET113[2])

The under/over voltage relay bases its trip decision on the effective value of the voltage calculated from the digital samples of instantaneous phase voltage at the generator's terminals with no time delay included. The power system frequency and rate of change of frequency is normally calculated from the digital samples of voltage or current. However for these performance studies the frequency is derived from the generator's speed, without the signal processing normally required to calculate the frequency.

The proposed loss of grid algorithm is set to just trip for a loss of grid resulting in a 1% change in generator loading with a six cycle moving average window resulting in a maximum trip time of 120 msec. The amplitude limiting function is set to give a minimum operating time of 20 msec (i.e. one cycle). This leads to a trip setting of ± 5 units on the scales shown in the results.

Since the loss of grid algorithm is designed to only operate for loss of grid and independent load change, its immunity to power system fault conditions requires analysis. To allow for the unbalanced fault conditions, the model used for the fault analysis combines both the direct phase quantities and the dq0 axes variables used for the previous analyses. The external system equations are solved in direct phase quantities and the results are then converted into dq0 axes variables to solve the equations representing the synchronous generator. Further details on the fault analysis can be found in reference 45.

As previously stated, a large number of tests were carried out using the simulation software, but only a select few of the results have been included in this thesis to allow for comparison with the actual real system results presented in chapter 5. The full results and analysis of this work can again be found in reference 45.

4.2 The P.C. Based Laboratory System - Hardware.

Following the software investigation into the loss of grid protection undertaken by Dr Usta, it was considered essential to investigate the performance of the algorithm using practical power systems.

In order to simplify the development of the loss of grid algorithm, a desktop personal computer (P.C.) was used which contains an analog to digital (A to D) converter board connected through transducers to the terminals of the synchronous machine. This allows the monitoring of the generator output terminal quantities and the use of signal processing software to develop the algorithm in a 'user-friendly' environment. Once the final algorithm has been developed, the code can be adapted and transferred to the microprocessor protection relay (M.P.R.) for additional testing and field trials.

To enable the monitoring of the generator output using a P.C. it was necessary to build an interface system. This consists of secondary transducer modules, anti-aliasing filters, sample and hold circuits, a phase locked loop frequency multiplier and a power supply. The resulting monitoring system closely resembles the M.P.R. system except for the obvious inherent advantages of using a P.C. (i.e. the Visual Display Unit and the Keyboard). The elements which make up the P.C. based scheme are detailed below and can be seen in figure 4.1.

4.2.1 The Analog to Digital Converter Board.

The analog to digital conversion board used for this work is a Data Translation DT2821 high speed analog and digital I/O board. It is designed to plug into one of the fully bussed expansion slots available in the backplane of an I.B.M. compatible computer. The board can then be programmed to perform A to D conversions, D to A conversions and digital input or output transfers. The programming can be done either directly by using assembly code, or in a high level language with the assistance of the support software 'ATLAB'. Further information about the operation and usage of the DT2821 board can be found in references 49 and 50.

4.2.2 The System Transducers.

The primary system transducers on the research bench provide the input signals for both the P.C. based system and the M.P.R. based system. They consist of seven primary current transformers (C.T.s) and three isolating voltage transformers (V.T.s). The connection diagram for the primary transducers can be seen in figure 4.3.

The C.T.s are class 'X' type with a turns ratio of 14.4 : 1 which provides a 1 amp. nominal current corresponding to the generator rated output current of 14.4 amps. The C.T.s are connected two per phase on the output terminal side of the generator and on the star point side. The seventh C.T. is connected on the star point itself. The three V.T.s have a turns ratio of 1:1 and are connected phase to ground to provide the generator terminal phase voltage. The outputs from these primary transducers are then fed directly into the corresponding secondary transducer module.

To reduce the levels of current and voltage to a level suitable for conversion into a digital signal by the A to D converter board, secondary transducers connected to the secondary circuits of the primary transducers were required. Two modules each containing four secondary current transformers (C.T.s) were constructed with the current output of each of the C.T.s being converted to a proportional voltage using burden resistors. To overcome the foreseen dynamic range problems, the value of the burden resistor was made switch selectable. This ensures that when high current levels are predicted, the resistance can be switched so that the output voltage does not exceed the maximum input voltage of ± 10 volts to prevent saturation of the A to D converter. The switched levels available give the full scale voltage (± 10 volts) for multiples of two, five and ten times the nominal current of the generator (which is 14.4 Amps).

One module containing three secondary V.T.s each connected to the secondary winding of a primary voltage transformer was also constructed. These secondary V.T.s are required to further reduce the power system voltage from the primary level of 115 volts phase to neutral (200 volts phase to phase) to a level suitable for the A to D converter. To provide for the measurement of overvoltages above the nominal value, the voltage transducers were designed to give a maximum of ± 10 volts at the A to D converter input for a system voltage of two times nominal voltage (i.e. 230 volts). The connection diagram for the secondary transducers can be seen in figure 4.4. In order to accommodate the different algorithms implemented on the research bench, the input transducers are switched into the filtering system in the configuration required.

4.2.3 Anti-aliasing Filters.

To prevent the problems of aliasing associated with analog to digital conversion it was necessary to design and build a set of anti-aliasing filters with the required cut-off frequency as defined by Nyquist's sampling theory. Each input to the A to D converter board requires pre-filtering to attenuate any frequency levels that may cause aliasing. The type of filter chosen for this application is a fourth order Bessel filter (also known as a Thomson filter). The full design of the anti-aliasing filter including the resulting circuit parameters can be seen in appendix C. Before the anti-aliasing filters were constructed, the frequency response of the design was predicted using the 'SPICEAGE' analysis

package. A total of eight anti-aliasing filters were constructed on a single printed circuit board (P.C.B). The schematic layout of this P.C.B can be seen in figure 4.5 together with the circuit diagrams of the anti-aliasing filter and sample and hold elements.

4.2.4 Sample and Hold Circuit.

A set of eight sample and hold circuits are included in the interface circuitry to allow for simultaneous sampling of up to eight channels. This is carried out by triggering each sample and hold circuit to 'hold' using a single trigger signal which is produced by a phase locked loop frequency multiplier circuit. This is of particular benefit when the inputs to a particular algorithm are required to be sampled at the same instant in time. (e.g. for biased differential protection algorithm[47]). The circuit diagram for the sample and hold circuit is included in figure 4.5.

4.2.5 Phase Locked Loop Frequency Multiplier Circuit.

The phase locked loop (P.L.L.) frequency multiplier produces an output frequency which is an integer multiple of the input frequency. The input to the circuit is taken from one of the input signals to the A to D board (i.e. one of the secondary transducer outputs). The output of the circuit is used to trigger both the sample and hold circuits to 'hold' and the A to D converter to start the conversion process. The A to D converter is triggered with a short low pulse which is generated from the output of the frequency multiplier using a glitch generator.

The phase locked loop frequency multiplier circuit consists of a single P.L.L. integrated circuit with two series connected 'Divide-by-N' counters connected into its feedback path (see figure 4.6). The output frequency is made switch selectable to allow multiple output frequencies to be generated. A schematic diagram of the circuit can be seen in figure 4.6, and the complete design can be found in reference 48. A slight variation from the design shown in the reference includes the need for the additional triggering signal to trigger the sample and hold circuit prior to the A to D conversion. This is obtained using two hex inverting buffer chips shown in the diagram.

Since the proposed loss of grid algorithm is dealing with instantaneous power, the P.C. data recording system is programmed to carry out simultaneous A to D data conversion on the six transducer inputs (i.e. three voltages and three currents) at a rate determined by the setting of the frequency multiplier. The frequency multiplier trigger firstly sets all the sample and hold circuits on the interface board to 'hold', the A to D board is then externally triggered to begin conversion of the first channel and then as rapidly as the software speed allows, the other channels are converted using software triggered conversions. This allows the simultaneous sampling of the six channels.

4.2.6 Bench Control Circuitry.

The trip outputs from both the P.C. and the M.P.R. provide a closing contact which results in tripping the main circuit breaker, disconnecting the synchronous machine terminals from the model power system. In order to provide for a delay in this tripping for laboratory experiment measurement purposes, a timer relay is included. The control circuitry for the protection scheme on the laboratory bench is shown in figure 4.7. This shows the indication lamps and relay interconnection required to carry out the generator protection undergraduate laboratory experiment using the microprocessor based system.

4.3 The P.C. Based Laboratory System - Software.

In the early stages of the loss of grid algorithm development it was considered an advantage to operate the P.C. system as a data recorder which could store the results of tests to file allowing post-processing using a signal processing package. This allows the algorithm to be developed with total flexibility and free from the constraints of real time operation using the signal processing package to test the effects on the various stages of the algorithm for a library of test data obtained from the laboratory. The 'DADiSP' signal processing package used for this work allows a number of data files to be imported into independent windows and mathematical operations carried out. Using this package, the basic power based algorithm can be fully implemented. In addition to the data recording function, the basic theoretical algorithm was also implemented in the P.C. to provide an indication of how the algorithm reacts to the situations tested.

The software written for the P.C. system consists of four parts (see figure 4.8):

- Assembly coded instructions operate the A to D conversion board to sample the required channel at the required time and store the result in a data register on the A to D board. The instant of conversion is determined by either an externally generated trigger signal or an internally generated software trigger. In these tests, the first channel is sampled on receipt of an external trigger signal, which allows system synchronization, and the subsequent five channels making up the sample data set are sampled using an internally generated software trigger which occurs at a rate determined by the on-board timer.

- Assembly coded instructions input the stored data sample values from the on-board data register into the computer's R.A.M. and applies the required mathematical operations to calculate the power which is stored in memory awaiting the next stage. Once the power is calculated the basic algorithm calculations can be applied if required and the intermediate results stored in memory for later extraction. The basic operation of the assembly coded modules is shown in the flow chart of figure 4.9.

- A 'C' coded data extraction module reads in the memory resident data arrays stored by the assembly code and writes them to file for post-test analysis.

- A B.A.S.I.C. program provides the overall system management and user interface functions and allows the operator to decide prior to the test what information is to be calculated and stored by the relevant assembly coded function. This program also sets up the number of data points to be stored which determines the duration of the test window. This information along with the file identification information is passed to the data extraction program after the completion of the test.

Using this package of software modules the user can complete real time tests in the laboratory at a rapid rate without the need for lengthy command line interaction.

4.4 The M.P.R. Based Laboratory System - Hardware.

Following completion of the preliminary tests using the P.C. based research system, development could move to the M.P.R. system. The microprocessor protection relay used in the laboratory facility and the field trials is a GEC Alsthom Protection and Control LZPK101 multi-module standard hardware microprocessor relay. This contains an Intel 80186 microprocessor, together with the input circuits required to monitor current and voltage transducer secondary signals and output circuits containing trip and alarm relays. There is also an RS232 serial communications channel for communication between the M.P.R. and a P.C.

The term 'standard hardware' signifies that this type of relay can be used for many different protection functions with the actual protection algorithm being encoded in software depending on the required application. The M.P.R. hardware and its operation in the laboratory research bench is described in this section.

4.4.1 The System Transducers.

The electrical inputs to the M.P.R. system from the generator originate from the same primary transducers used by the P.C. based system as described in section 4.2.2 and seen in figure 4.3. The secondary connections from these transducers are then screwed into the terminals on the back-plane of the M.P.R. The secondary transducer modules for the M.P.R. slot into the relay housing and the connections to the terminals on the backplane are made automatically. The secondary transducer module in the M.P.R. contains three C.T.s and three V.T.s, the analog anti-aliasing filters for each channel, a 12 bit A to D converter and six opto-isolated digital status inputs.

4.4.2 The Standard Hardware Microprocessor Relay.

In addition to the secondary transducer module described above, the standard hardware relay also contains a microprocessor module, an output module, a power supply module and an operator interface. Each of these modules fits into the relay housing giving the complete M.P.R. system shown in figure 4.10.

The microprocessor module contains the Intel 80186 processor together with the necessary auxiliary circuitry and system memory. The memory area of the board allows standard 28 pin memory integrated circuits to be plugged into sockets to provide up to 256kByte of memory. The configuration of this memory depends upon the application and for the research bench the top two memory sockets consist of E.P.R.O.M. programmed with the relay operating system software and the remaining 6 sockets are filled with 32kByte blocks of R.A.M. The use of R.A.M. in the usable areas of system memory means that the encoded algorithm must be downloaded into memory on power-up and is lost once the relay is powered-down. This situation is acceptable and actually desirable in the algorithm development stage, but the R.A.M. would be replaced by E.P.R.O.M. and E^2P.R.O.M. in the final system to allow automatic algorithm restart after a power-down.

The output module contains eight P.C.B. mounted miniature hinged armature relays which provide the outputs from the relay to circuit breakers and alarms.

The operator interface system for the standard hardware relay is mounted in the hinged front panel. It consists of a 2-row x 16-character alpha numeric liquid crystal display (L.C.D.) and a 7-key keypad. Also included in the front panel are four indication L.E.D.s and two 25-pin D-type sockets. One of these D-type sockets is for RS232 serial communications with the relay which is used to download the application software and transfer the results back to the supervisory computer.

4.4.3 The Supervisory Personal Computer.

The personal computer which forms part of the test facility is a COMPAQ 286 which is also used in the P.C. based system. In its supervisory capacity it performs two additional functions, it provides the user interface for programming the M.P.R. by offering a full 'C' compiler and communications software for algorithm development and downloading. It also allows receipt of the temporarily stored test data from the M.P.R. and writes these values to file for post-test analysis. The bi-directional transfer of information is carried out over the serial link already described.

4.5 The M.P.R. Based Laboratory System - Software.

4.5.1 The Basic Input/Output System (B.I.O.S.).

The M.P.R. has a number of input/output (i/o) devices which it is not possible to directly control using the 'C' programming language since it doesn't support i/o facilities. The purpose of the Basic Input/Output System (B.I.O.S.) is to isolate the application program from the system hardware that it operates. It consists of a series of macros which can be incorporated into the application software to provide a hardware/software interface that can control the i/o devices and peripherals of the multi-module standard hardware. The B.I.O.S. therefore handles the following four categories of commands:

- Input and Output: low level i/o for status inputs, output L.E.D.s and parallel port,
- Communications: string and single character operations for the serial port, parallel port, L.C.D. and keypad,
- Analog Input: data acquisition for analog channels,
- Timer: setting and reading the system timer and timer related commands.

The B.I.O.S. also returns information about the execution of a command to provide for detection and handling of errors. Complete details about the B.I.O.S., including a listing of the available commands, can be found in the reference manual written by the manufacturers of the multi module standard hardware relay.[51]

4.5.2 The Multi-Tasking Executive (M.T.E.).

A major difficulty encountered when writing embedded real-time software is to manage concurrency and any single program that attempts to process multiple, concurrent, asynchronous events is bound to be complex. Multi-tasking is a technique that reduces complexity by allowing a single piece of software to separate into several, individual processes called 'tasks' which are independent programs that can run either alone or in conjunction with other tasks. However, this independence does not exclude coordination among tasks or the sharing of resources. The M.T.E. is a collection of functions that provides an environment to support execution of several tasks concurrently.

At the centre of the executive is the scheduler which arbitrates the control of the central processing unit (C.P.U.) among tasks according to the priority level of an individual task. This ensures that more urgent tasks are run before less urgent tasks. Since only one task can be run at one time, the other ready tasks are held in the C.P.U. queue until they are the highest priority task not being executed. This situation will occur when all higher priority tasks are in a state where they are either waiting for data to be updated or waiting for the completion of another task. The executive supports '0' to '255' levels of C.P.U. priority with '0' being the highest level.

The tasks that exist within the multi-tasking environment will, at any given instant, be in one of the following states:

Dormant - task was never activated or has been deactivated because its operation is complete.

Waiting - task has been temporarily suspended and is waiting for a change in system status or new sets of data before it can recommence. A waiting task will be reactivated on occurrence of an event by a signal called a 'semaphore'.

Running - task is currently using the C.P.U..

Ready - task is in C.P.U. queue and is waiting to become the highest priority task.

If a task is being executed by the C.P.U., its execution will halt as soon as a task of higher priority moves from either the dormant or waiting state to a ready state. The halted task will return to the C.P.U. queue and wait to become the highest priority task again. This method allows the system to respond quickly to external events.

It is common in multi-tasking environments for tasks to communicate with each other or mutually exclude each other when accessing a common resource. This interaction is resolved using exchanges and the M.T.E. supports two types of exchange: semaphore and mailbox. Semaphores allow the synchronizing of task events by suspending operations until a particular semaphore is received, and mailboxes allow passage of messages between tasks. The full multi-tasking environment is explained in the M.T.E. version 2 manual written by the manufacturers.[52]

4.5.3 The Supervisory Computer Software.

As mentioned earlier, the role of the supervisory P.C. is twofold. For algorithm development, it provides the tools necessary to write and encode the source file to a hexadecimal file ready for downloading into the M.P.R. The original source code is written partly in the 'C' language and partly in assembly, which both require compiling and linking. For this work, the Microsoft C6 Compiler and Linker is used with the MASM 6 assembler. The resulting hexadecimal application code block must then be located at a specific memory location within the memory map of the M.P.R. processor. This process is carried out using the Paradigm Locater package which allows specific regions of memory to be reserved for specific applications in order to keep the application workspace separate from the M.T.E./B.I.O.S. workspace.

Once the application software has been compiled, linked and located, it is necessary to download the hexadecimal file into the M.P.R. memory. This is carried out using a communications package called Procomm and by making use of the off-line monitor facility which is part of the user interface of the M.P.R. The off-line monitor is an E.P.R.O.M. resident program which facilitates debugging of user programs. Once invoked, the user can communicate directly with the microprocessor via the RS232 data terminal (using Procomm) which allows the downloading of programs in hexadecimal format, the execution of programs and the examination of system registers and memory contents.

The second role for the supervisory computer system is to receive and decode the sample data values sent via the serial link from the M.P.R. This is achieved using a 'C' coded communication program which waits for a synchronizing character at the start of the data blocks and then stores the data following it in temporary arrays. These arrays are then written to file for post-processing. In this way, following each laboratory test, the stored data can be extracted from the M.P.R. memory leaving it ready to carry out another test.

4.5.4 The Application Software.

As with the P.C. based system, two test programs are written for the M.P.R. based system. The first, a data recording function, simply stores a predetermined time window

of data to memory and then transfers the data via the serial link to the supervisory P.C. The basic flow diagram for this mode of operation using the M.T.E. is shown in figure 4.11.

With reference to this diagram, in the multi-tasking environment, each semaphore and task must be initialized and activated before it can be used. This occurs in the background task along with the serial link and A to D converter initialization. The background task has the lowest priority and is first to be executed. Once the other tasks have been activated, control switches according to the relative task priorities and the background task only provides an infinite 'do nothing' loop to prevent the M.T.E. from crashing during periods where no other task is running..

TaskC, the error handling task, is activated first and it immediately suspends waiting for an error semaphore which will be signalled should any system error occur during program execution. Following a key press, the main data recording task (TaskA) is activated and this also suspends and waits for a Got_Data semaphore which is signalled by the A to D converter system when a set of sample data has been captured. The final task to be activated is TaskB, the data export task, and this suspends waiting for a Trip semaphore which is signalled by TaskA once the data recording cycle has been completed and the data is ready for export to the supervisory P.C..

With each of the three primary tasks suspended waiting for semaphores, control returns to the background task which continues by initializing the A to D converter system. As soon as a data set is sampled, the Got_Data semaphore is signalled and TaskA regains C.P.U. control. Once the data recording loop is complete, TaskB is triggered via the Trip semaphore and it proceeds to export the sampled values down the serial link. During this export procedure the A to D converter continues to produce Got_Data semaphores which require action and these are serviced by TaskA with no further action. Once the export is complete the system is reset and the next test initialized by a 'SET' button press.

The timer for the A to D converter system is set to provide 12 samples per cycle and the sampling frequency therefore must be adjusted to allow for variations in the power system frequency. This is done using a frequency tracking algorithm, called from TaskA, which

calculates the system frequency from the phase angle of one of the signals and adjusts the timer circuit to maintain 12 samples per cycle. The phase angle is calculated using the data obtained by full cycle Fourier filtering the raw sample values.

Once the raw sample values have been stored in the M.P.R. memory for a particular test, the values are downloaded to the P.C. for post-processing. All the data manipulation and algorithm calculation can therefore be carried out on the P.C., following the test, to determine the response of the algorithm.

One major difference between the M.P.R. based system and the P.C. based system is that sampling in the P.C. based laboratory system occurs effectively simultaneously for each of the six channels. This is achieved using the sample and hold circuitry previously explained. In the M.P.R. system, the samples are taken in succession which means that there will be an error introduced into the instantaneous power calculation which assumes simultaneous sample values. This error is reduced by time alignment of the data samples such that it appears that all the channels have been sampled simultaneously. The time alignment process makes use of the Fourier filtered sample values to generate the phasor representation of the input waveform. These phasors can then all be time aligned by rotating them backwards through an angle determined by the time delay between their respective sample instances. In addition to time alignment by phasor rotation, the errors due to the data acquisition system can also be reduced by including a scaling term for each channel which compensates for the errors associated with that channel. The software for implementing the phasor compensation process is also written for operation on the P.C. to provide greater accuracy during the post-test analysis procedure.

The second test program written for the M.P.R. system implements the full loss of grid algorithm with the intermediate calculated data values stored in memory on the occurrence of a trip decision. This allows the algorithm to be tested under various system conditions and once a trip decision occurs, the disturbance which caused the trip can be observed using the exported data files. The final form of the power based loss of grid algorithm is explained in the next chapter along with the reasons for certain refinements to the theoretical algorithm but the structure of the algorithm encoded in the M.P.R. is very similar to that of the data recording function already described. One key difference

is the need to include the phasor rotation function for time aligning the sample values and the phasor compensation function to reduce data acquisition errors, within the body of the main task. This is carried out in TaskA prior to the calculation of the instantaneous power for the algorithm. The loss of grid algorithm is implemented in TaskA with TaskB only triggered to export the results once TaskA has made a decision to trip. The flow diagram for this mode of operation is shown in figure 4.12.

4.6 Laboratory Test System Configuration.

The laboratory research facility uses a 5KVA, 2 pole synchronous machine which is driven by an 8 H.P. d.c. motor. The synchronous machine is connected to a model power system which contains a similar machine set and interties into a 200 volt three phase system. The synchronous generator may be synchronized with the 200 volt system allowing bidirectional power flow across the intertie. In addition to this, local loads can be connected to the system and wattmeters placed at various points. The schematic diagram for this model power system can be seen in figure 4.13. The system contains a double bus arrangement similar to that found in a medium range generating station. The model power system ('DANE' panel) is fed via a 500kVA three phase transformer which is situated about 100 metres from the laboratory.

4.6.1 System Setup for Biased Differential Scheme.

In order to test the full operation of the laboratory bench test facility, a second year undergraduate experiment into biased differential protection of synchronous generators was setup. The laboratory experiment is designed to teach undergraduates about the technique of biased differential protection as well as introduce them to the new microprocessor technology being used in relay protection schemes. The complete laboratory was therefore implemented using the P.C. system, with an application program written to guide the operator through the laboratory and then subsequently implemented in the M.P.R with the P.C. providing the user interface requirements for the laboratory. Faults are placed on the generator via taps along the stator windings and the M.P.R. exports results allowing the relay characteristics to be determined.

4.6.2 System Setup for Loss of Grid and Load Change Tests.

Using the various isolators and circuit breakers in the model power system shown in figure 4.13, it is possible to obtain the required test system configuration. In addition to the elements shown in this diagram, some load is required which can be connected into the system at convenient points. This load consists of a bank of six double bar electric fires rated at 240 volts and 1 kilowatt per bar and a set of three large variable resistors. The amount of load is made variable by means of three phase variacs connected before the load bank. The configuration of the system used for the loss of grid and load change tests can be seen in figure 4.14 along with a simplified line diagram.

With the bus section circuit breaker closed (C.B.5) the two generators can be connected together on a local busbar with local load attached at the bus coupling point. The second load bank acts as a grid load and is connected between the intertie breaker and the 'loss of grid' breaker. To assist in the setting of the required power flows from the generator and the mains supply, three pairs of wattmeters were used to measure the power into the load, from the generator and from or to the mains.

Since a purely resistive load was used, the output from the generator was maintained at around unity power factor by controlling both the power input and the generator excitation controls. This means that the reactive power in the intertie between the generator/local load busbar and the mains was kept to a minimum.

During the loss of grid and load change tests, the local load can be connected to either the generator, the mains or both together by means of the isolators and circuit breakers. A synchroscope can be used on any circuit breaker to synchronize the two systems together. With reference to figure 4.14, the circuit breakers C.B.6 or C.B.8 can be used to cause a loss of grid event.

The loss of grid tests were carried out at a number of generator output power levels with different combinations of local and grid load determining the load change that occurs at the instant of the loss of connection.

The independent load change tests use a similar setup, apart from the grid supply remains unconnected and so the generator output before the load change was set to match the site load to maintain the correct voltage and frequency levels. A load increase or decrease was then applied to the local busbar using the load banks.

The parallel load change tests required the mains supply to be synchronized to the local busbar and a change in the level of local or grid loading applied. The change was either a sudden step increase or decrease, or a variation induced by increasing the variac setting manually.

It is also possible to synchronize the unprotected machine (Generator 1) into the system to test the effects of multiple generator sites on the operation of the algorithm. The measurements for these tests were still taken from the terminals of the protected generator (Generator 2).

4.6.3 System Setup for Fault Tests.

To test the response of the loss of grid algorithm to faults on the system, it was necessary to apply faults involving any phase and earth to the laboratory system. This was carried out using a remote circuit breaker as a switch to apply a low resistance connection between whichever phases and earth as required. This fault switch was connected as shown in figure 4.14. The connection configuration was set using links in positions 'a' to 'd' as required.

During earth fault conditions, the connection of the generator star point has a significant effect on the fault test results. The star point is made available in the test generator to allow for either direct, resistive or isolated connection of the star point. The whole laboratory test system can be connected to a common neutral which is then connected to the incoming three phase mains neutral taken from the star point of the main supply transformer.

4.7 Field Trials on a Diesel Generator Set.

A second source of real time test data was used to verify the security and operation of the loss of grid algorithm. The M.P.R. was again used in data recording operation with the input to the relay coming from the terminals of a 625 kVA diesel driven generator set. The diesel generator is one of three which are used for peak-lopping on an industrial site. The generator can be connected to the utility grid supply operating in parallel and local changes in site configuration can be performed to test the effect on the algorithm.

For these tests, the M.P.R. was connected into a system used for testing a multifunctional generator protection relay.[8.9] The connection diagram for this relay on the local industrial site is shown in figure 4.15. The load requirements for the various tests was satisfied by attaching a load bank to the busbars of the protected diesel generator set. Multiple generator tests were also possible using the other generators which make up the industrial site generation.

The tests carried out in the laboratory and in the field trials provided results from practical systems with all the challenges that real systems introduce, along with the limitations imposed by having to operate in real-time using sampled input data. The theoretical algorithm was developed using a simulation test system which was free from many of the practical challenges and as a result, high levels of sensitivity and accuracy were demonstrated. The test system described in this chapter has been used to verify and refine the basic theoretical algorithm to allow it to operate in a real system. The results of the tests undertaken are the subject of the next chapter, together with the refinements made to the algorithm.

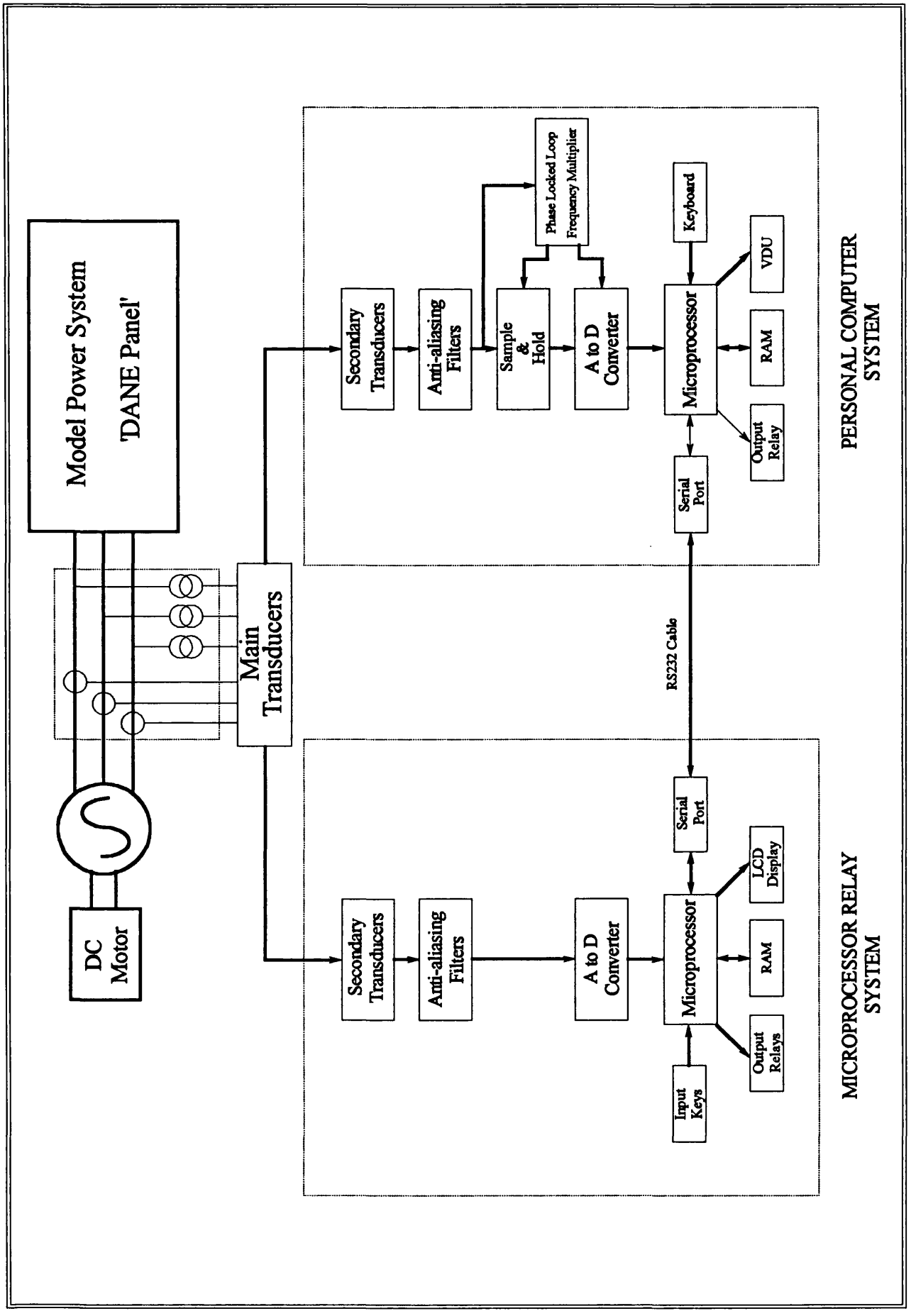

Figure 4.1 : Schematic Diagram of the Laboratory Research Bench.

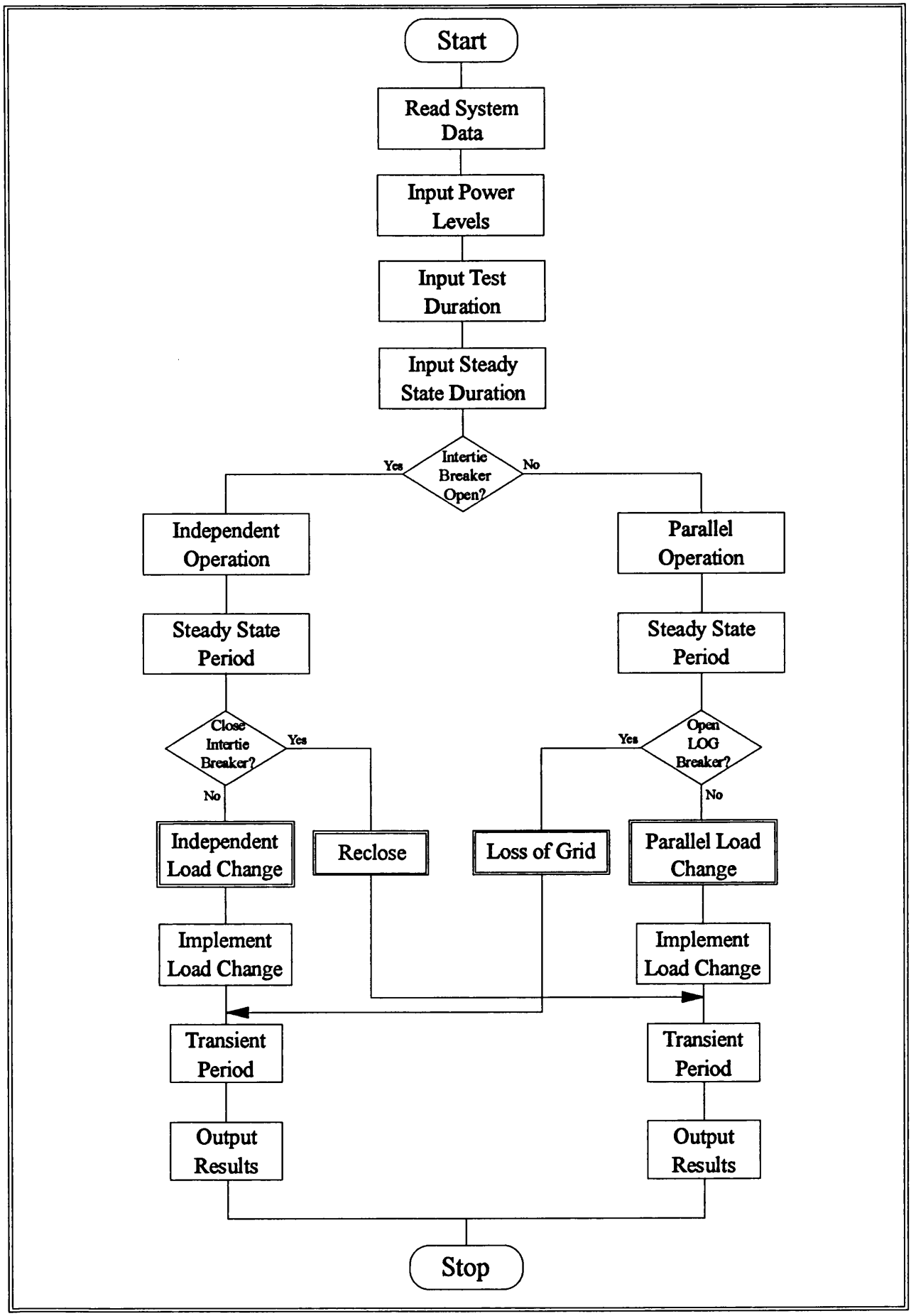

Figure 4.2 : Flow Chart for the Loss of Grid Simulation Software.

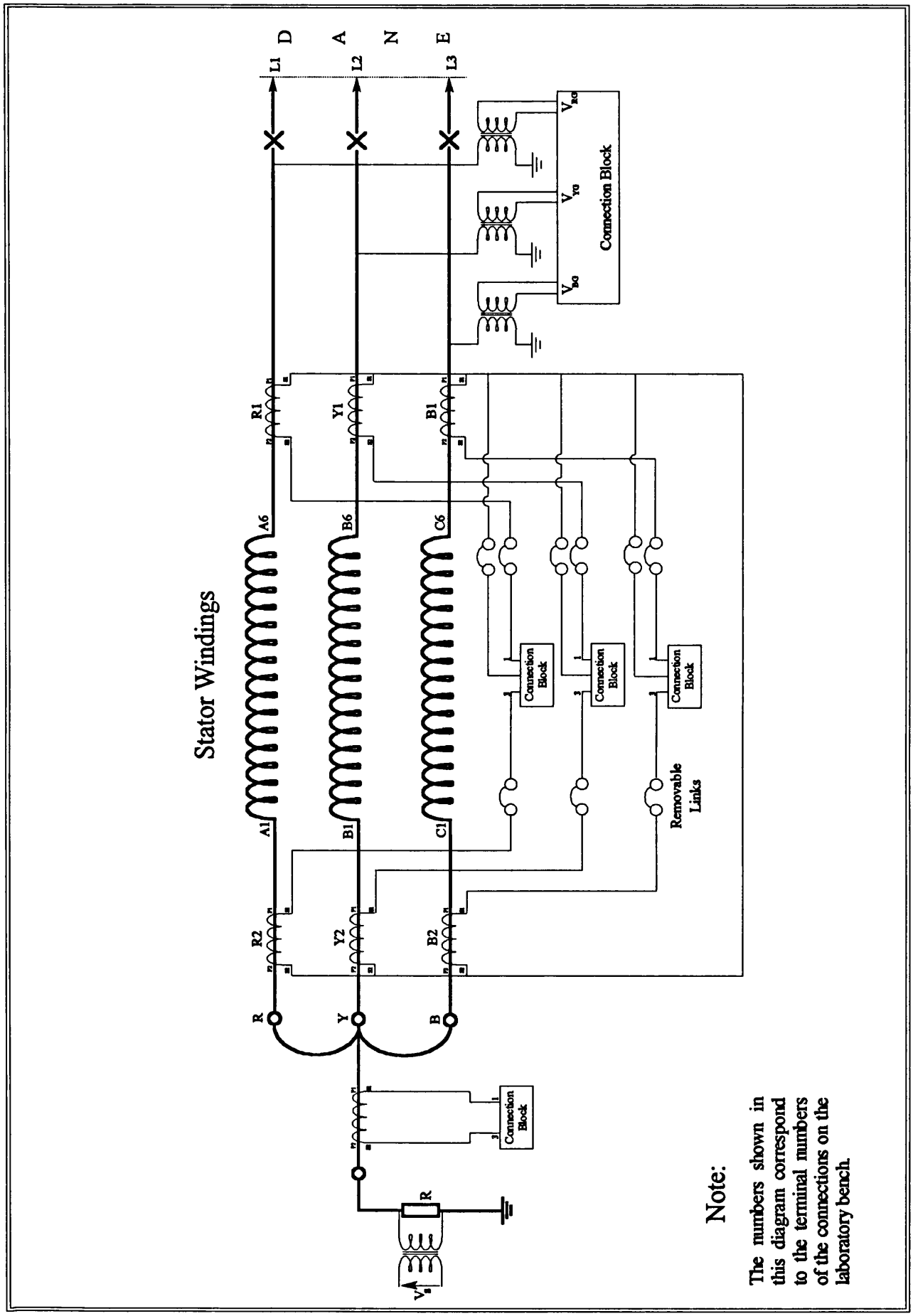

Figure 4.3 : Connection of Primary Transducers to Laboratory Synchronous Generator.

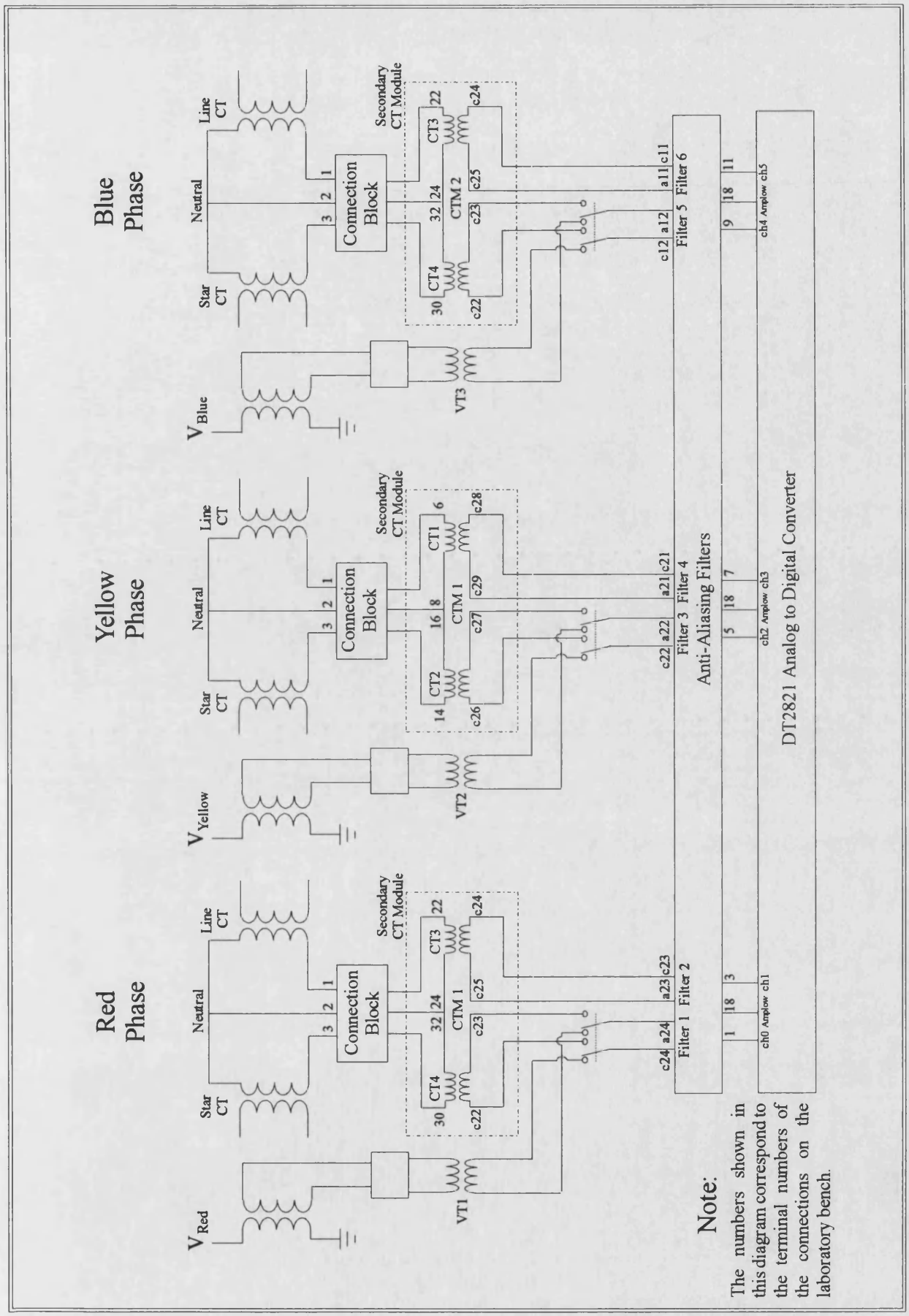

Figure 4.4 : Connection of Secondary Transducers in the Laboratory Research Bench.

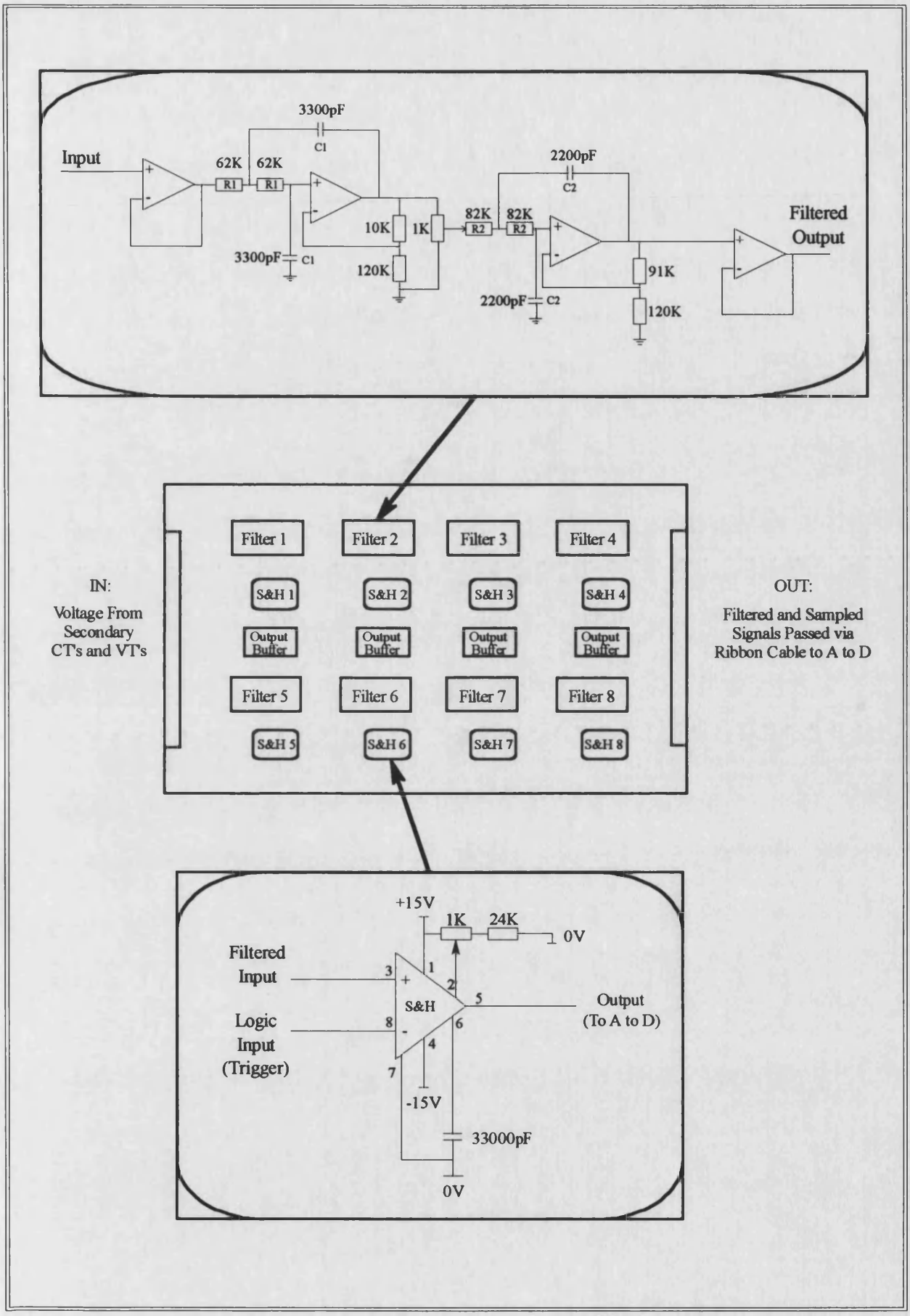

Figure 4.5 : Anti-aliasing Filter and Sample and Hold Printed Circuit Board Layout.

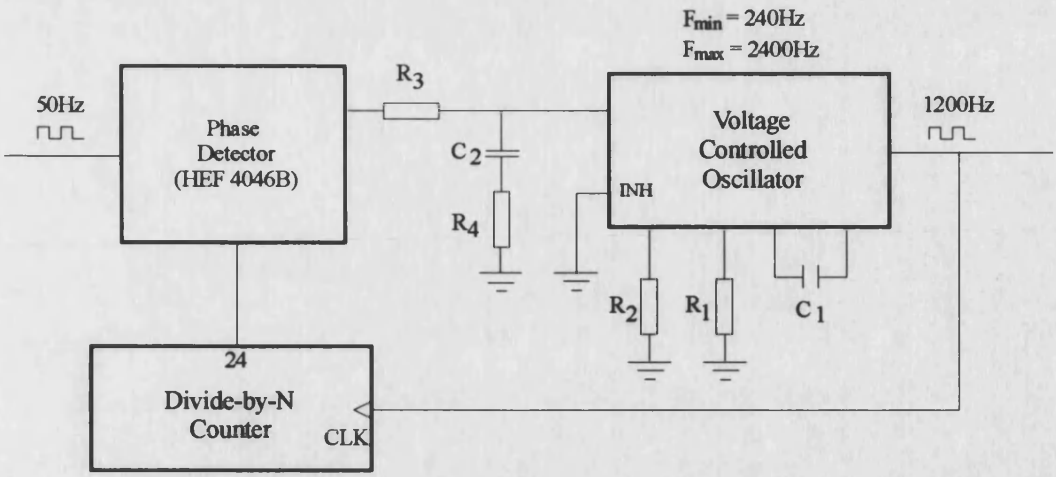

a) Phase Locked Loop (PLL) as a Frequency Multiplier.

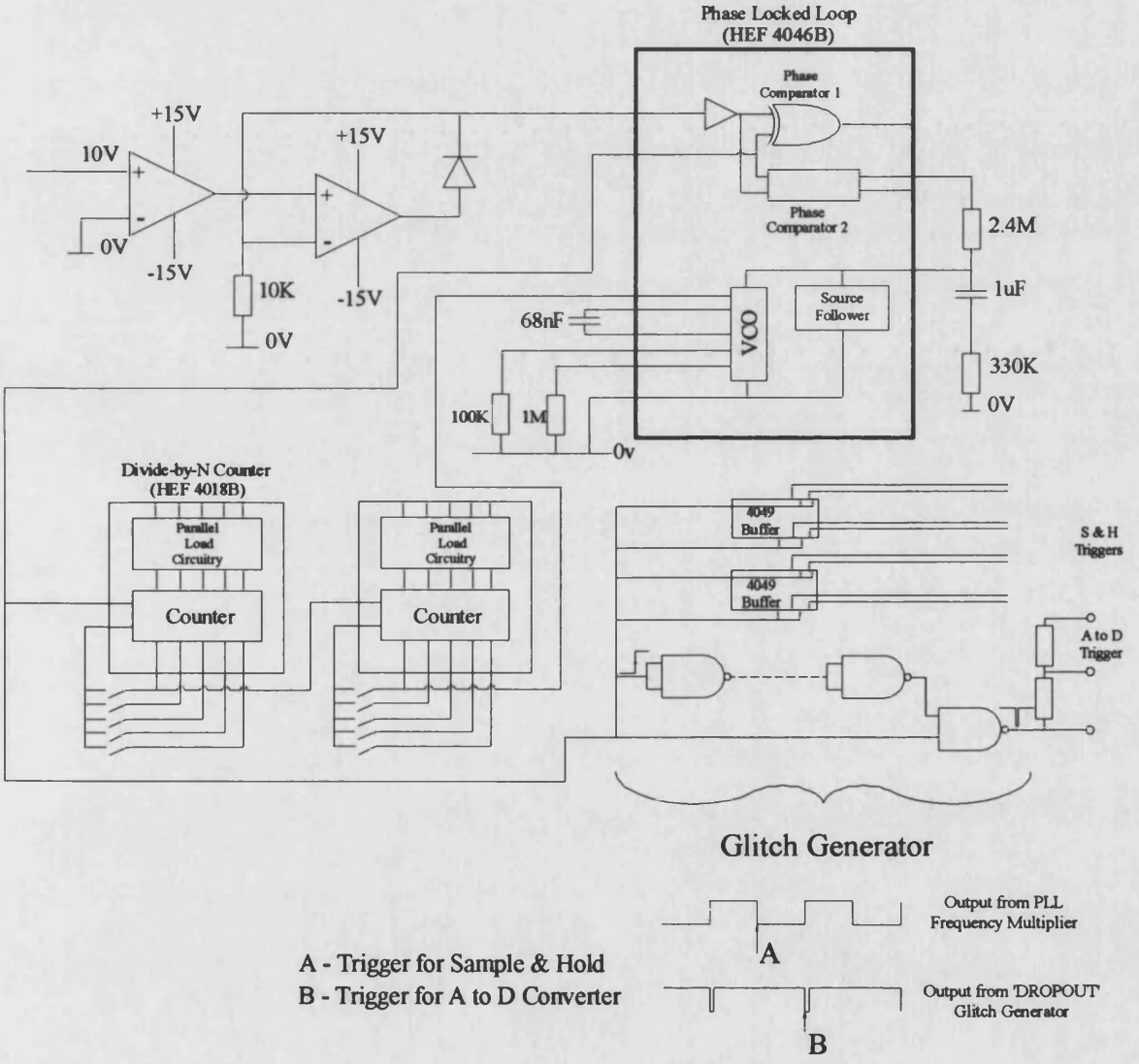

b) Schematic of the PLL Frequency Multiplier Circuit.

Figure 4.6 : Phase Locked Loop Frequency Multiplier Circuit Diagrams.

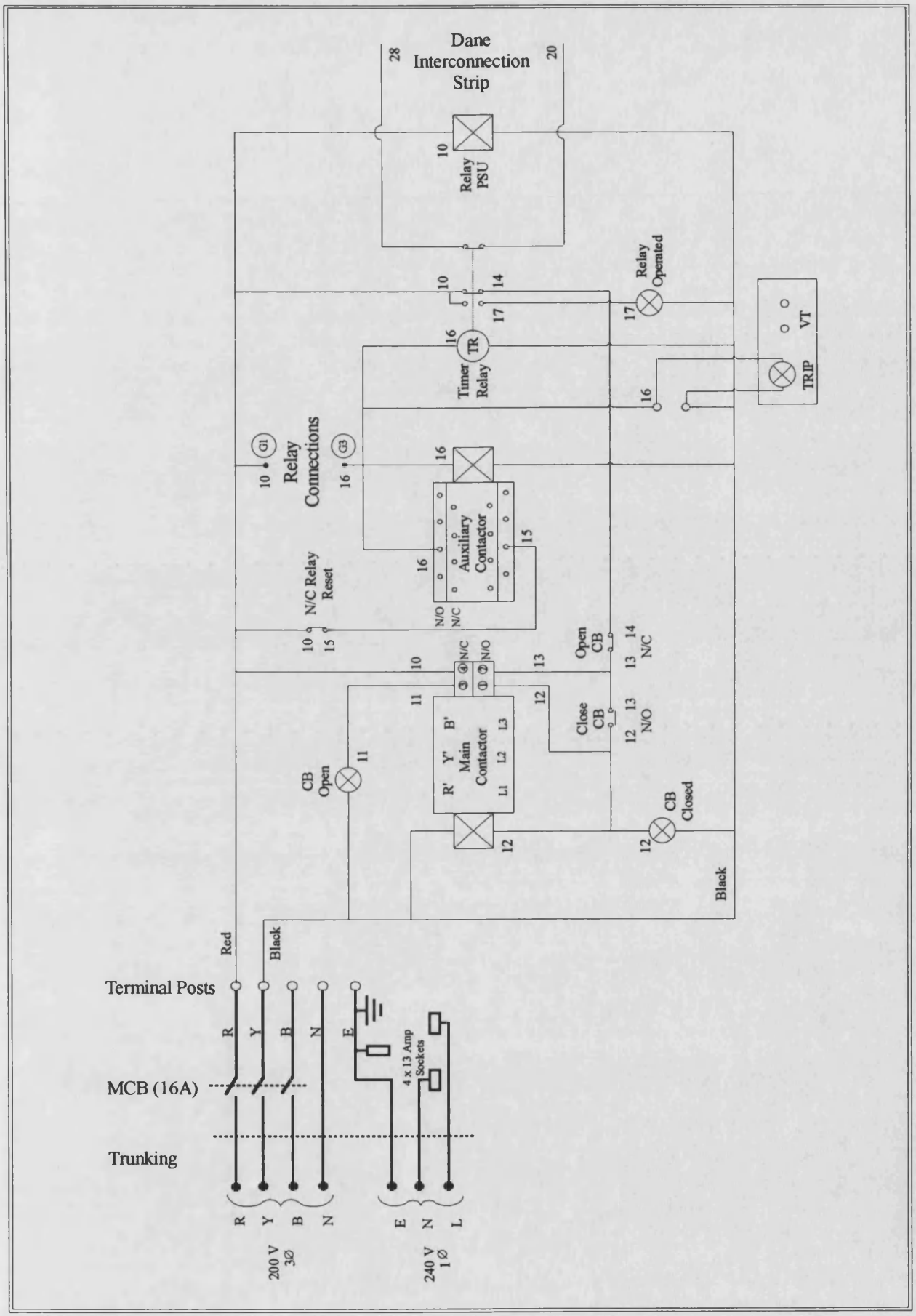

Figure 4.7 : Laboratory Research Bench Trip Circuitry.

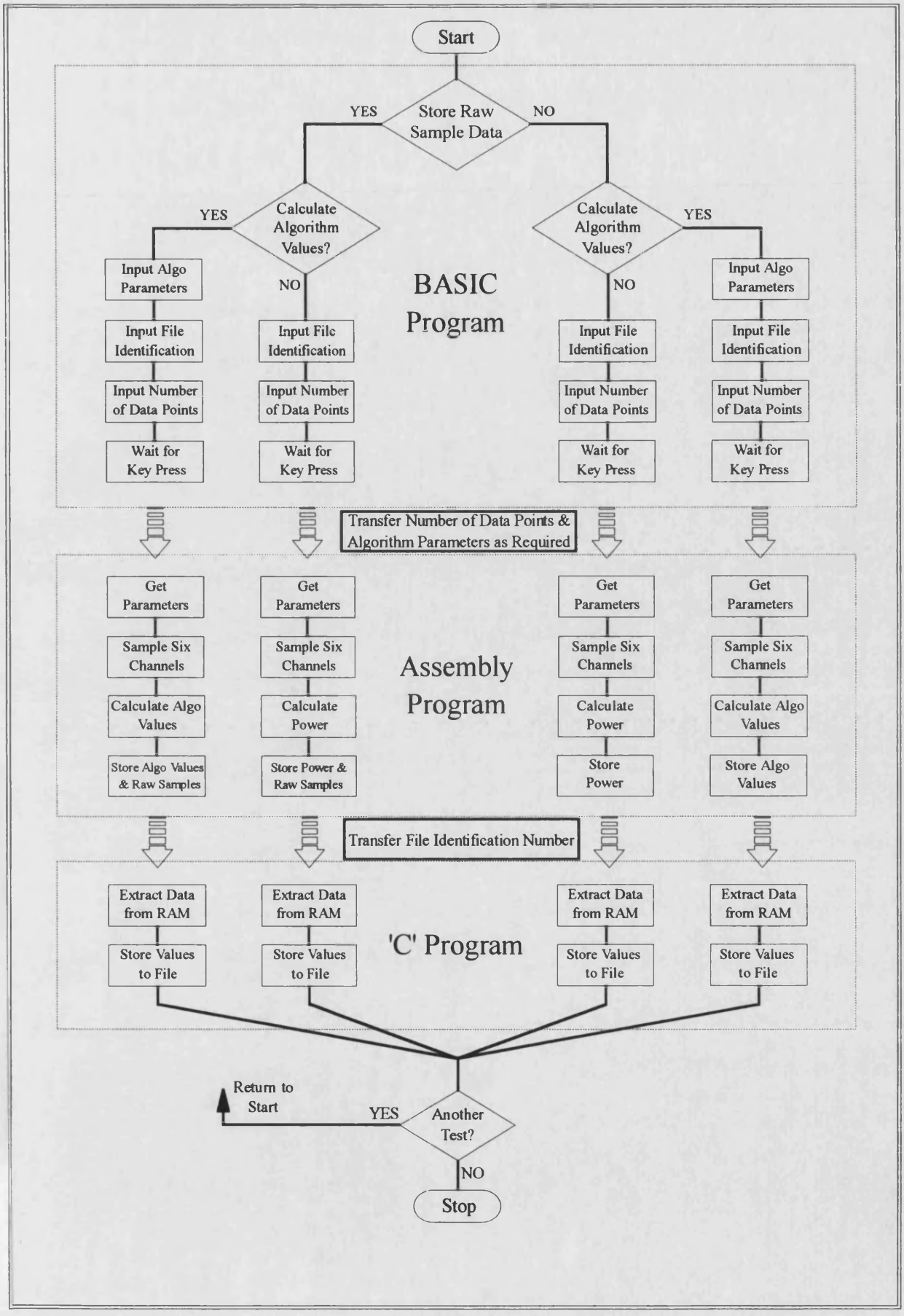

Figure 4.8 : Flow Chart for the Personal Computer Based Software.

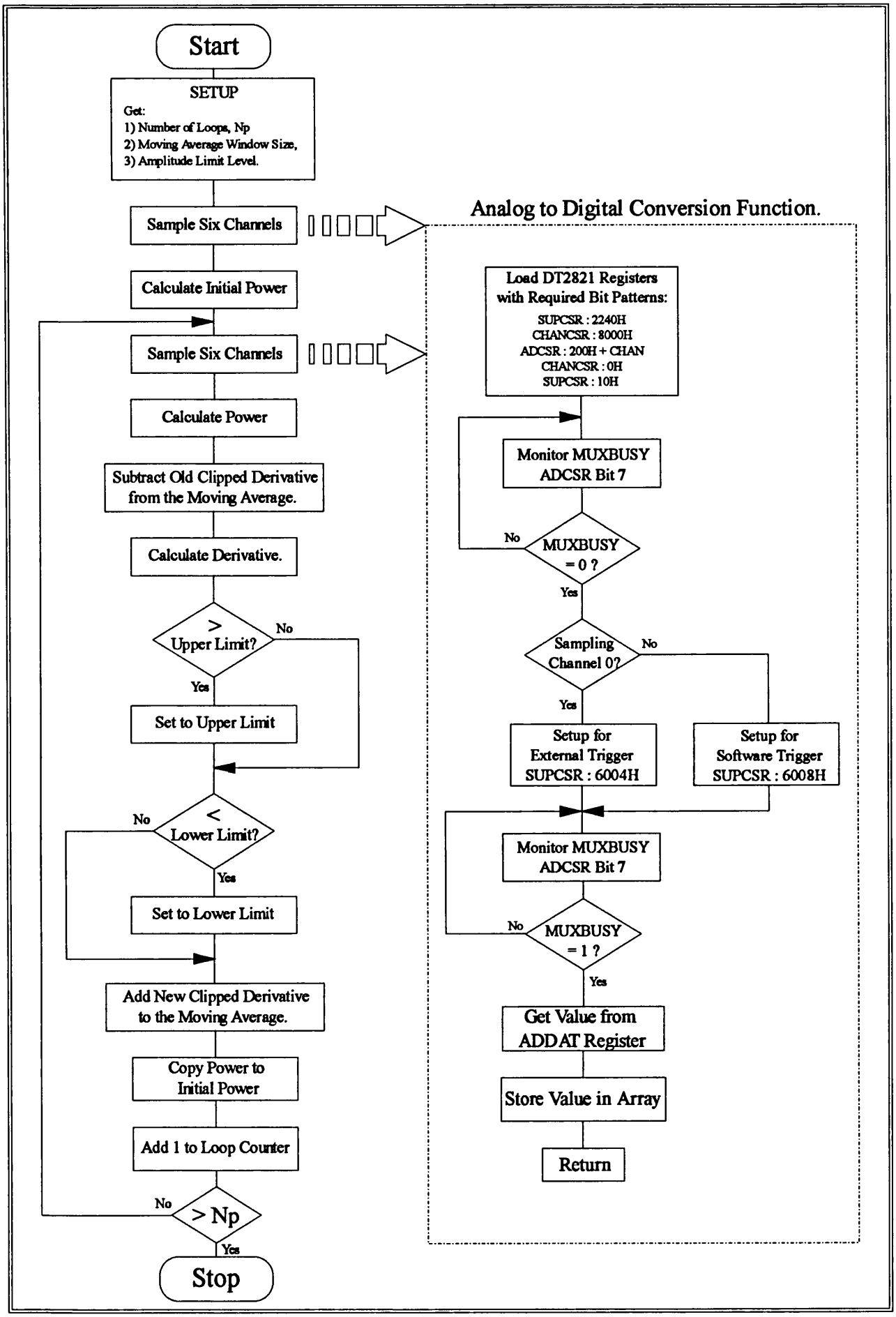

Figure 4.9 : Flow Chart of Assembly Coded Modules for the Personal Computer Based Research Facility.

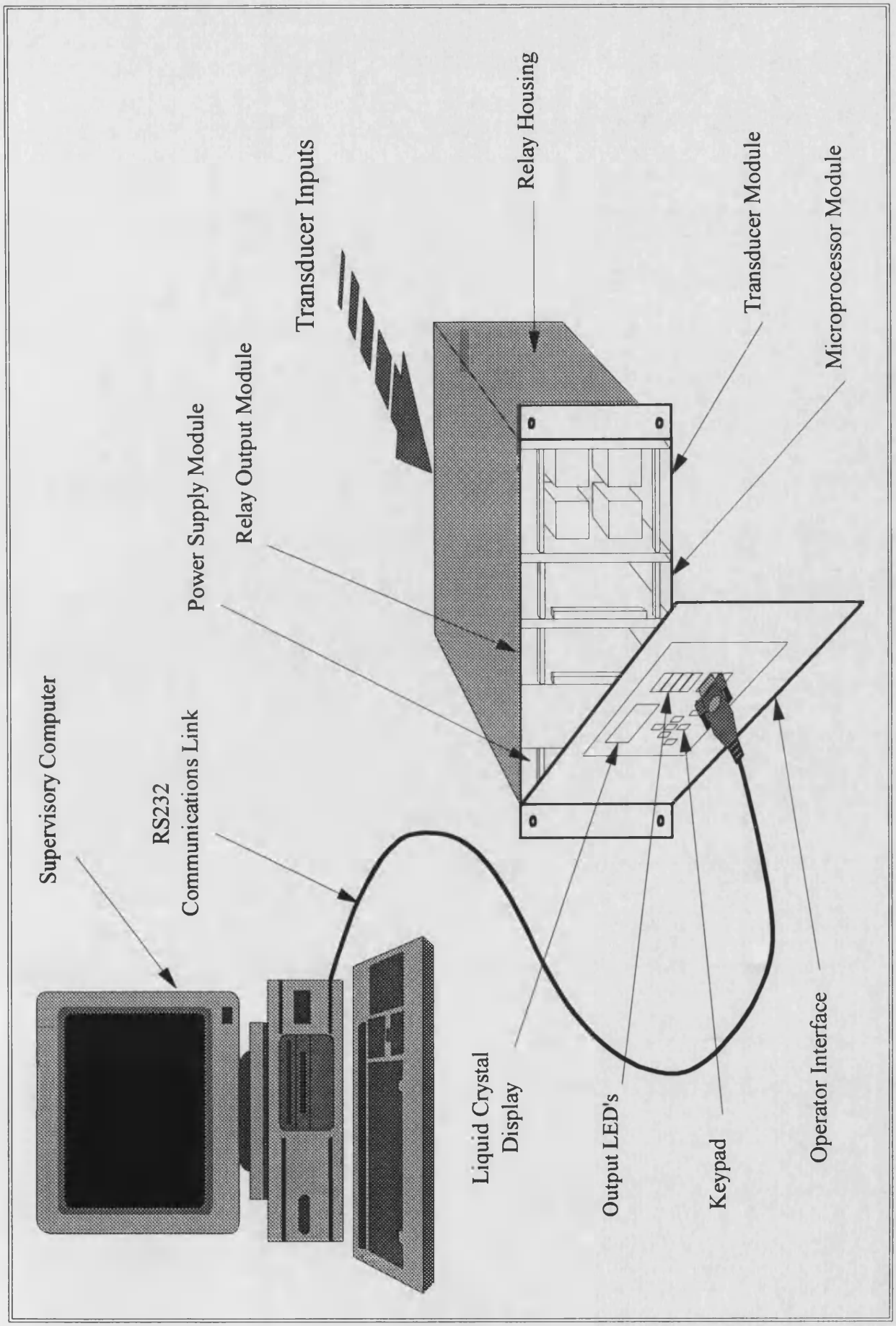

Figure 4.10 : The Microprocessor Relay Research System Hardware.

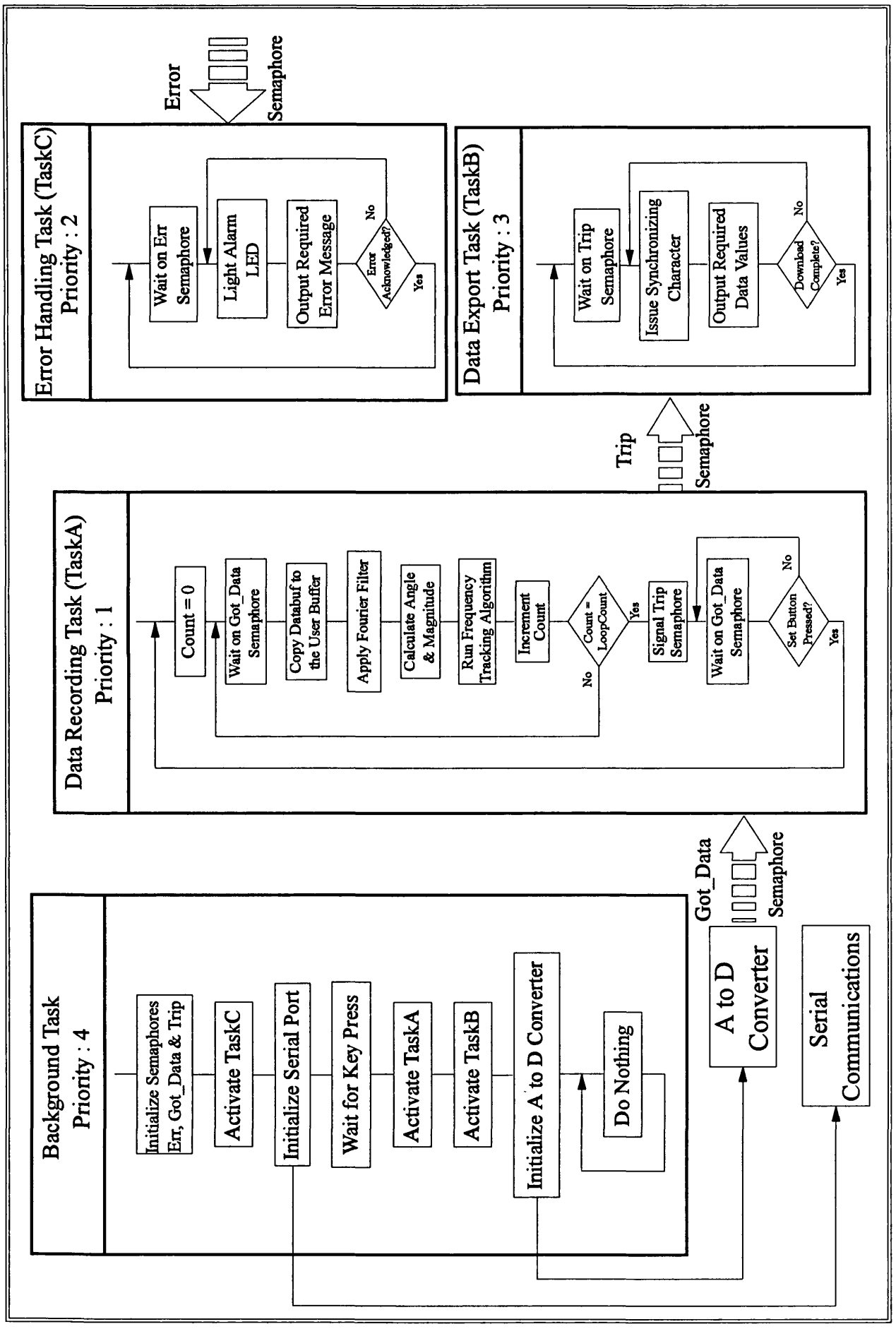

Figure 4.11 : Data Recording Software for the M.P.R. Multi-Tasking Environment.

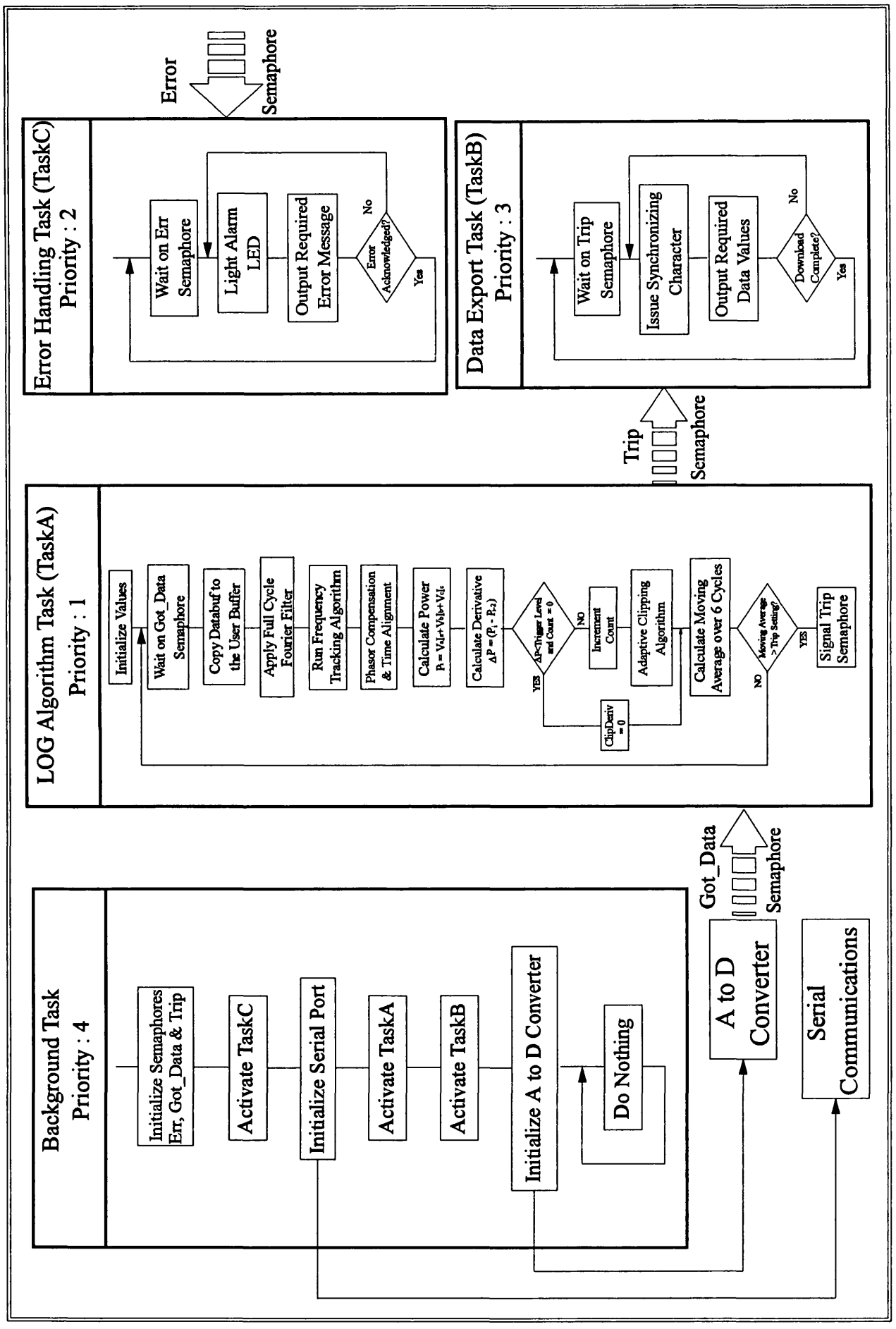

Figure 4.12 : Full Algorithm Implementation in the M.P.R. Multi-Tasking Environment.

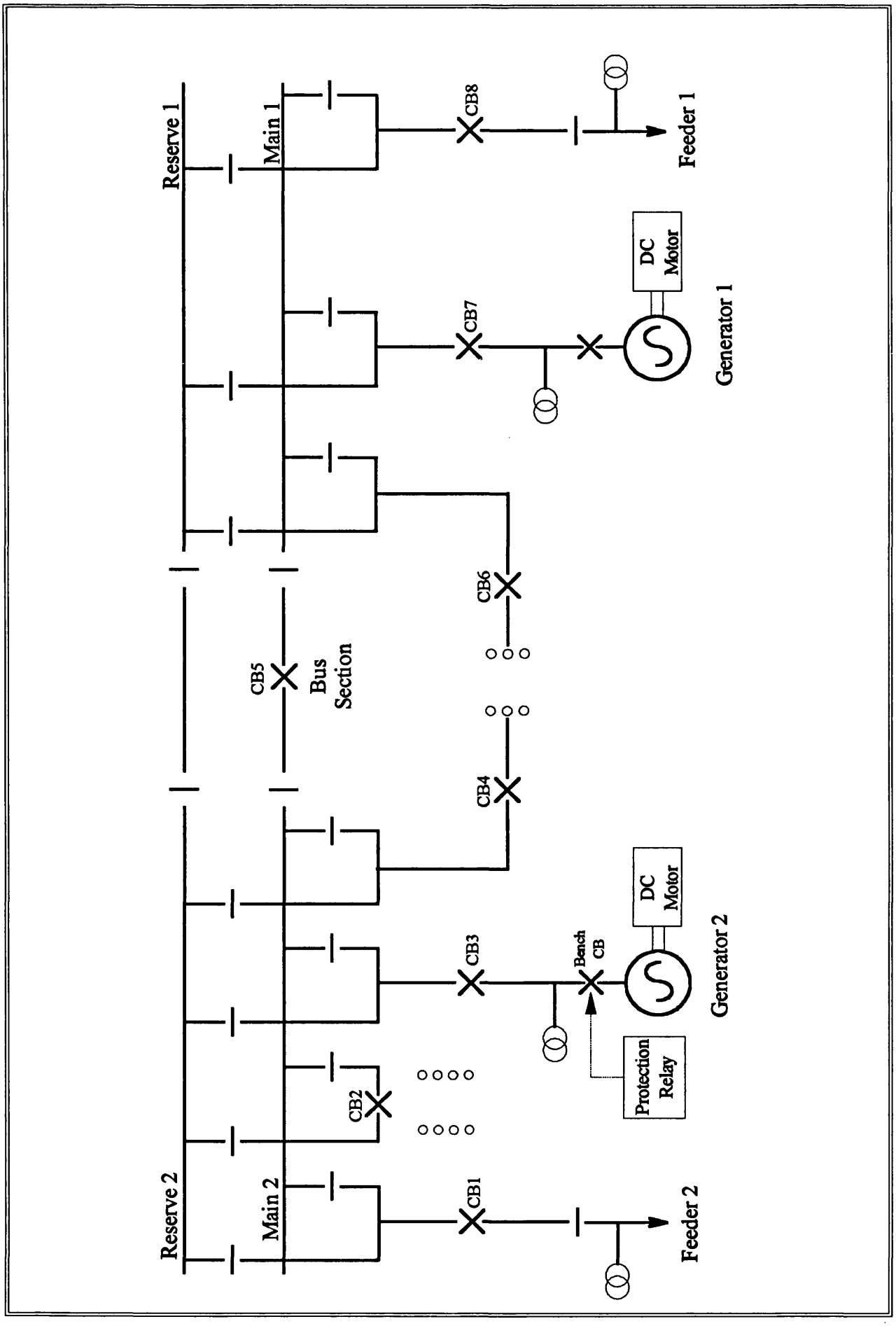

Figure 4.13 : Schematic Diagram of the Laboratory Model Power System.

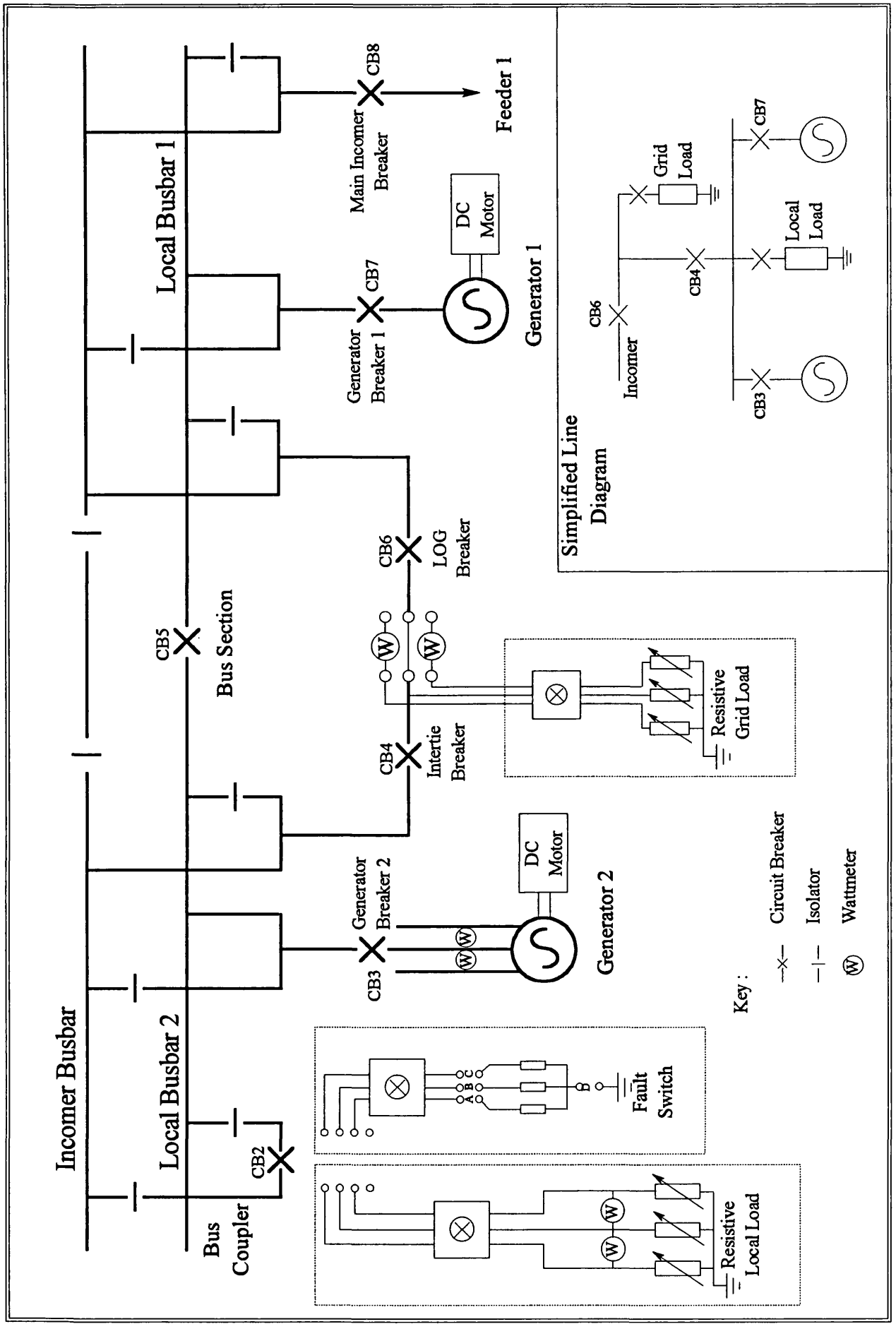

Figure 4.14 : Laboratory Test Setup Using the Model Power System.

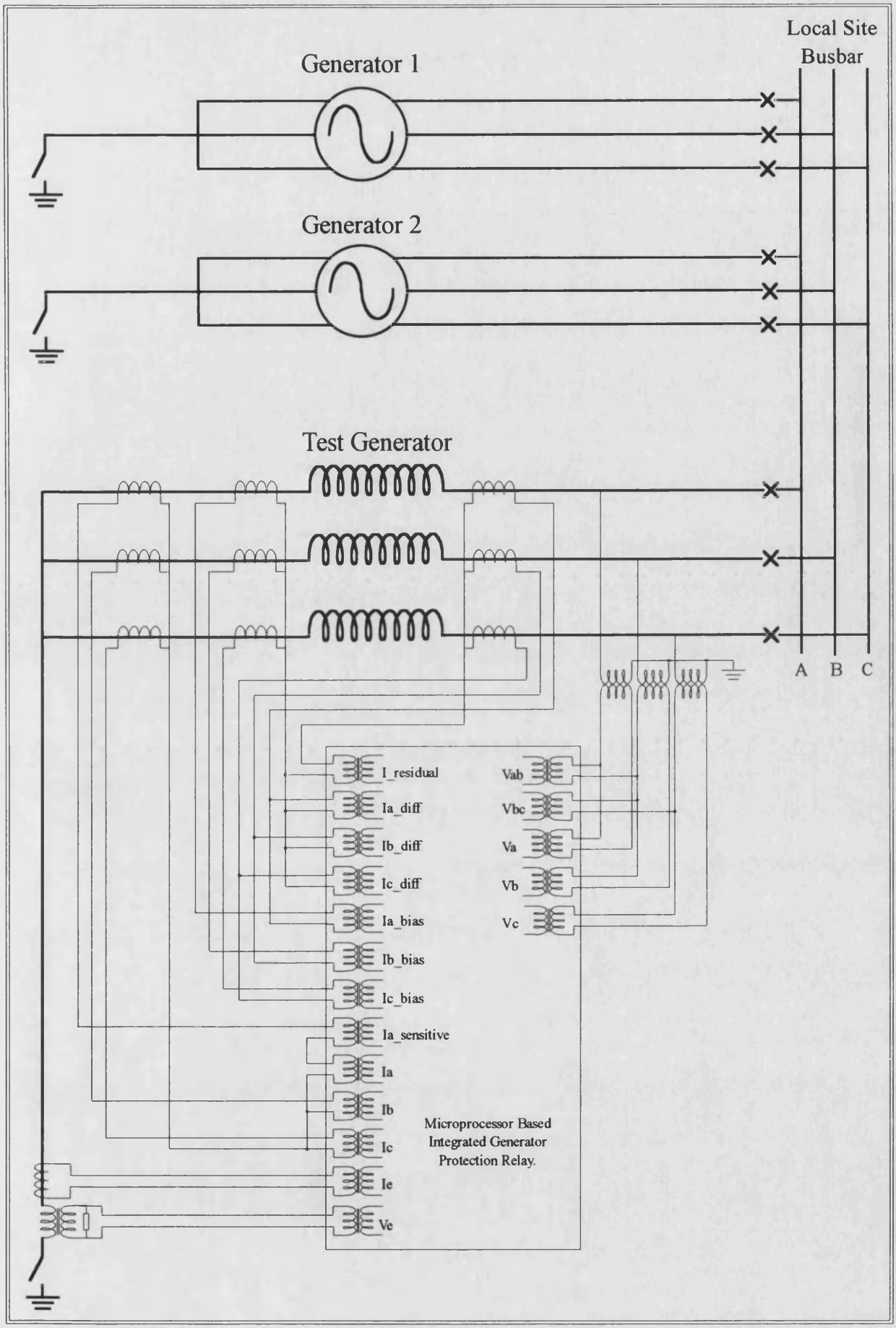

Figure 4.15 : Connection Diagram of M.P.R. System for Field Trials.

Chapter 5

Refinements to Theoretical Algorithm

This chapter presents results obtained from tests undertaken in the laboratory using the system described in chapter 4 as well as some of those taken from the preliminary field trials. The format of the chapter is based around the sequential order of events carried out during the testing process. The work is therefore presented in a progressive manner which shows the challenges encountered and the methods used to overcome them.

Before proceeding to the results a brief review of the basic algorithm implementation will be of benefit. The algorithm in its basic form consists of four distinct operations or calculations:

- **Calculation of the Instantaneous Power.** The phase voltages and currents are sampled at the same instant and the instantaneous power is calculated using:

$$P = v_a i_a + v_b i_b + v_c i_c \tag{5.1}$$

- **Calculation of the Rate of Change of Power.** Using the present instantaneous power value from equation 5.1 and the power value calculated at the previous sample instant, the rate of change of power is calculated using:

$$\Delta P_n = P_n - P_{n-1} \tag{5.2}$$

- **Amplitude Limiting the Rate of Change of Power.** For the reasons specified in chapter 3, the rate of change of power signal requires amplitude limiting. This is carried out by simply setting the output variable from this stage to the limit if the rate of change signal exceeds this limit in either the positive or negative sign. Otherwise the value is left unchanged.

$$\Delta P_{Limited} = \Delta P \Big]_{-Limit}^{Limit} \tag{5.3}$$

- **Moving Average to Produce Trip Calculation.** The final stage of the algorithm is to calculate the moving average of the signal from equation 5.3 over a pre-determined window size. This is implemented using:

$$MovAvg = \sum_{n=1}^{WinSize} \Delta P_{Limited} \tag{5.4}$$

The trip decision then simply compares the modulus of the final value of the moving average term with the trip level and a trip occurs if it exceeds this level. Trip if:

$$| MovAvg | > TripLevel \tag{5.5}$$

5.1 The Theoretical Algorithm.

Before the results obtained from the laboratory system and field trials are addressed, some simulation results are presented for comparison purposes. These show the basic theoretical operation of the algorithm before any refinements are applied, along with comparison studies with some of the other passive forms of loss of grid detection techniques.

5.1.1 Loss of Grid Studies.

Case Study 1: The first set of results shown in figure 5.1 from the simulation tests show how the system reacts to a loss of grid which causes an increase in generator loading of 65% of its rating. In this case, the generator is supplying some of the utility system load following the opening of the 'loss of grid' circuit breaker in the system. The loss of grid therefore causes a step increase in the generator's loading and the terminal current (5.1a) and output power (5.1e) rapidly increase to supply the islanded load, then decrease to a steady state value (Note that the effects of a speed governor or A.V.R. have not been included in the simulation studies). This sudden current increase causes the system voltage to decrease (5.1b) and with an under voltage element set to 6% (5970 volts), a trip will occur 8 milliseconds following the event. This trip time does not allow for any time delay included in the under voltage element or any data acquisition delays.

The prime mover governor cannot respond immediately so the input power remains constant and the increase in loading causes the machine to slow down releasing some of its inertia power to supply the load increase. This slowing of the machine can be observed in figure 5.1c which shows the islanded system frequency which is determined by the embedded generator alone once connection to the grid is lost. The under frequency element set to 1% of nominal will trip on 49.5 Hz after 36 milliseconds.

The fourth plot (5.1d) shows how the rate of change of frequency (R.O.C.O.F.) responds to the loss of grid. This relay element would be set to around 0.3 Hz/sec and would therefore see the loss of grid almost instantaneously. This study does not take into account the data acquisition or the calculation method required by the R.O.C.O.F. The frequency for these studies is determined directly from the machine speed.

To determine how the proposed change of power algorithm would react to this loss of grid, the instantaneous power must first be calculated using equation 5.1. The instantaneous power waveform shown in figure 5.1e shows how the output power of the machine reacts under the loss of grid and the sharp increase in output power due to the energy stored in the machine windings (sub-transient response as mentioned earlier) can be clearly seen. The subsequent decay of the output power occurs at a rate determined by the machine's inertia constant.

The derivative (or rate of change) of the power signal is shown in figure 5.1f. This signal then requires amplitude limiting for the reasons mentioned in section 3.2.2 and the resulting clipped signal is shown in figure 5.1g. The final stage of the algorithm, the moving average filter, leads to the algorithm output shown in figure 5.1h and the trip level is included to show that a trip occurs after 28 milliseconds. A comparison of the various trip times can be seen in table 5.1.

Case Study 2: As well as looking at the loss of grid occurrence which results in an overloading of the embedded generator, the response of the system to a load decrease as a result of a loss of grid needs to be addressed. The system response to a 50% decrease in loading as a result of a loss of grid is shown in figure 5.2. In this event the generator loading suddenly drops resulting in a decrease in the generator's output current (5.2a) and

instantaneous power (5.2e) with a subsequent increase in the terminal voltage and armature speed (or local system frequency). Figure 5.2b shows the voltage increase as seen by the under/over voltage relay element and a trip occurs at 6732 volts (i.e. +6%) after 7 milliseconds. The over frequency element (5.2c) trips at 50.5 Hz after 42 milliseconds and the R.O.C.O.F. (5.2d) again detects the loss almost immediately.

The response of the rate of change of power algorithm can be seen in figures 5.2e-h. Each stage of the algorithm is shown and a trip occurs after 23 milliseconds (5.2h). The algorithm therefore detects both load increases and decreases following a loss of grid.

Case Study 3: A loss of grid which results in only a small change in the generator's loading is of greatest interest. Should the power flow be low through the circuit breaker which opens to cause the loss of grid, then the change in generator loading may be very small. Consider the case where the loss of grid results in only a 2% increase in the loading of the generator as shown in figure 5.3. The resulting isolated system voltage again becomes depressed as the output current rises, but for this case, the voltage does not decrease below the under voltage relay setting of 5970 volts during the one second test period. This means that the under voltage element will not detect this loss of grid before the governor and A.V.R. respond to restore the system to within the prescribed limits. The same applies to the under frequency element (5.3c) which also fails to detect the loss of grid in sufficient time.

The R.O.C.O.F. relay however, if set to 0.3 Hz/sec should detect the event in a short time period as shown by figure 5.3d. The output of each stage of the rate of change of power algorithm can be seen in figure 5.3e-h. and under these conditions a trip occurs after 77 milliseconds. (See Table 5.1)

The effectiveness of the under/over voltage and under/over frequency relay elements for detecting a loss of grid resulting in only a small change of loading can be seen to be suspect. The R.O.C.O.F. and the new change of power algorithm can both detect and clear the situation in a short period of time, but for the reasons highlighted in section 3.1.2 the new power based algorithm has some benefits over the R.O.C.O.F.

5.1.2 Load Change Under Independent Operation.

Case Study 4: As previously discussed in section 3.2, the operation of the algorithm is unchanged under conditions when the generator operates independently from the utility grid. This situation is beneficial should a loss of grid occur undetected. Any subsequent change in the islanded load would lead to the algorithm detecting the lack of grid connection and removing the local site from the remaining islanded utility load allowing grid reconnection. The characteristics of the generator operating independently from the grid are the same as for the case when a loss of grid occurs since the generator characteristics determine the response in both cases. Therefore the algorithm simply detects the same characteristic output power waveform. The occurrence of a 2% local load increase with the generator operating independently can be seen in figure 5.4. The reaction of the algorithm can be seen to be almost identical to that for the similar loss of grid (figure 5.3) and an algorithm trip occurs after 64 milliseconds.

5.1.3 Load Change Under Parallel Operation.

Case Study 5: It is important in these studies to determine the response of the generator to local load changes which occur whilst operating in parallel with the grid since the protection algorithm should remain stable under these conditions.

The response of the embedded generator to a load increase equivalent to its rating is shown in figure 5.5. The simulated load increase causes a current rise (5.5a) and a corresponding voltage and frequency fall (5.5b & c), but these are insufficient to cause mal-operation of the under/over voltage and under/over frequency relays over the time frame analysed. The R.O.C.O.F. waveform (5.5d) however, falls below the trip setting of 0.3 Hertz leading to a possible mal-operation due to this normal operating condition.

The reaction of the theoretical power based algorithm to this parallel load change is shown by figures 5.5e - h. The power signal (5.5e) oscillates leading to oscillations in the derivative waveform which in turn causes the amplitude to be limited equally in both the positive and negative sign. The resulting algorithm output (5.5h) shows the stability of the new algorithm under parallel operation load changes for the simulated system.

5.1.4 System Fault Study.

Case Study 6: The occurrence of an unbalanced fault either on the local busbar or somewhere in the connected system should not cause mal-operation from the loss of grid protection function. In the case of the power based loss of grid algorithm, its response to a single phase to ground fault can be observed in figure 5.6. The high levels of unbalance due to this type of fault lead to a double system frequency (100 Hertz) term in the instantaneous power waveform (5.6a) for the duration of the fault. This unbalance term also appears in the derivative waveform and subsequently in the amplitude limited derivative waveform. However, the amplitude limiting function was included such that under extreme unbalanced conditions, its moving average over six cycles sums to zero. This effect can be seen in the algorithm output (5.6d) where the output becomes zero after twice the length of the moving average window. This example demonstrates the algorithm's stability under unbalanced faults which allows the dedicated protection functions to detect and clear the single phase fault in the required manner.

5.1.5 Conclusions.

A few of the results obtained from the simulation system have been presented to show the response of the simulated generator and the theoretical algorithm to a number of system disturbances including loss of grid. The operation of the algorithm for all the tests shown has been as desired with adequate trip times demonstrated for the loss of grid. The limitations of some of the current passive techniques have also been highlighted.

Case Study	U/O Voltage	U/O Frequency	R.O.C.O.F	Change of Power
1	8 msecs	36 msecs	Instantaneous	28 msecs
2	7 msecs	42 msecs	Instantaneous	23 msecs
3	No Trip	No Trip	1 msec	77 msecs

Table 5.1 : Comparison of trip times for simulation case studies 1 to 3.

5.2 Laboratory Tests.

The next stage in the algorithm development required a comprehensive set of experimental laboratory data to be accumulated from the test system. This is used to show the response of the algorithm to a number of system conditions. The provisional tests undertaken and used in this section are:

- Steady State Parallel Operation } To demonstrate the stability of the
- Steady State Independent Operation } algorithm under steady state conditions.

- Loss of Grid } To demonstrate the operation of the
- Independent Operation Load Change } algorithm in the required manner.

- Parallel Operation Load Change } To demonstrate the immunity of the
- System Fault Conditions } algorithm to these conditions.

A few examples from each of these tests are used in this section to show the need for the relevant algorithm refinements.

5.2.1 Steady State Parallel Operation.

Case Study 7: The first tests undertaken in the laboratory were with the generator operating in parallel with the laboratory supply under steady state conditions. These tests allow the resulting output power signal from the generator to be observed and the steady state stability of the algorithm proved.

The first set of results shown in figure 5.7 show the distorted waveforms that are obtained from the laboratory generator at low output power levels. These results are for nominal excitation at an output power of around 400 watts (i.e. 10% of rated). The distortion is highest in the current waveform (5.7c) and this leads to a distorted power waveform as shown in figure 5.7e. The theoretical instantaneous power should be a smooth straight line (i.e. a d.c. level) for a balanced situation as shown in appendix B. An harmonic analysis of these waveforms can be seen in figures 5.7b,d and f and these reveal the presence of

3^{rd}, 5^{th} and 7^{th} harmonics in the current and voltage waveforms. The power waveform has harmonics at 50Hz, 200Hz and 300Hz in addition to the double frequency term (i.e. 100Hz) which is due to unbalance in the connected system.

Case Study 8: At a higher output power level the harmonic content of the waveforms reduces. The resulting waveforms for a test carried out at rated power (i.e. 5 KVA at 0.8 power factor) can be seen in figure 5.8. The shape of the distortions to the power waveform (5.8e) is different to that for the previous low power test (5.7e) due to the lower levels of harmonic content of the waveform. These results indicate the presence of harmonics and unbalance on the laboratory system which are particularly prevalent at low excitation and low output power levels.

Under steady state conditions the algorithm output should be around zero due to there being no noticeable change in the power measured. By applying the four stages of the algorithm to the output power obtained under steady state operation at nominal output power, the stability of the algorithm can be determined. The resulting waveforms after each stage of the process for an algorithm setting of 10% can be seen in figure 5.9.

The first thing to notice is that the output of the six cycle moving average window (i.e. the algorithm output figure 5.9d) is not zero. This indicates that the algorithm is not totally stable under normal conditions which is of fundamental importance. The trip setting is unity on the scales shown and therefore the algorithm cannot be assumed to be stable as the output approaches unity even under steady state conditions. The presence of the harmonics and unbalance in the system changes the response of the algorithm from that for the simulated system and under steady state conditions, the combination of third harmonic noise and unbalance results in an amplitude limited derivative signal (5.9c) which has a non-zero average value over the six cycle moving average window (5.9d).

To overcome the problems introduced by the unbalance and harmonics, a number of filtering processes were considered. Two types of filter are discussed in this section, each of which has properties which improves the algorithm's operation. The effect of both of these filters is shown for a number of different tests and the final decision on which filter to use is left until the end of the section.

The removal of the harmonics alone can be achieved by applying a full cycle fourier filter to the measured sinewaves. A full analysis of the full cycle fourier filter can be seen in appendix D.1. With the harmonic content removed, the double frequency term present in the power waveform under unbalanced conditions and due to unbalanced faults is filtered out by the algorithm resulting in inherent stability. This is shown by figure 5.10 where a full cycle fourier filter is applied to the input sinusoidal quantities to remove the harmonics which then produces the power waveform shown in figure 5.10a. The unbalance is also present in the derivative term (5.10b), but the amplitude limiting function (5.10c) produces a waveform which has zero average output over the six cycle moving average filter period resulting in a zero output from the algorithm as shown in figure (5.10d). This result indicates the adverse effect of harmonics on the stability of the algorithm which was not detected during the theoretical simulation study.

An alternative method for reducing the effects of both the harmonics and the unbalance is to use a half cycle moving average filter applied to the power waveform. This simply involves taking the moving average of the power waveform over a window size which is half the number of samples taken per 50Hz cycle. The characteristics of this filter can be seen in appendix D.2. This filter is more easily implemented than the full cycle fourier filter and was therefore chosen in the early stages of the algorithm's development to improve the stability of the algorithm under normal conditions. The result of using the half cycle moving average filter can be seen in figure 5.11 which shows the individual stages of the algorithm with this filter included. Stability under steady state conditions can therefore be obtained using the half cycle moving average filter, instead of the fourier filter. However, as figure 5.11d shows, the algorithm output is still non-zero for steady state conditions (algorithm trip level is ± 1 on the scales shown). The discussion on filter choice continues with further case studies and test results in the following sections.

5.2.2 Steady State Independent Operation.

Case Study 9: The source of the harmonics can be investigated by operating the generator independently from the supply with only local load attached. The output power waveform for the generator running with only independent resistive load and no parallel connection into the mains system can be seen in figure 5.12. The power level was set to

around 3000 Watts with the voltage and frequency maintained at 200 volts and 50 hertz respectively. The results show the lower distortion levels that occur when operating independently of the grid and this is confirmed by the harmonic analysis which shows reduced levels of harmonics compared to those for parallel operation. Obviously the amount of unbalance present depends upon the local load connected to the generator. This result shows that most of the harmonic effects occur due to the system to which the generator is connected and this cannot be predicted with any degree of certainty.

5.2.3 Loss of Grid.

Case Study 10: The basic operation of the algorithm and the waveforms produced can be shown using the practical system. The instantaneous power waveform obtained from a practical loss of grid test which results in a 65% increase in the generator's loading after the loss can be seen in figure 5.13a. The waveform shows the characteristic shape that can be attributed to the occurrence of a loss of grid. This should be compared with the theoretical results obtained using the simulation program which were discussed in section 5.1 and are shown in figures 5.1 to 5.4.

The main difference between this result and that from the simulation arises from the presence of harmonics and unbalance whose effects were not included in the simulation studies. The effects of these factors will be discussed shortly. The application of the half-cycle moving average filter (5.13b) reduces the level of these distortions and brings the resulting power waveform closer to that obtained by the simulation and this filtered signal is used in the algorithm calculation.

The need for the amplitude limitation of the derivative signal is shown by the results in figure 5.13c and 5.13d. Without the limitation of the derivative signal the algorithm output (5.13d) would produce a trip in only a few milliseconds which may lead to algorithm stability problems and doesn't take into account the relative inertias of the machine and system. By limiting the derivative signal spike, the effect of the sub-transient response is greatly reduced and the post-spike portion of the derivative waveform, which is related to machine inertia, provides the basis for the algorithm's operation. The trip time is increased as a result to around 51 milliseconds. The amplitude limited derivative signal

and the resulting algorithm output after the six cycle moving average window can be seen in figures 5.13e and 5.13f respectively.

Case Study 11: The loss of grid resulting in a 65% increase in generator loading provides a large power change which the algorithm has no difficulties in detecting in its current form. By using the half-cycle moving average filter on the power waveform, the similarity between the practical results and the simulation test results is demonstrated. However, the effectiveness of the algorithm in detecting a smaller change of around 10% increase in load is of greater interest particularly with respect to the effect of the two filters on the algorithm.

From the steady state results (section 5.2.1), the problems associated with the unbalance and harmonics would appear to be best solved simply by the use of the full-cycle fourier filter on the input sinusoidal quantities. However, the effect of this type of filter on the algorithm for a loss of grid resulting in a small load change must be addressed.

Consider the case of a loss of grid which results in a 10% increase in generator loading shown in figure 5.14. With no filtering present, the combination of the harmonics and unbalance mean that the loss of grid event is almost indistinguishable in the derivative waveform (5.14b). The amplitude limiting function (5.14c) results in an algorithm output (5.14d) which is actually zero when the loss of grid occurs.

By applying the full cycle fourier filter to the input waveforms, the harmonics in the power waveform (5.15a) are removed. However, the improvements in the derivative (5.15b) and final algorithm output (5.15d) waveforms are small. This also results in the loss of grid event passing undetected by the algorithm (trip level = ± 1).

If the half cycle moving average filter is applied to the power signal then the result is quite different as shown by figure 5.16. The derivative signal shows the occurrence of the loss of grid with a large positive spike and the algorithm output produces a trip decision after 110 milliseconds (5.16d).

With reference to the amplitude limited derivative waveform (5.16c), the positive spike is clipped which results in only a small deviation in the algorithm output (ie the effect of the sub-transient response is reduced). The negative portion of the derivative, following the spike, is the portion on which the operation of the algorithm is based. Both figures 5.15c and 5.16c show that the presence of the double frequency term in the derivative waveform reduces the duration for which the signal is actually set to the negative clip level. This in turn reduces the deviation in the algorithm output and in the case of figure 5.15 where the fourier filter is used, the deviation is insufficient to cause trip. This indicates that the unbalance present in the system has a detrimental effect on the algorithm's ability to detect a loss of grid.

Despite removing the harmonic content very successfully the fourier filter does not improve the algorithm's operation under loss of grid. In contrast, the moving average filter does improve algorithm operation, but the presence of unbalance during the loss of grid is still detrimental to the algorithm.

5.2.4 Local System Fault.

The fault tests were carried out with the grid connected and present for the duration of the fault (i.e. the laboratory protection is disabled). Each fault type was tested in the laboratory with the generator star point either connected directly to the system neutral or left open circuit. Of particular interest in the current analysis is the unbalanced fault condition. During this type of fault the loss of grid protection algorithm should remain stable to allow the fault to be cleared by the dedicated protection scheme.

Case Study 12: Application of an A-phase-to-ground fault to the system results in the waveform shown in figure 5.17a. It has already been shown in section 5.2.1 that false tripping is liable to occur unless the level of harmonics in the power waveform is reduced. The effect of these harmonics on the algorithm can also be observed in figure 5.17 where the unfiltered instantaneous power waveform is used in the algorithm resulting in a non-zero algorithm output even before the fault has been applied.

In section 5.1, where the effects of the simulation results on the algorithm were discussed,

the power waveform had no unbalance or harmonics present and therefore no pre-filtering was required. The simulation results for the fault tests show immunity to tripping for single-phase-to-ground, phase-to-phase and double-phase-to-ground faults due to the high level of unbalance which is present in the power signal during these faults and the algorithm's inherent stability under extreme levels of unbalance.

The application of the half-cycle moving average filter to the power waveform for the practical tests reduces the high levels of unbalance and nearly causes a false trip to occur for this unbalanced fault. The effect of the half-cycle moving average filter can be seen in figure 5.18a which shows the removal of the 100Hz unbalance component. The resulting deviation of the algorithm output close to the trip level is still in agreement with the simulated results if the half-cycle moving average filter is applied to them.

As a result of removing the unbalance term with the half-cycle moving average filter, the algorithm's inherent stability to unbalanced faults is reduced. This result can be further reinforced by applying the full-cycle fourier filter to the sinusoidal inputs and calculating the instantaneous power using these signals. The resulting power waveform still contains the 100Hz term due to unbalance (5.19a), but the harmonics are removed. In this situation the stability of the algorithm to the same unbalanced fault is total with only the fault-on and fault-off points being noticeable in the algorithm output (5.19d).

5.2.5 Load Change Under Independent Operation.

Case Study 13: The rate of change of power output from the isolated generator under load change conditions is dictated by the inertia constant of the generator (i.e. without the inertia of the grid). The response of the generator for load changes therefore results in very similar power fluctuations to those for a loss of grid as previously mentioned. To prevent repeating results already discussed, the independent load change waveforms have not been included in this section. The effect of the various filters was examined for this situation and the performance of the algorithm in detecting the load change assessed, but for the purposes of filter choice the results offer no further information to that from the loss of grid results.

5.2.6 Load Change Under Parallel Operation.

Case Study 14: The algorithm must remain stable under all normal operating conditions which includes changes in local load whilst the generator is operating in parallel with the grid supply. Under these conditions the basic theoretical algorithm responds as shown by figure 5.20. This set of plots shows the response of the algorithm to a 100% load increase when the unfiltered instantaneous power is used as the input to the algorithm. Under these conditions, the algorithm remains stable during the load change, however some 200 milliseconds after the load change the algorithm output deviates from zero due to the harmonic and unbalance effects previously discussed.

Applying the fourier filter to the power waveform results in no change to the stability of the algorithm as shown in figure 5.21, but this stability is solely due to the presence of unbalance in the waveform, disguising the load change.

Reducing the unbalance and harmonics using the half-cycle moving average filter as shown in figure 5.22 causes the algorithm output to deviate from zero due to the load change. For the algorithm at this setting a false trip does not occur, but the output does come close to the trip level of ±1.

5.2.7 Effect of the Filters on the Algorithm.

The previous sections have shown the need for filtering of either the power waveform or its constituent sinewaves to obtain stable steady state operation of the algorithm. The problems for the algorithm in its original theoretical form can be summarized as follows:

- If the power signal is left unfiltered, the harmonics and unbalance combine to produce possible false tripping under steady state conditions. This is due to the non-zero average value of the amplitude limited signal. The algorithm also fails to detect a loss of grid due to these distortions. However, the natural immunity of the algorithm to unbalanced faults is preserved due to the presence of very high levels of the double frequency unbalance term in the power waveform.

- Using a half cycle moving average filter to suppress the harmonics and unbalance results in good steady state stability and loss of grid detection. However, the immunity to unbalanced faults is reduced as is the immunity to parallel load changes.

- If a full cycle fourier filter is used to remove the harmonics leaving the unbalance term unaffected, the immunity to unbalanced faults returns. However, the effect of only removing the higher order harmonics is to reduce the sensitivity of the algorithm to the loss of grid since the sharp derivative characteristics are removed. A failure to operate for a loss of grid occurs due to the unbalance in the system.

5.2.8 Proposed Methods to Improve the Theoretical Algorithm.

Two possible methods for overcoming these problems have been developed.

1) By using the intermediate derivative signal to determine, by a simple form of pattern recognition, whether the shape of the waveform corresponds to a fault condition, a loss of grid or a parallel load change. The result can be used to provide a permissive inter-trip with the algorithm output.

2) Using a similar pattern recognition technique to control the amplitude limiting function on the derivative signal.

Since both of the above methods are able to detect the occurrence of an unbalanced fault, the immunity of the algorithm to the fault-on and fault-off portions of the waveform is no longer required. This means that the unbalance term in the power waveform can be removed using the half cycle moving average filter to improve the sensitivity of the algorithm for a loss of grid despite the presence of unbalance. However, the fourier filter would also be beneficial to remove the unwanted harmonics.

Using both the fourier filter and the half-cycle filter results in a large group delay. To overcome this problem a new method for removing the unbalance has been developed. This method also reduces the required processing time to allow faster operation in a microprocessor based integrated generator protection package.

By simply reducing the processing rate of the power calculation to 4 times per cycle the sinusoidal double frequency term in the power signal is converted into a triangular wave of the same frequency. Calculating the derivative term using a quadratic approximation method, the result is zero providing there is no underlying change in the power. To simplify the derivative calculation, rather than using the quadratic approximation, the derivative is calculated using the difference between the current value and the previous but one value. This results in a derivative term which follows the underlying changes in the power despite the presence of the unbalance (ie the effect of the unbalance is completely removed).

Thus by using:

$$\Delta P_n = P_n - P_{n-2} \tag{5.6}$$

instead of:

$$\Delta P_n = P_n - P_{n-1} \tag{5.7}$$

with a processing rate for the power of four times a cycle, the unbalance term in the derivative is removed.

The sampling rate of the sinusoidal input signals is still maintained at twelve samples per cycle to allow for accurate calculation for the full cycle Fourier filter, but the power term used in the algorithm is only calculated four times per cycle. The effectiveness of this technique of removing the unbalance by reducing the processing rate can be seen in figures 5.23-5.26.

Figure 5.23 shows the same loss of grid results as shown earlier (i.e. 10% load increase), but with the reduced processing rate and fourier filter applied. The derivative term (5.23b) can be seen to be free from the unbalance which is present in the power waveform, however it does follow the underlying changes in the power waveform. This result should be compared to that obtained previously shown in figure 5.15.

The effect of the technique on the unbalanced fault condition can be seen in figure 5.24. Now that the unbalance term has been removed, the derivative signal shows up the

change in the level of unbalance from before the fault to during the fault. The immunity of the algorithm to this type of fault is therefore lost by the removal of the unbalance term associated with the fault. The outcome is a near trip decision from the algorithm (5.24d) for both the fault-on and fault-off periods.

For the parallel load change (figure 5.25), the effect of removing the unbalance term using the reduced sampling rate gives a similar result to that obtained when the unbalance was removed using the half-cycle moving average filter (figure 5.22). The algorithm output approaches the trip level but stability is just maintained for a 10% setting.

To counteract the effect of removing the double frequency term from the unbalanced fault and parallel load change results, the amplitude limiting function is changed from the simple clipping function to one which makes the decision to clip on the basis of previous conditions as mentioned at the beginning of this section.

To show the effect of the improvement to the amplitude limiting function, the trip setting is firstly reduced to a more sensitive level such that it produces a trip decision when a loss of grid results in a **2.5% change** in the generator's loading. The resulting algorithm response for the original basic clipping function is shown for comparison for each of the three possible events (ie loss of grid, unbalanced fault and parallel load change) in figures 5.26a, 5.27a and 5.28a respectively. The output power and derivative waveforms are not shown since they are unchanged from those used with the 10% setting earlier (figures 5.23 - 5.25). Only the last two stages (i.e. amplitude limiting and 6 cycle moving average filter) are shown to demonstrate the operation of the new adaptive clipping function.

With reference to the amplitude limited signal for the loss of grid condition (5.26a & b), the output from the algorithm can be seen to reach the trip level of one due to the first clipped derivative spike (point 'a'). This is due to a non-zero derivative signal before the loss of grid event causing the moving average term to deviate from zero.

For the unbalanced fault test (5.27a & b), a false trip occurs for the reduced trip setting as a result of the portion of the clipped derivative waveform indicated by the letter 'e', during the fault-on period.

For the parallel load change results (5.28a & b) the third portion of the clipped signal, shown by the letter 'c', gives rise to the algorithm's false trip. In the case of the loss of grid condition the trip decision should have already been made before a third change of clip sign can occur. The portion of the amplitude limited derivative signal on which the algorithm's operation is based is shown by the letter 'b' in figure 5.26a.

This theory provides the basis for the new pattern recognition based amplitude limiting function. The basic operation of which can be described as:

- If the present derivative sample value does not exceed the clip level then that sample value is set to zero,

- If the value does exceed the clip level then the sample value is set to the clip level,

- If the sign of the clipped derivative signal changes three times in succession, then after the third change has been detected, the next sample value is set to zero until the derivative signal value settles to below the clip level for 10 consecutive samples.

With the addition of a few extra routines to overcome possible deviations from the normal, this is the basic operation of the refined amplitude limiting function. It has been designed to enhance the operation of the algorithm without affecting the basic theory upon which the whole algorithm is based.

The result of this change to the amplitude limiting function for the same three sets of test results can be seen in figures 5.26c & d to 5.28c & d.

For the case of the loss of grid (figure 5.26), the addition of the adaptive clipping algorithm removes the trip on the positive deviation of the algorithm output since the clipped signal is set to zero when it is below the clip level. A clear trip occurs after 100 milliseconds and the effects of the distortions on the system are completely removed.

For the case of the unbalanced fault, the derivative signal changes from positive clip to negative clip in successive samples. It can be seen in figure 5.27c that after the third

change the clipped derivative output is written to zero (point f). This increases the stability of the algorithm in the presence of unbalanced faults.

With the parallel load change result shown in figures 5.28c & d, the third change in the sign of the derivative term is again detected (point d) and the false trip which occurred with the original clipping method (5.28a & b) is removed.

The pattern recognition based amplitude limiting function therefore improves the ability of the algorithm to detect a loss of grid or independent load change occurrence even in the presence of high levels of unbalance. It also improves the stability of the algorithm to unbalanced faults occurring on the system and for load changes which occur while the generator is connected in parallel with the utility supply. The technique does not change the basic operation of the algorithm which still relies upon the relative sizes of the inertia constants of the two interconnected systems.

5.2.9 Conclusions.

The problems of algorithm stability in the presence of noise and unbalance have been shown in this section. A method to overcome these problems has been introduced which has no great effect on the basic operation of the algorithm, but has numerous advantages.

These include:

- improved stability of the algorithm under all conditions of load unbalance and harmonic noise,
- greater sensitivity to loss of grid or independent load change,
- improved discrimination between unbalanced faults and loss of grid conditions,
- greater stability in the presence of large local load fluctuations whilst operating in parallel with the main source of supply.

The technique used requires little additional encoding in the present algorithm and the processing time required is actually reduced.

5.3 Field Trials.

In order to demonstrate the response of the algorithm to actual loss of grid phenomena on an embedded generator, field trials have been carried out using a diesel driven industrial generator. Details of the system configuration can be found in section 4.7. Some of the results from these tests have been included in this section to show the requirements for further refinements to the algorithm.

As for the laboratory test results, a number of different tests are included starting with simple steady state operation, moving onto loss of grid studies and finally load changes both with and without the utility grid connected. Unfortunately, due to the nature of the industrial site to which the generator is connected, it was not practical to carry out system fault studies. Once again the results in this section are presented in a progressive manner, with the need for refinements indicated and conclusions drawn at the end.

5.3.1 Steady State Parallel Operation.

Case Study 15: The first set of results taken from the field trials show the operation of the generator under normal steady state conditions whilst connected to the grid supply. The resulting instantaneous output power waveform for a generator output of 50kW (i.e. 10% of rating) calculated at 12 samples/cycle before any applied filtering is shown in figure 5.29a. It is clear from this waveform that there is a low frequency oscillation in the output power from the generator and the spectrum analysis (5.29b) shows that it oscillates at a frequency of 4 Hertz. The effect of this oscillation on the new loss of grid algorithm can be seen in figures 5.29c & d. The derivative of the filtered power waveform (5.29d) shows that this 4 Hertz oscillation propagates through to the pre-clipped derivative term and the amplitude of the oscillation means that a false trip may occur even under steady state conditions.

Case Study 16: A similar situation is found when the generator operates at a higher output power level as shown by figure 5.30, except that the amplitude of the oscillation as a percentage of the fundamental is lower and the frequency is 3.4 Hertz. Once again these low frequency oscillations in the output power result in similar oscillations in the

calculated derivative term within the algorithm and the outcome of this may again be poor steady state stability of the algorithm in its present form. Before discussing a technique to overcome this phenomenon an interesting observation will be addressed.

5.3.2 Steady State Independent Operation.

Case Study 17: In order to test the possible reasons for this oscillation, tests were undertaken with the generator operating in isolation from the utility supply. The instantaneous output power from the diesel generator whilst it operates independently with only a 50kW matched local load is shown in figure 5.31a. In this waveform and in the spectrum analysis shown in figure 5.31b, there is no sign of the 4 Hertz oscillation present for the same loading under parallel operation. This indicates that the presence of the utility connection either causes or allows this low frequency oscillation to occur. The subsequent effect of the oscillation on the derivative term in the algorithm is also removed for this steady state operation. The same situation is found for steady state independent operation tests carried out at higher output power levels.

5.3.3 Loss of Grid.

Case Study 18: A simple but highly effective method for overcoming the undesirable effects on the algorithm of these low frequency oscillations is to introduce a starter element technique which makes use of a characteristic of the derivative waveform which is present in the event of a loss of grid (and independent load change). This characteristic can be clearly seen in the next set of results. Figure 5.32a shows the response of the diesel generator to a loss of grid which results in an increase in its loading of 20%. As with all the previous loss of grid and independent load change results, the output power rapidly changes at the point of the load change due to the stored electrical energy of the machine being released. This change in turn produces a large spike in the derivative waveform calculated by the algorithm. The starter element technique simply states that if a pre-determined level is exceeded by the derivative waveform then operation of the algorithm should continue for a preset period of time, sufficient for a loss of grid event to be detected, after which the starter unit is reset. Under normal steady state conditions, the amplitude of the derivative term will not approach this level and this therefore

provides a method for screening the algorithm response from these low frequency oscillations.

An additional and very important outcome of using this technique is that during normal operating conditions the algorithm remains in a 'dormant' mode, with minimal processor overhead, awaiting this starter unit level to be triggered. This greatly reduces the processing requirements of the algorithm which is an important consideration for its implementation in a multi-function microprocessor relay.

The response of the further refined algorithm for the loss of grid resulting in a 20% load increase is shown in the remaining waveforms in figure 5.32. The derivative of power waveform shows the spike which triggers the starter element (set to 1,000,000 on the scales used) and the subsequent algorithm response is to trip after 130 milliseconds.

5.3.4 Load Change Under Independent Operation.

Case Study 19: A similar situation occurs with the independent operation load change results shown by figure 5.33. The starter element level is again exceeded and algorithm operation initiated which produces a trip decision after 120 milliseconds. However, under independent operation the starter unit is superfluous since there is no low frequency oscillations in the generator output power before the load change.

5.3.5 Load Change Under Parallel Operation.

Case Study 20: The final set of results in this section (figure 5.34) show the response of the diesel generator and the new algorithm to a 50% load change under parallel operation. The load is applied at around 1 second and removed at about 4 seconds. The derivative waveform calculated by the algorithm (5.34b) shows that the starter element level of 1,000,000 is not exceeded during this test therefore the rest of the algorithm does not continue and the algorithm output remains at zero (5.34c & d).

5.3.6 Conclusions

The field trial results have highlighted the need for a further refinement to the new loss of grid algorithm. This refinement is necessary to overcome the phenomenon of low frequency oscillations in the diesel generator's output power under parallel operating conditions. The use of a starter unit which initiates the remaining algorithm stages based upon the level of the derivative term also has the important benefit of cutting the processor requirements of the algorithm even further. Therefore under steady state conditions the algorithm runs extremely quickly. In the event of some disturbance it effectively 'switches on' and investigates the characteristics of the disturbance to determine if the generator site has become isolated from the main source of utility supply. The final operational form of the algorithm is demonstrated by the flow chart in figure 5.35. This shows the adaptive amplitude limiting function and the starter element included in the basic theoretical algorithm. Implementation of the final form of the algorithm in the microprocessor relay occurs in the form of a specific protection task as specified in section 4.5.4 and shown in figure 4.12.

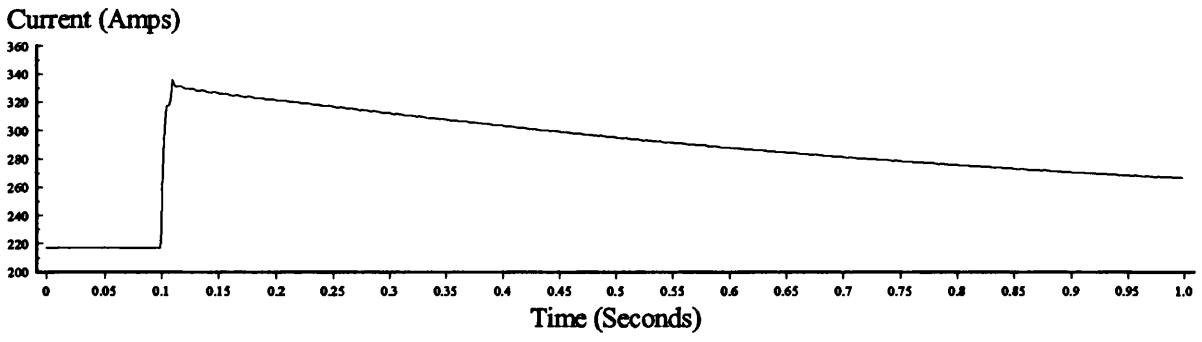

5.1a) A-Phase Generator Line Current.

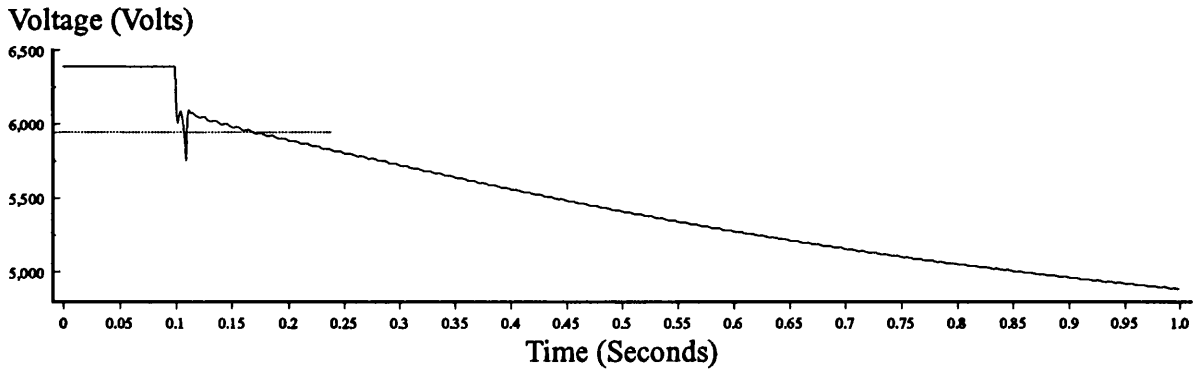

5.1b) A-Phase Generator Terminal Voltage.

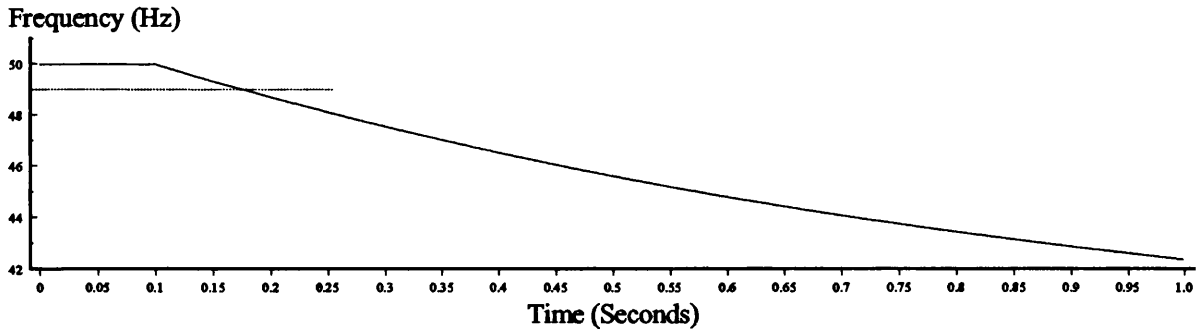

5.1c) Local System Frequency.

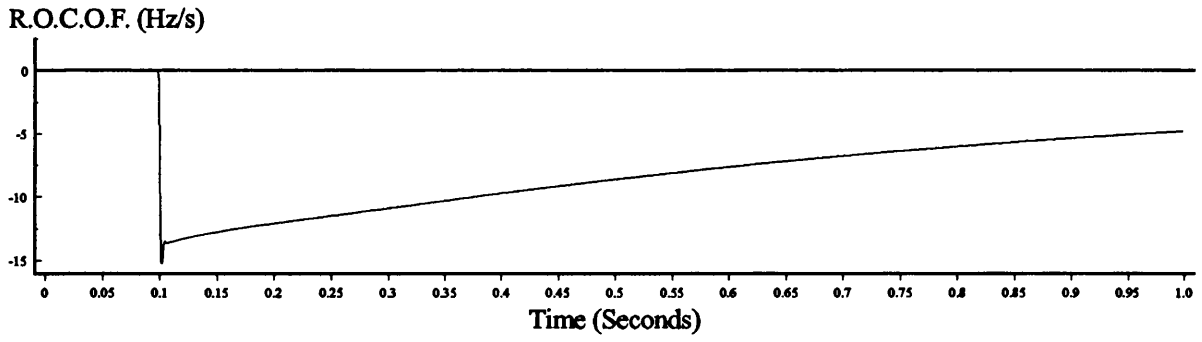

5.1d) Rate of Change of Frequency.

Figure 5.1a-d : System Response to a Loss of Grid Resulting in a 65% Load Increase. (Simulation Result)

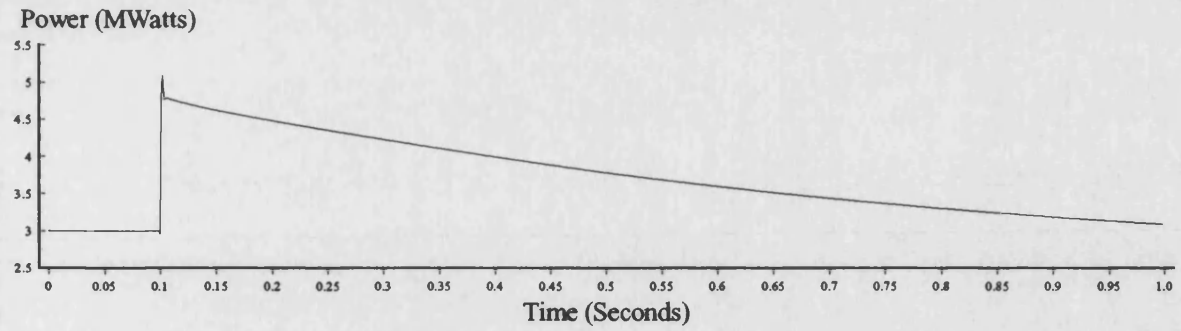

5.1e) Instantaneous Generator Output Power.

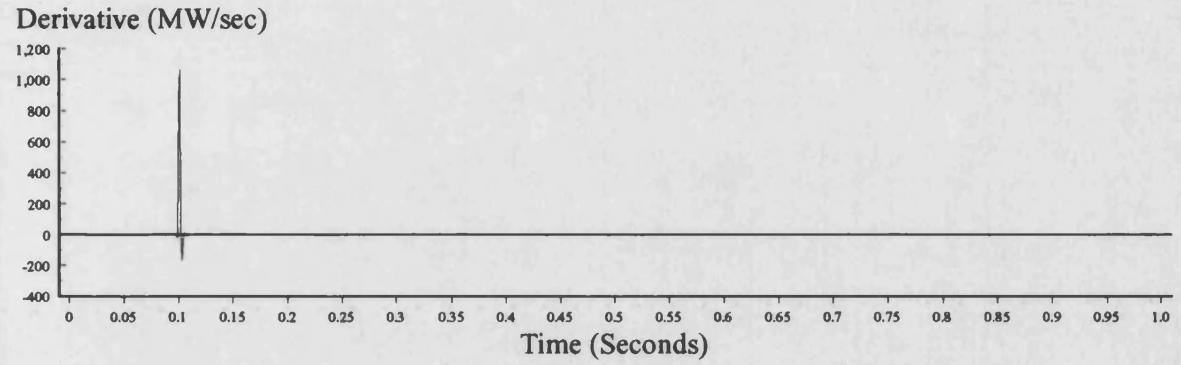

5.1f) Derivative of Power.

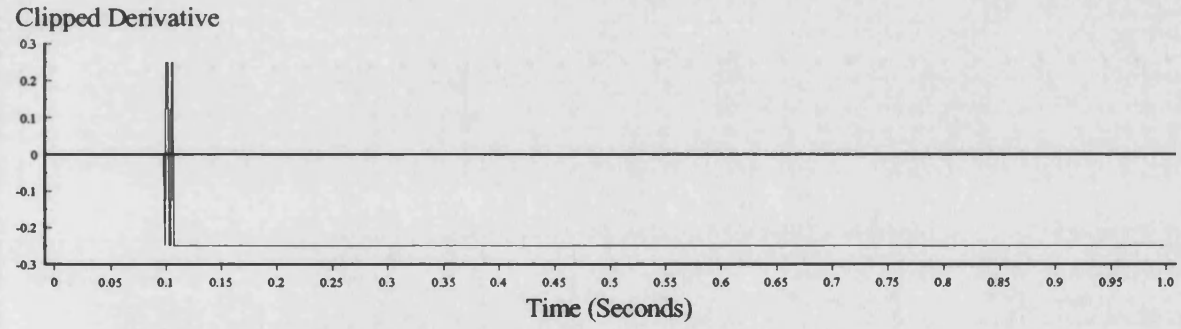

5.1g) Amplitude Limited Derivative.

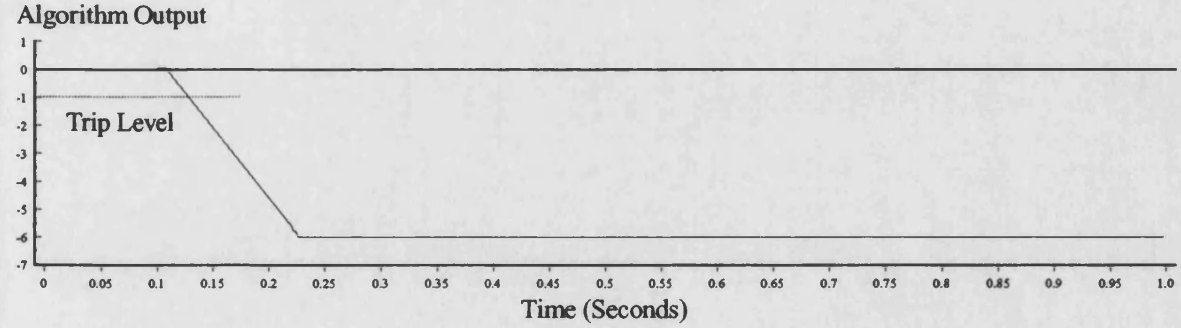

5.1h) Algorithm Output (6 Cycle Moving Average Filter).

Figure 5.1e-h : Algorithm Response to a Loss of Grid Resulting in a 65% Load Increase. (Simulation Result)

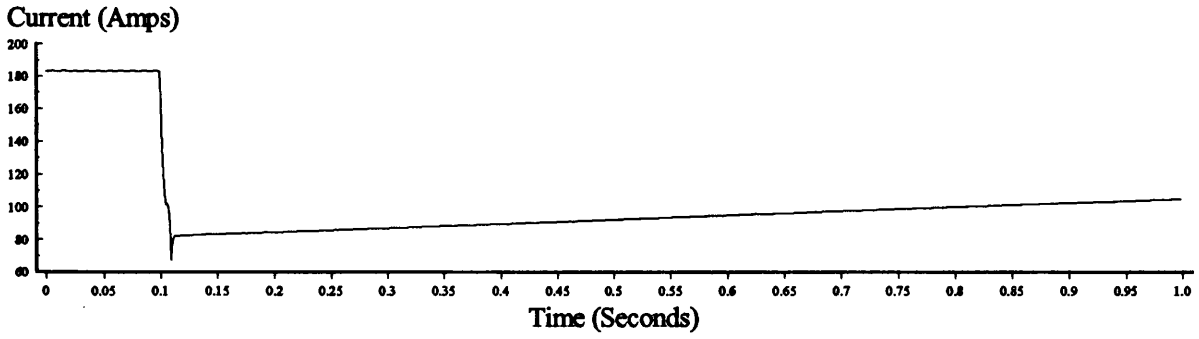

5.2a) A-Phase Generator Line Current.

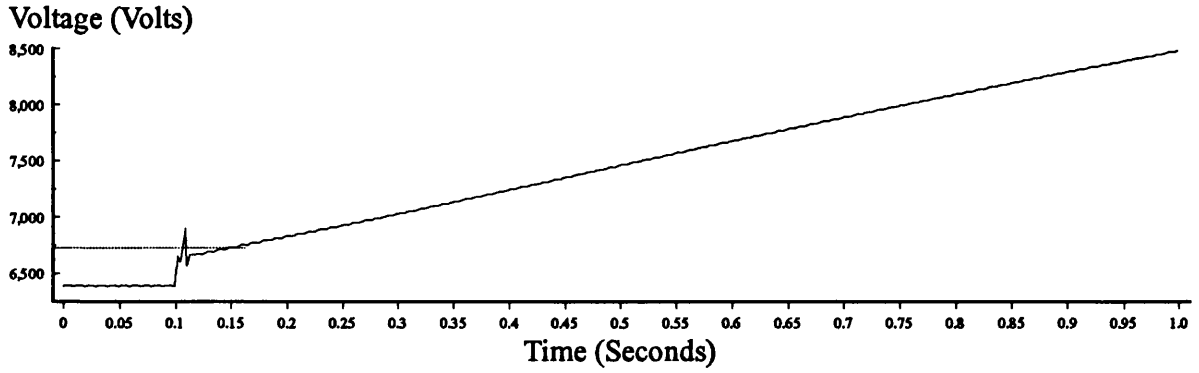

5.2b) A-Phase Generator Terminal Voltage.

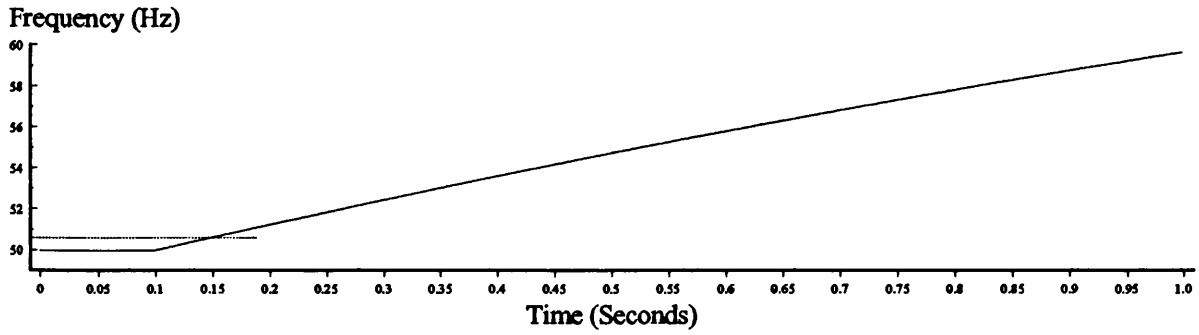

5.2c) Local System Frequency.

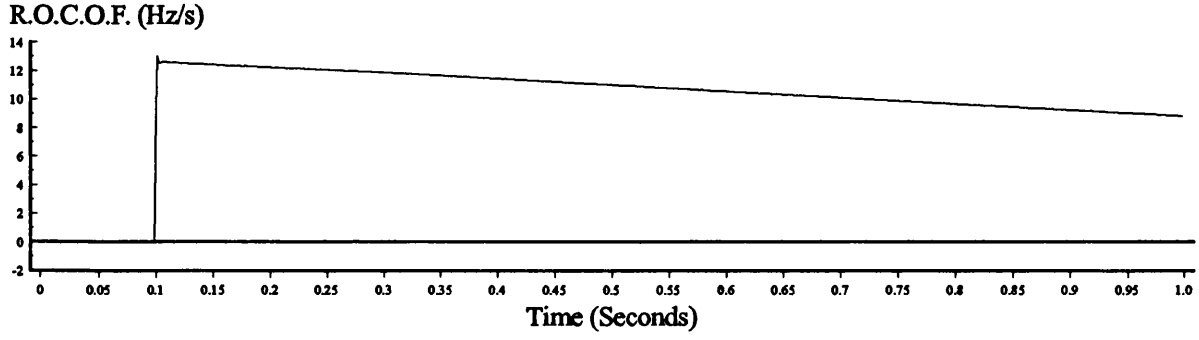

5.2d) Rate of Change of Frequency.

Figure 5.2a-d : System Reponse to a Loss of Grid Resulting in a 50% Load Decrease. (Simulation Result)

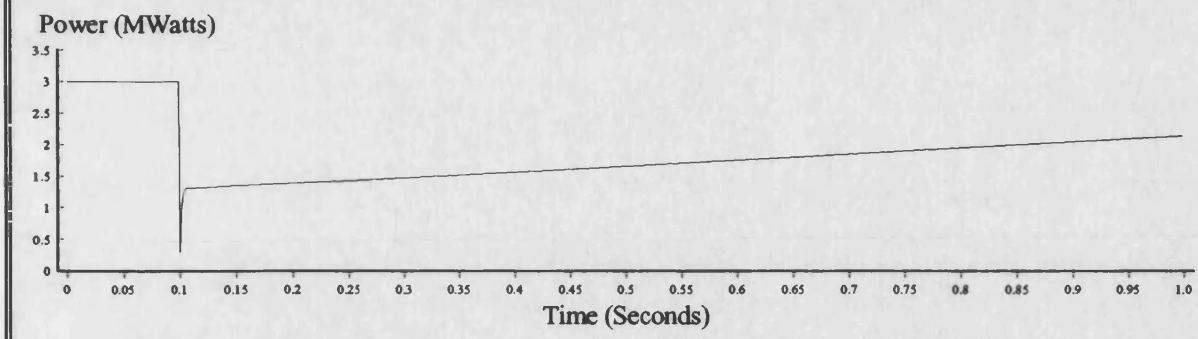

5.2e) Instantaneous Output Power.

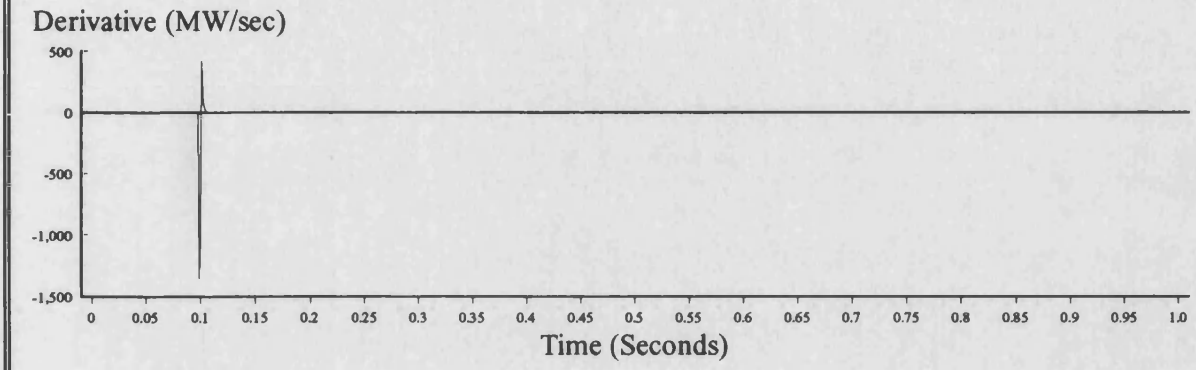

5.2f) Derivative of Power.

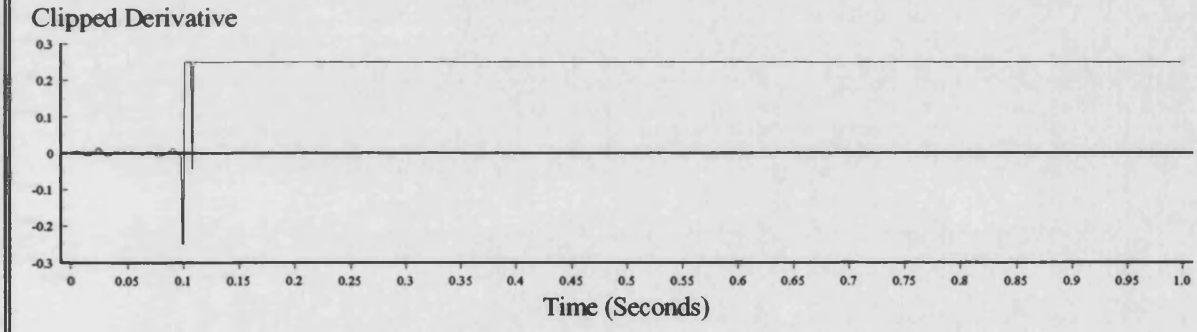

5.2g) Amplitude Limited Derivative.

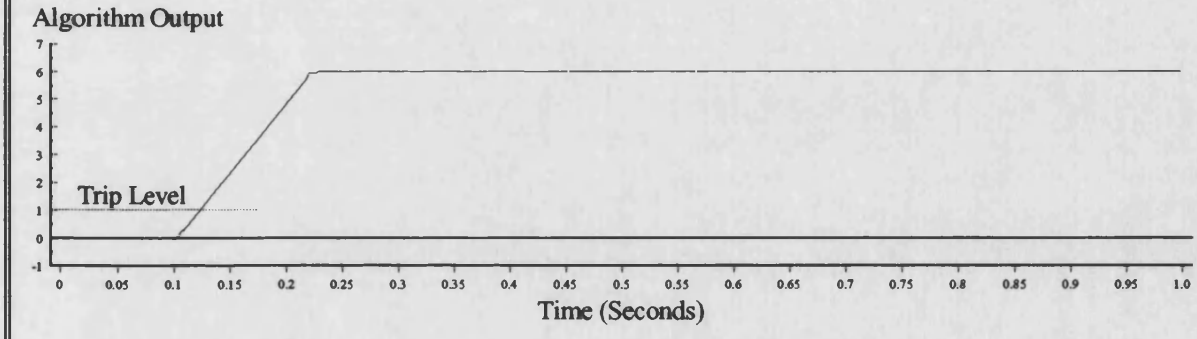

5.2h) Algorithm Output (6 Cycle Moving Average Filter).

Figure 5.2e-h : Algorithm Response to a Loss of Grid Resulting in a 50% Load Decrease. (Simulation Result)

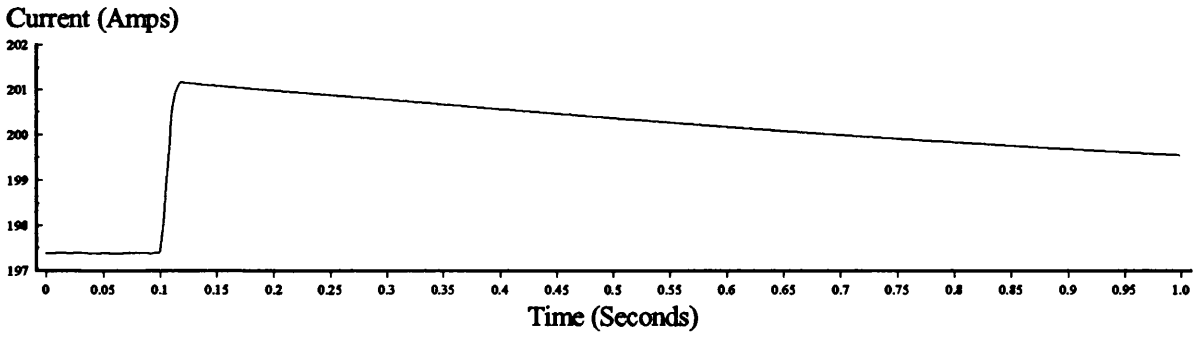

5.3a) A-Phase Generator Line Current.

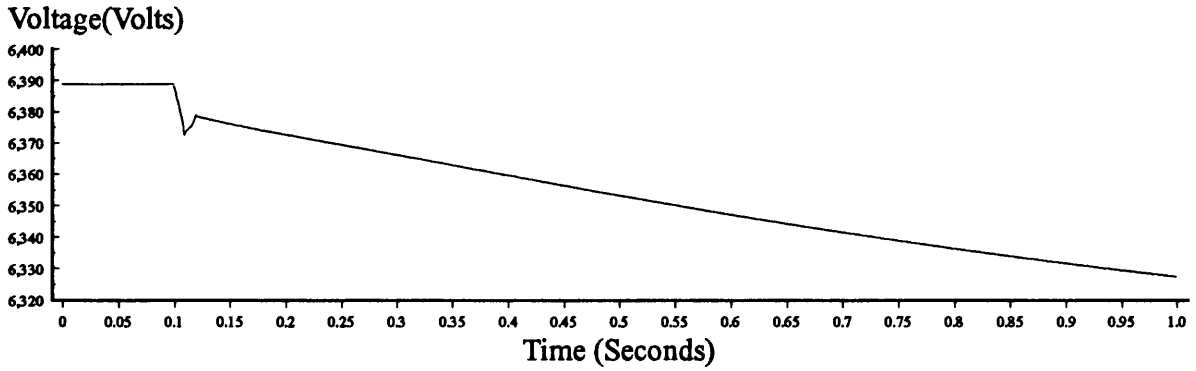

5.3b) A-Phase Generator Terminal Voltage.

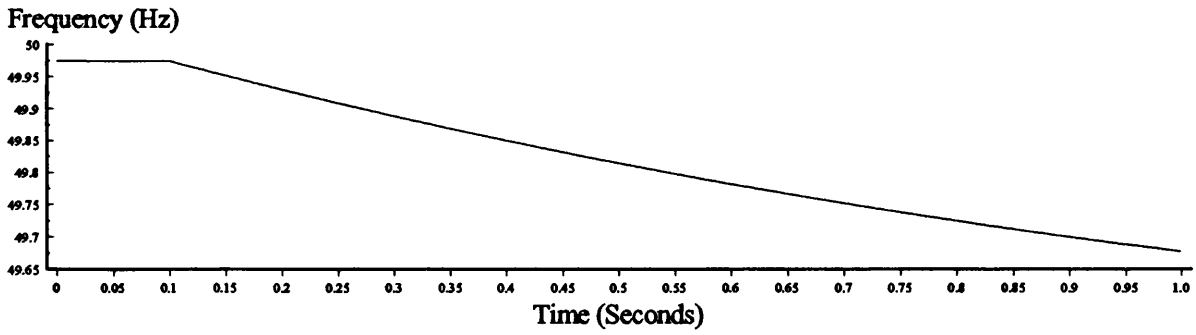

5.3c) Local System Frequency.

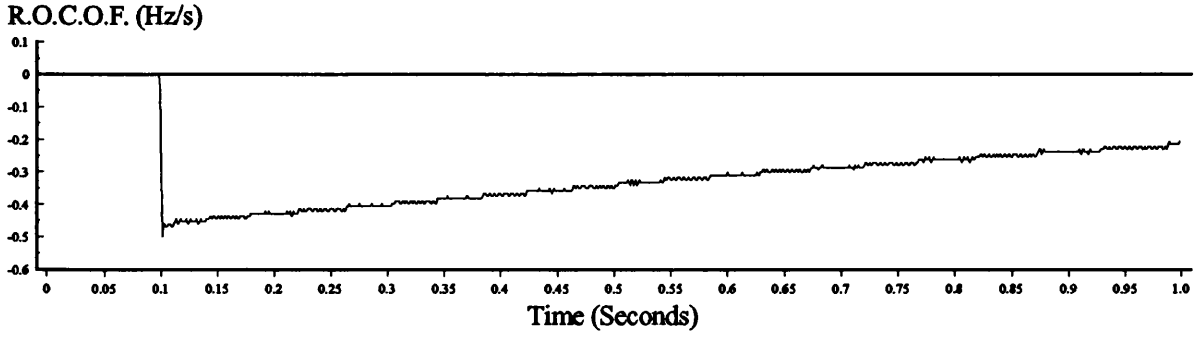

5.3d) Rate of Change of Frequency.

Figure 5.3a-d : System Response to a Loss of Grid Resulting in a 2% Load Increase. (Simulation Result)

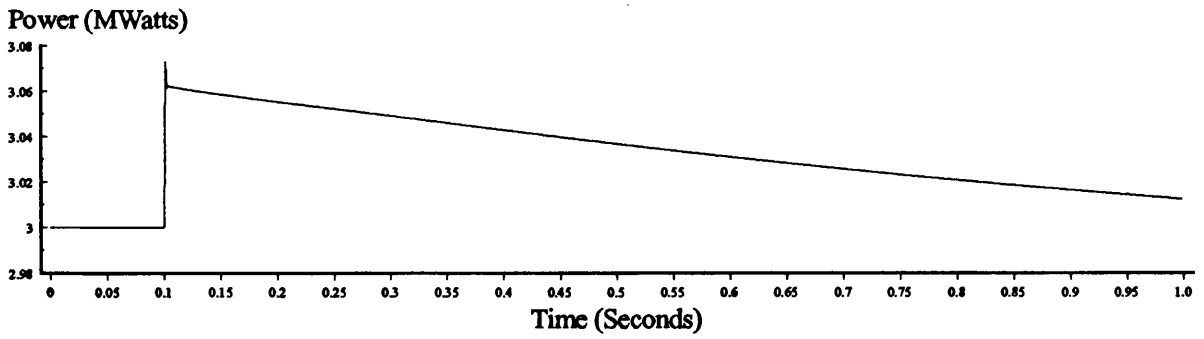

5.3e) Instantaneous Output Power.

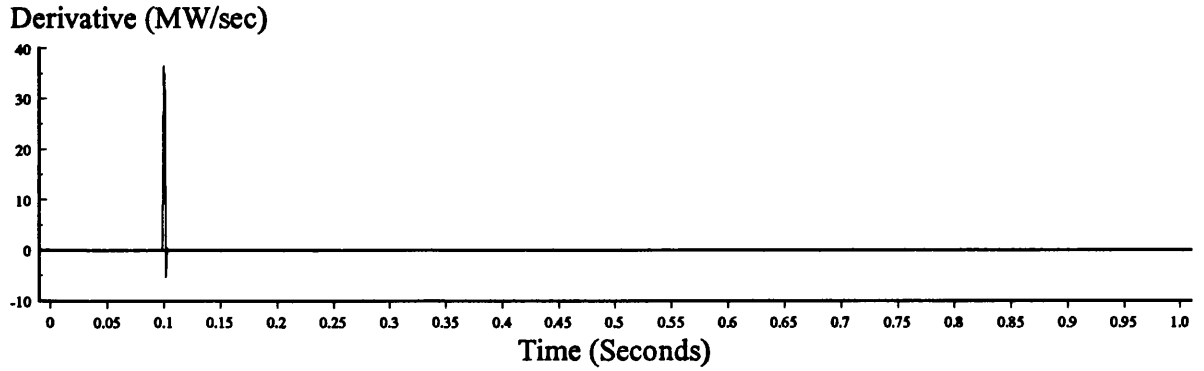

5.3f) Derivative of Power.

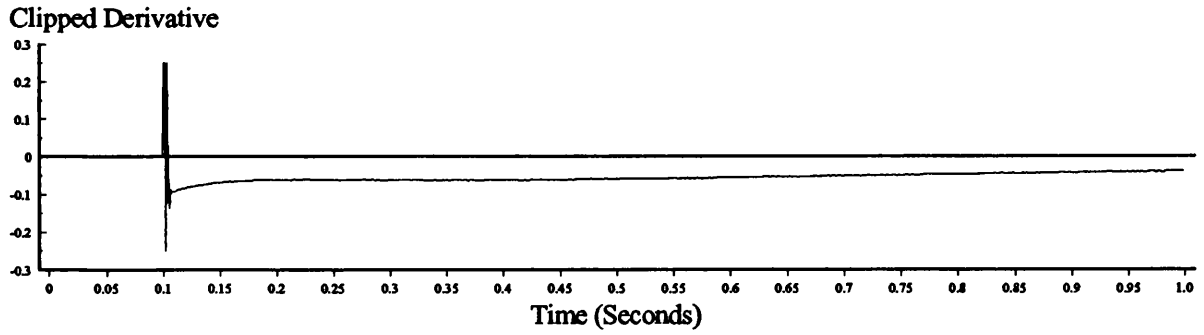

5.3g) Amplitude Limited Derivative.

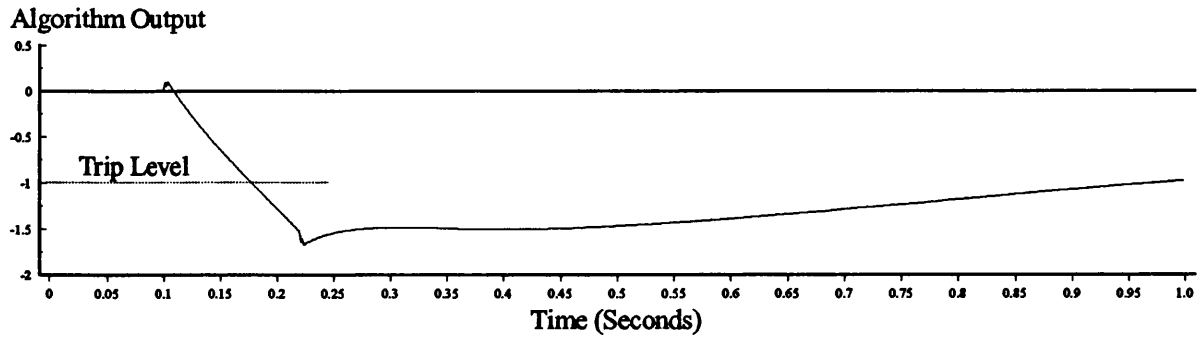

5.3h) Algorithm Output (6 Cycle Moving Average Filter).

Figure 5.3e-h : Algorithm Response to a Loss of Grid Resulting in a 2% Load Increase. (Simulation Result)

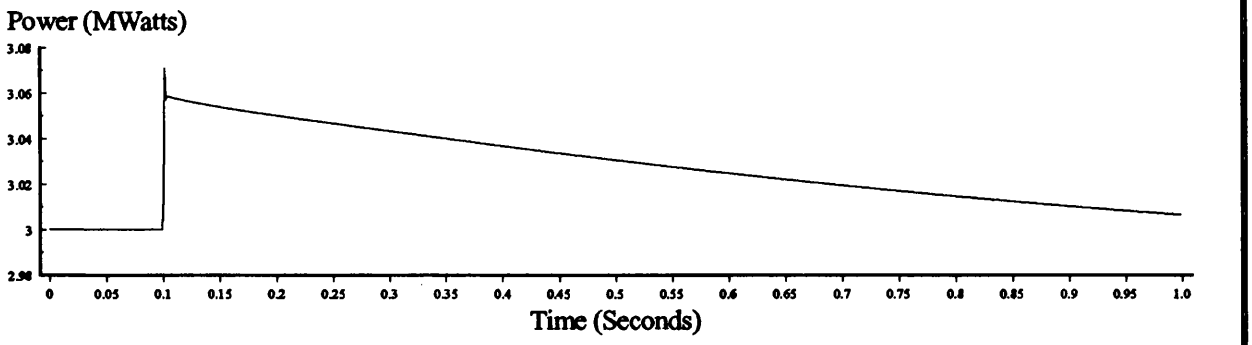

5.4a) Instantaneous Output Power.

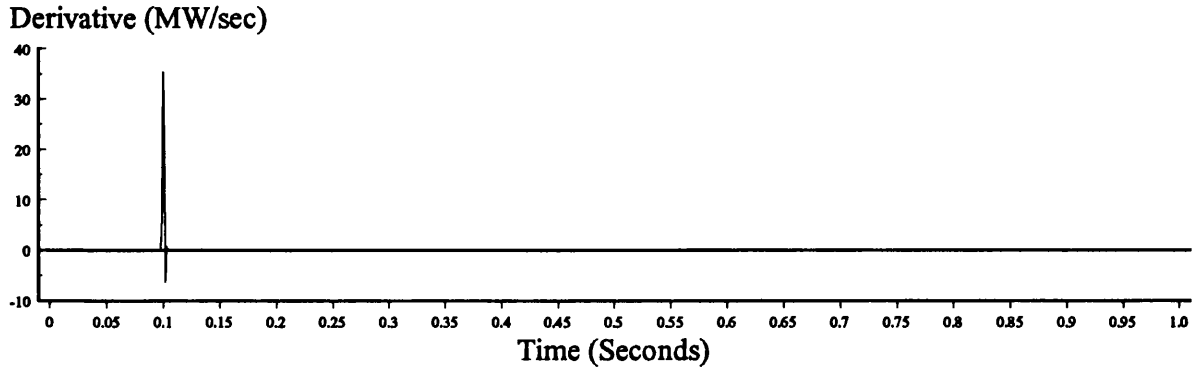

5.4b) Derivative of Power.

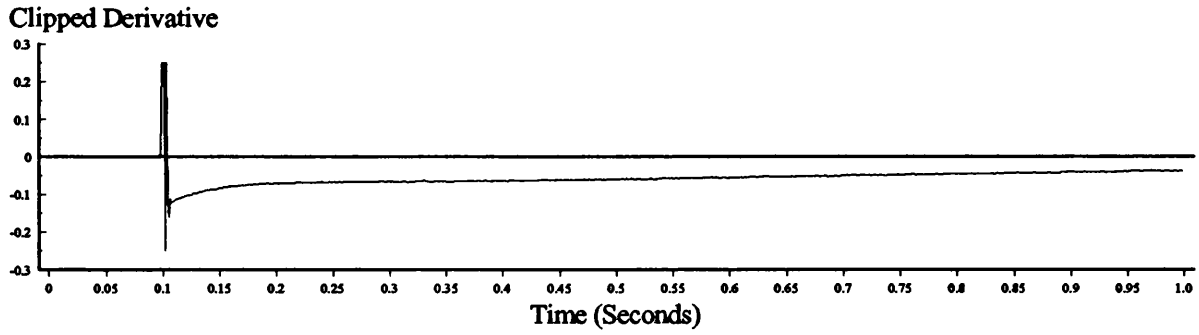

5.4c) Amplitude Limited Derivative.

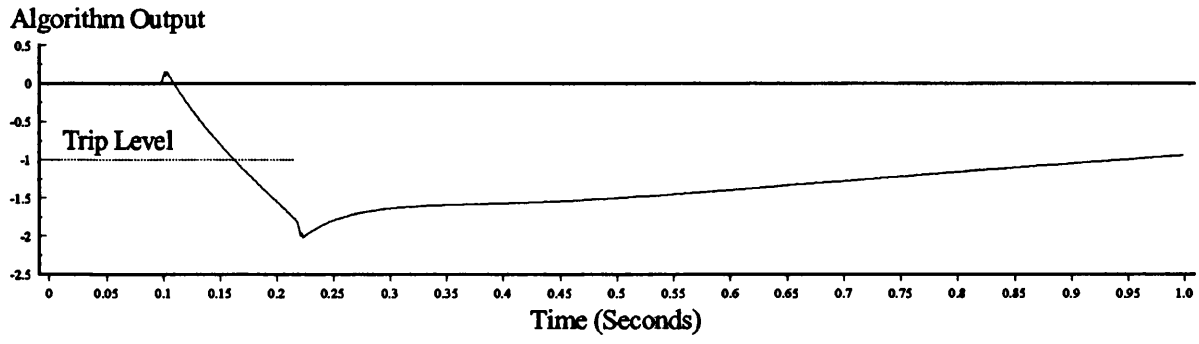

5.4d) Algorithm Output (6 Cycle Moving Average Filter).

Figure 5.4 : Algorithm Response to a 2% Load Increase under Independent Operation. (Simulation Result)

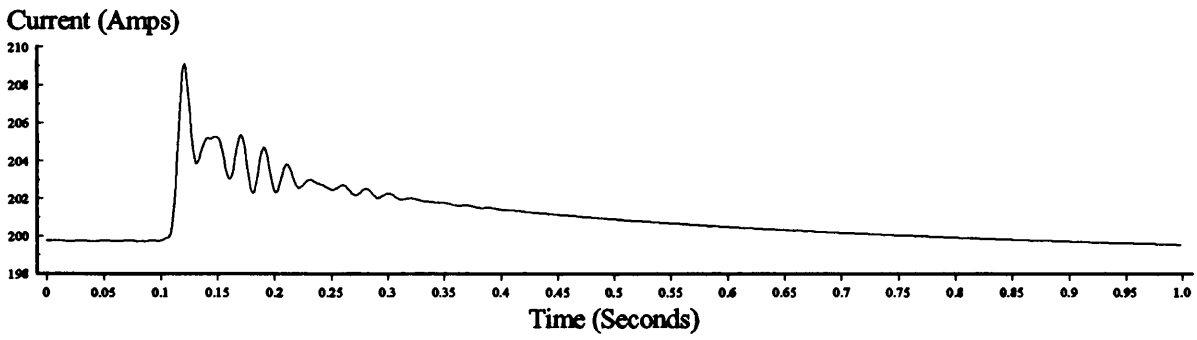

5.5a) A-Phase Generator Line Current.

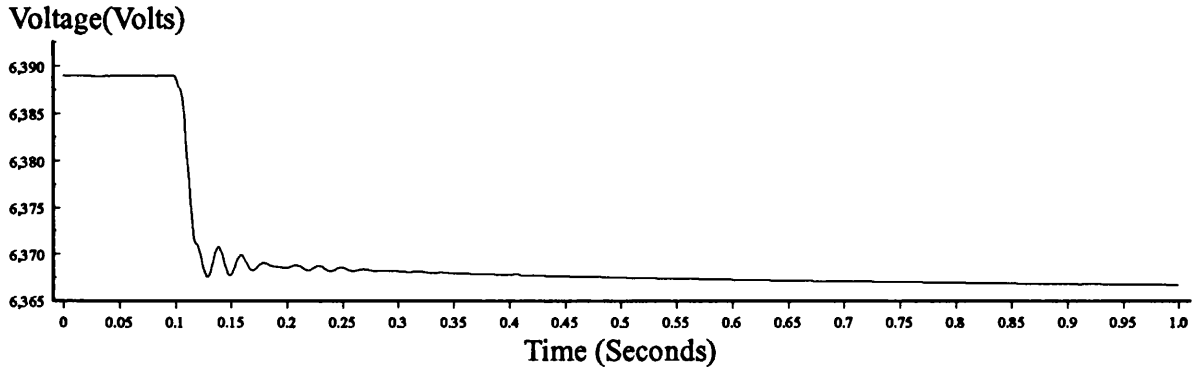

5.5b) A-Phase Generator Terminal Voltage.

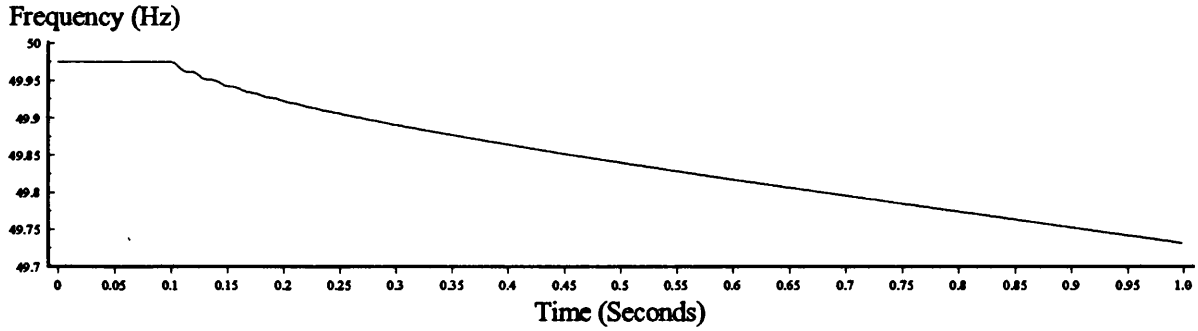

5.5c) Local System Frequency.

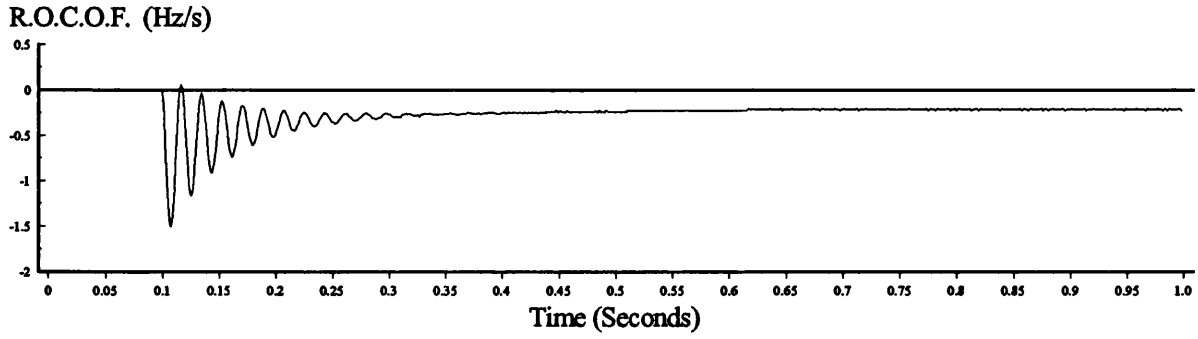

5.5d) Rate of Change of Frequency.

Figure 5.5a-d : System Response to a 100% Load Increase under Parallel Operation. (Simulation Result)

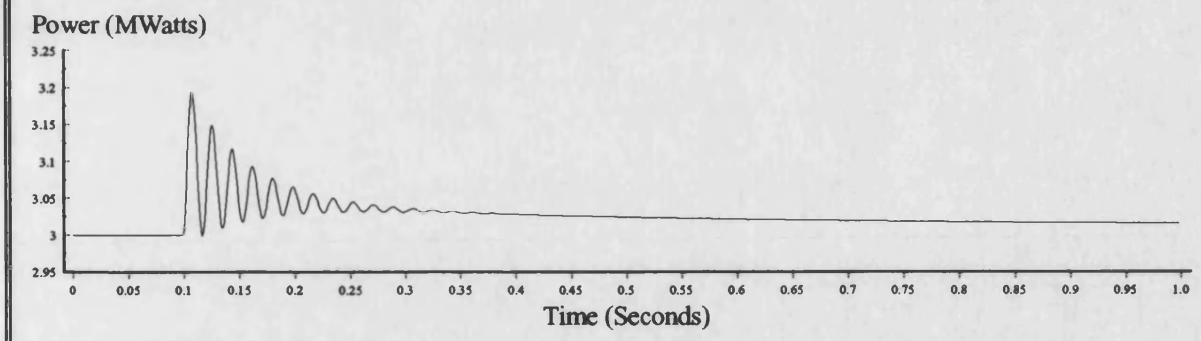

5.5e) Instantaneous Output Power.

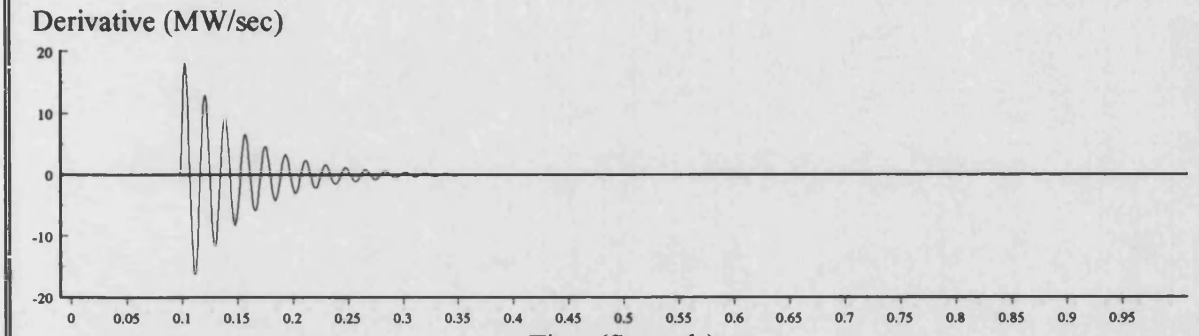

5.5f) Derivative of Power.

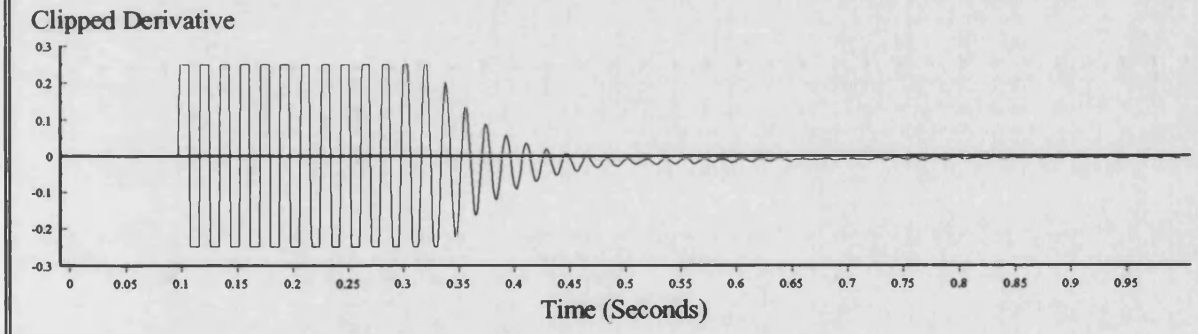

5.5g) Amplitude Limited Derivative.

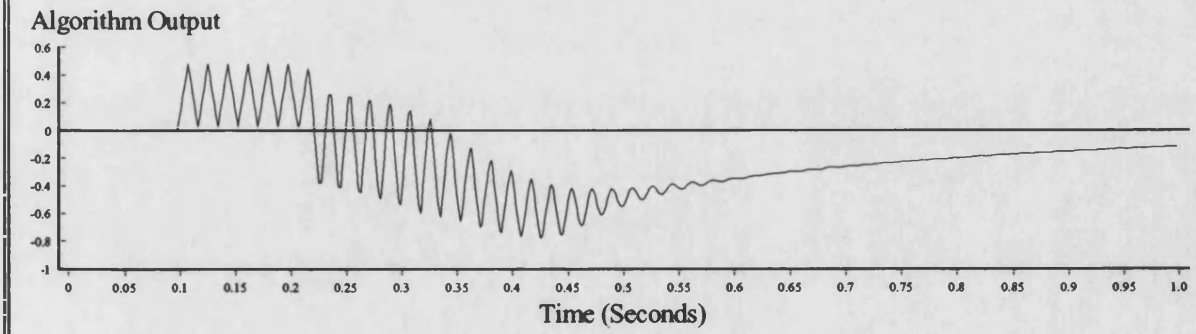

5.5h) Algorithm Output (6 Cycle Moving Average Filter).

Figure 5.5e-h : Algorithm Response to a 100% Load Increase under Parallel Operation. (Simulation Result)

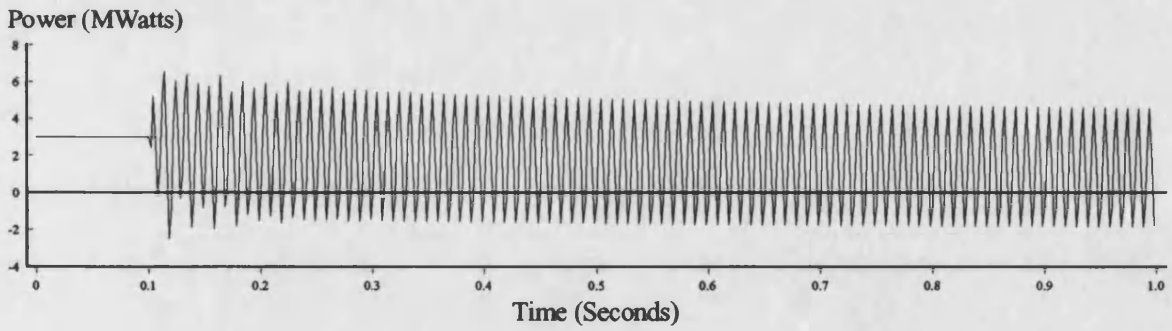

5.6a) Instantaneous Output Power.

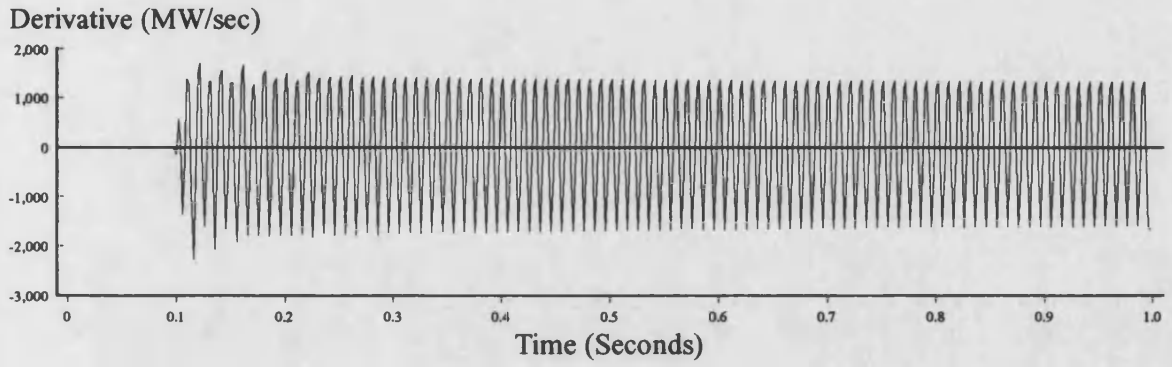

5.6b) Derivative of Power.

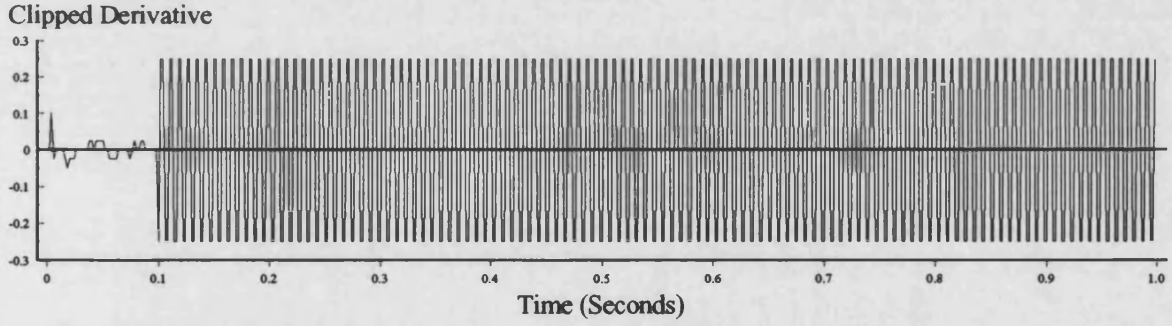

5.6c) Amplitude Limited Derivative.

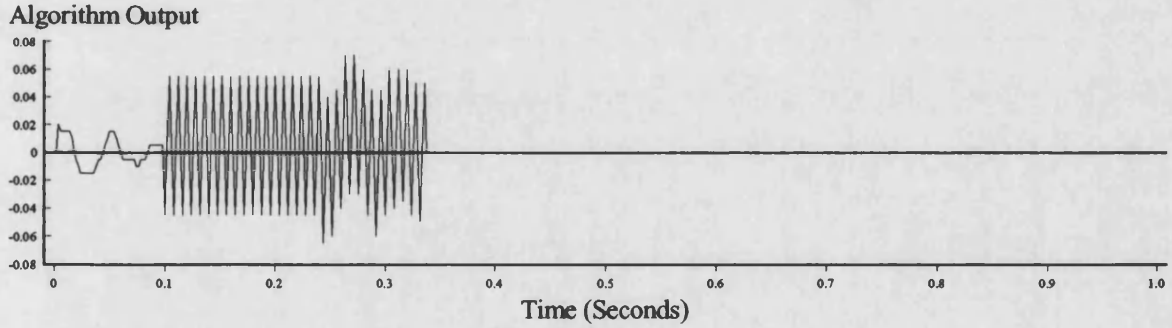

5.6d) Algorithm Output (6 Cycle Moving Average Filter).

Figure 5.6 : Algorithm Response to a Single Phase to Ground Fault on the Local Busbar. (Simulation Result)

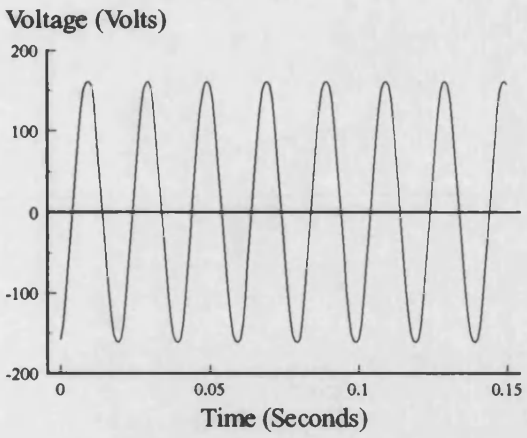

5.7a) A-Phase Generator Terminal Voltage.

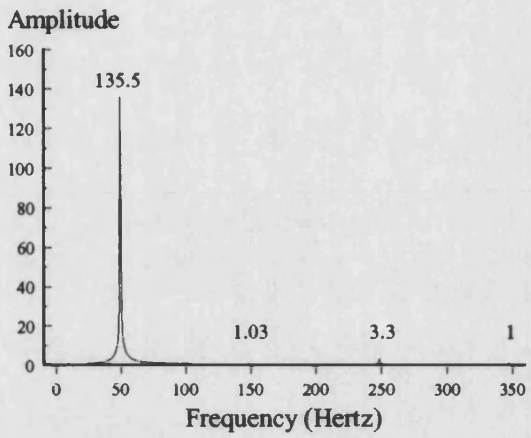

5.7b) Harmonic Analysis of Voltage.

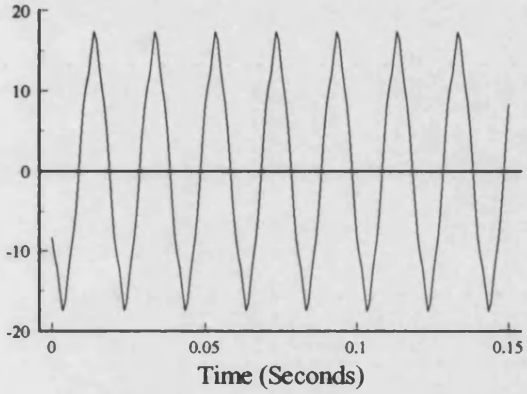

5.7c) A-Phase Generator Line Current.

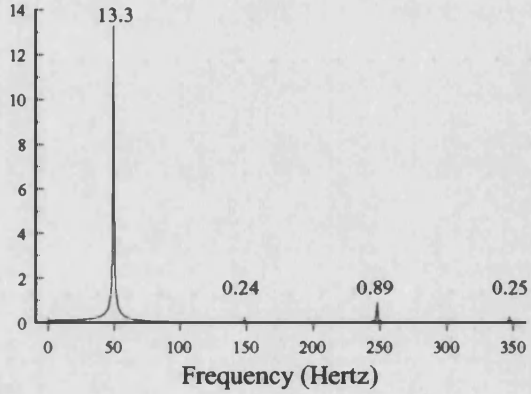

5.7d) Harmonic Analysis of Current.

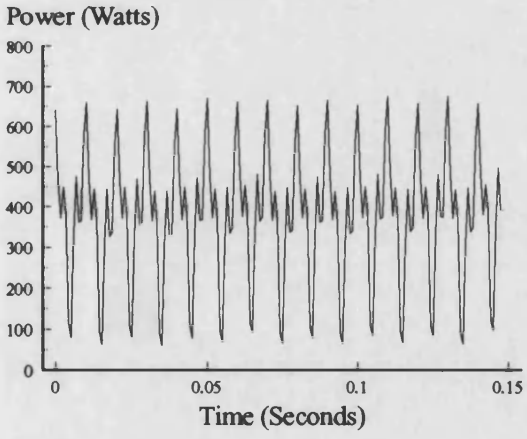

5.7e) Instantaneous Three Phase Output Power.

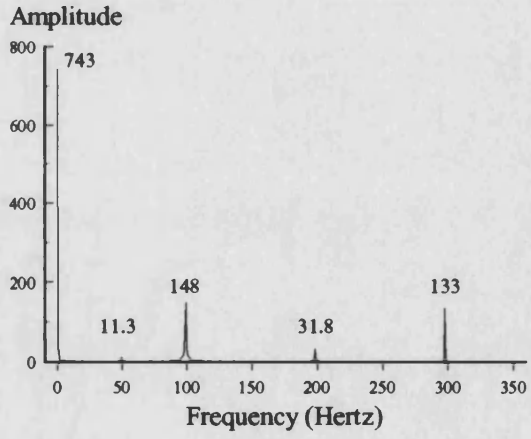

5.7f) Harmonic Analysis of Power.

Figure 5.7 : Steady State Parallel Operation (400 Watts/Lagging p.f.).
(Laboratory System Result)

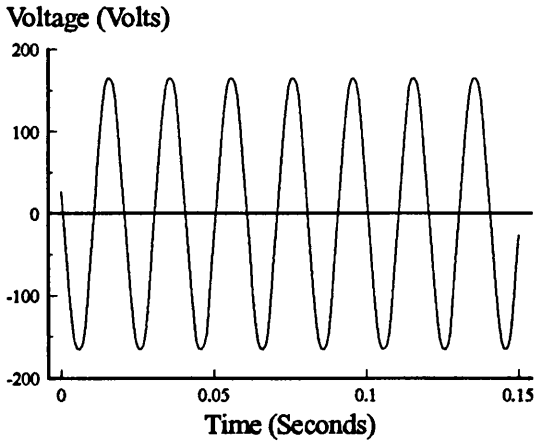

5.8a) A-Phase Generator Terminal Voltage.

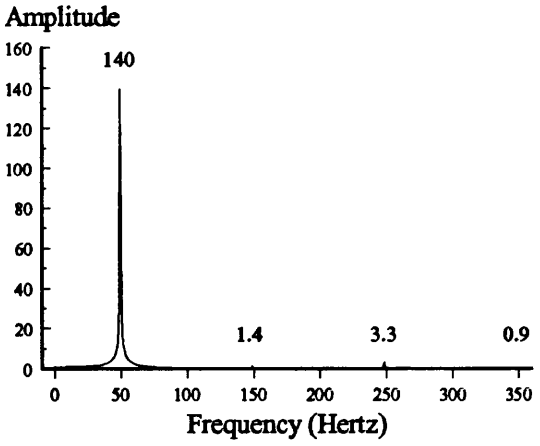

5.8b) Harmonic Analysis of Voltage.

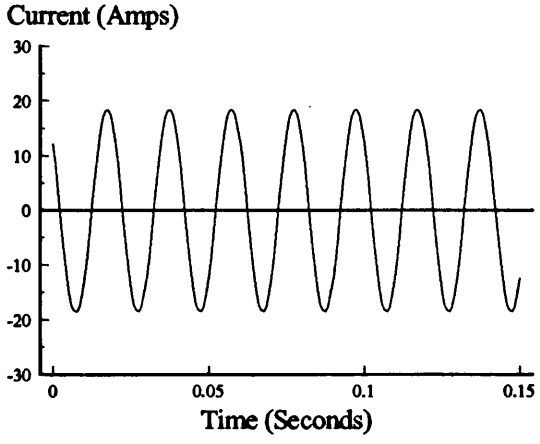

5.8c) A-Phase Generator Line Current.

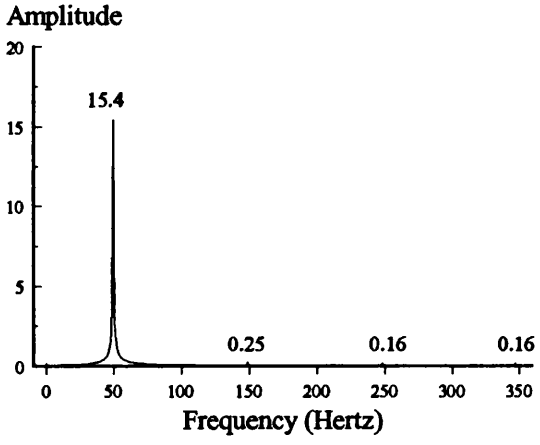

5.8d) Harmonic Analysis of Current.

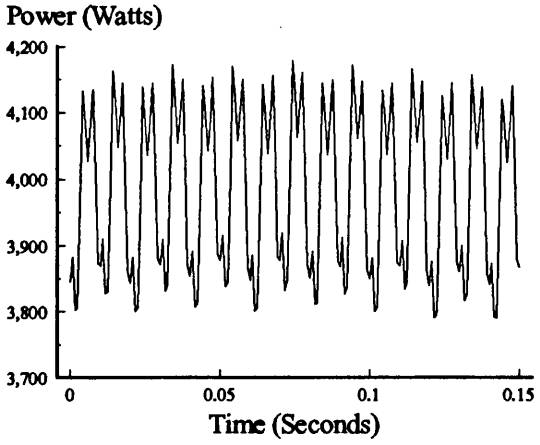

5.8e) Instantaneous Three Phase Output Power.

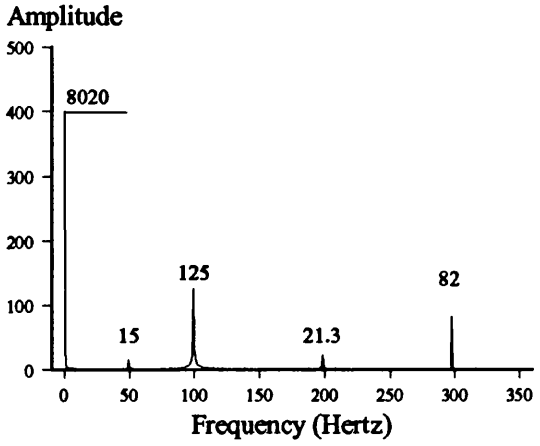

5.8f) Harmonic Analysis of Power.

Figure 5.8 : Steady State Parallel Operation (4000 Watts/Lagging p.f.).
(Laboratory System Result)

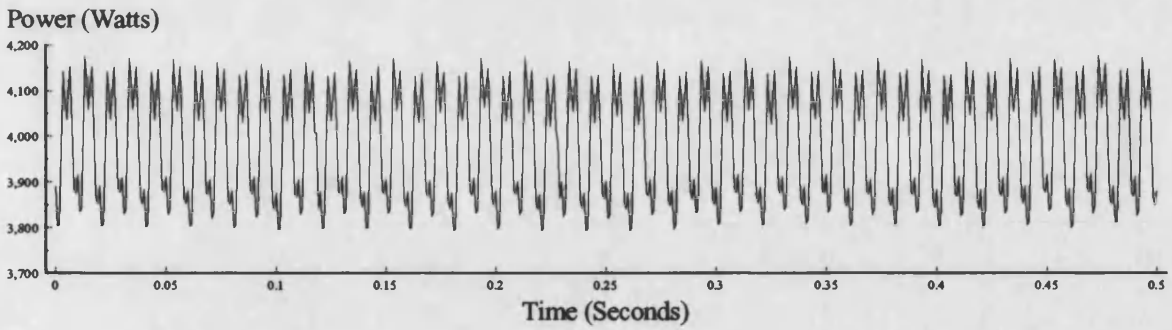

5.9a) Instantaneous Three Phase Output Power.

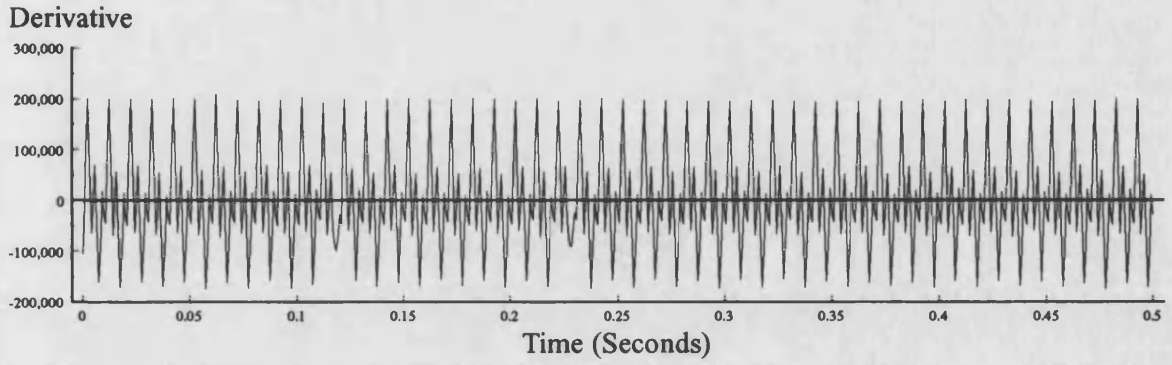

5.9b) Derivative Of Power.

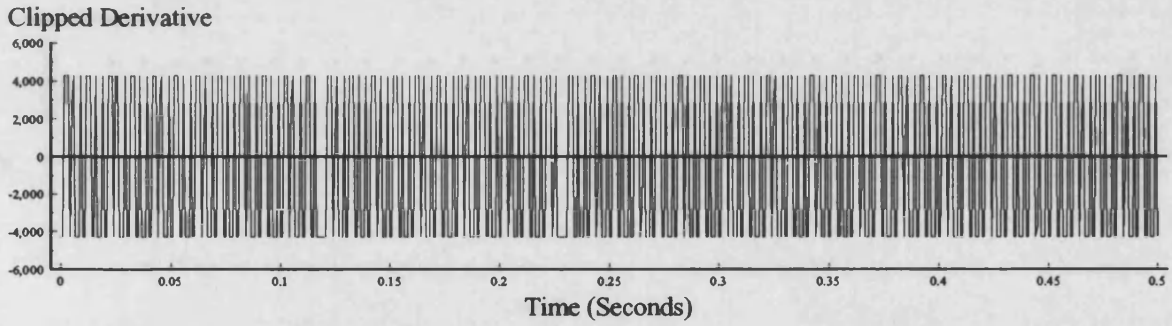

5.9c) Amplitude Limited Derivative.

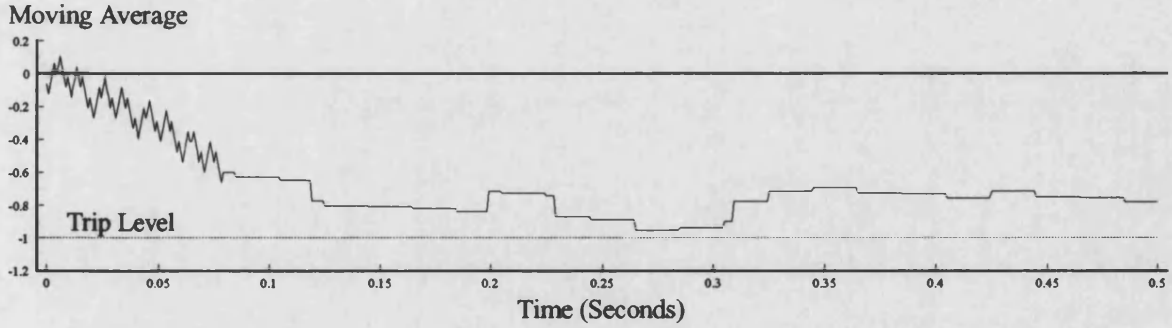

5.9d) Algorithm Output (6 Cycle Moving Average Filter).

Figure 5.9 : Algorithm Response Under Steady State Conditions with 10% Setting.
(Laboratory System Result)

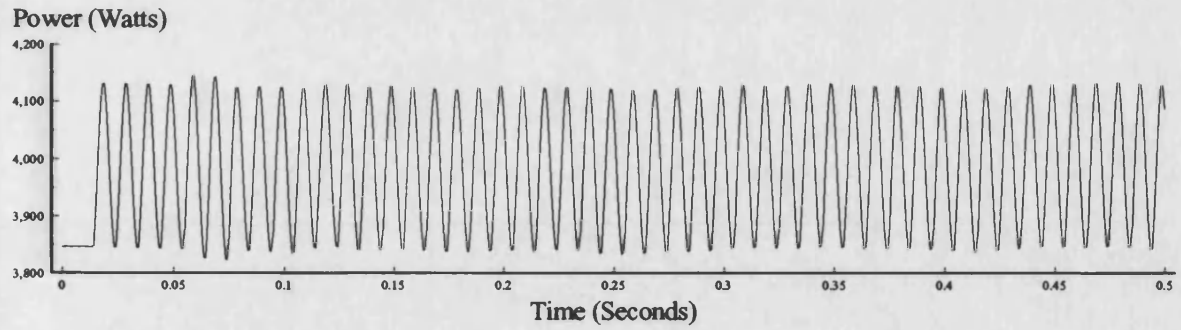

5.10a) Full Cycle Fourier Filtered Power.

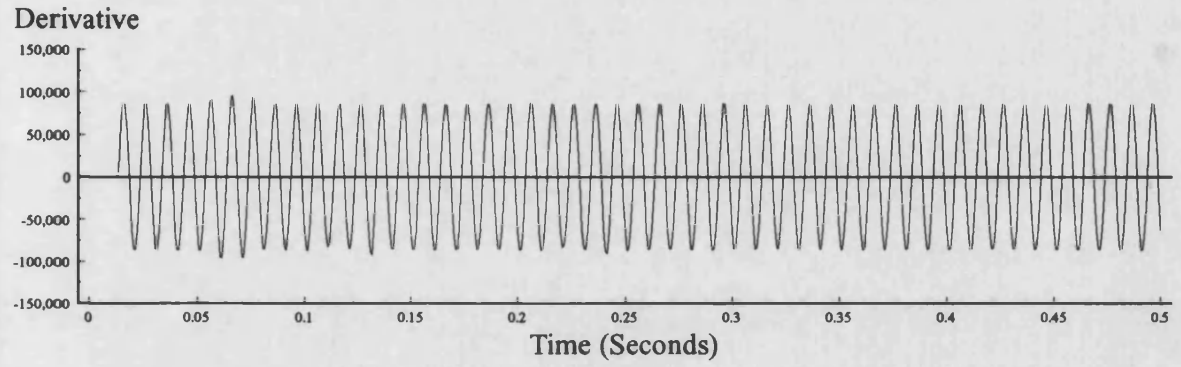

5.10b) Derivative of Filtered Power.

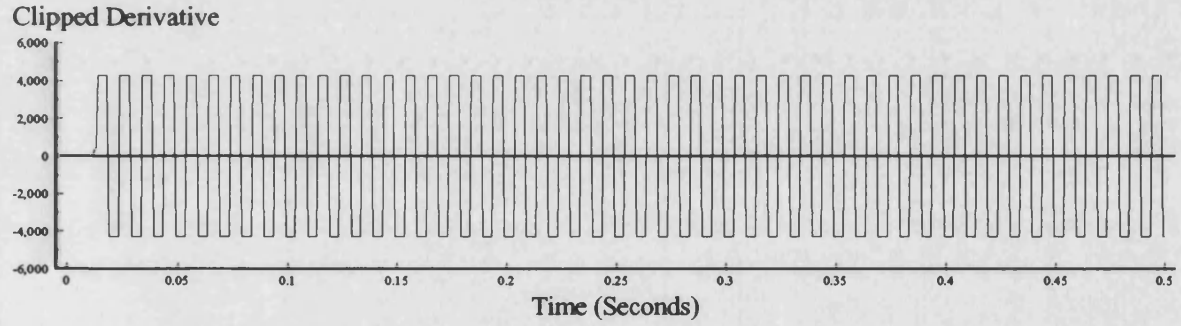

5.10c) Amplitude Limited Derivative.

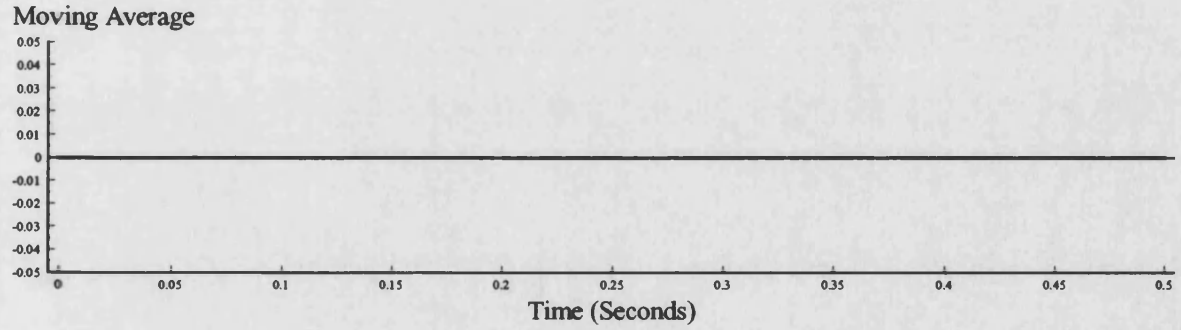

5.10d) Algorithm Output (6 Cycle Moving Average Filter).

Figure 5.10 : Algorithm Response Under Steady State Conditions With Fourier Filtered Power (Laboratory System Result)

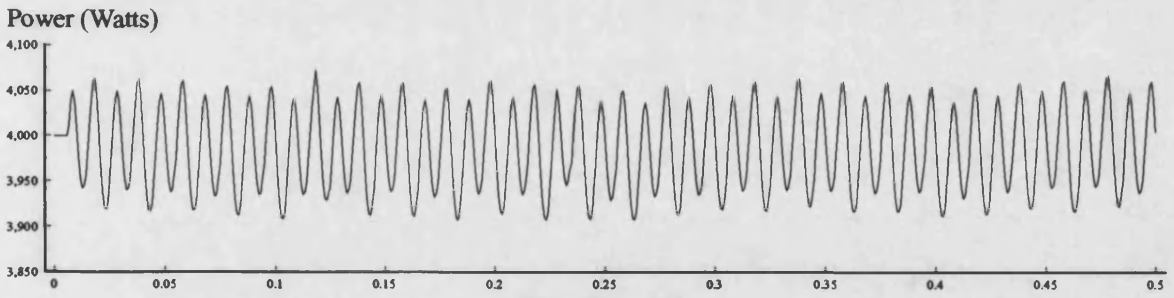

5.11a) Half Cycle Moving Average Filtered Power.

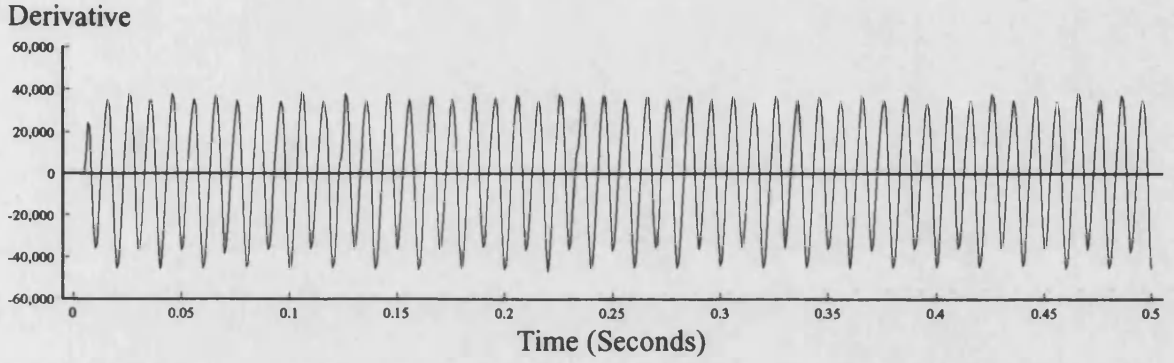

5.11b) Derivative of Filtered Power.

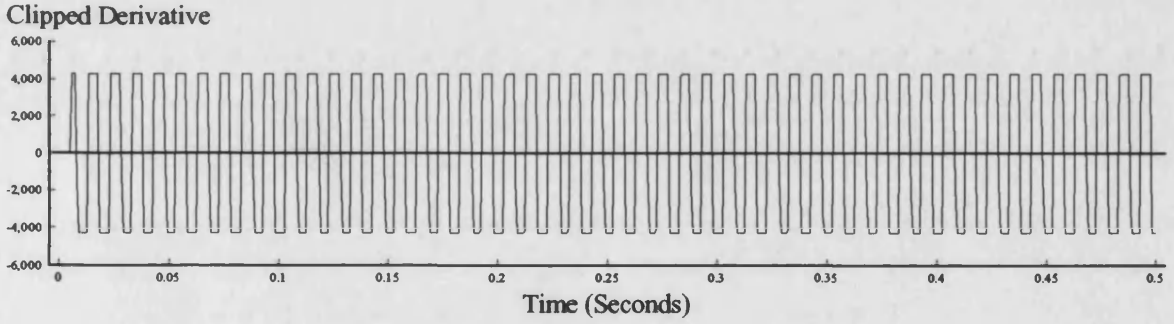

5.11c) Amplitude Limited Derivative.

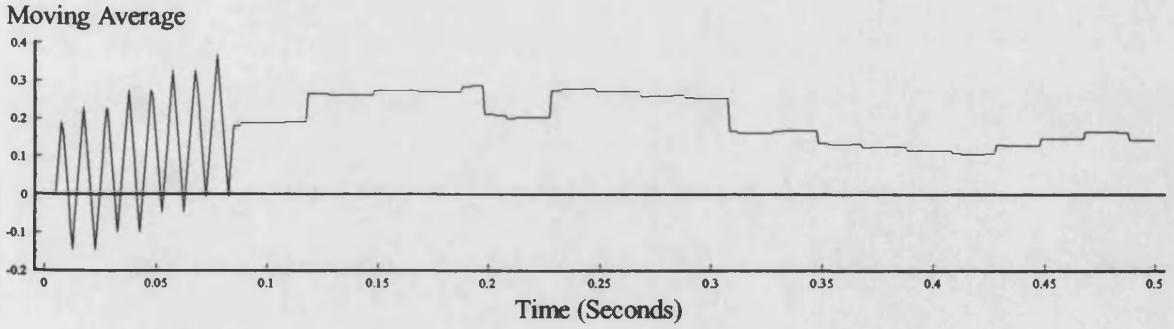

5.11d) Algorithm Output (6 Cycle Moving Average Filter).

Figure 5.11 : Algorithm Response Under Steady State With 1/2 Cycle Moving Average Power. (Laboratory System Result)

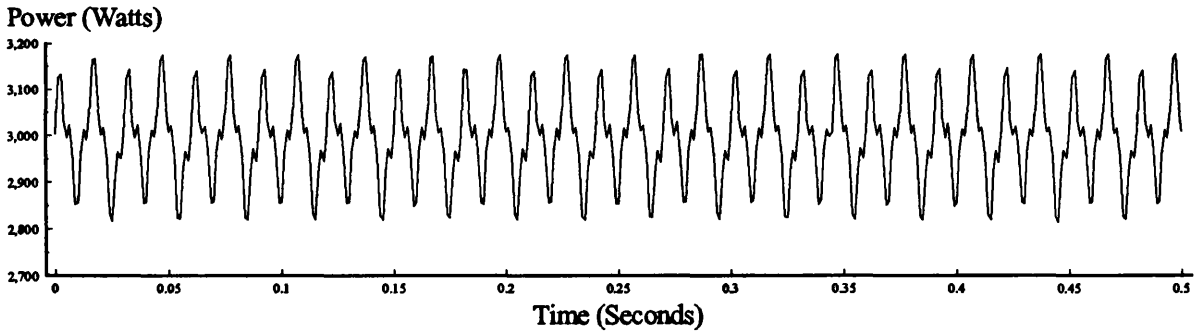

5.12a) Instantaneous Three Phase Ouput Power.

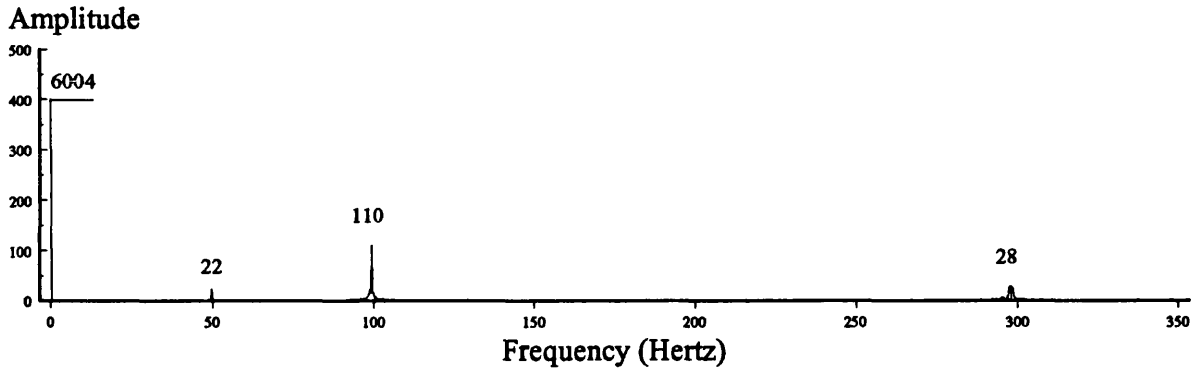

5.12b) Harmonic Analysis of Power

Figure 5.12 : Steady State Independent Operation (3000 Watts)
(Laboratory System Result)

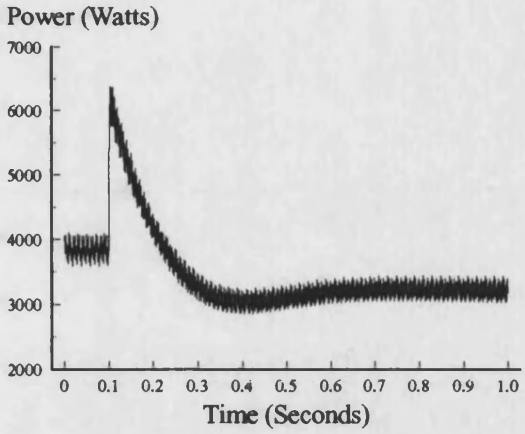

5.13a) Instantaneous Three Phase Output Power.

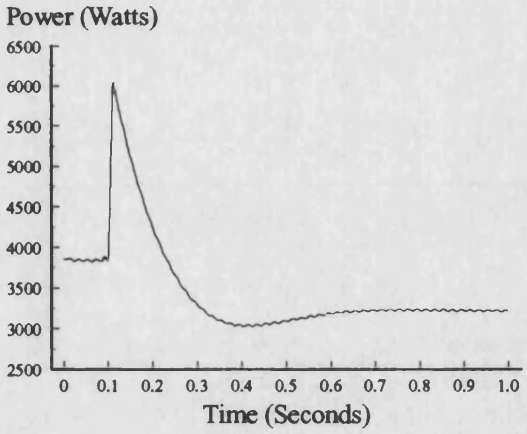

5.13b) Half Cycle Moving Average of Power.

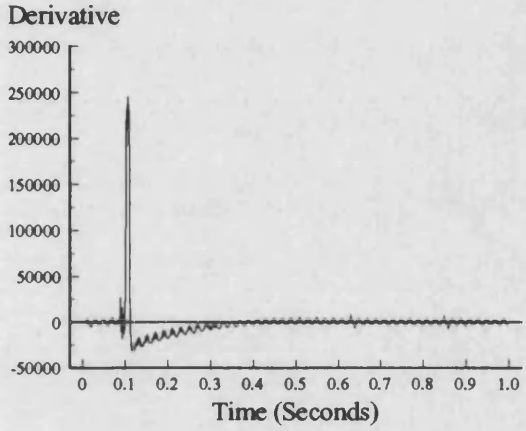

5.13c) Derivative of Power.

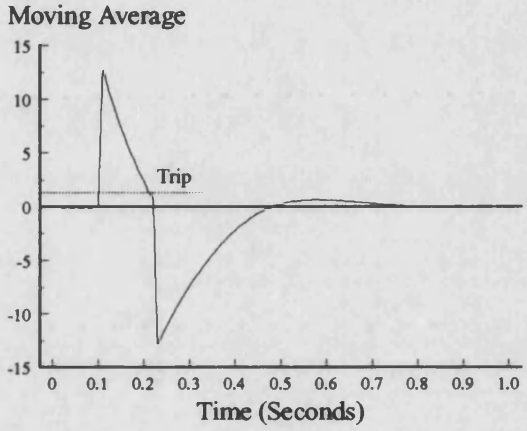

5.13d) Algorithm Output With no Clipping.

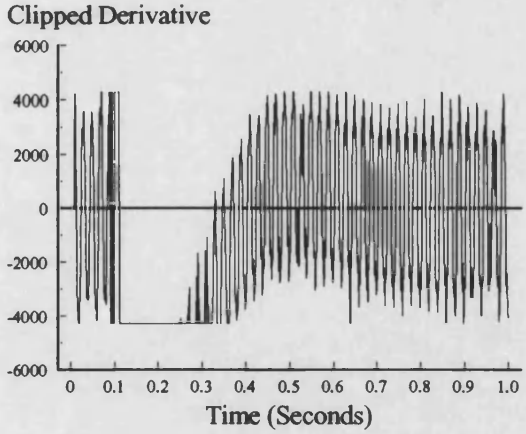

5.13e) Amplitude Limited Derivative.

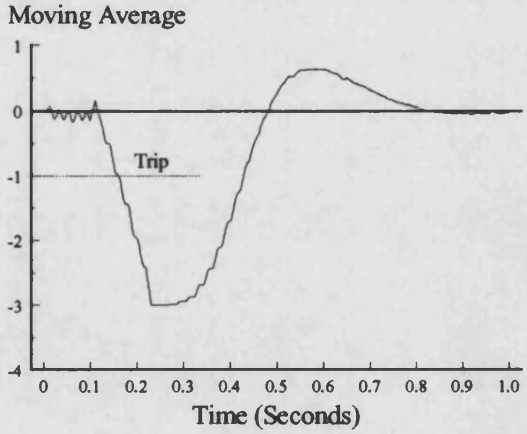

5.13f) Algorithm Output With Clipped Derivative.

Figure 5.13 : Algorithm Response to a Loss of Grid Resulting in a 65% Increase in Loading. (Laboratory System Result)

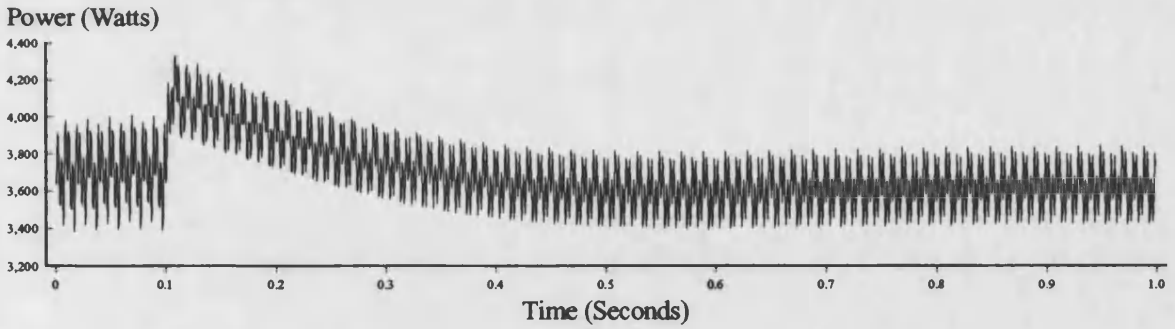

5.14a) Instantaneous Three Phase Output Power

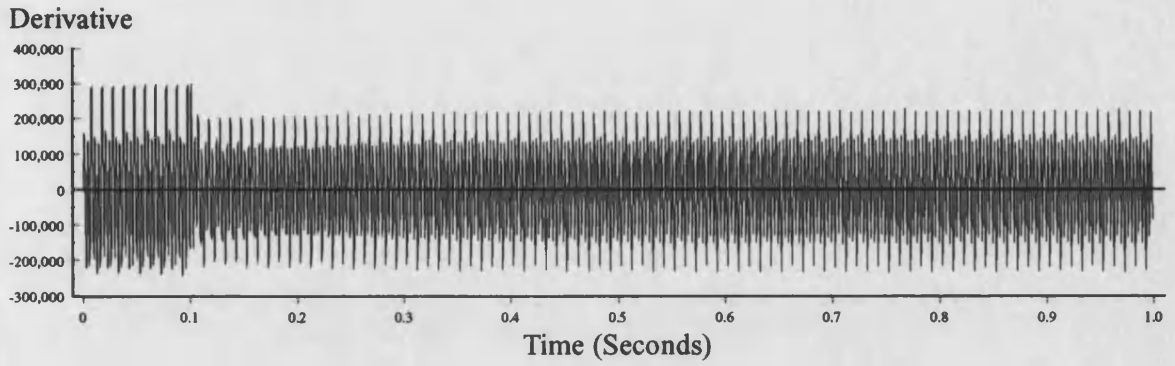

5.14b) Derivative of Power.

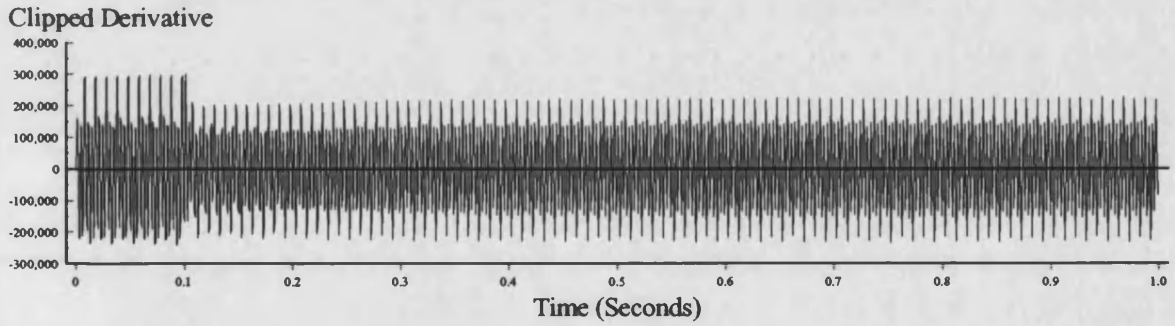

5.14c) Amplitude Limited Derivative.

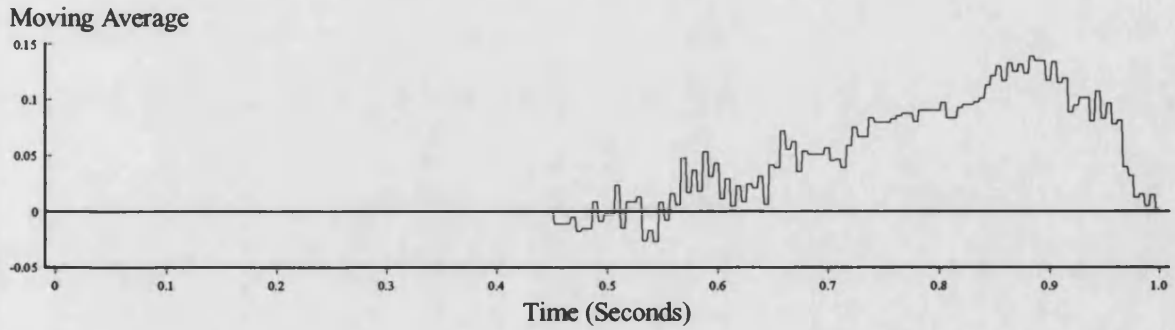

5.14d) Algorithm Output (6 Cycle Moving Average Filter).

Figure 5.14 : Algorithm Response to a Loss of Grid Resulting in a 10% Load Increase using Instantaneous Power at 24 Samples/Cycle.
(Laboratory System Result)

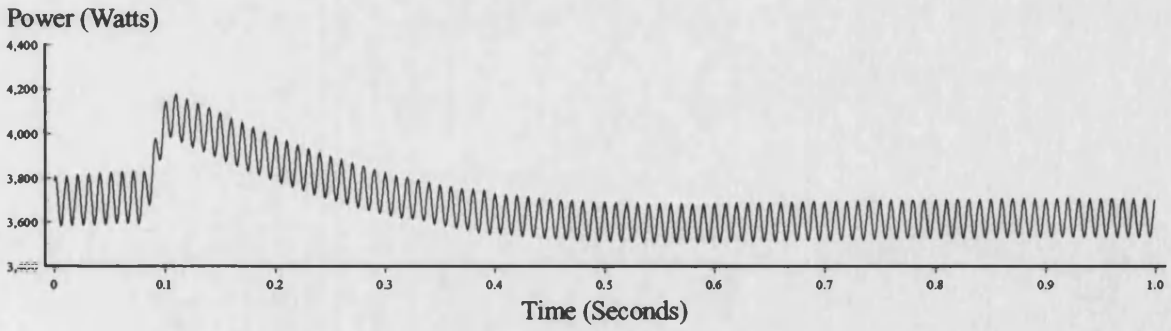

5.15a) Full Cycle Fourier Filtered Power.

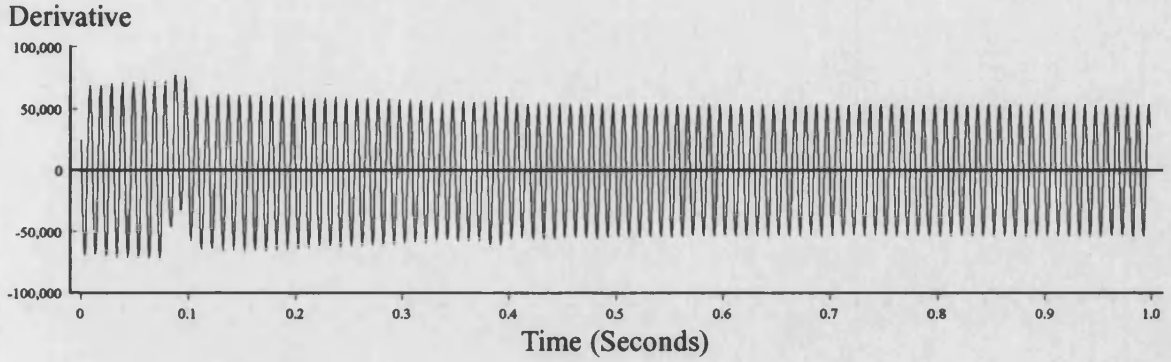

5.15b) Derivative of Filtered Power.

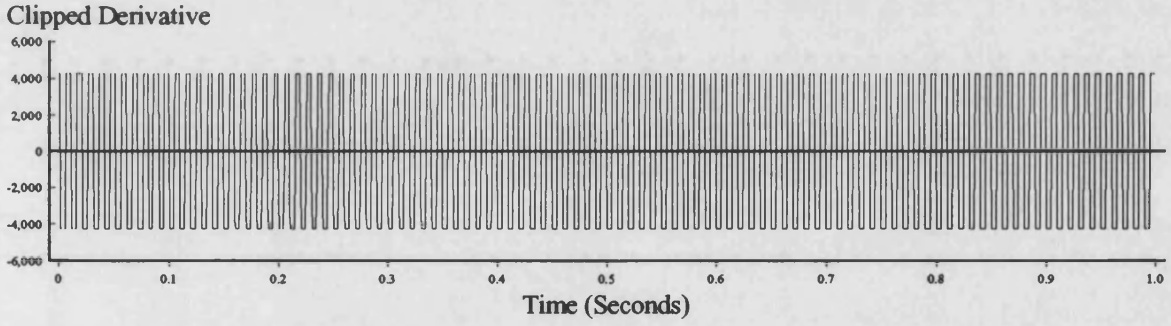

5.15c) Amplitude Limited Derivative.

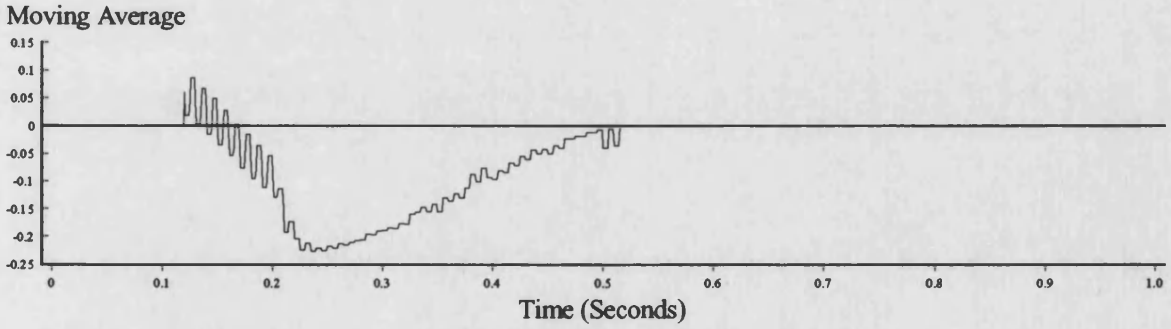

5.15d) Algorithm Output (6 Cycle Moving Average Filter).

Figure 5.15 : Algorithm Response to a Loss of Grid Resulting in a 10% Load Increase using Fourier Filtered Power at 24 Samples/Cycle.
(Laboratory System Result)

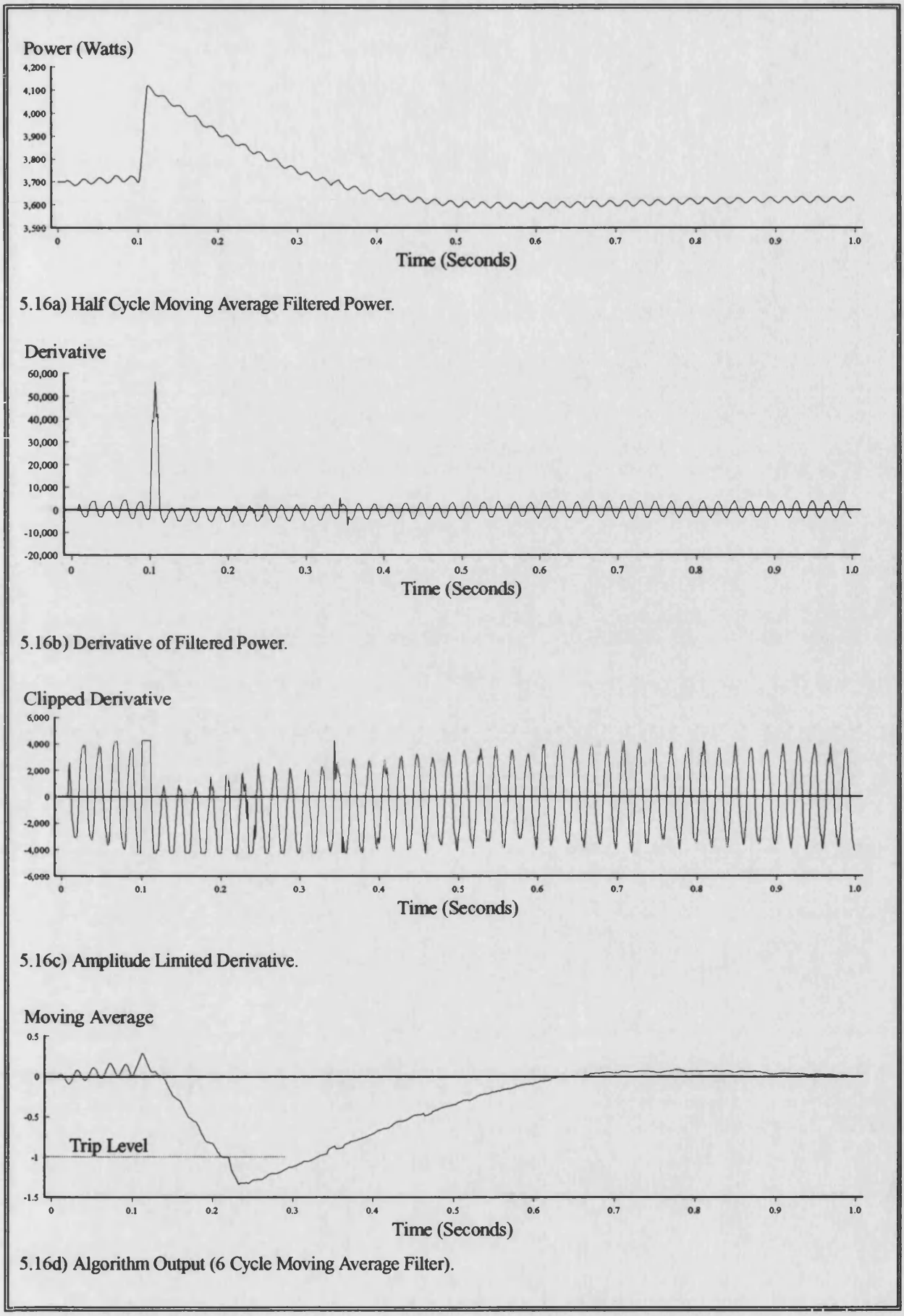

Figure 5.16 : Algorithm Response to a Loss of Grid Resulting in a 10% Load Increase using 1/2 Cycle Moving Average Power at 24 Samples/Cycle.
(Laboratory System Result)

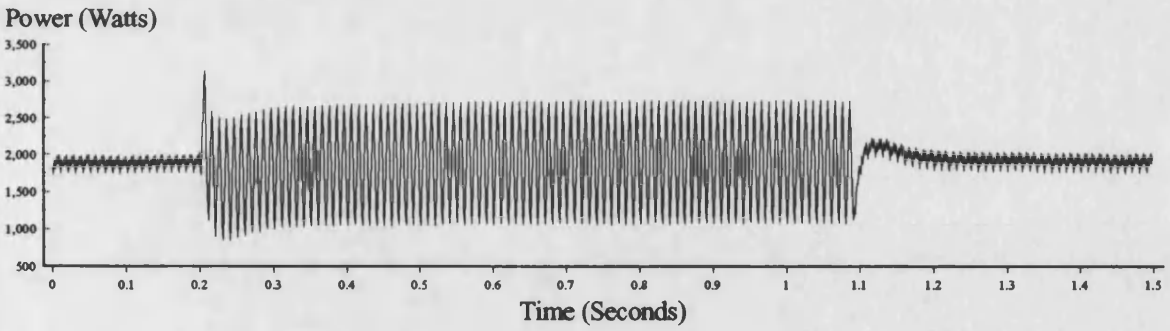

5.17a) Instantaneous Three Phase Output Power.

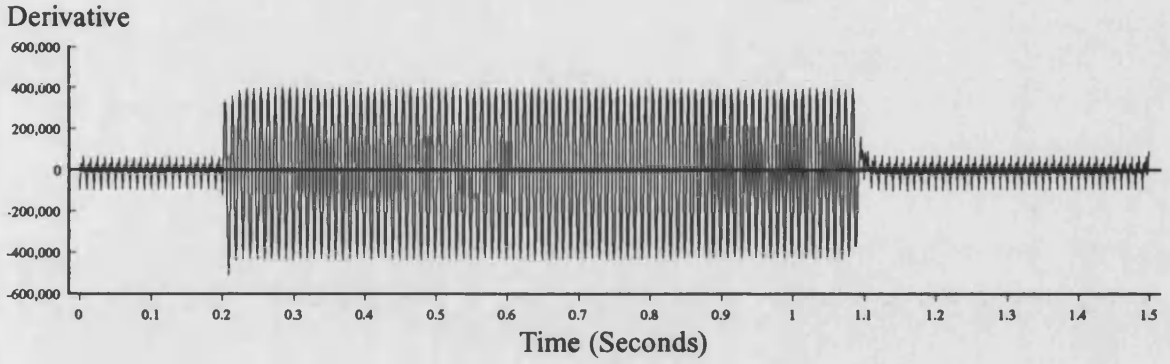

5.17b) Derivative of Power.

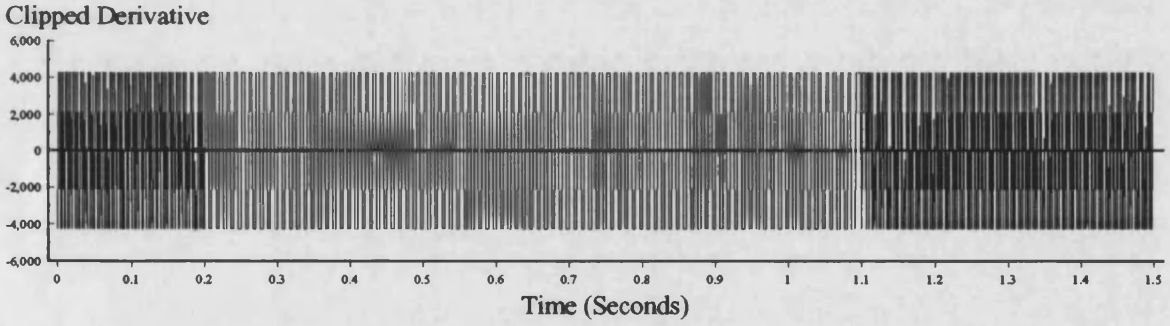

5.17c) Amplitude Limited Derivative.

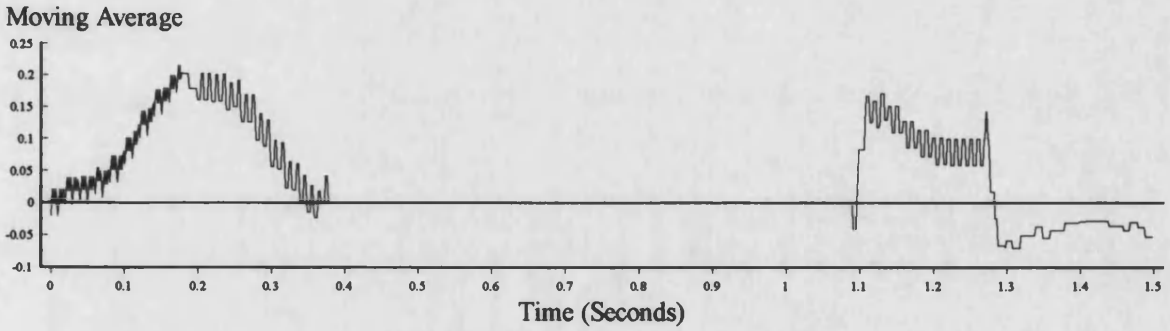

5.17d) Algorithm Output (6 Cycle Moving Average Filter).

Figure 5.17 : Algorithm Response to an A-Phase to Ground Fault
using Instantaneous Power at 24 Samples/Cycle.
(Laboratory System Result)

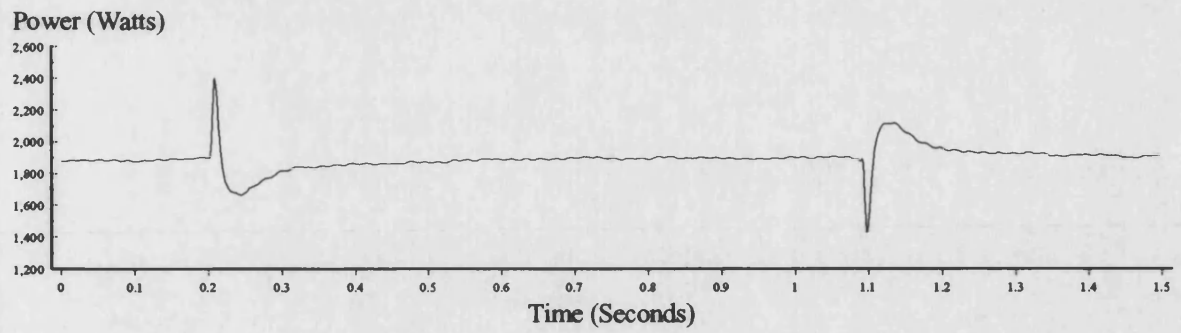

5.18a) Half Cycle Moving Average Filtered Power.

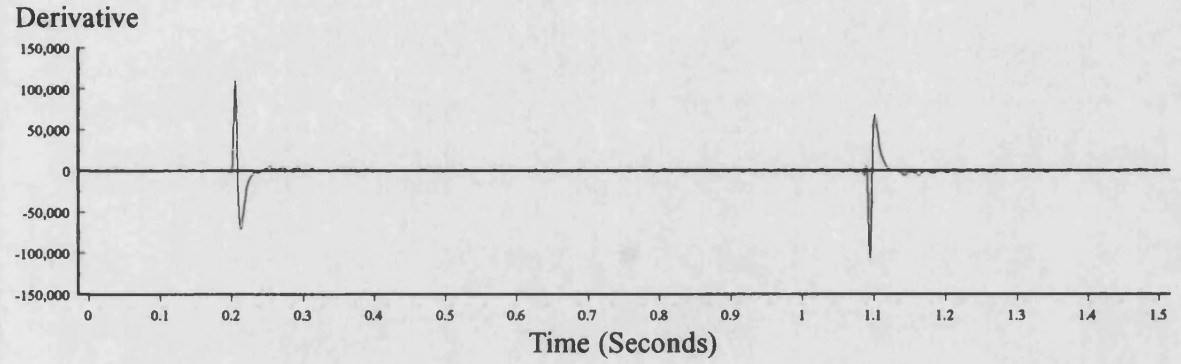

5.18b) Derivative of Filtered Power.

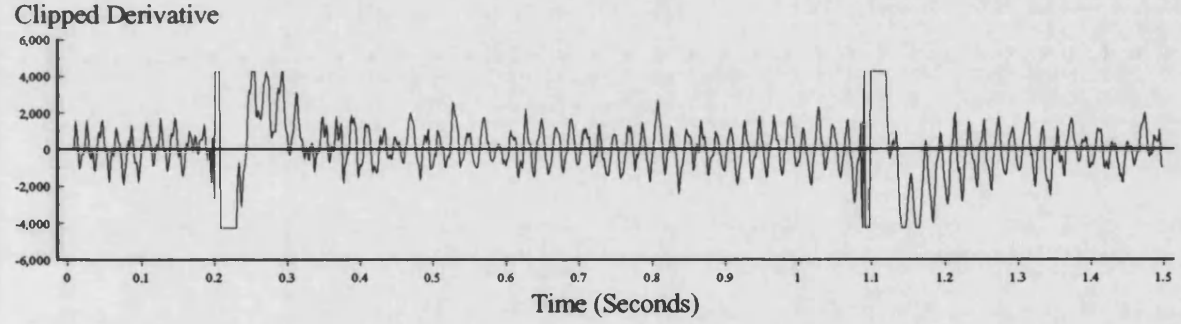

5.18c) Amplitude Limited Derivative.

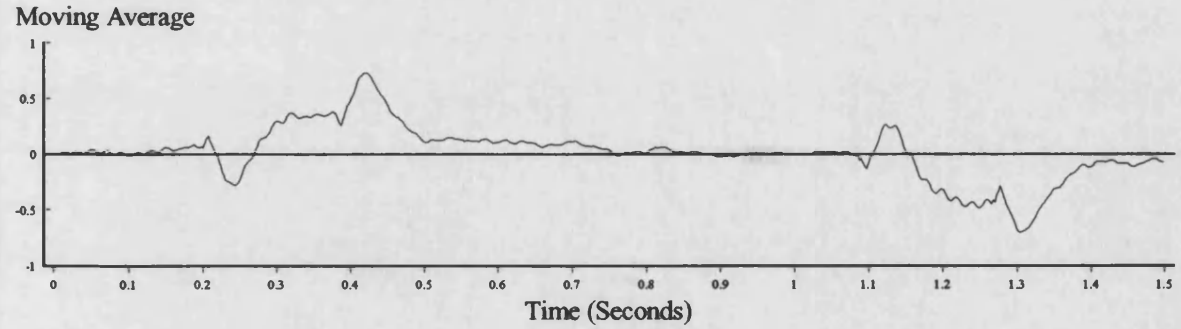

5.18d) Algorithm Output (6 Cycle Moving Average Filter).

Figure 5.18 : Algorithm Response to an A-Phase to Ground Fault using 1/2 Cycle Moving Average Power at 24 Samples/Cycle. (Laboratory System Result)

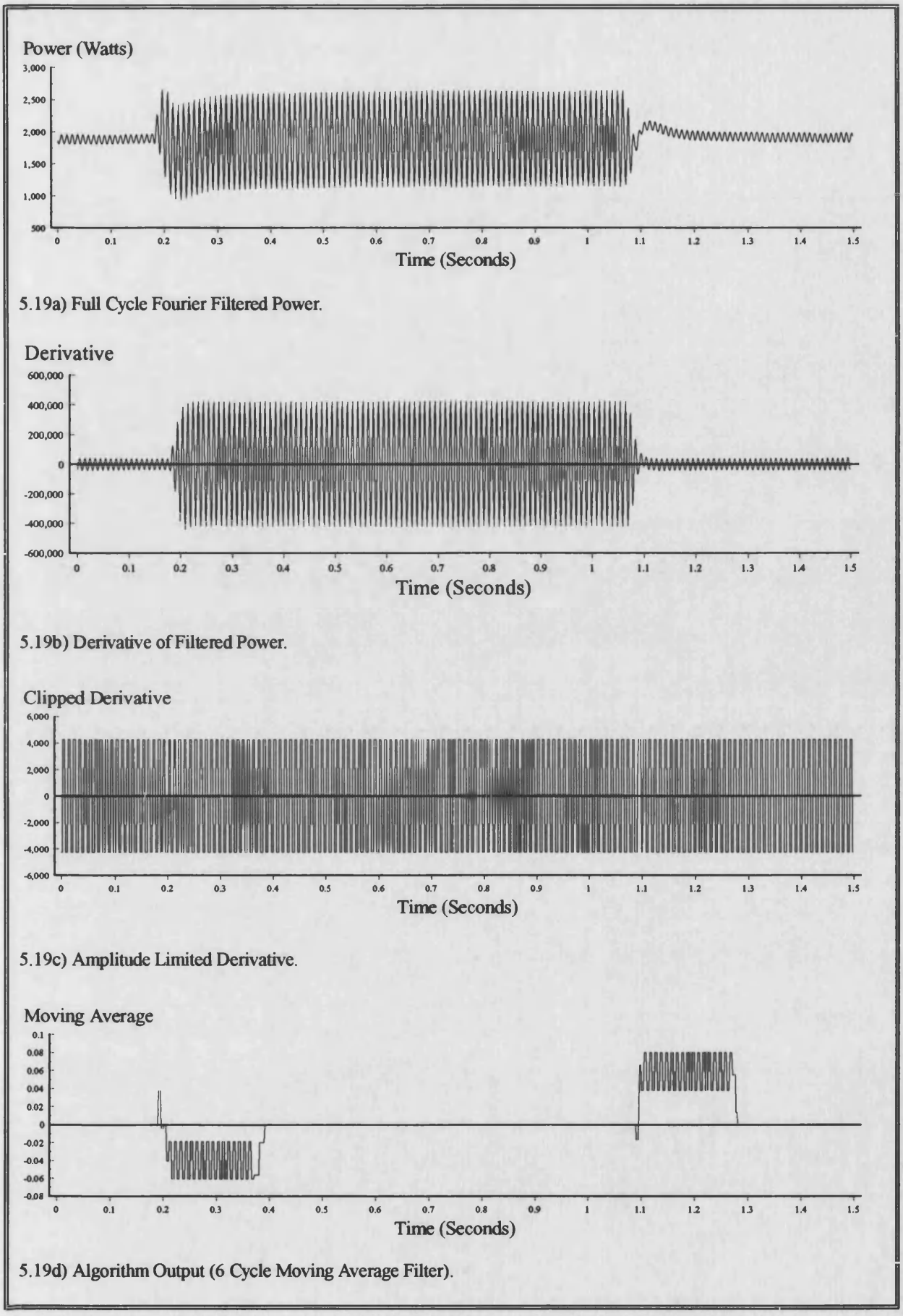

Figure 5.19 : Algorithm Response to an A-Phase to Ground Fault using Fourier Filtered Power at 24 Samples/Cycle. (Laboratory System Result)

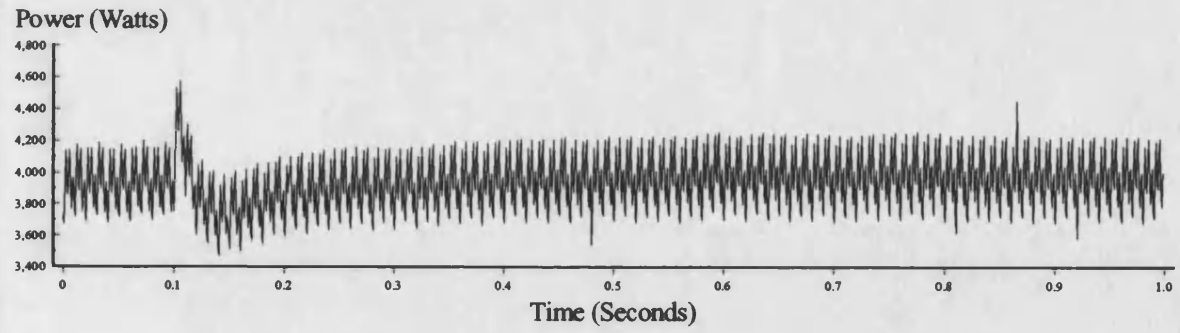

5.20a) Instantaneous Three Phase Output Power.

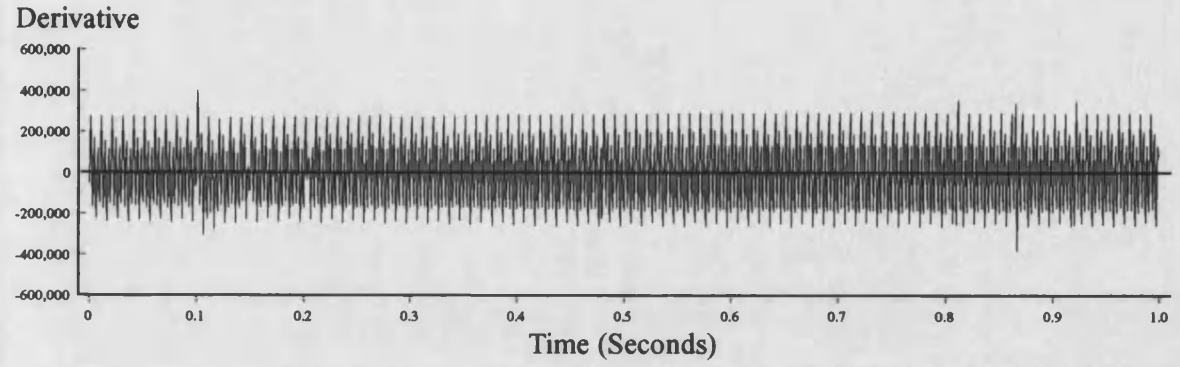

5.20b) Derivative of Power.

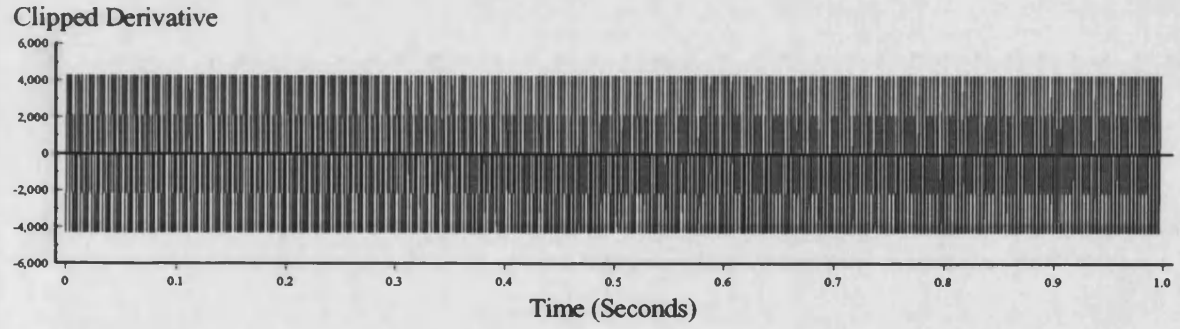

5.20c) Amplitude Limited Derivative.

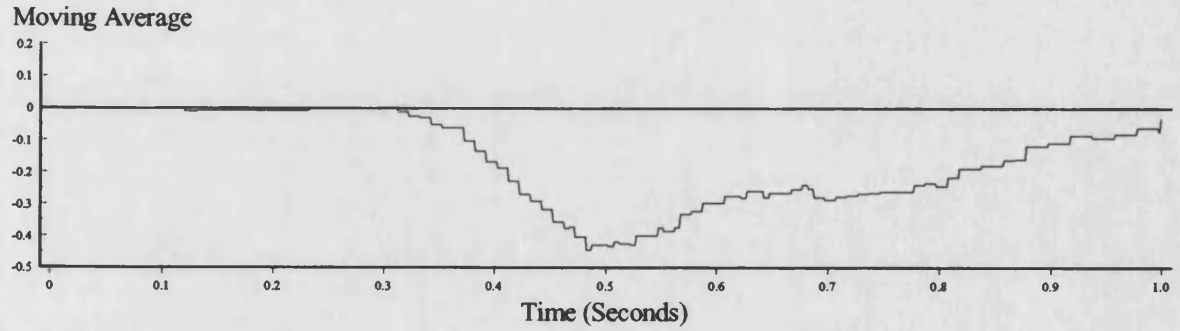

5.20d) Algorithm Output (6 Cycle Moving Average Filter).

Figure 5.20 : Algorithm Response to a 100% Load Increase under Parallel Operation using Instantaneous Power at 24 Samples/Cycle.
(Laboratory System Result)

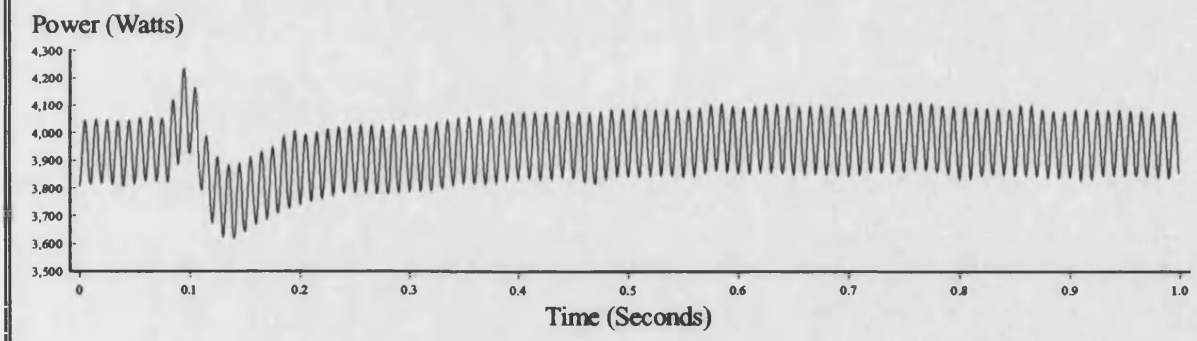

5.21a) Full Cycle Fourier Filtered Power.

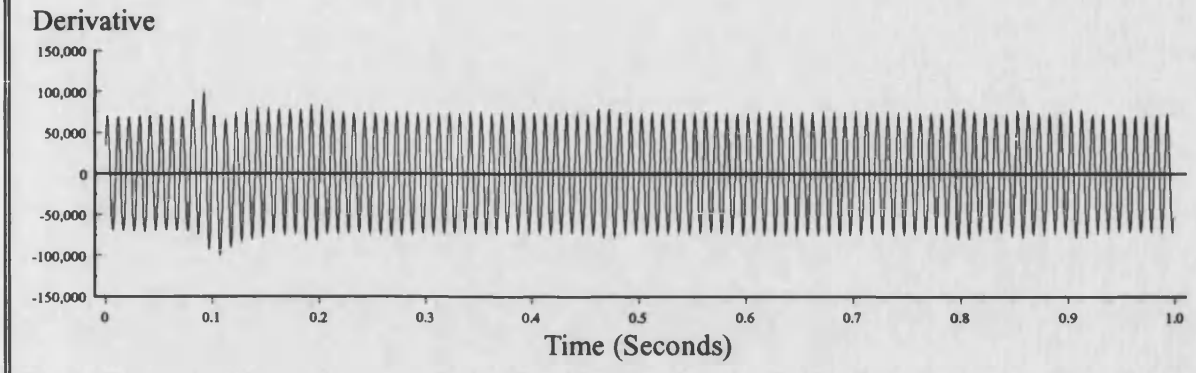

5.21b) Derivative of Filtered Power.

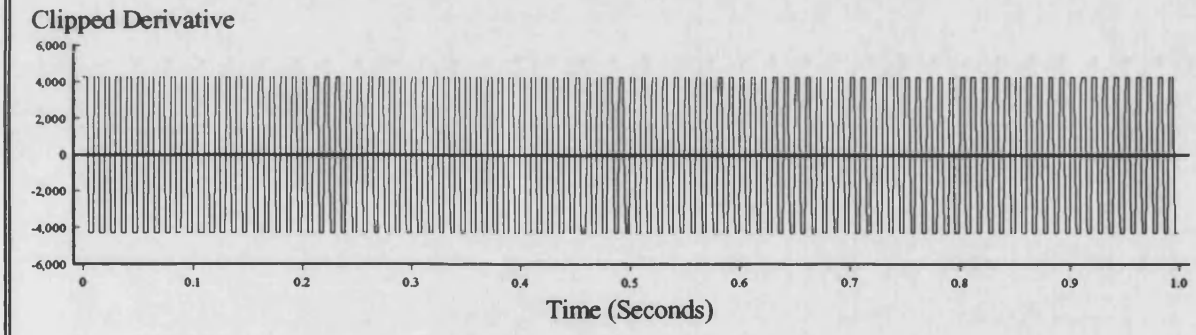

5.21c) Amplitude Limited Derivative.

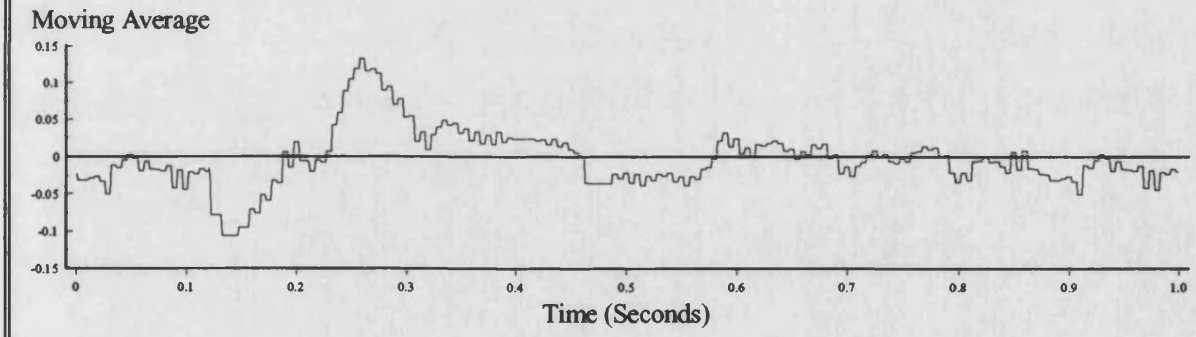

5.21d) Algorithm Output (6 Cycle Moving Average Filter).

Figure 5.21 : Algorithm Response to a 100% Load Increase under Parallel Operation using Fourier Filtered Power at 24 Samples/Cycle.
(Laboratory System Result)

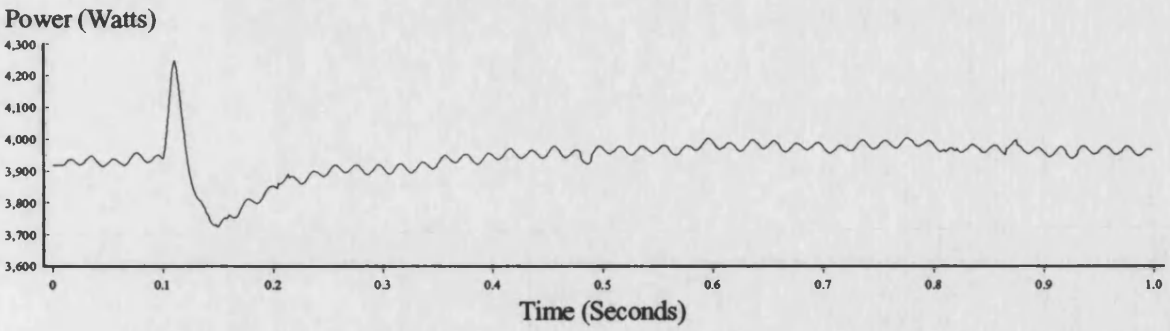

5.22a) Half Cycle Moving Average Filtered Power.

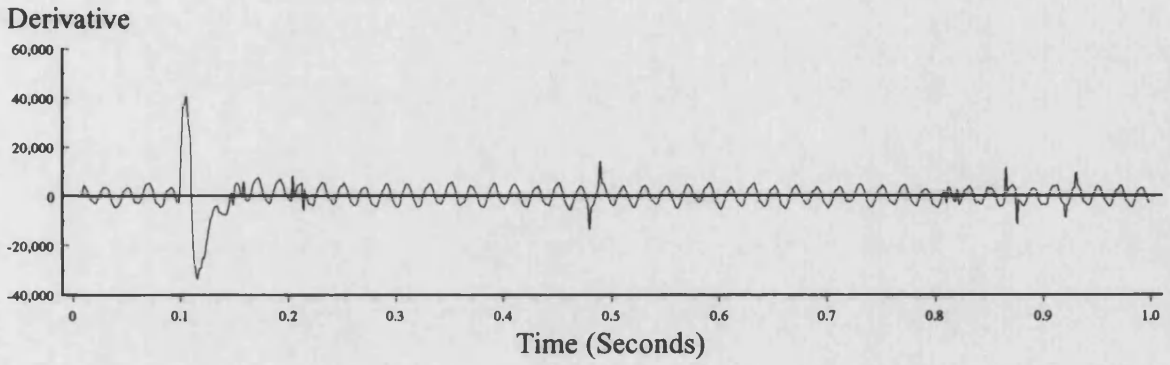

5.22b) Derivative of Filtered Power.

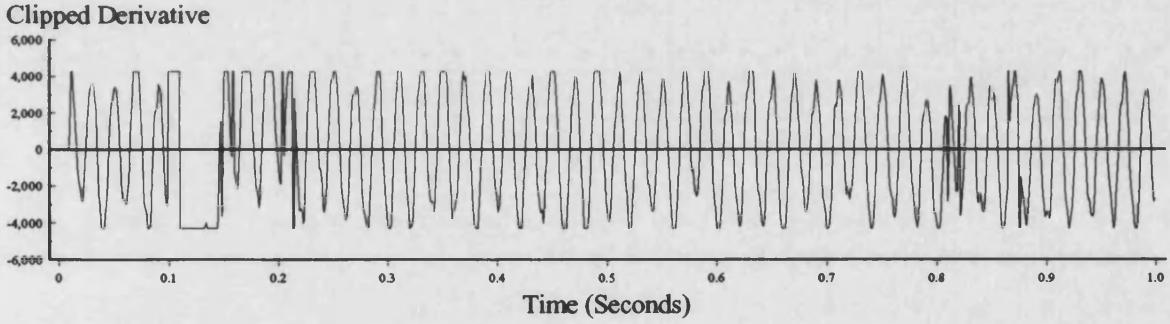

5.22c) Amplitude Limited Derivative.

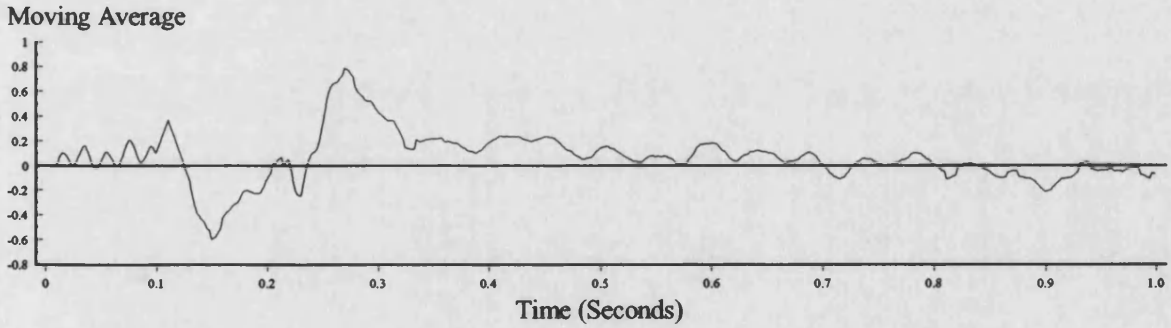

5.22d) Algorithm Output (6 Cycle Moving Average Filter).

Figure 5.22 : Algorithm Response to a 100% Load Increase under Parallel Operation using 1/2 Cycle Moving Average Power at 24 Samples/Cycle. (Laboratory System Result)

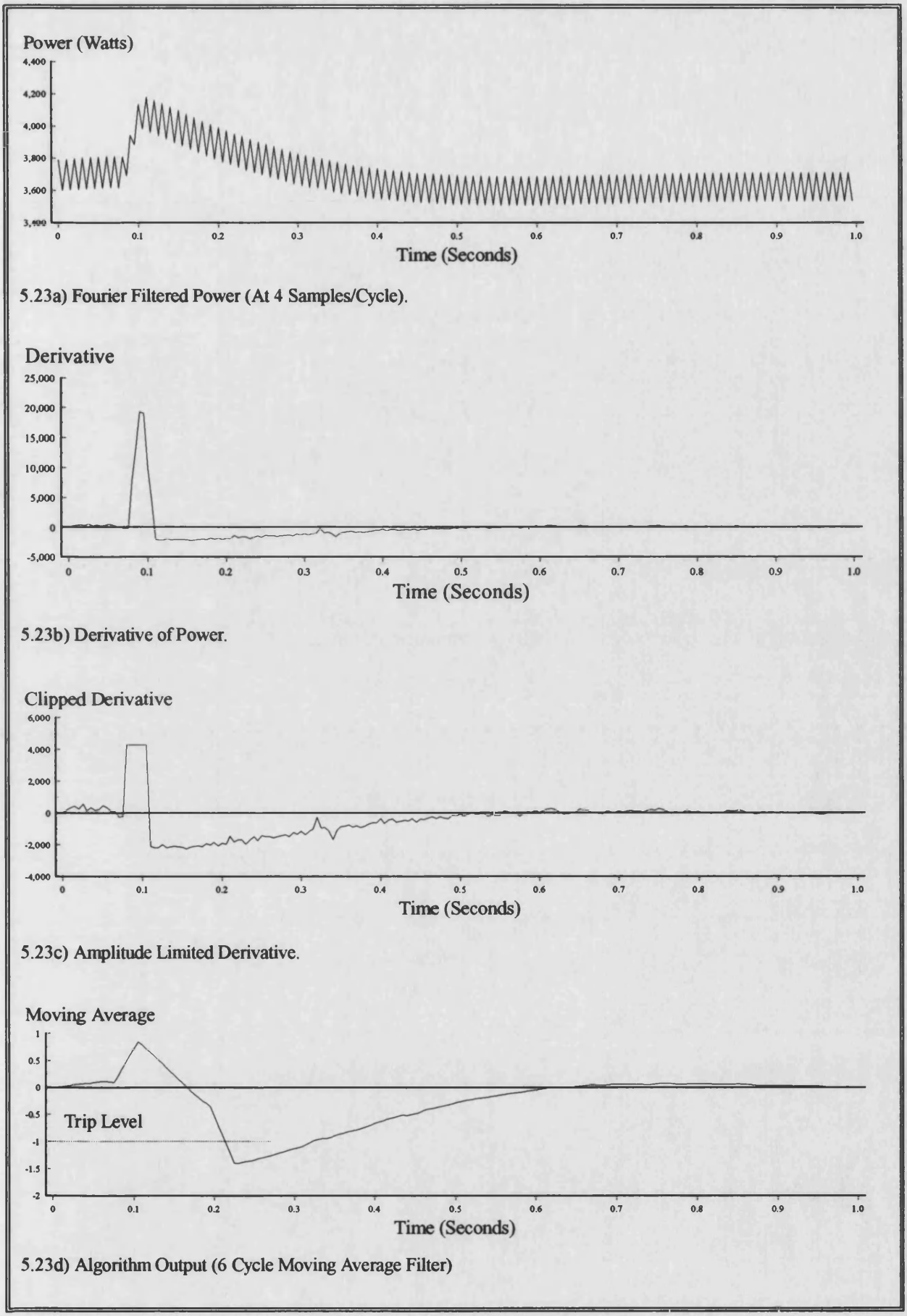

5.23a) Fourier Filtered Power (At 4 Samples/Cycle).

5.23b) Derivative of Power.

5.23c) Amplitude Limited Derivative.

5.23d) Algorithm Output (6 Cycle Moving Average Filter)

Figure 5.23 : Algorithm Response to a Loss of Grid Resulting in a 10% Load Increase using Fourier Filtered Power at 4 Samples/Cycle.
(Laboratory System Result)

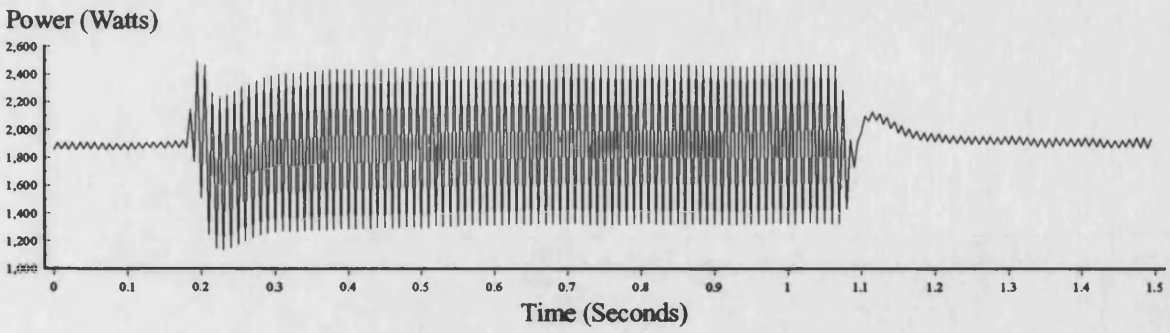

5.24a) Fourier Filtered Power (At 4 Samples/Cycle).

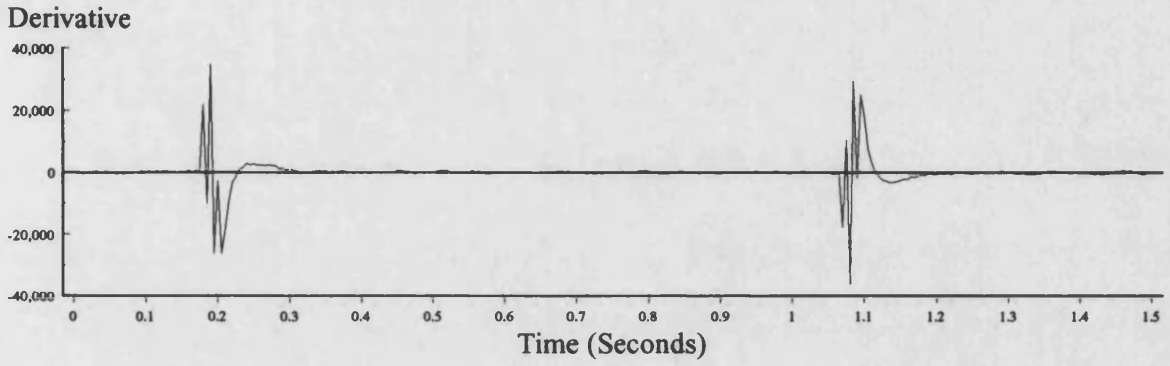

5.24b) Derivative of Power.

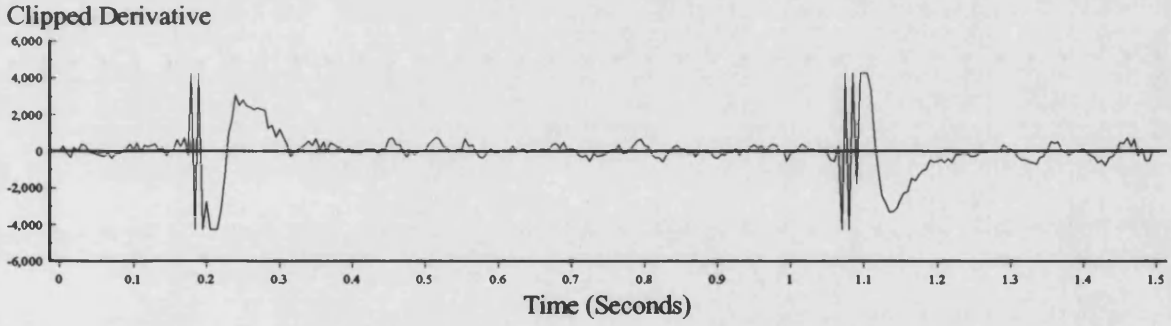

5.24c) Amplitude Limited Derivative.

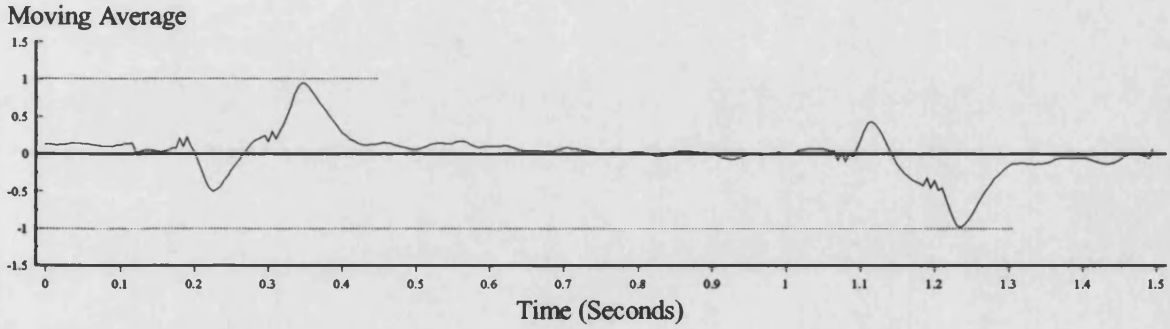

5.24d) Algorithm Output (6 Cycle Moving Average Filter).

Figure 5.24 : Algorithm Response to an A-Phase to Ground Fault
using Fourier Filtered Power at 4 Samples/Cycle.
(Laboratory System Result)

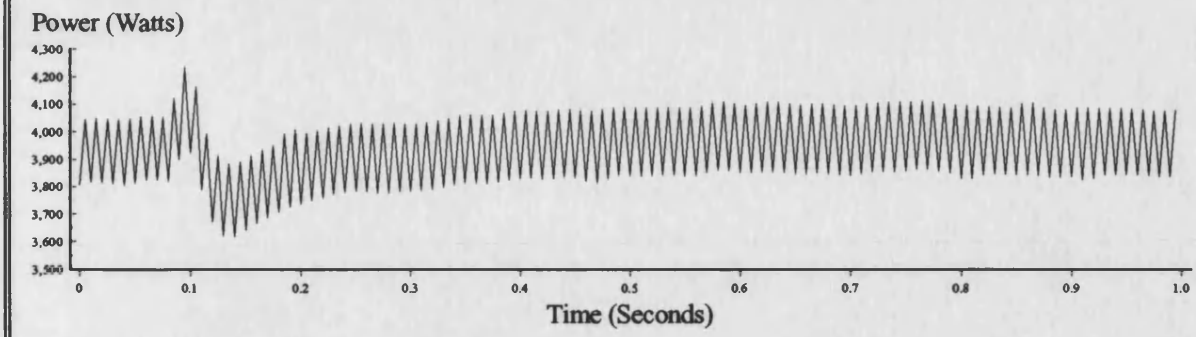

5.25a) Fourier Filtered Power (At 4 Samples/Cycle).

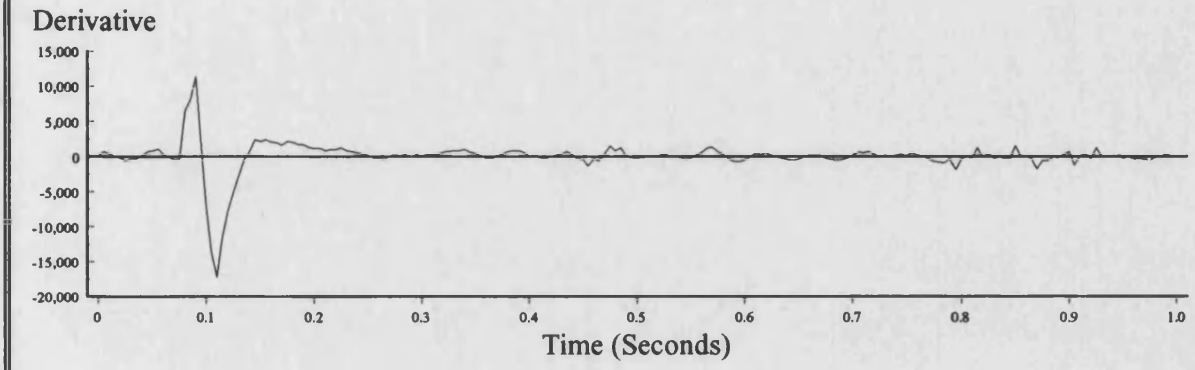

5.25b) Derivative of Power.

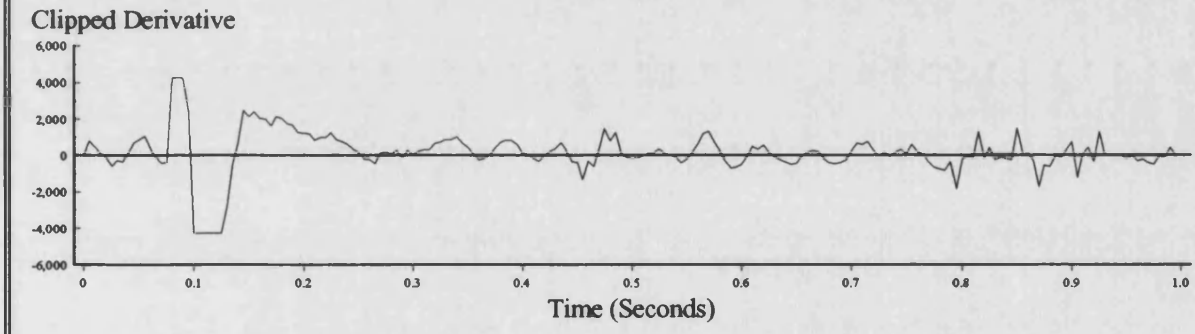

5.25c) Amplitude Limited Derivative.

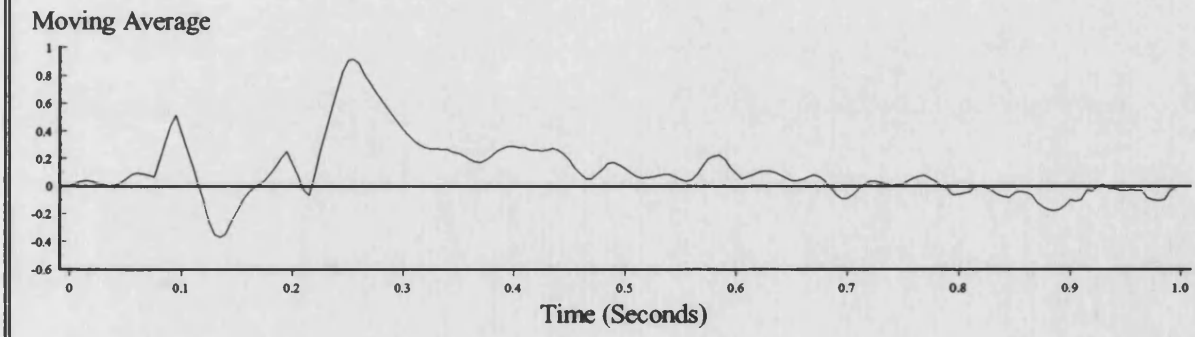

5.25d) Algorithm Output (6 Cycle Moving Average Filter).

Figure 5.25 : Algorithm Response to a 100% Load Increase under Parallel Operation using Fourier Filtered Power at 4 Samples/Cycle.
(Laboratory System Result)

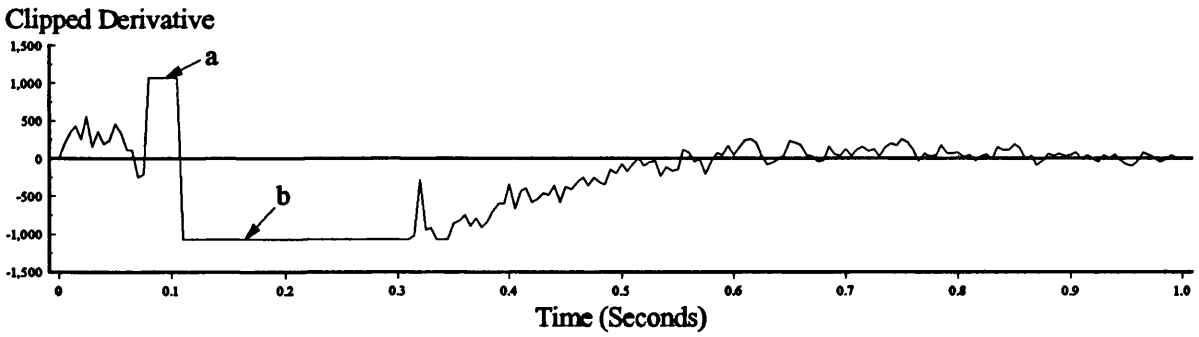

5.26a) Amplitude Limited Derivative for 2.5% Setting.

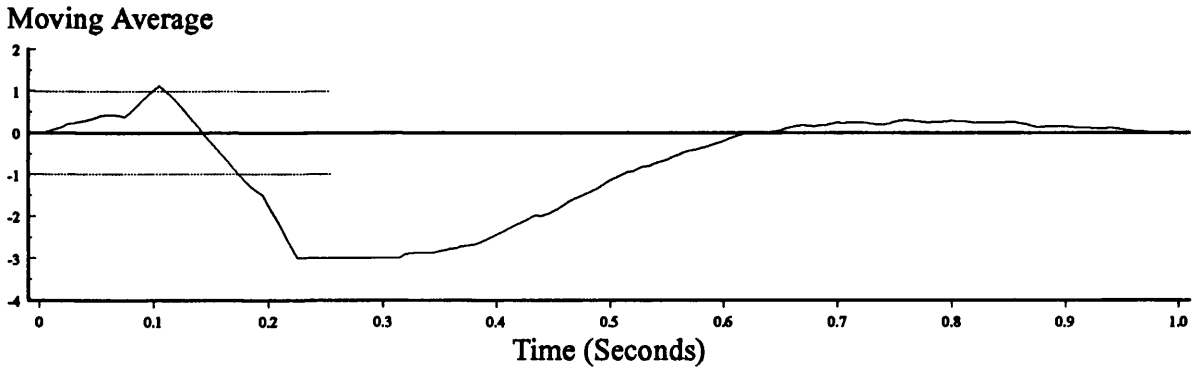

5.26b) Algorithm Output for 2.5% Setting.

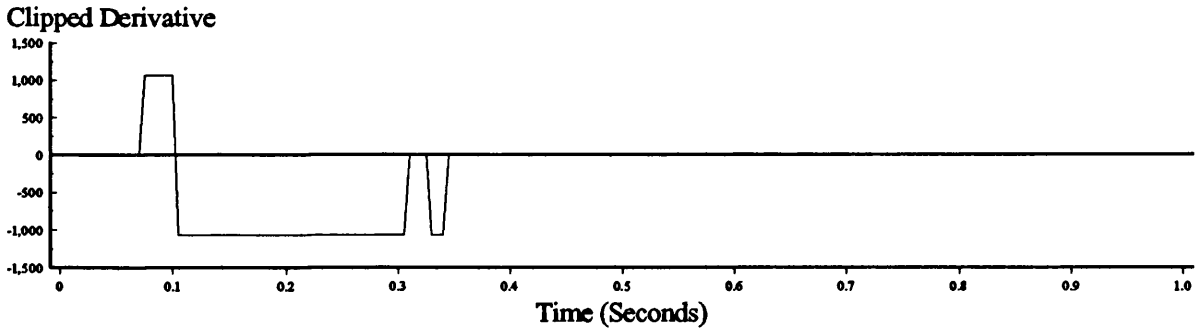

5.26c) Amplitude Limited Derivative for 2.5% Setting with Pattern Recognition.

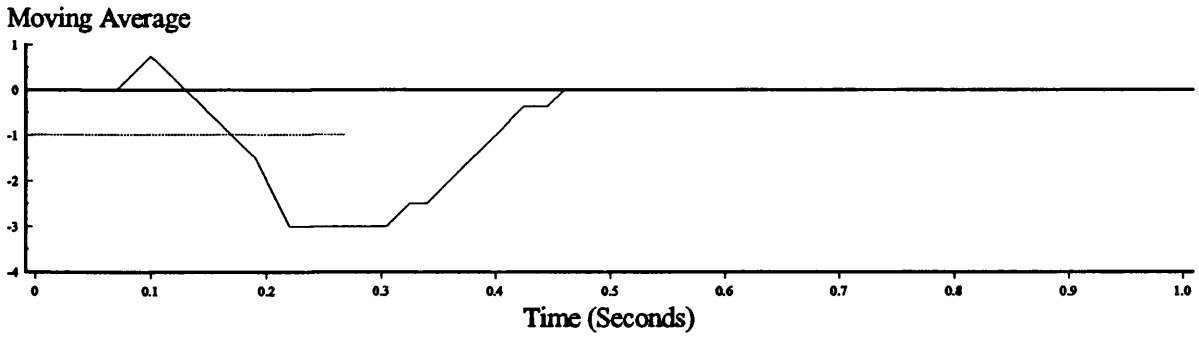

5.26d) Algorithm Output for 2.5% Setting with Pattern Recognition.

Figure 5.26 : Algorithm Response to a Loss of Grid Resulting in a 10% Load Increase using Fourier Filtered Power at 4 Samples/Cycle with 2.5% Setting. (Laboratory System Result)

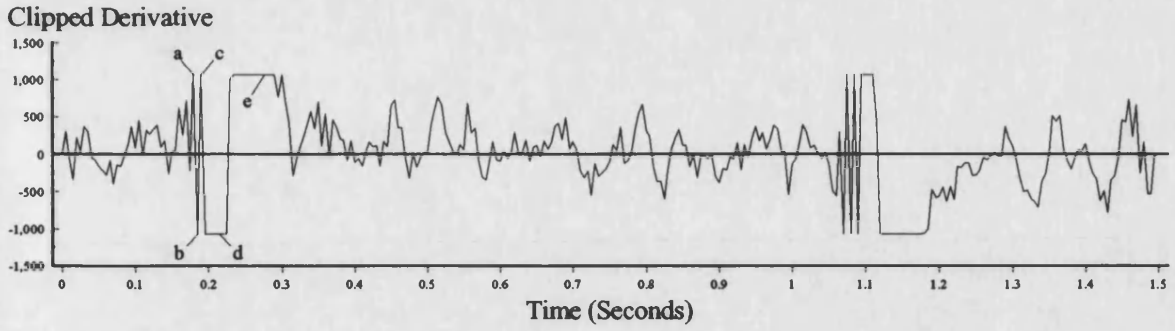

5.27a) Amplitude Limited Derivative for 2.5% Setting.

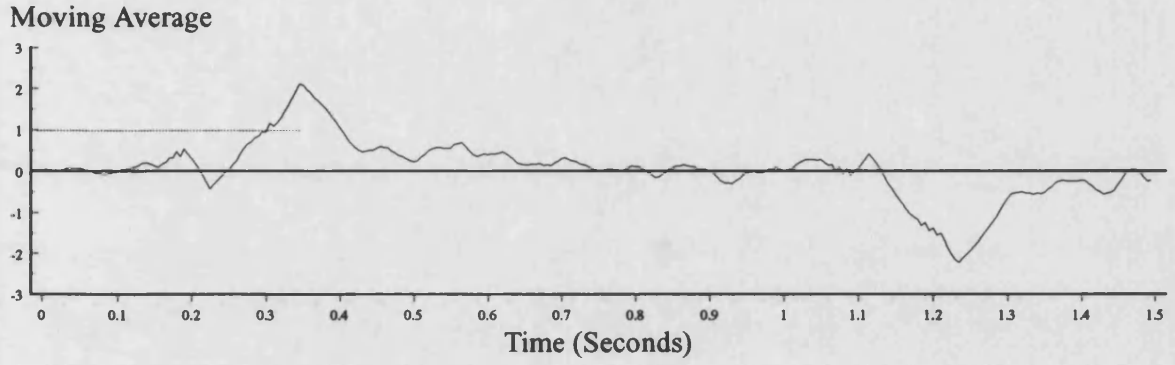

5.27b) Algorithm Output for 2.5% Setting.

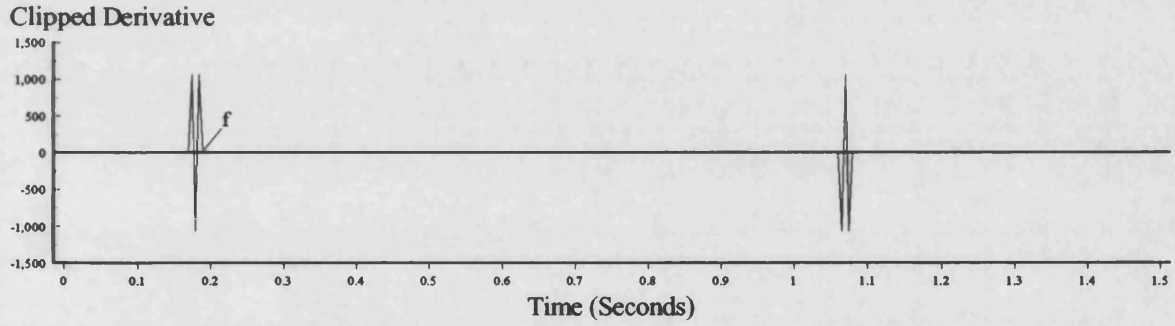

5.27c) Amplitude Limited Derivative for 2.5% Setting with Pattern Recognition.

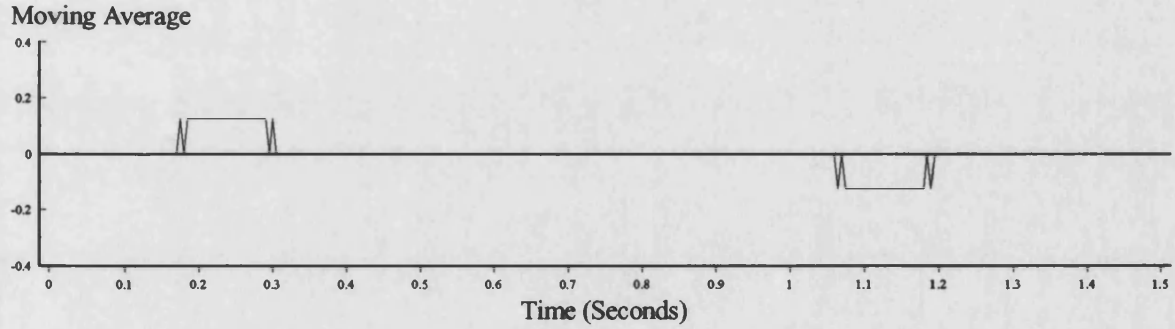

5.27d) Algorithm Output for 2.5% Setting with Pattern Recognition.

Figure 5.27 : Algorithm Response to an A-Phase to Ground Fault using Fourier Filtered Power at 4 Samples/Cycle with 2.5% Setting. (Laboratory System Result)

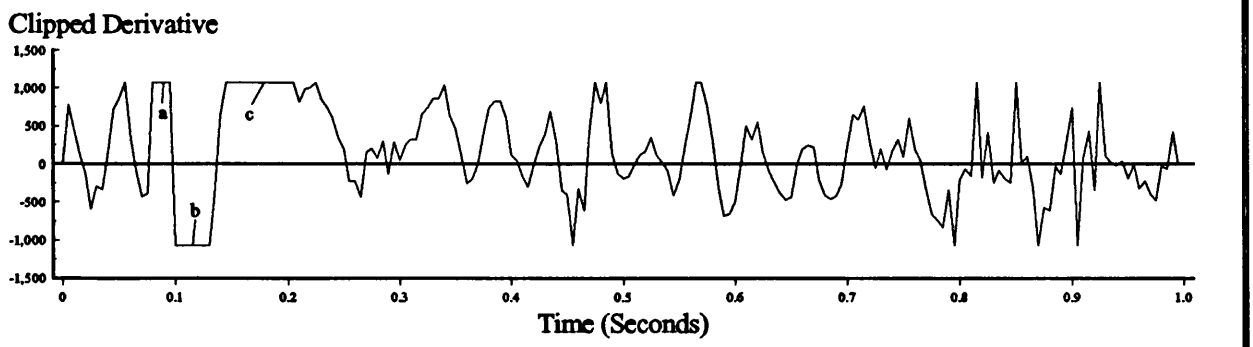

5.28a) Amplitude Limited Derivative for 2.5% Setting.

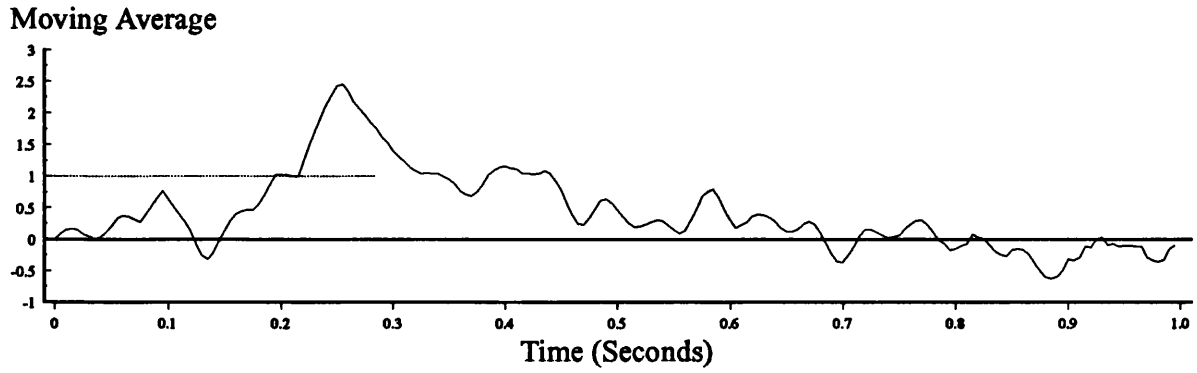

5.28b) Algorithm Output for 2.5% Setting.

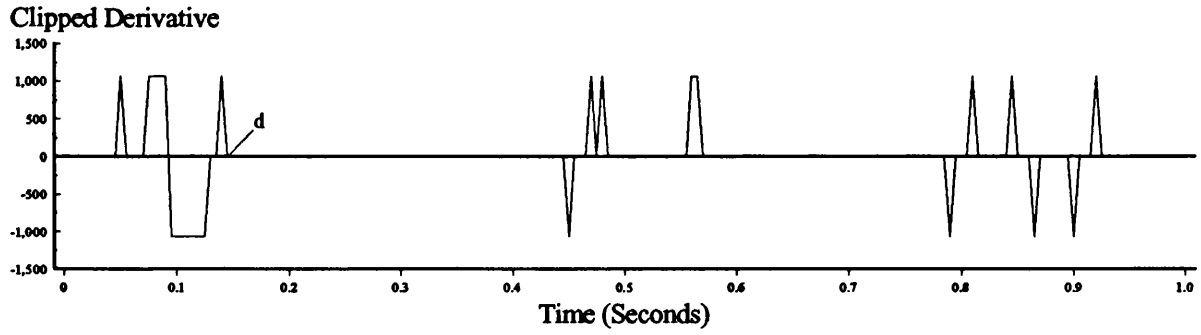

5.28c) Amplitude Limited Derivative for 2.5% Setting with Pattern Recognition.

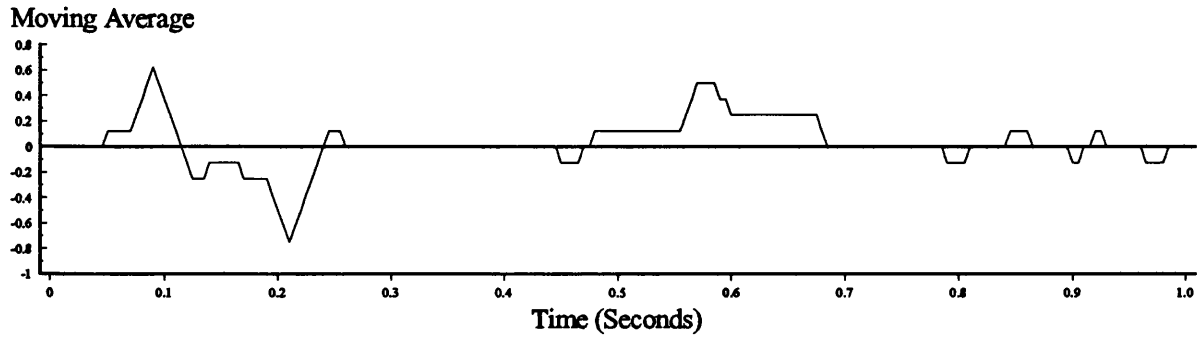

5.28d) Algorithm Output for 2.5% Setting with Pattern Recognition.

Figure 5.28 : Algorithm Response to a 100% Load Increase under Parallel Operation using Fourier Filtered Power at 4 Samples/Cycle for 2.5% Setting. (Laboratory System Result)

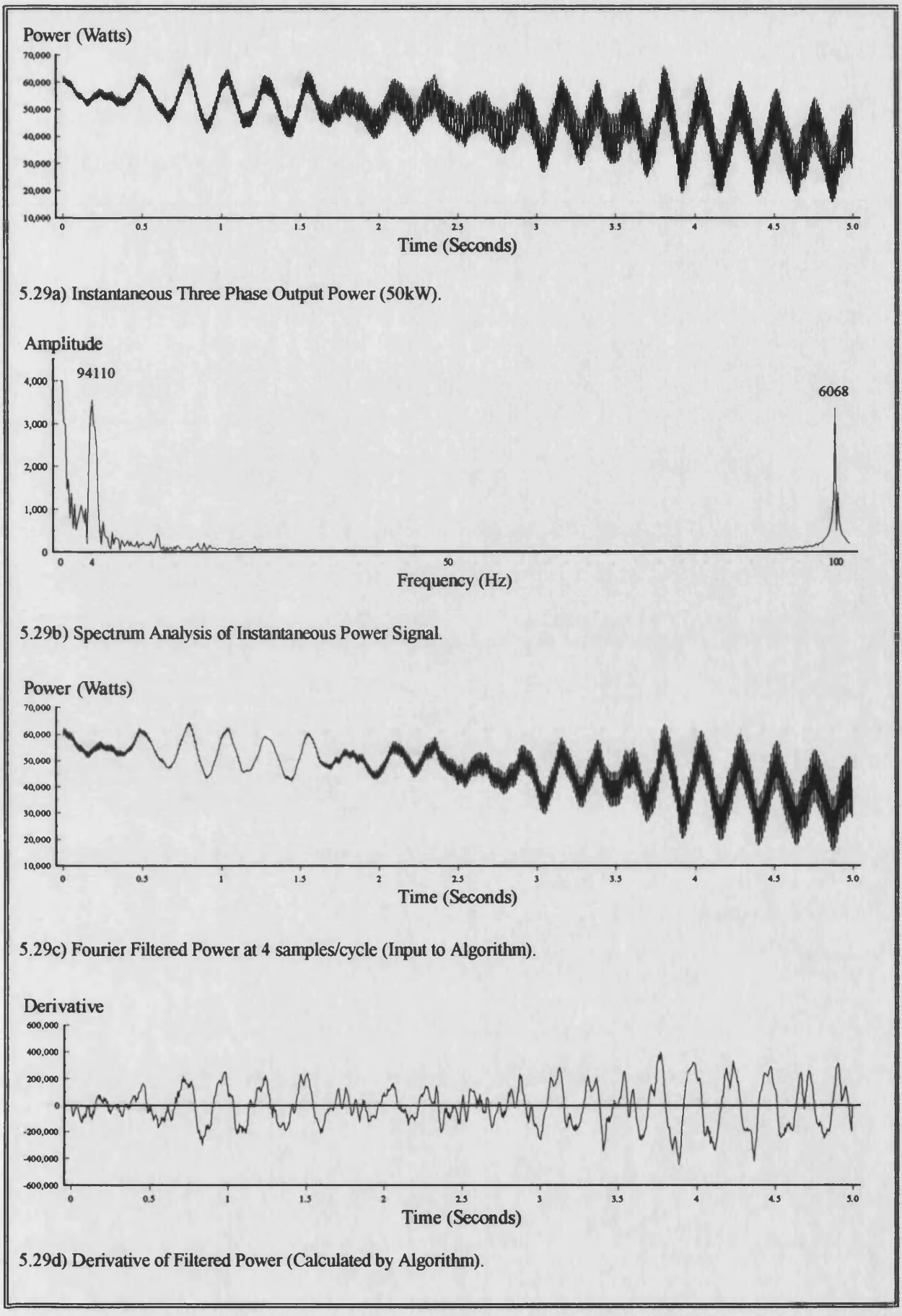

Figure 5.29 : Steady State Parallel Operation (50kW).
(Field Trial Result)

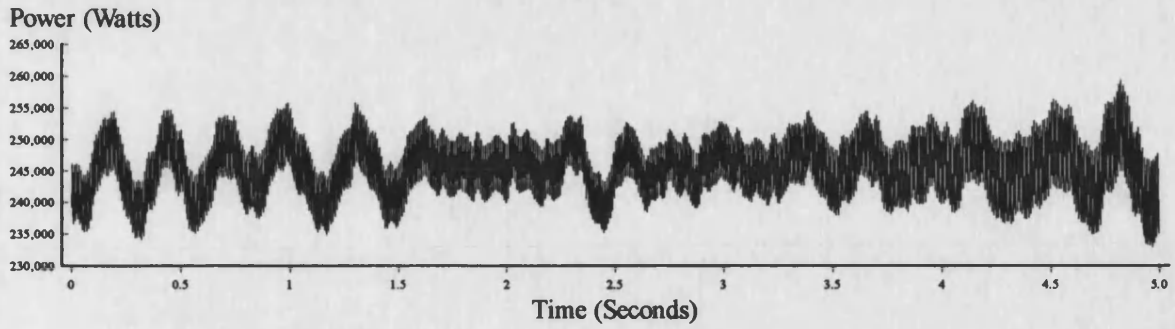

5.30a) Instantaneous Three Phase Output Power (250kW).

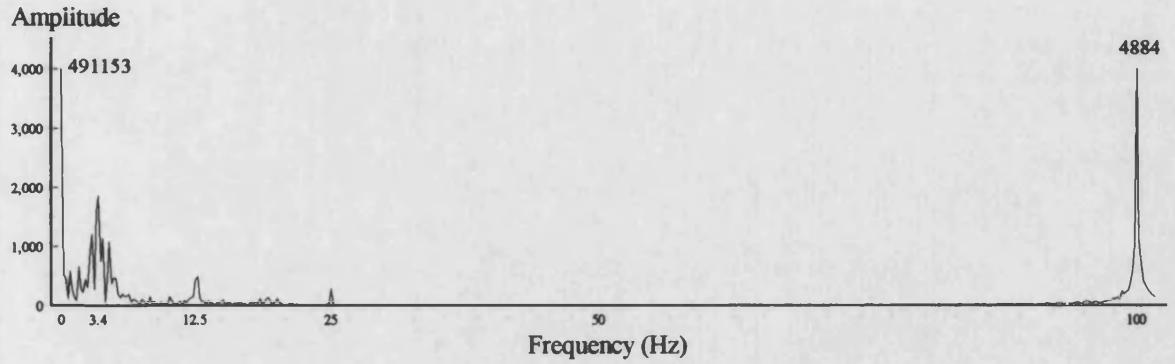

5.30b) Spectrum Analysis of Instantaneous Power Signal.

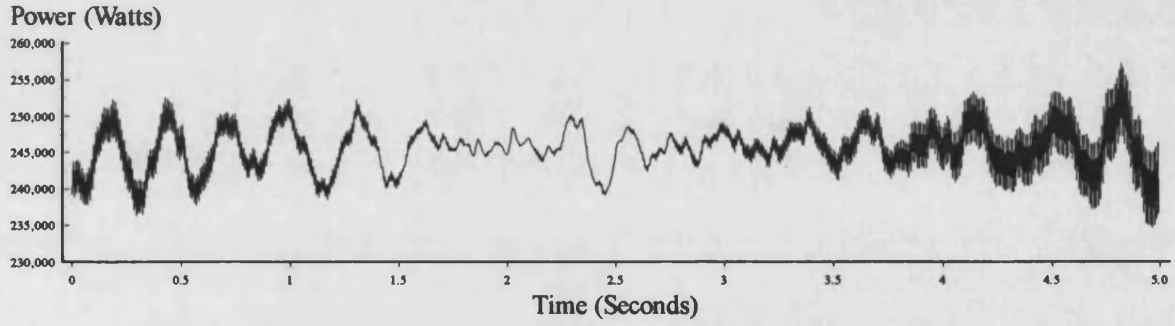

5.30c) Fourier Filtered Power at 4 samples/cycle (Input to Algorithm).

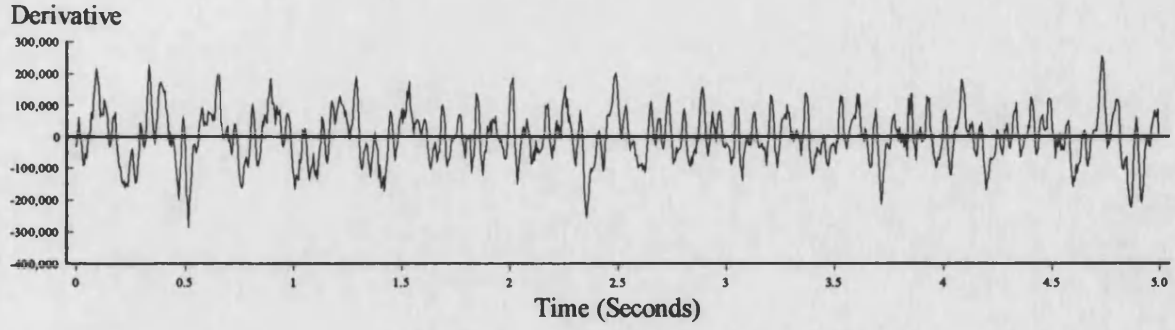

5.30d) Derivative of Filtered Power (Calculated by Algorithm).

Figure 5.30 : Steady State Parallel Operation (250kW).
(Field Trial Result)

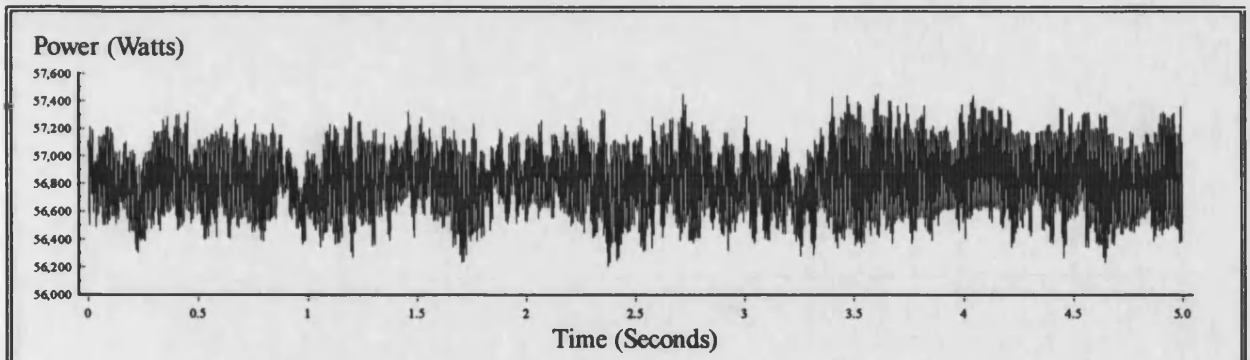

5.31a) Instantaneous Three Phase Output Power (50kW).

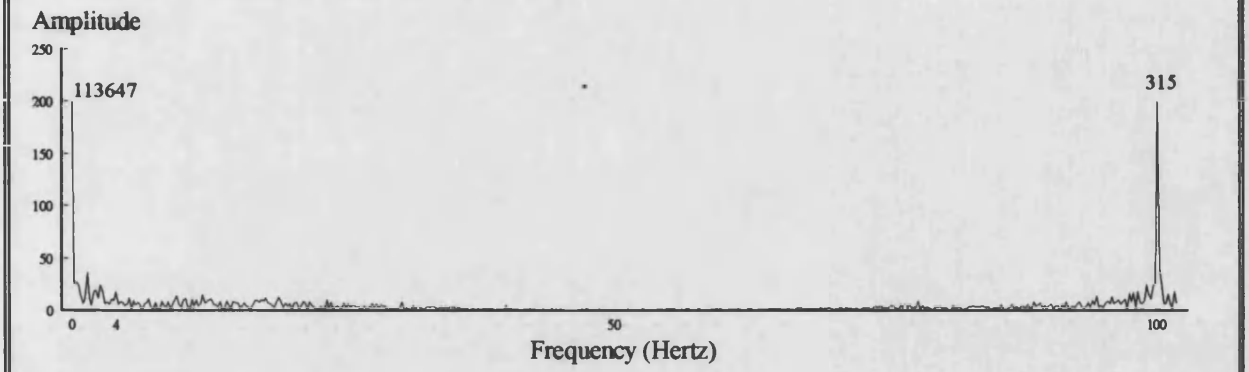

5.31b) Spectrum Analysis of Instantaneous Power Signal.

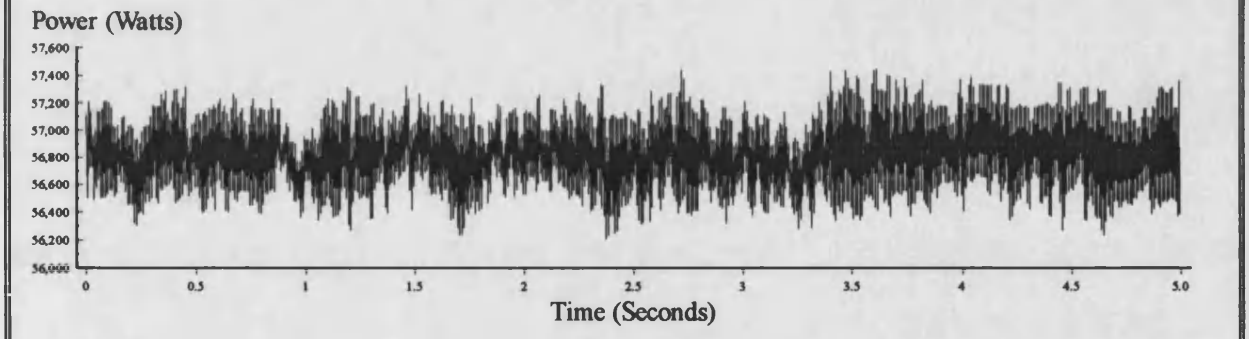

5.31c) Fourier Filtered Power at 4 samples/cycle (Input to Algorithm).

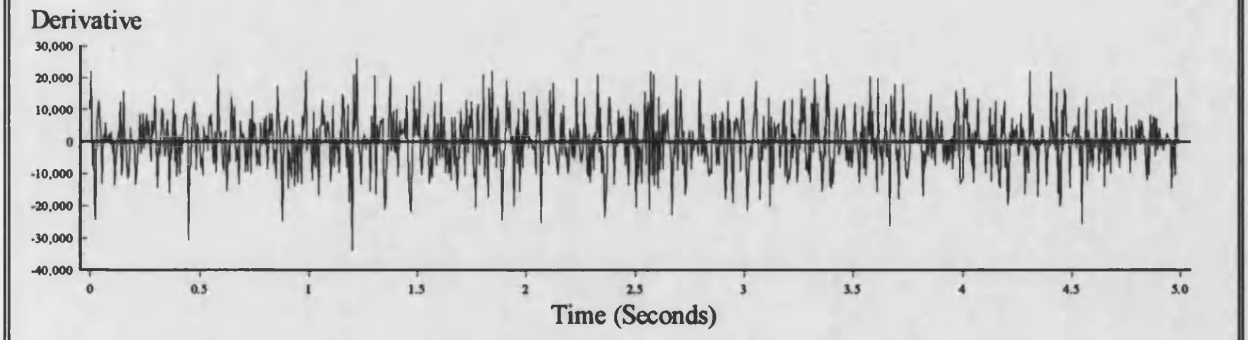

5.31d) Derivative of Filtered Power (Calculated by Algorithm).

Figure 5.31 : Steady State Independent Operation (50kW).
(Field Trial Result)

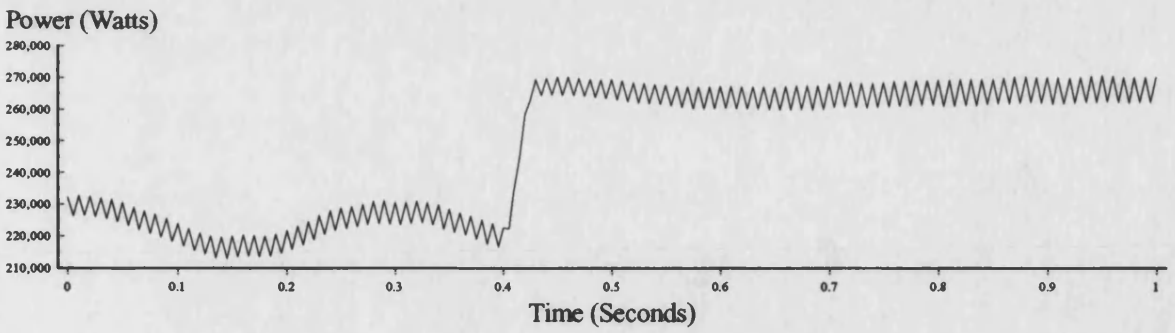

5.32a) Fourier Filtered Power at 4 samples/cycle (Input to Algorithm).

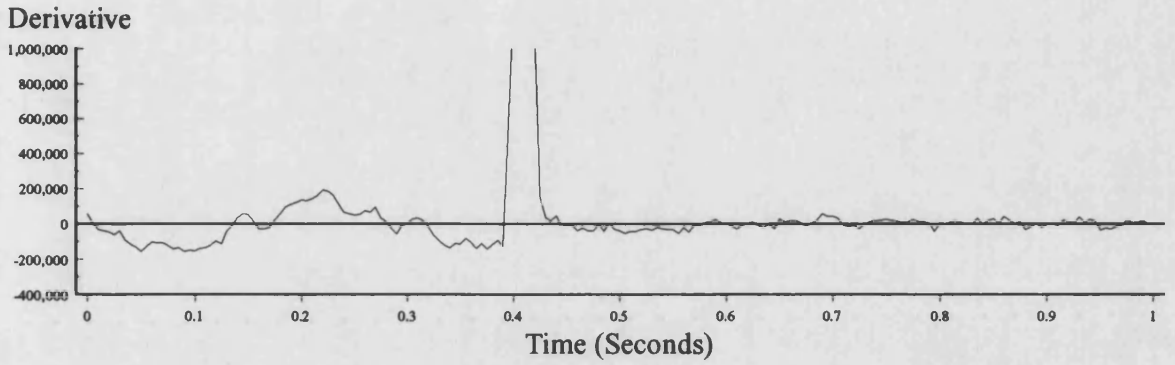

5.32b) Derivative of Filtered Power.

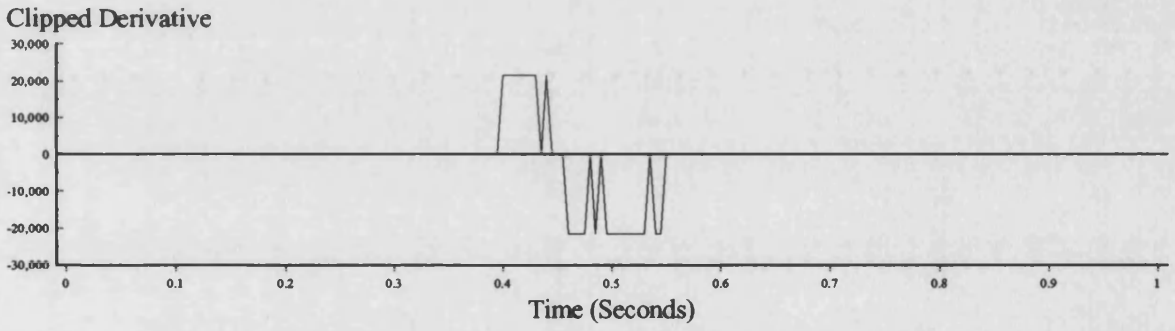

5.32c) Amplitude Limited Derivative.

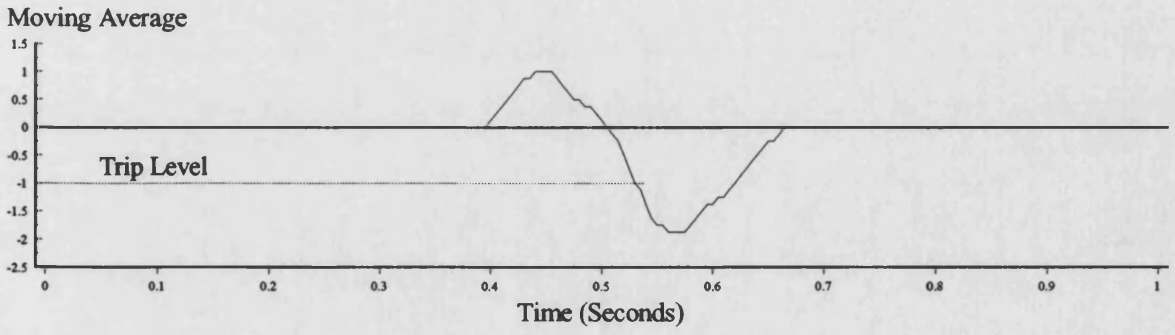

5.32d) Algorithm Output (6 Cycle Moving Average Filter).

Figure 5.32 : Algorithm Response to a Loss of Grid Resulting in a 20% Increase in Loading. (Field Trial Results)

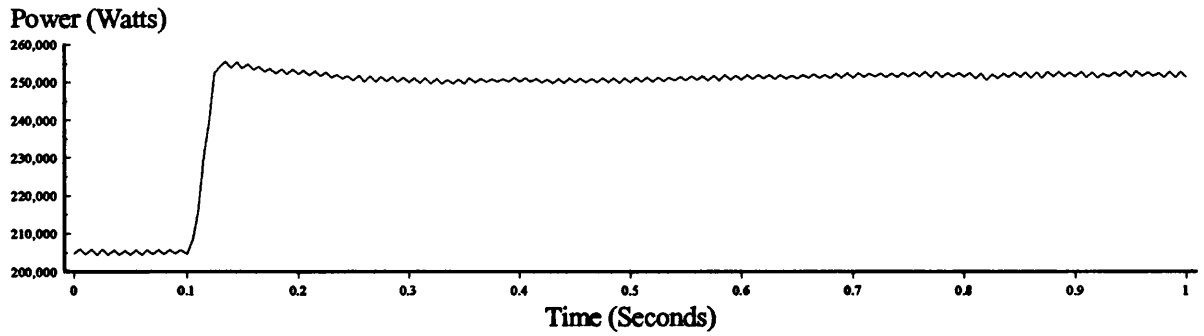

5.33a) Fourier Filtered Power at 4 samples/cycle (Input to Algorithm).

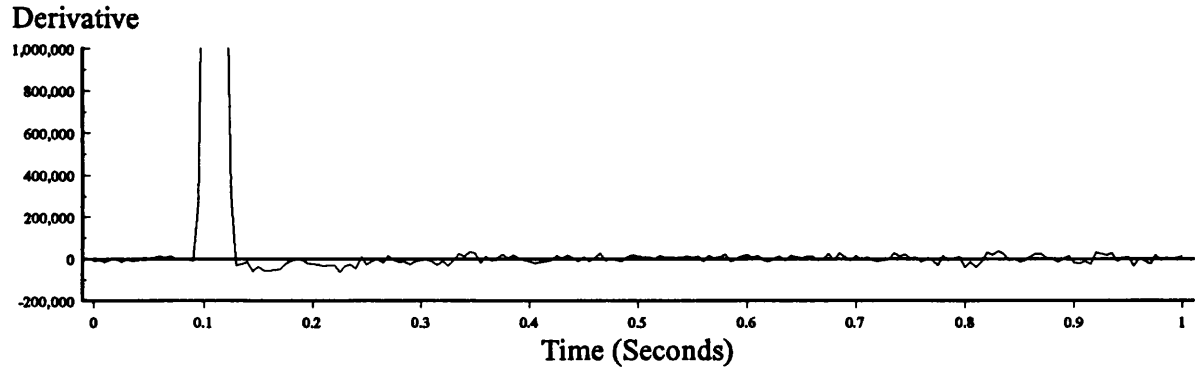

5.33b) Derivative of Filtered Power.

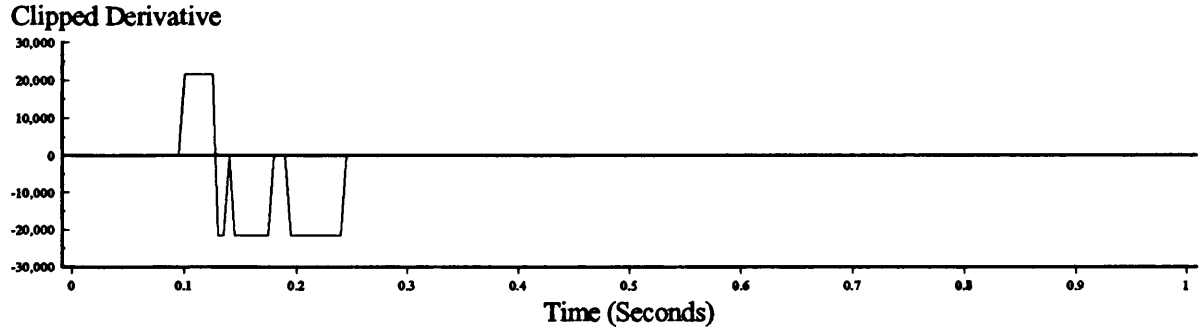

5.33c) Amplitude Limited Derivative.

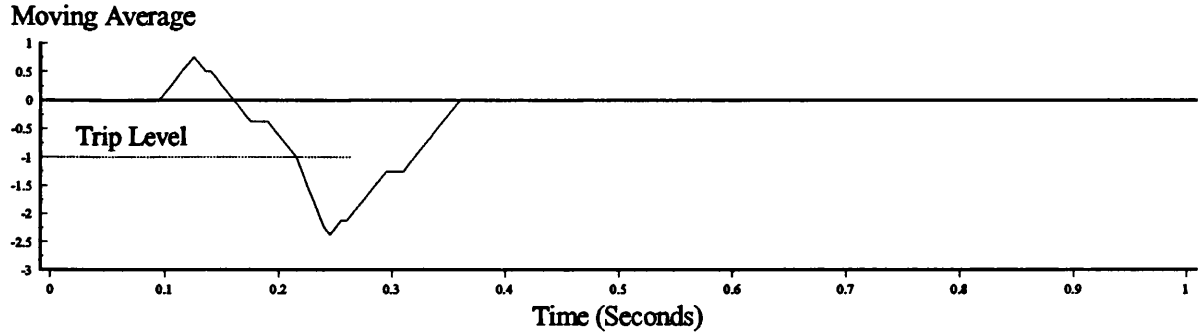

5.33d) Algorithm Output (6 Cycle Moving Average Filter).

Figure 5.33 : Algorithm Response to a 20% Load Increase under Independent Operation. (Field Trial Result)

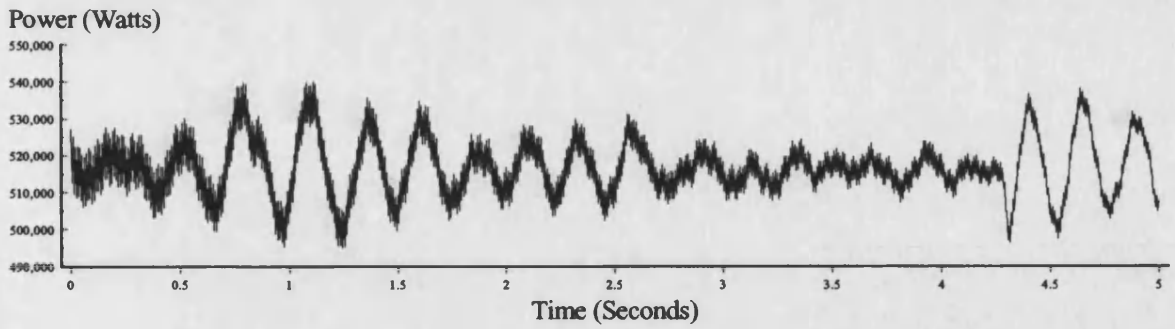

5.34a) Fourier Filtered Power at 4 samples/cycle (Input to Algorithm).

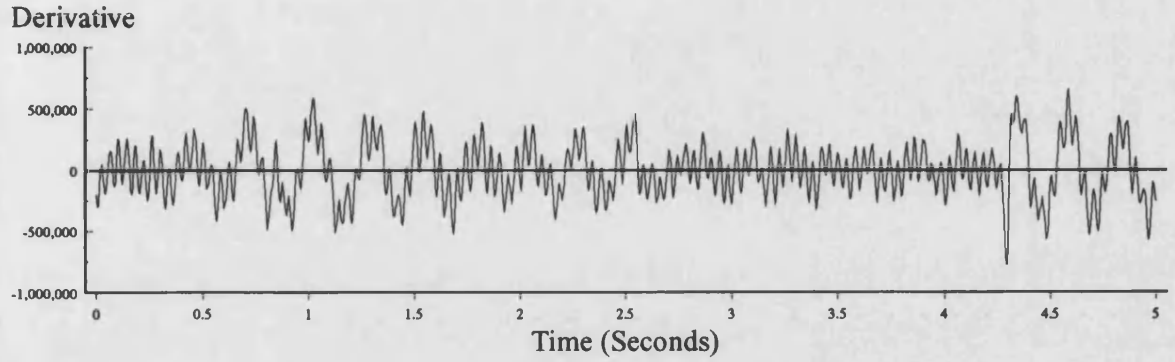

5.34b) Derivative of Filtered Power.

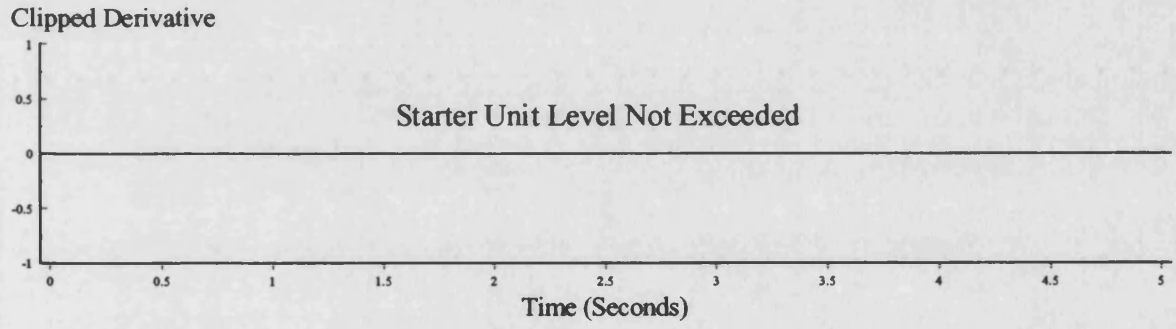

5.34c) Amplitude Limited Derivative.

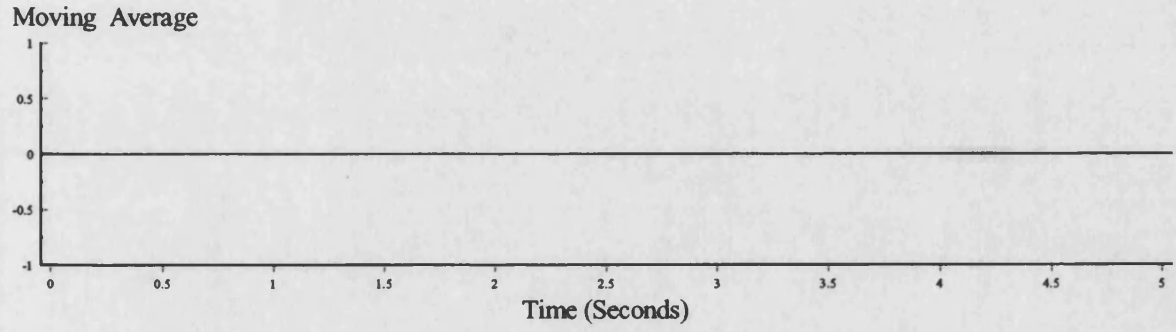

5.34d) Algorithm Output (6 Cycle Moving Average Filter).

Figures 5.34 : Algorithm Response to a 50% Load Increase under Parallel Operation. (Field Trial Result)

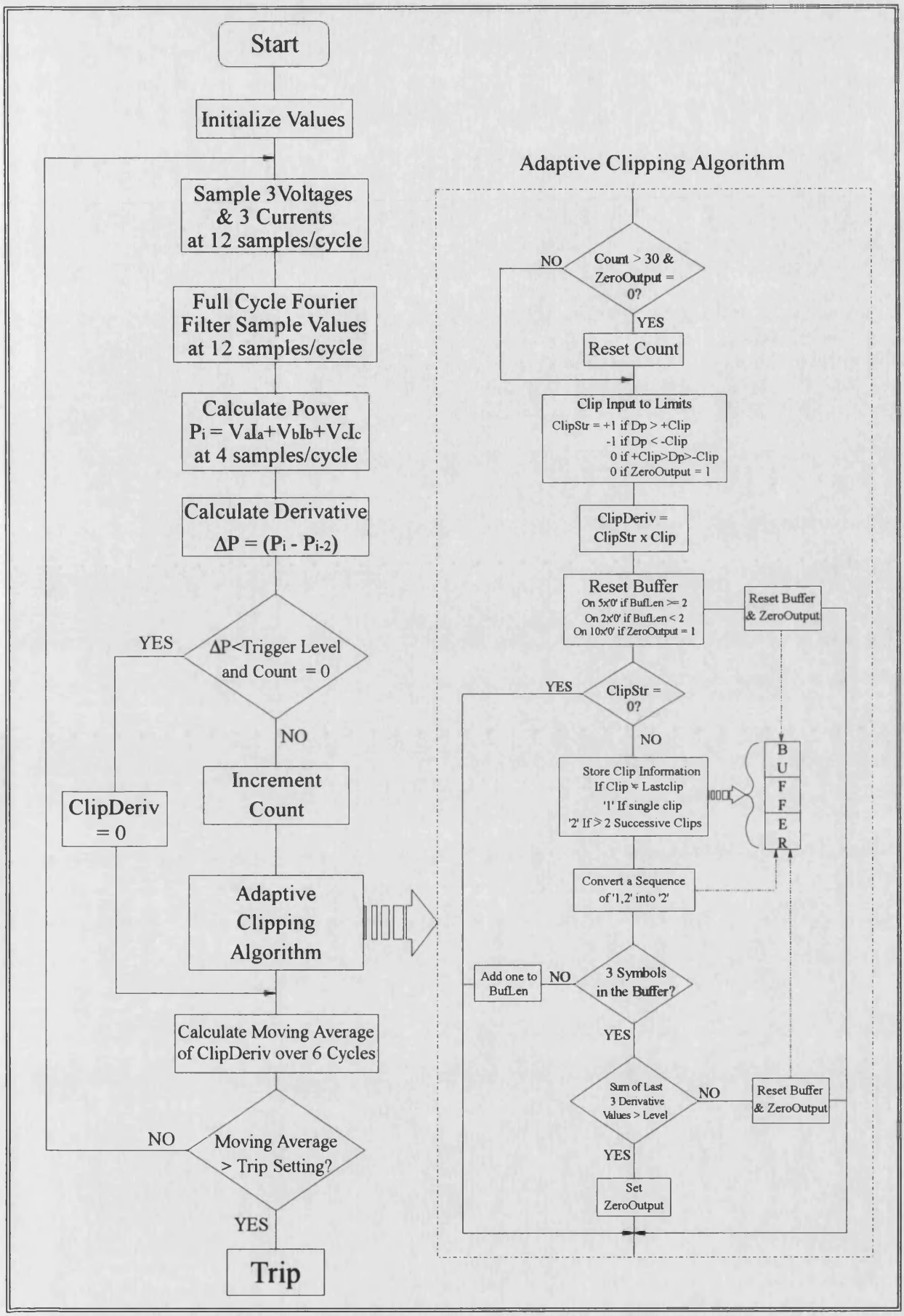

Figure 5.35 : Flow Chart of Final Loss of Grid Algorithm Operation.

Chapter 6

Presentation and Analysis of Final Results

This chapter completes the analysis of the performance of the algorithm by showing its final operation under various system conditions using the three sources of test data available (i.e. simulation, laboratory and field trial). For completeness the results will include further cases of loss of grid connection as well as parallel and independent load change, system faults and out of step reclosure. The steady state stability of the algorithm has already been proved up to this point therefore no further results are necessary.

The results and analysis in this chapter will demonstrate slight variations in the observed responses from the different test systems for the same test type. These variations will be discussed with possible explanations put forward for the differences, but more importantly, the response of the algorithm will be shown to be essentially unaffected.

The format of the chapter will therefore be to introduce a particular test condition and present results from each of the test systems, where available, before discussing the responses. For the results shown in this chapter, the starter unit level is set to:

- 8,000 Watts/second for the 5kVA generator in the laboratory system,
- 1 Megawatt/second for the 625kVA generator in the field trial system,
- 6 Megawatts/second for the 3.75MVA generator in the simulation system.

This corresponds to a required change in the output power level of 1% of rated power in a quarter cycle period. These values were derived empirically from the studies undertaken.

6.1 Loss of Grid.

Since loss of grid is the most important condition for the algorithm to detect the first set of results show the final algorithm's response for a few different recorded loss of grid events.

Case Study 1: The loss of grid results shown to date in chapter 5 have been for the generator operating at near rated output power. However, the response of the generator is essentially the same for loss of grid events which occur with the generator operating at very low output power levels. This situation may occur if the required contribution from the embedded generator is only small or if the generator is in the process of being run-up to meet the demand.

The responses of the laboratory generator and the diesel driven generator to a loss of grid event whilst operating at low output power are shown in figures 6.1 and 6.2 respectively. The result of the loss of grid is to increase the loading of the generators by 900%. For both the laboratory and field trial systems the loss of grid algorithm operates in the required manner which shows that the level of the output power from the generator prior to a loss of grid is irrelevant to the operation of the algorithm.

With reference to the output power waveforms for the two systems (figures 6.1a and 6.2a), the differences in the power following the loss of grid can be attributed to the governor response on the diesel generator. The additional loading of the diesel generator is matched quite rapidly by an increase in the input power from the diesel engine due to the governor opening the throttle. This situation does not occur with the d.c. driven generator in the laboratory which has a fixed input motive power to the generator and no governor. As stated in chapter 3 the governor response time is too slow to effect the operation of the algorithm and this can be seen by the rest of figure 6.2 where a trip occurs for the loss of grid after 130 milliseconds. The response of the algorithm for the two tests shown can therefore be seen to be very similar with the initial fast change in power causing the starter unit to be triggered and the subsequent machine characteristics whilst it slows down leading to an algorithm trip.

Case Study 2: The similarity in response for the two practical test systems is equally apparent for a loss of grid which results in a reduction in the loading of the machines. In addition, their similarity with the simulated system will be shown. Figures 6.3 to 6.5 show the outcome of a loss of grid which causes a reduction in loading of around 50% at rated output power (70% in the case of the laboratory result). For each of the tests the algorithm responds as designed and except for the fact that the governor was not

modelled in the simulation system and is not present in the laboratory system, the responses are almost identical.

The loss of grid results presented to date show that from all the data currently available from the three test systems, the fundamental principles on which the algorithm's operation is based appear to be sound.

6.2 Load Change under Independent Operation.

Case Study 3: Throughout this thesis it has been stated that the response of the generator, and therefore the algorithm, is the same for a load change which occurs whilst the generator operates in isolation from the grid as for that following a loss of grid itself. However for completeness, in this section, the response of each of the generators used in the performance assessment of the algorithm will be shown for load changes under independent operation. The results shown in figures 6.6 to 6.8 are for a load increase of around 25% under independent operation for each of the test systems available. They once again confirm the similarity between the results obtained from each of the test systems and show the way in which the algorithm reacts to the output power signals. The algorithm trips for each case in a time between 90 and 120 milliseconds. The only noticeable difference between the three results is again due to the effect of the governor responding to match the load change in the case of the diesel generator after about 250 milliseconds.

Case Study 4: In order to demonstrate the sensitivity of the algorithm to small load changes as a result of a loss of grid or under independent operation, a 2.5% load increase whilst the laboratory generator operates in isolation is shown in figure 6.9. The output power waveform shown in figure 6.9a shows that the presence of the unbalance in the system is now of comparable amplitude to the load change itself, however the method used by the algorithm to remove the effect of this unbalance can clearly be seen to be working with the derivative (figure 6.9b) completely free from this double frequency term. The corresponding algorithm response is a trip after 85 milliseconds.

6.3 Load Change under Parallel Operation.

Case Study 5: The next group of three results shown in figures 6.10 to 6.12 present the response of each of the generators used in the analysis to a load increase equal to their individual rating whilst they operate in parallel with the utility grid.

Under this situation, the theoretical response is for the generator electrically closest to the load change to 'see' the majority of the load change during the first few milliseconds, and the effect of the relative inertias of the generator and mains system to have an effect after this period.

The response of the laboratory system to the load increase (figure 6.10a) is an initial power increase, followed by a period where the power appears to 'swing back'. The duration of this period however, is insufficient to cause algorithm operation and the subsequent third change in sign of the derivative waveform causes the adaptive clipping function to zero the clipped output for the remaining period of the disturbance. In this situation the algorithm response is governed by the adaptive clipping function carrying out one of the tasks for which it was included in the algorithm.

A slightly different response is obtained from the field trials, where the load increase at 0.1 seconds is almost indistinguishable within the oscillations of the output power from the diesel generator. In order to explain the observed differences in the characteristics from the two systems requires greater information about the mains system to which the embedded generator is connected. In the laboratory, the mains source is obtained via a 500kVA transformer situated some 100 metres or so from the laboratory which results in a fairly high impedance source. Thus, the load change applied to the local busbar in the laboratory, which is effectively the terminals of the laboratory generator, results in a greater proportion of the load increase being 'taken up' by the local generator than would be the case if the mains was a lower impedance source (see appendix A for theory on distribution of load impacts). In the case of the field trial results, the mains has a much lower source impedance which results in a larger proportion of the local load change being 'taken up' by the mains system.

It is interesting to note at this point that the new power based algorithm requires only limited knowledge about the mains system to which it is connected since it bases its decision on the characteristics of the local generator alone. However, even if the system to which the embedded generator is connected does not have the characteristics of an infinite bus system, the algorithm response is not to trip for load changes whilst operating in parallel as shown by the laboratory result. The field trial results (figure 6.11) clearly show the desired and more typical response of the embedded generator under load changes whilst operating in parallel with the mains.

The effect of the source impedance of the mains system was investigated further using the simulation system which provides an ideal method for testing the effect of the impedance between the local busbar and the inter-connected mains system. The results of this simple study further demonstrated that the source impedance dictates the proportions of the load distribution in the period immediately following a load change.

From the simulation system, a load increase applied to the local busbar with the generator operating in parallel with the utility grid produces the resulting output power plot shown in figure 6.12a. The output power waveform in turn produces oscillations in the derivative term which results in the adaptive clipping function zeroing the clipped output (figure 6.12c). The response from the algorithm is once again not to trip.

6.4 System Fault Conditions.

The immunity of the new loss of grid algorithm to single phase to ground faults has already been demonstrated in section 5.2. This immunity arises from the double frequency (100 Hertz) oscillations present in the power waveform during the unbalanced fault. The effect of the unbalance term is actually filtered out by the method of processing the power term four times a cycle as previously discussed, but the fault-on and fault-off portions of the waveform are still present in the derivative waveform despite this filtering. This occurs because of the transient characteristics under fault conditions and the resulting oscillation in the derivative signal provides the adaptive clipping function with the information to cause it to zero the output after the third successive sign change.

Case Study 6: A similar situation to that described for the single phase to ground fault occurs for a double phase to ground fault applied to the local busbar. In this situation the unbalanced fault once again produces a double frequency oscillation in the output power waveform. However, under these conditions, the generator frequency is slightly less 'firmly' fixed by the presence of the grid connection and it is therefore free to vary slightly from 50 Hertz. Any variation in the system frequency during the fault leads to a change in the amplitude in the power waveform when processed at four times per cycle and this can be seen in figure 6.13a.

The response from the algorithm is for the adaptive clipping function to zero the output due to the oscillations in the derivative waveform (figure 6.13b) as for single phase faults. The algorithm therefore remains stable for both the fault-on and fault-off portions as shown by figure 6.13c & d.

Case Study 7: A different situation occurs with a three phase to ground fault applied to the local busbar. This is a balanced fault condition and as a result there is no double frequency term present in the power waveform apart from that due to any unbalanced loads. The generator response to the three phase to ground fault is shown in figure 6.14a. Due to the need for resistance in the fault path to prevent laboratory fuse rupture, the response is less severe than for zero resistance faults. The output power from the generator has the characteristics of a load change under parallel operation, which is effectively what the three phase to ground fault with fault resistance produces.

The response of the algorithm is shown by the remaining plots of figure 6.14 and these show the algorithm restraining due to the adaptive clipping function zeroing the clipped derivative output.

It could be argued that the three phase fault either with or without ground is equivalent to a loss of connection between the two sides of the system involved with the fault and as such it constitutes a loss of grid connection for which the algorithm should operate. In the situation tested in the laboratory, the fault does not produce a large change in the loading of the machine following the transient period and the algorithm restrains. Despite the argument that the three phase fault is the same as a loss of grid connection, the fact

that the algorithm restrains is of benefit since it allows the dedicated protection functions, which are included in the scheme to detect fault conditions, to clear the fault and indicate the cause of the trip. Loss of grid, as mentioned earlier, is not a fault condition but is highly undesirable and should the algorithm trip for a three phase fault before the dedicated protection function, then the presence of the fault would not be indicated and reconnection may occur onto a faulted feeder.

6.5 Out of Step Reclosure.

One of the requirements originally specified for the loss of grid protection algorithm was that in the event of an undetected loss of grid followed by a period of isolation without a load change, as a last resort, the algorithm should detect an out of step reclosure between the power island and the main utility grid. Although an out of step reclosure may lead to immediate damage to the generator shaft, prolonged exposure following reconnection should still be minimised. Therefore the algorithm should detect the reclosure and clear the embedded generator from the system as quickly as possible.

Case Study 8: The response of the laboratory generator to a reclosure when the two systems were 90 degrees out of step is shown in figure 6.15a. It can be seen that the output power from the generator immediately shifts from around 4kW generating to 20kW motoring as the two systems are reconnected. The response from the algorithm is a trip after 105 milliseconds.

The recording of a severe out of step reclosure in the field trials was impossible due to machine fatigue considerations. However, the point of resynchronizing the diesel generator onto the utility network was captured. The synchronizing event was supervised by a check-sync relay which provides a permissive scheme to prevent non-exact synchronizing attempts. With this scheme the two systems cannot be reconnected until they are within 5 degrees phase difference. The response of the diesel generator to a normal synchronization onto the mains is shown in figure 6.16a. Following connection the power oscillations take over 5 seconds to decay and had the phase difference been greater, the damage to the generator shaft could lead to a costly premature failure.

For this situation the algorithm produces a trip decision to remove the generator after 85 milliseconds. Obviously when synchronizing the generator onto the utility system the loss of grid algorithm would therefore require a blocking signal to prevent its operation, but the result does show that for more severe events the generator could be removed quickly.

6.6 Multiple Machine Loss of Grid.

Since many embedded generator schemes involve multiple generators on a single site, the effect of other generators on the characteristics obtained for a loss of grid requires analysis. This actually leads to the question of whether to apply the loss of grid protection function on a per-generator basis or a per-site basis with all the generators considered as a single large generator. For the work detailed in this thesis the algorithm has been designed for inclusion within an integrated generator protection package which will be applied on a per-generator basis and therefore the effect of the other generators in the site does become important.

Case Study 9: The effect of a second generator on the response of the test generator in the laboratory for a loss of grid which produces a power island in which both generators are present is shown in figure 6.17a. The response is not noticeably different from those obtained earlier with a single machine in the power island and the algorithm responds in a similar manner with a trip after 90 milliseconds.

For the diesel generator set used in the field trials, with another diesel generator brought in to share some of the total site load, when a loss of grid occurs the test generator responds as shown in figure 6.18a. It is interesting to see that the low frequency oscillations which were present in the output power from the single diesel generator under parallel operation with the utility are maintained after the loss of grid connection when the second machine is present. This does not agree with the steady state independent operation tests carried out with the single machine where the oscillations were not present. We can conclude from this result that the presence of the utility grid or another generator either causes or allows a low frequency oscillation to occur in the output power from the diesel generator. The presence of these oscillations after the loss of grid connection due

to the presence of the other machine does not prevent the algorithm from tripping under these conditions and a trip occurs after 110 milliseconds.

6.7 Conclusions.

This final results chapter has shown the response of the refined algorithm to some additional test scenarios which were not shown in chapter 5. In addition it has compared the responses obtained from each of the test systems available to show the similarity of response from three very different test setups.

The algorithm in its final form has been shown to operate correctly when required to trip and restrain when not. In the particular case of the diesel driven generator set, it has produced a trip decision before the governor has been able to respond to correct the generator/load mismatch.

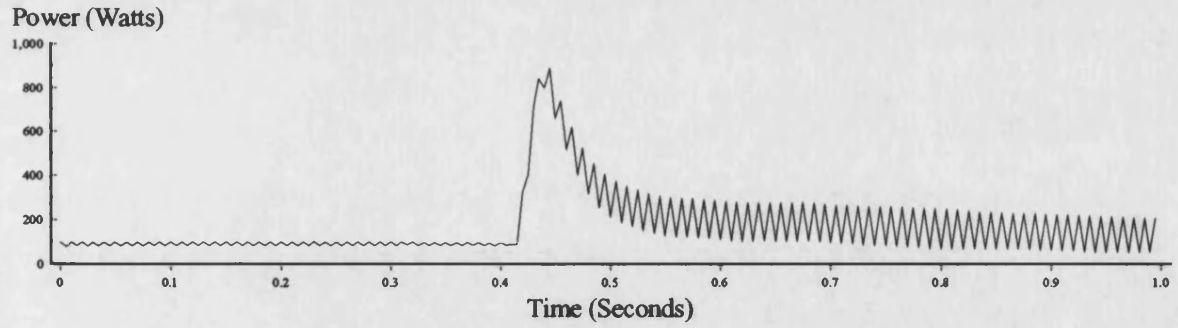

6.1a) Fourier Filtered Power at 4 Samples/Cycle (Input to Algorithm).

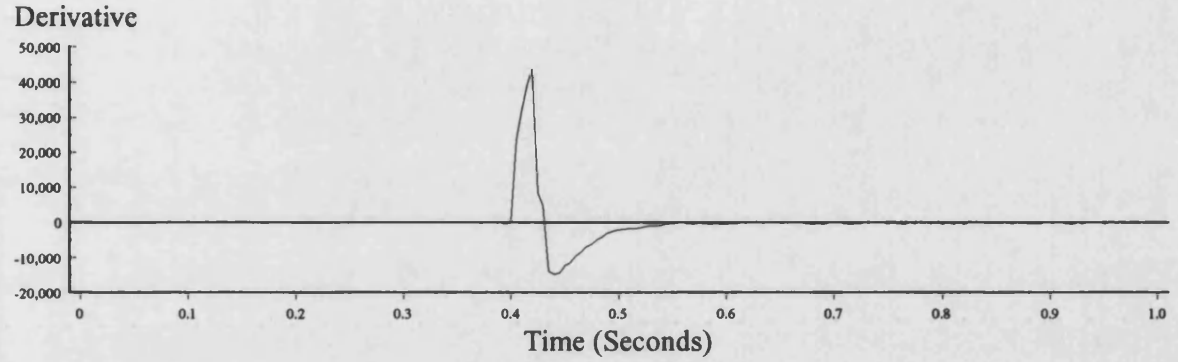

6.1b) Derivative of Filtered Power.

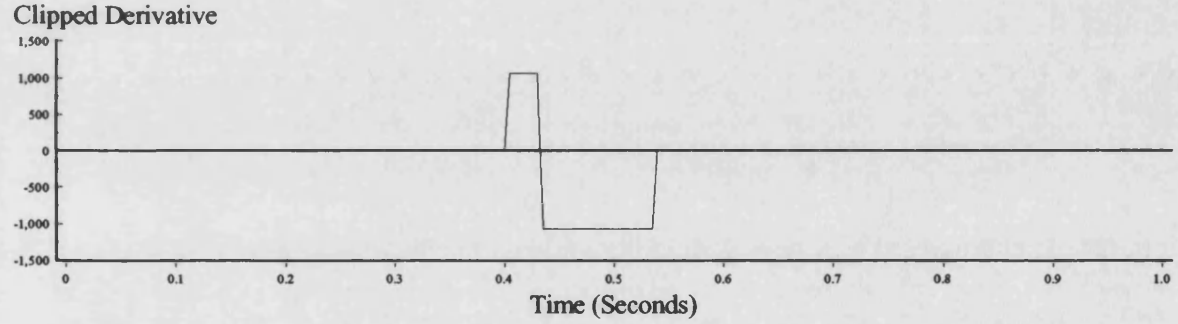

6.1c) Amplitude Limited Derivative.

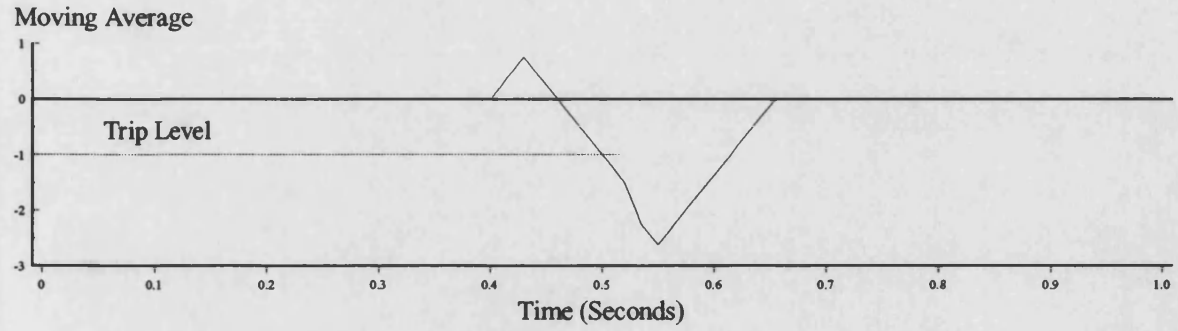

6.1d) Algorithm Output (6 Cycle Moving Average Filter).

Figure 6.1 : Loss of Grid Resulting in a 900% Increase in Generator Loading.
(Laboratory Results)

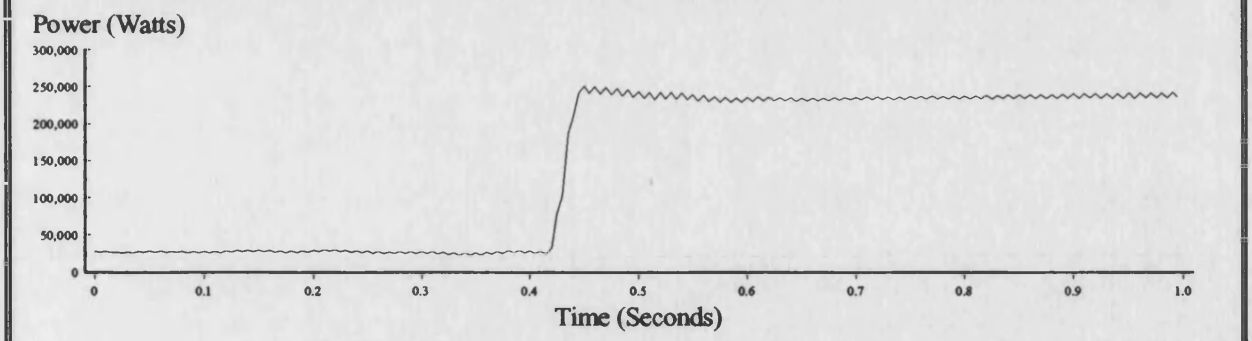

6.2a) Fourier Filtered Power at 4 Samples/Cycle (Input to Algorithm).

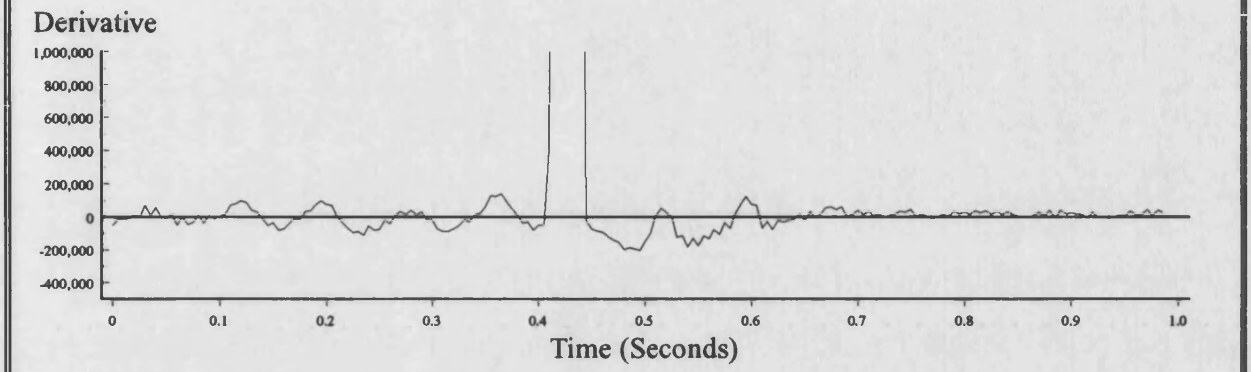

6.2b) Derivative of Filtered Power.

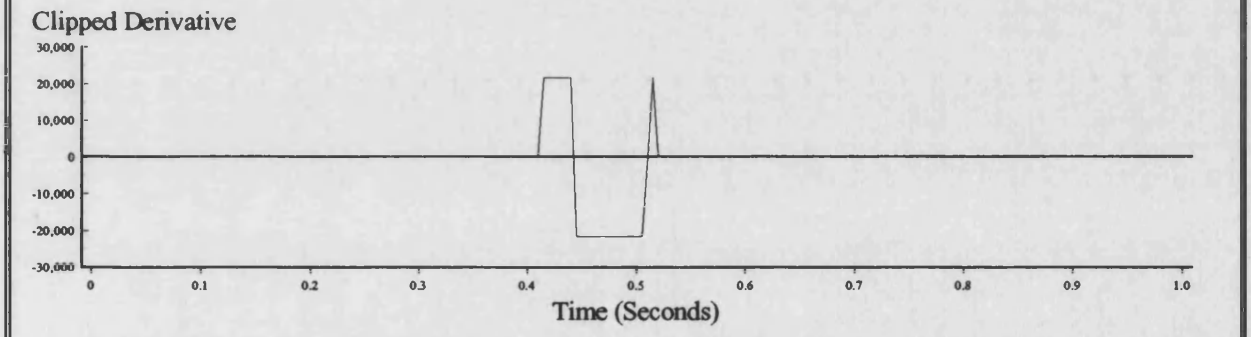

6.2c) Amplitude Limited Derivative.

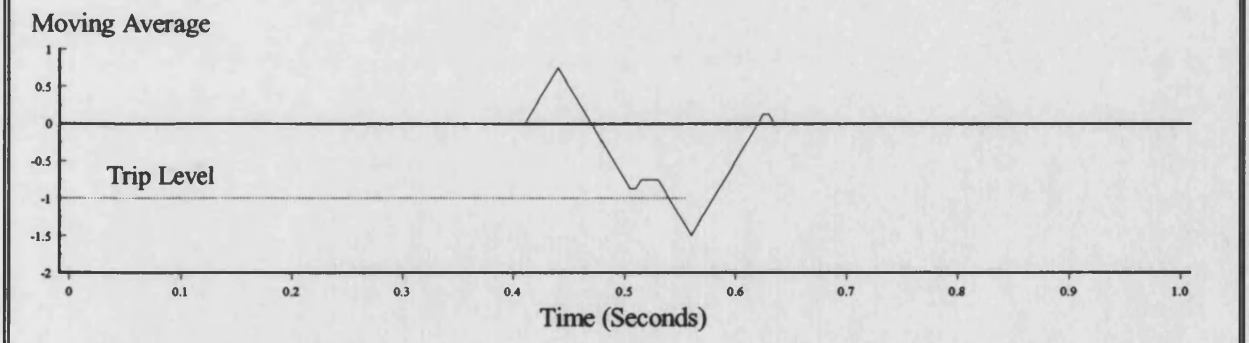

6.2d) Algorithm Output (6 Cycle Moving Average Filter).

Figure 6.2 : Loss of Grid Resulting in a 900% Increase in Generator Loading.
(Field Trial Results)

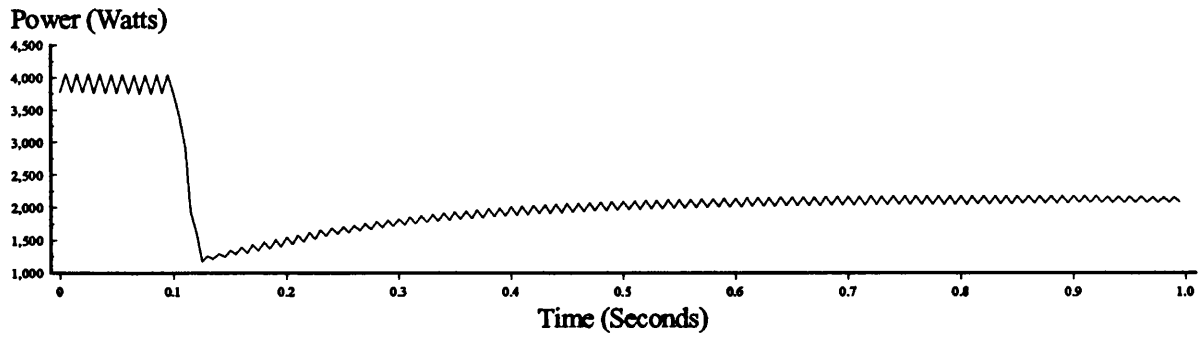

6.3a) Fourier Filtered Power at 4 Samples/Cycle (Input to Algorithm).

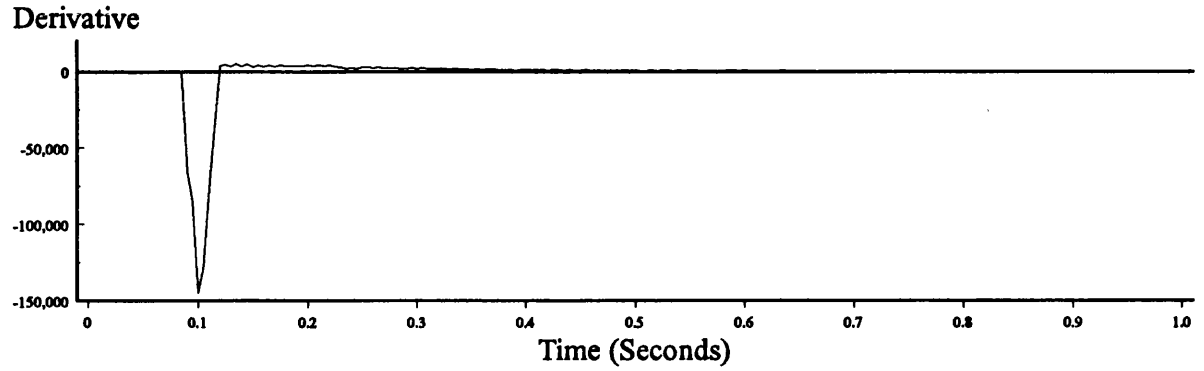

6.3b) Derivative of Filtered Power.

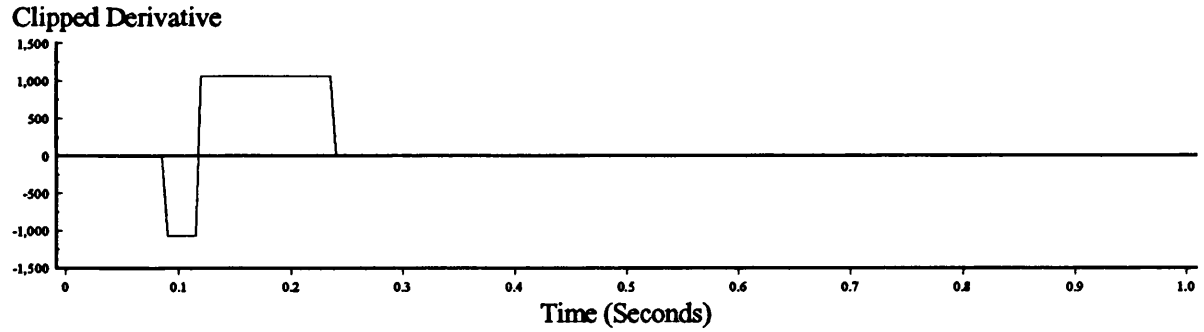

6.3c) Amplitude Limited Derivative.

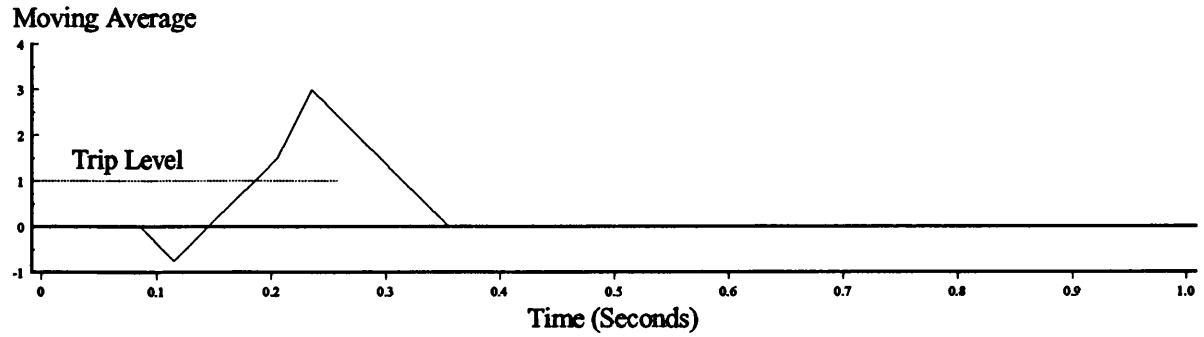

6.3d) Algorithm Output (6 Cycle Moving Average Filter).

Figure 6.3 : Loss of Grid Resulting in a 70% Decrease in Generator Loading.
(Laboratory Results)

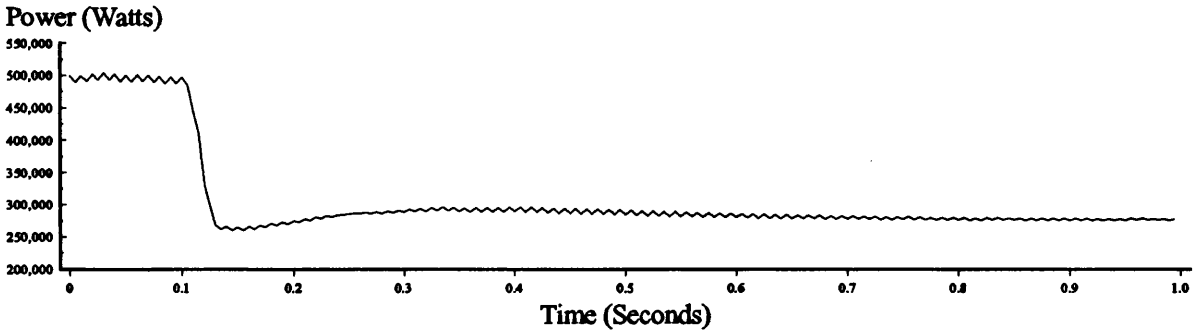

6.4a) Fourier Filtered Power at 4 Samples/Cycle (Input to Algorithm).

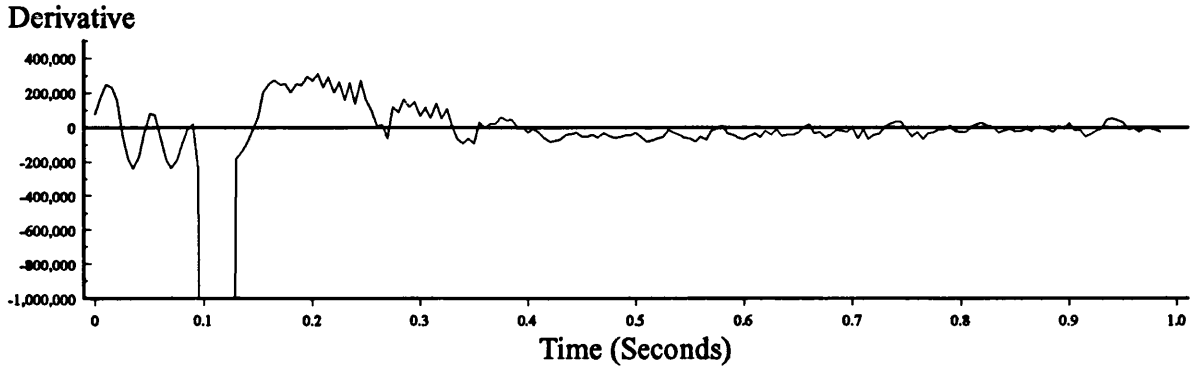

6.4b) Derivative of Filtered Power.

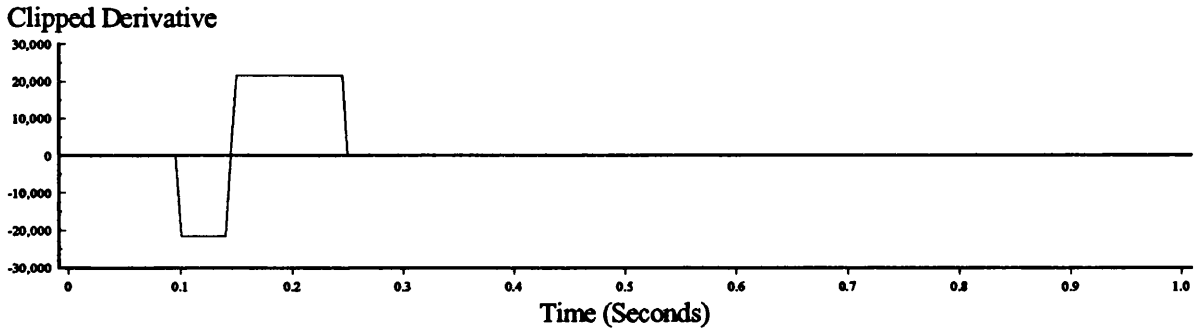

6.4c) Amplitude Limited Derivative.

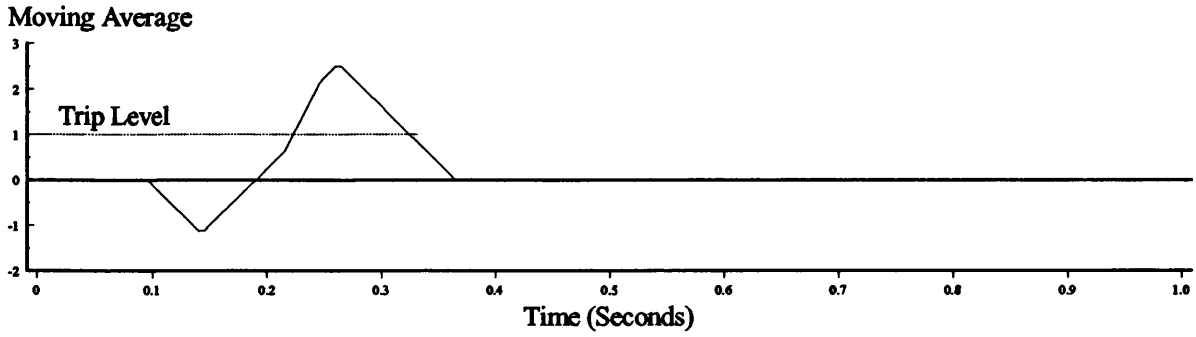

6.4d) Algorithm Output (6 Cycle Moving Average Filter).

Figure 6.4 : Loss of Grid Resulting in a 50% Decrease in Generator Loading.
(Field Trial Results)

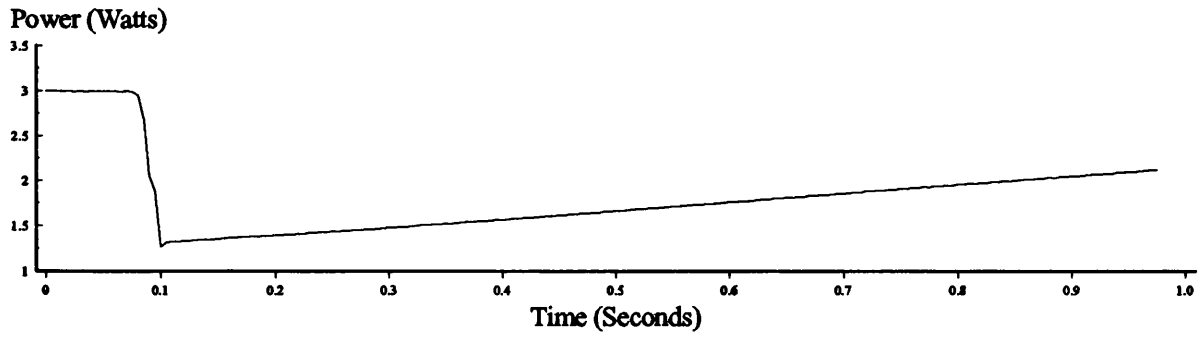

6.5a) Fourier Filtered Power at 4 Samples/Cycle (Input to Algorithm).

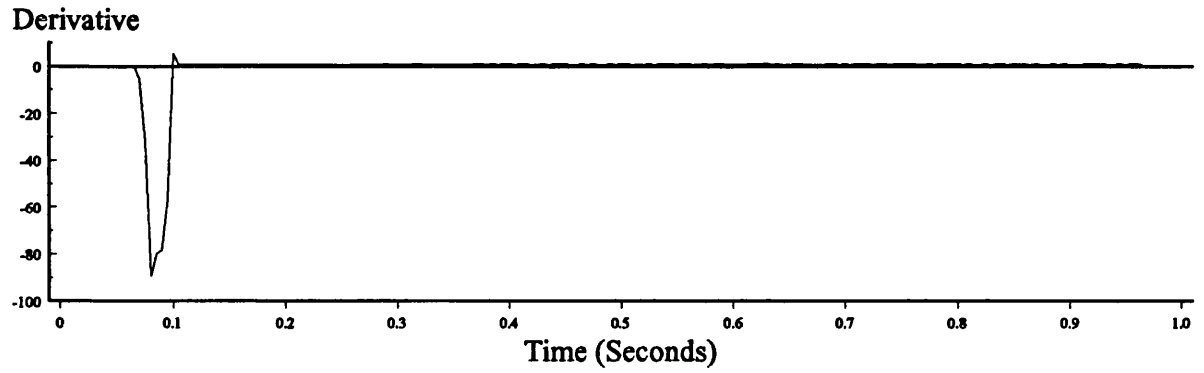

6.5b) Derivative of Filtered Power.

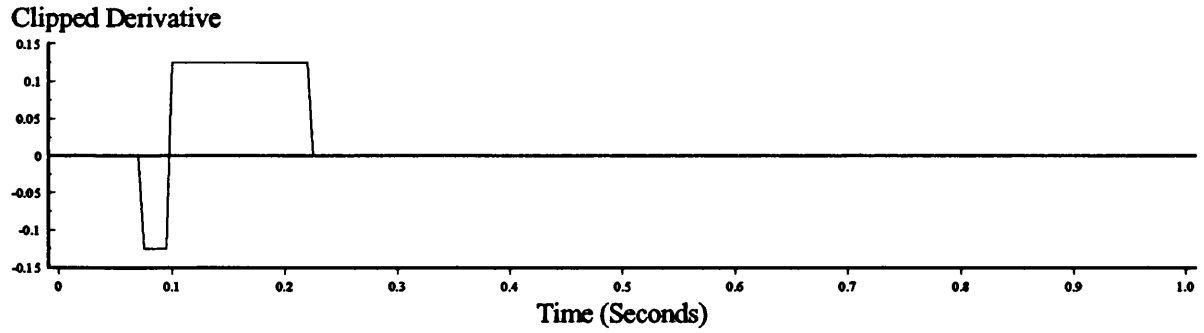

6.5c) Amplitude Limited Derivative.

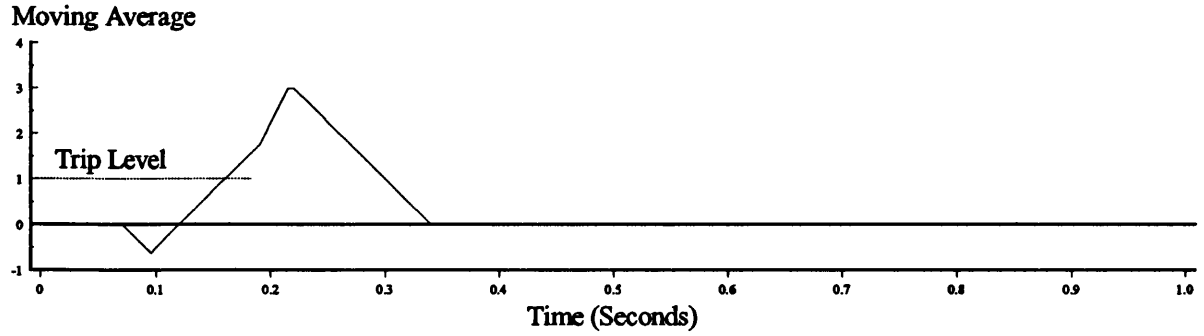

6.5d) Algorithm Output (6 Cycle Moving Average Filter).

Figure 6.5 : Loss of Grid Resulting in a 50% Decrease in Generator Loading. (Simulation Results)

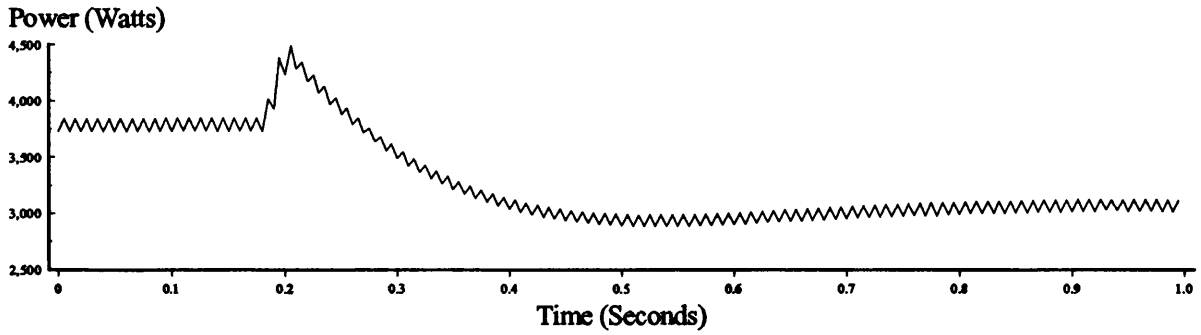

6.6a) Fourier Filtered Power at 4 Samples/Cycle (Input to Algorithm).

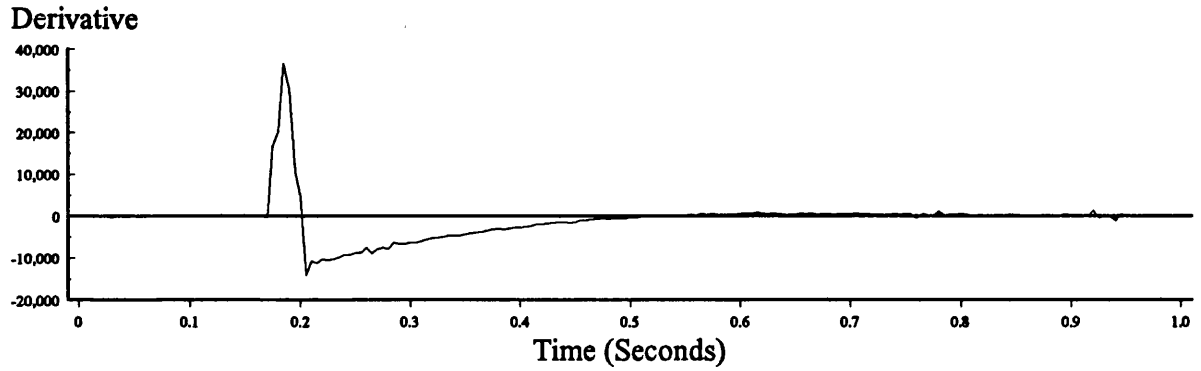

6.6b) Derivative of Filtered Power.

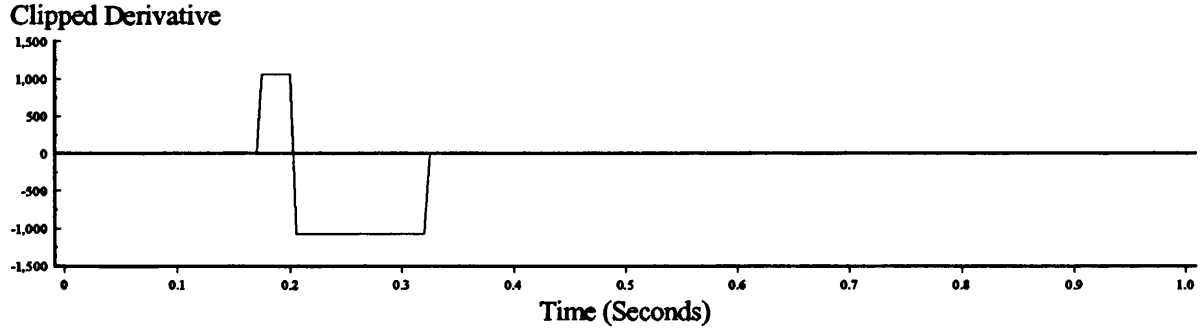

6.6c) Amplitude Limited Derivative.

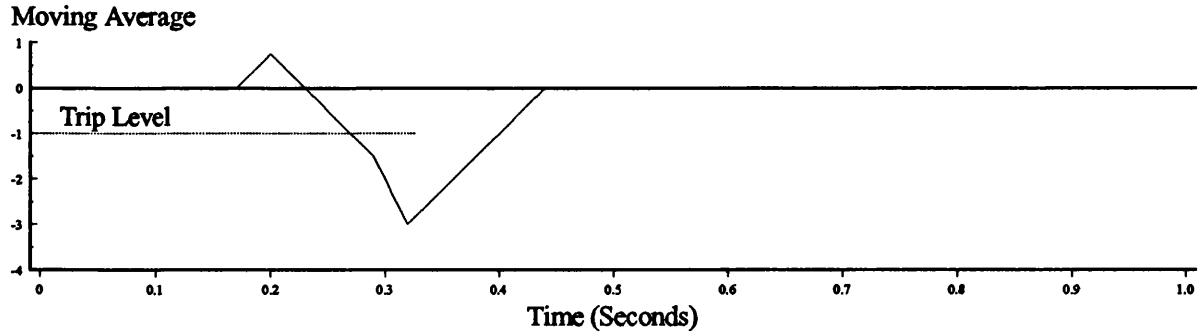

6.6d) Algorithm Output (6 Cycle Moving Average Filter).

Figure 6.6 : A 20% Increase in Generator Loading under Independent Operation. (Laboratory Results)

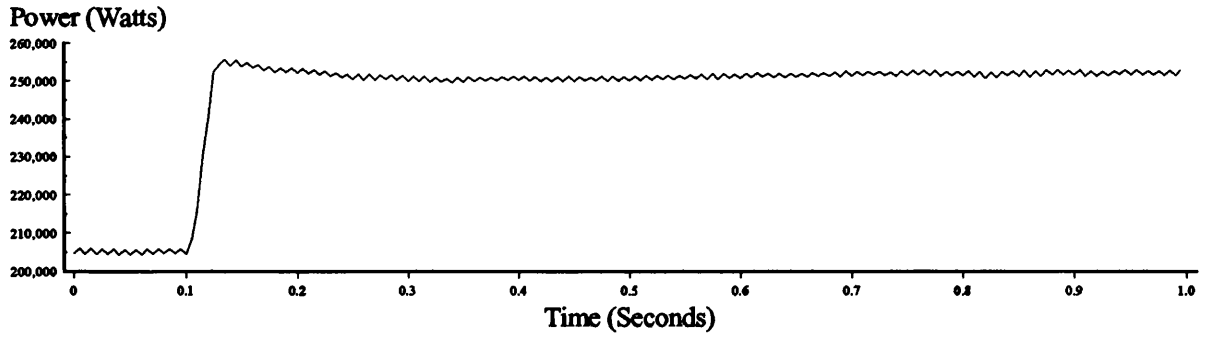

6.7a) Fourier Filtered Power at 4 Samples/Cycle (Input to Algorithm).

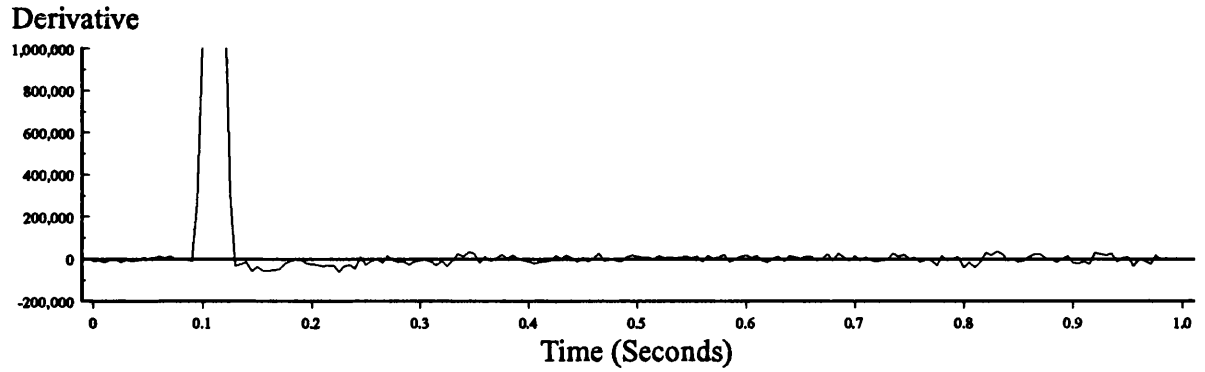

6.7b) Derivative of Filtered Power.

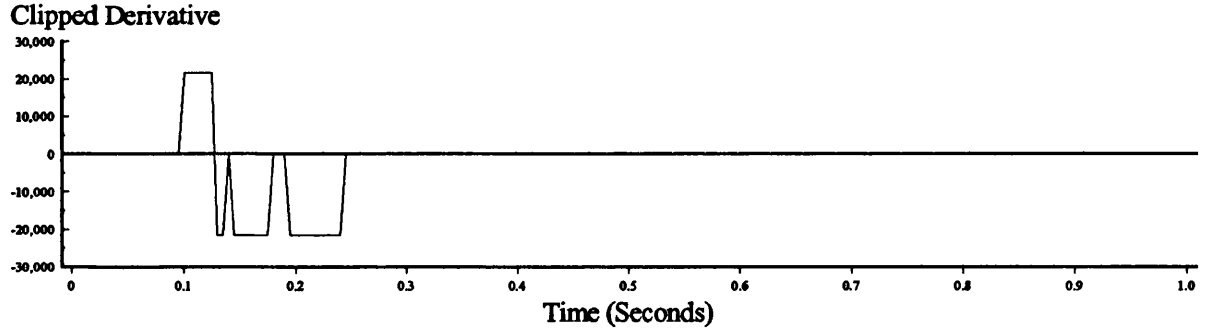

6.7c) Amplitude Limited Derivative.

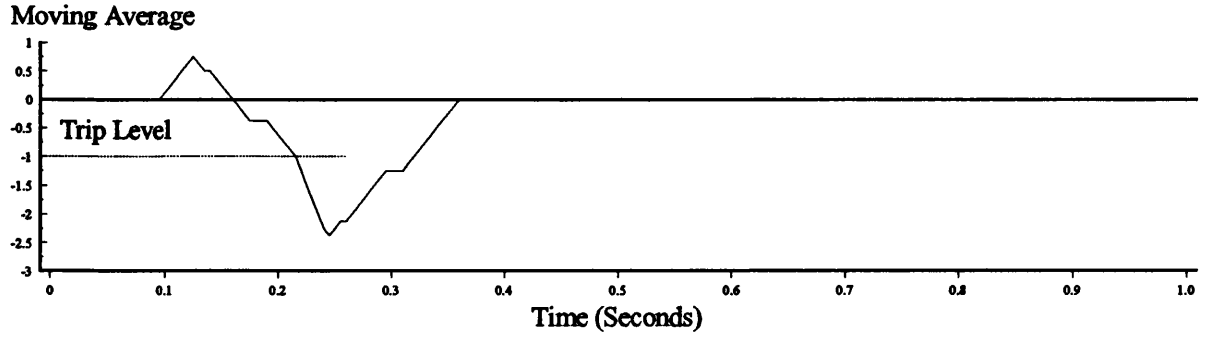

6.7d) Algorithm Output (6 Cycle Moving Average Filter).

Figure 6.7 : A 25% Increase in Generator Loading under Independent Operation.
(Field Trial Results)

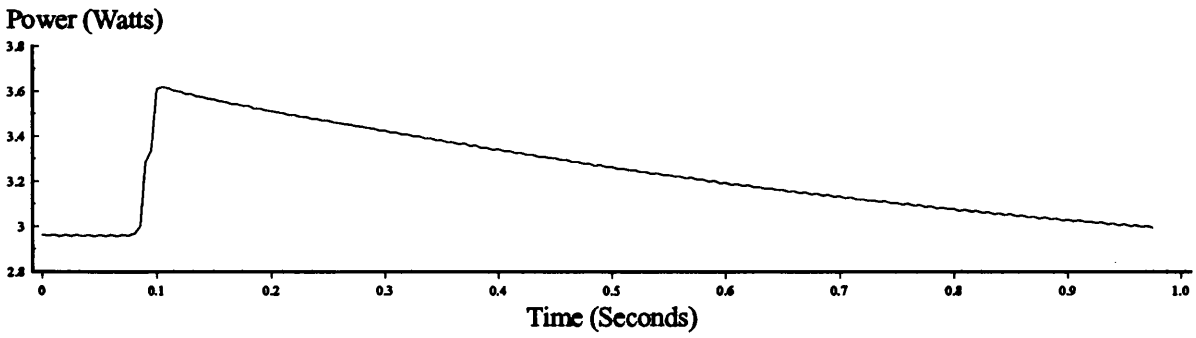

6.8a) Fourier Filtered Power at 4 Samples/Cycle (Input to Algorithm).

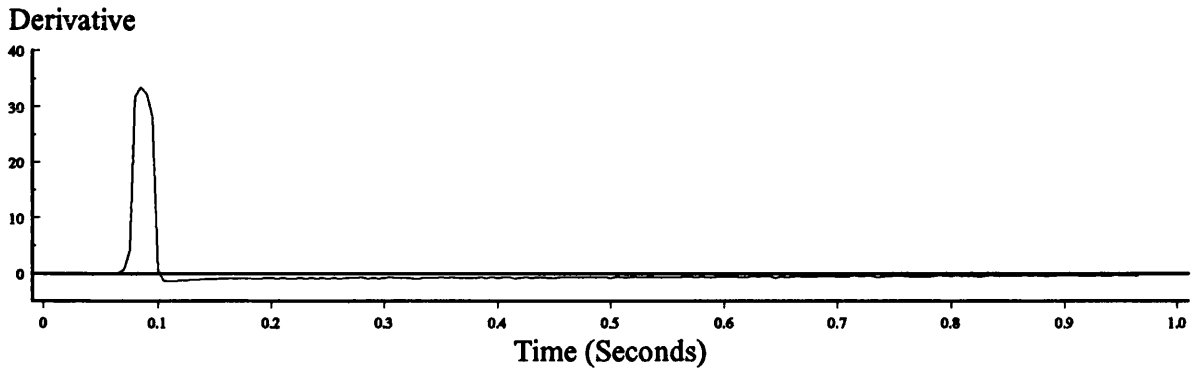

6.8b) Derivative of Filtered Power.

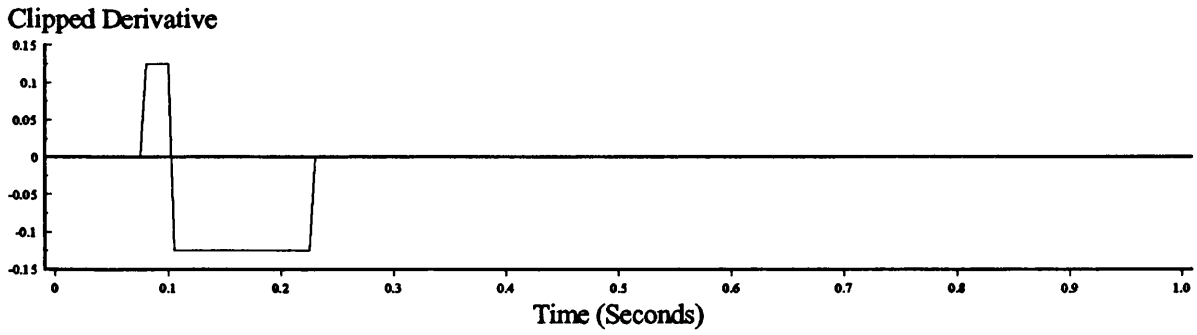

6.8c) Amplitude Limited Derivative.

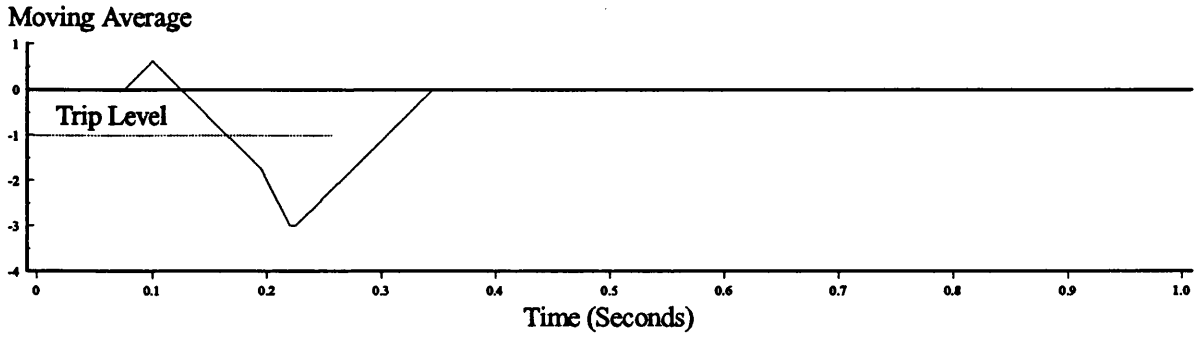

6.8d) Algorithm Output (6 Cycle Moving Average Filter).

Figure 6.8 : A 25% Increase in Generator Loading under Independent Conditions. (Simulation Results)

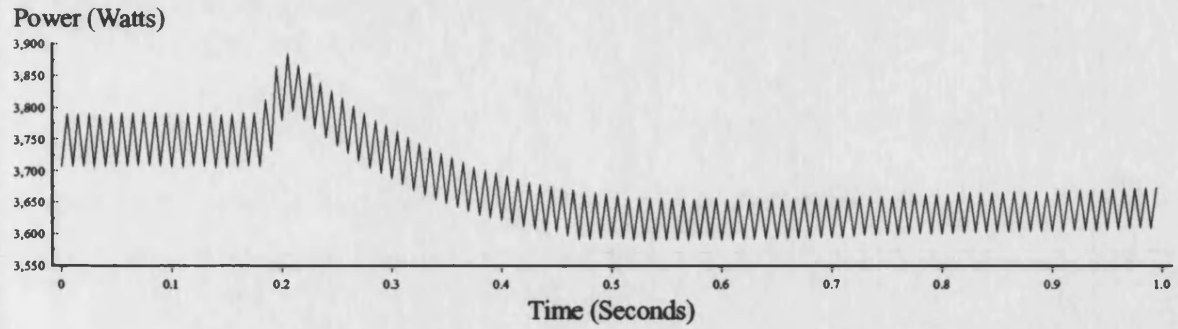

6.9a) Fourier Filtered Power at 4 Samples/Cycle (Input to Algorithm).

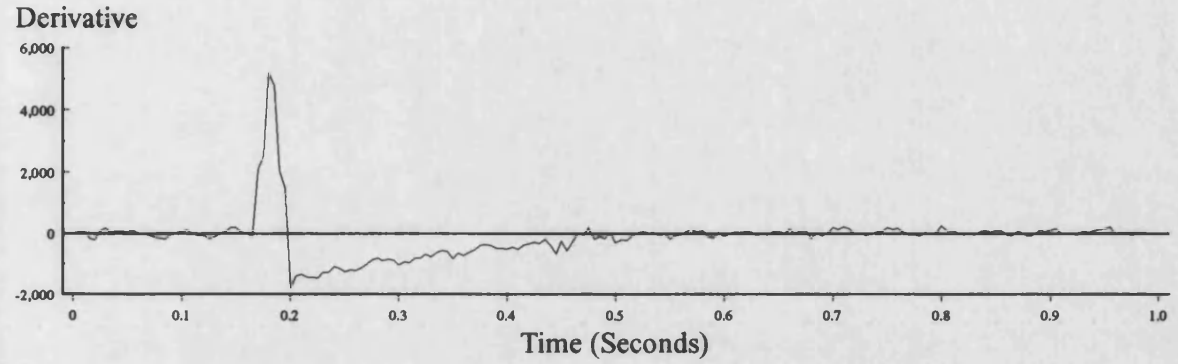

6.9b) Derivative of Filtered Power.

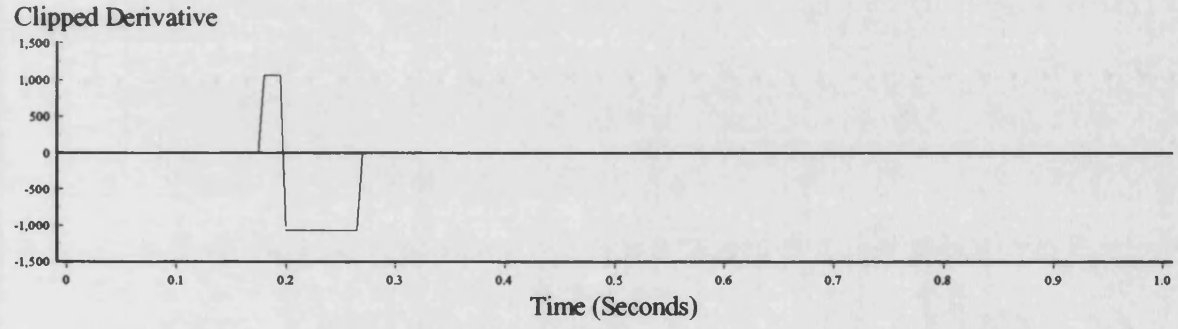

6.9c) Amplitude Limited Derivative.

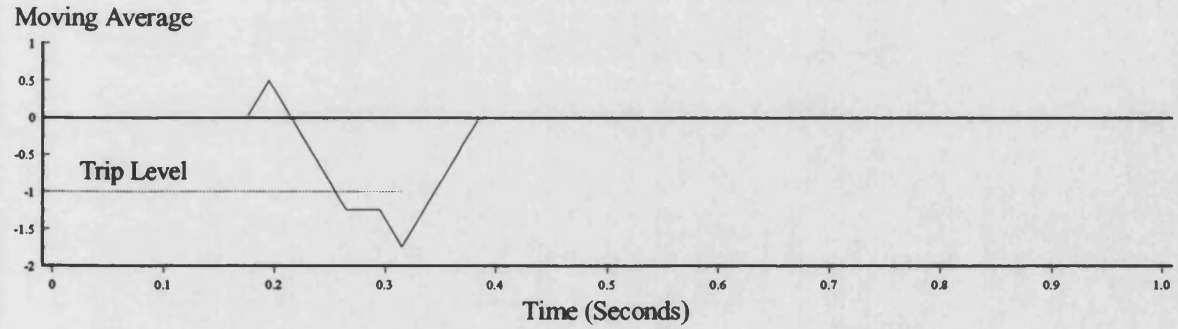

6.9d) Algorithm Output (6 Cycle Moving Average Filter).

Figure 6.9 : A 2.5% Increase in Generator Loading under Independent Operation. (Laboratory Results)

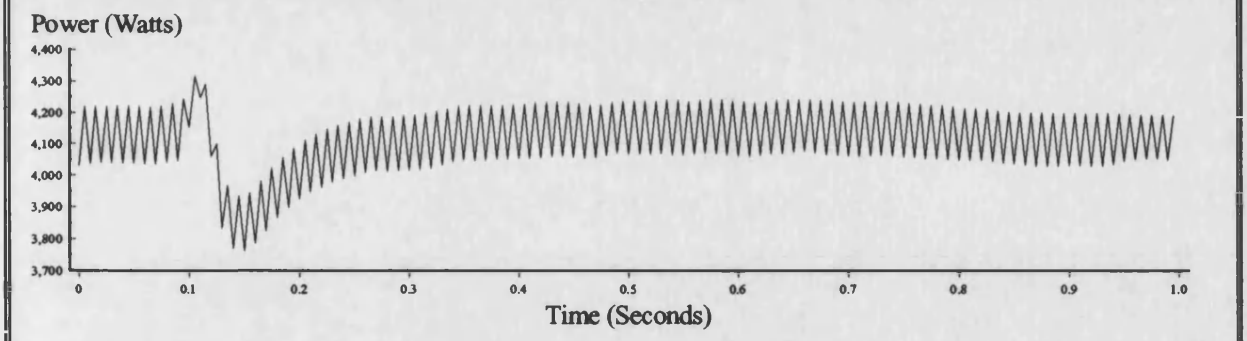

6.10a) Fourier Filtered Power at 4 Samples/Cycle (Input to Algorithm).

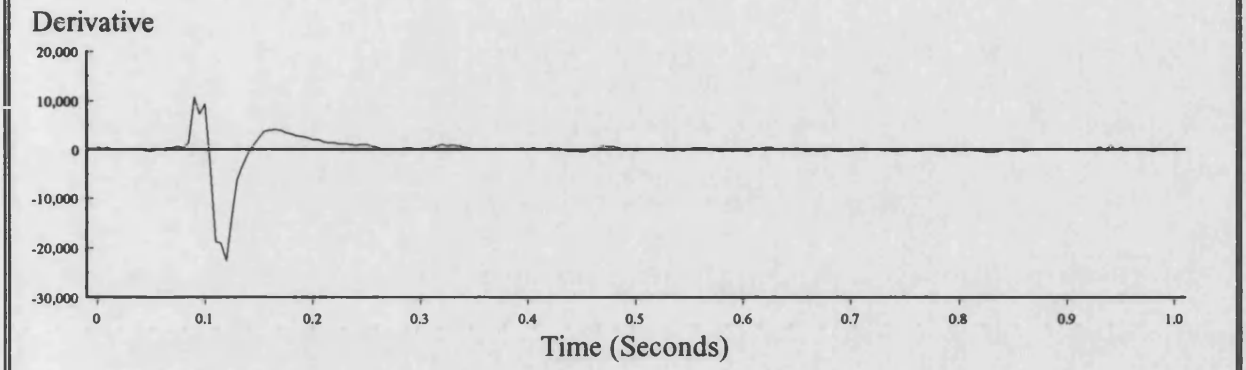

6.10b) Derivative of Filtered Power.

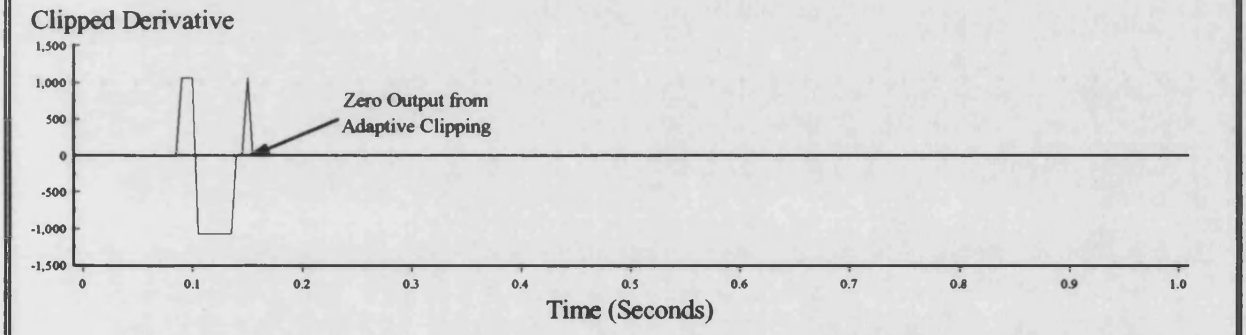

6.10c) Amplitude Limited Derivative.

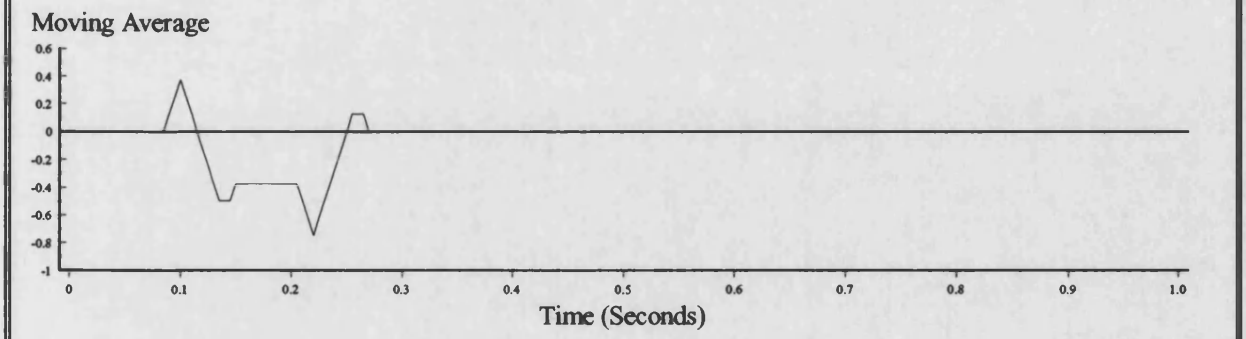

6.10d) Algorithm Output (6 Cycle Moving Average Filter).

Figure 6.10 : A 100% Increase in Generator Loading under Parallel Conditions.
(Laboratory Results)

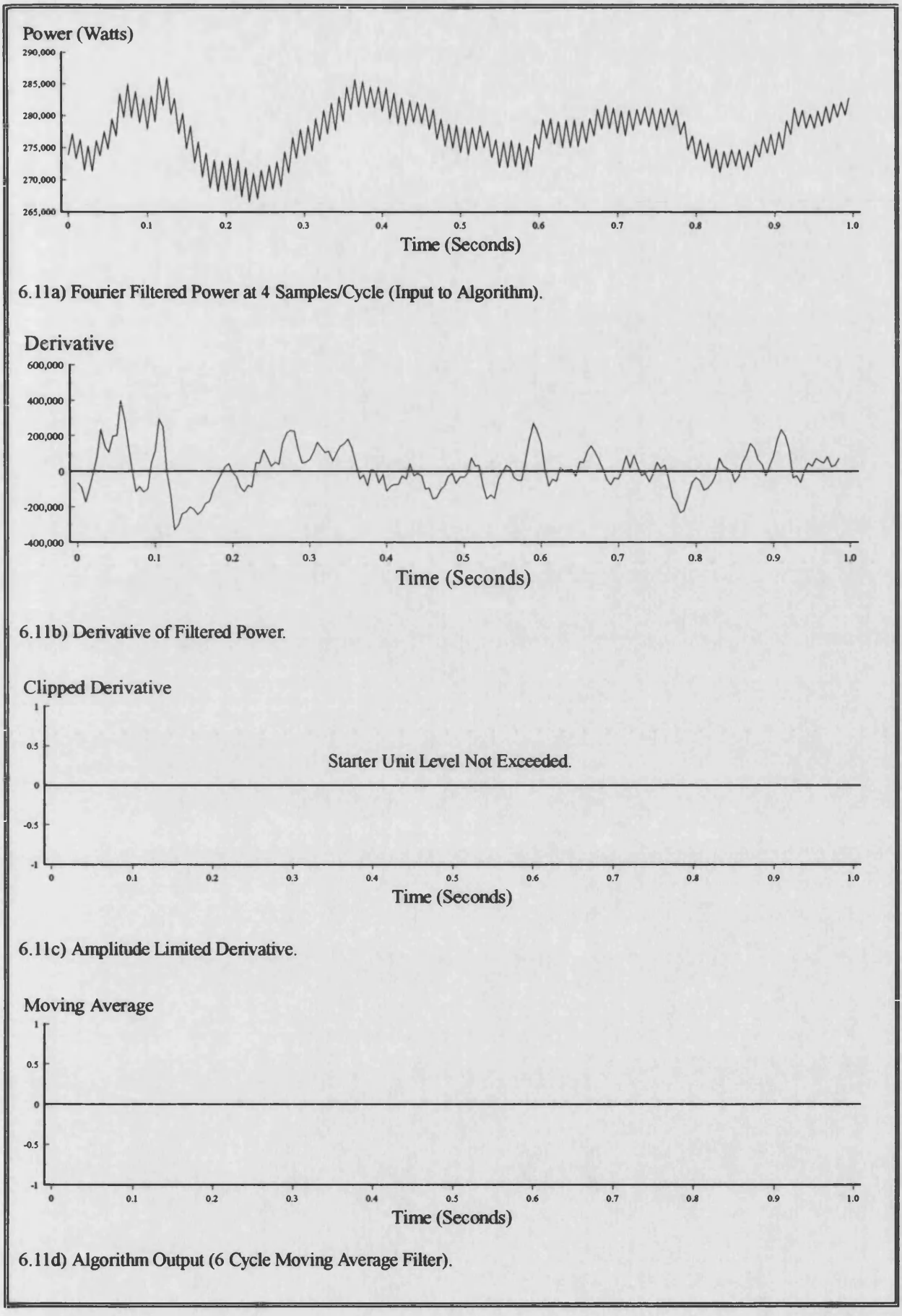

6.11a) Fourier Filtered Power at 4 Samples/Cycle (Input to Algorithm).

6.11b) Derivative of Filtered Power.

6.11c) Amplitude Limited Derivative.

6.11d) Algorithm Output (6 Cycle Moving Average Filter).

Figure 6.11 : A 100% Increase in Generator Loading under Parallel Conditions.
(Field Trial Results)

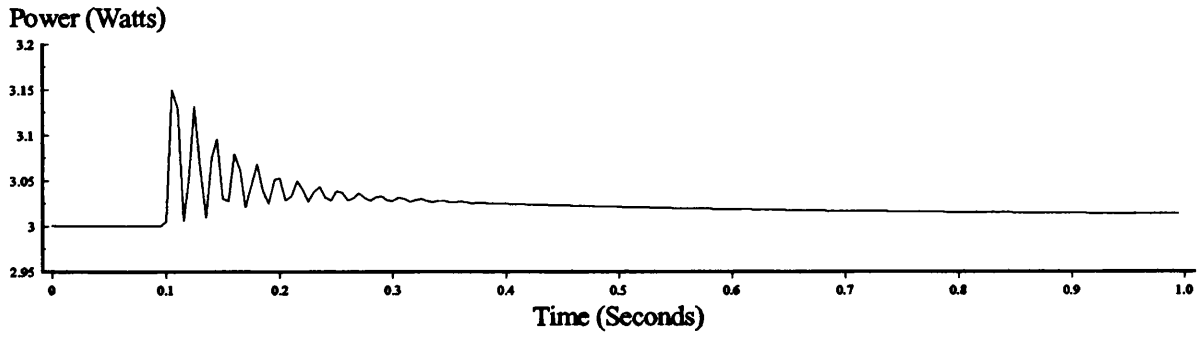

6.12a) Fourier Filtered Power at 4 Samples/Cycle (Input to Algorithm).

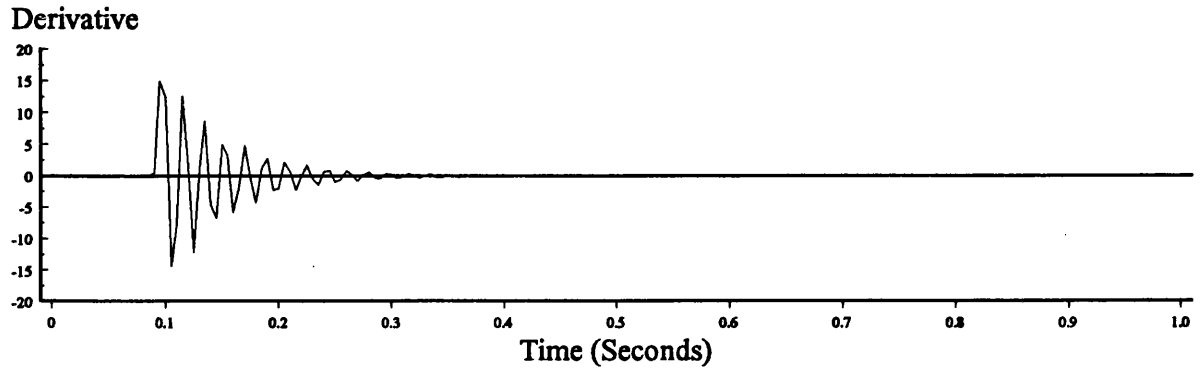

6.12b) Derivative of Filtered Power.

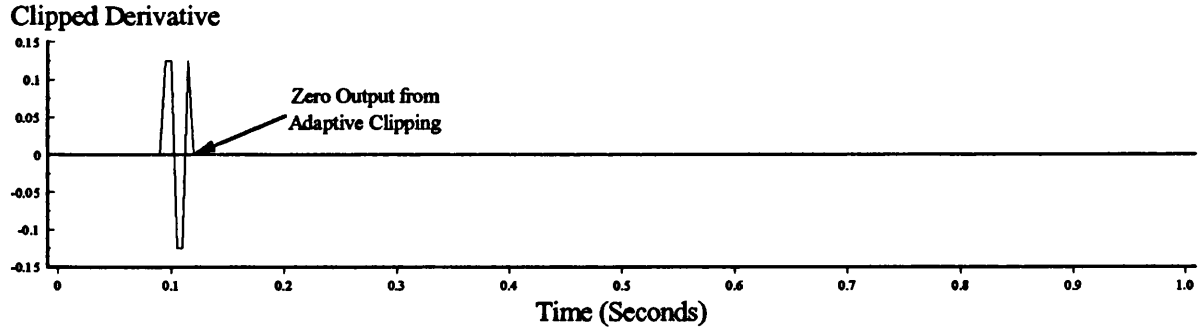

6.12c) Amplitude Limited Derivative.

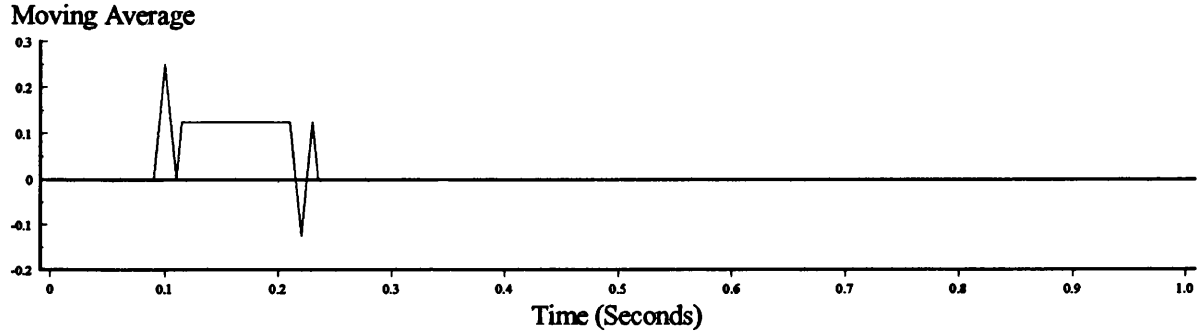

6.12d) Algorithm Output (6 Cycle Moving Average Filter).

Figure 6.12 : A 100% Increase in Generator Loading under Parallel Conditions. (Simulation Results)

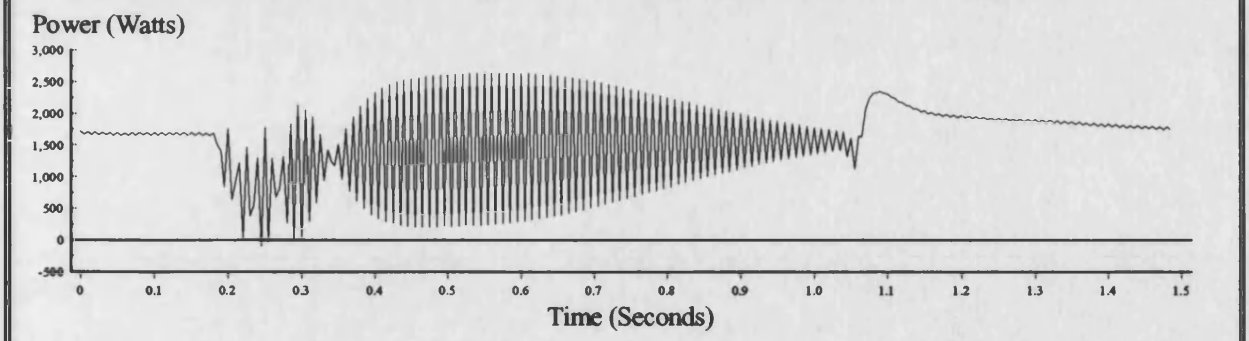

6.13a) Fourier Filtered Power at 4 Samples/Cycle (Input to Algorithm).

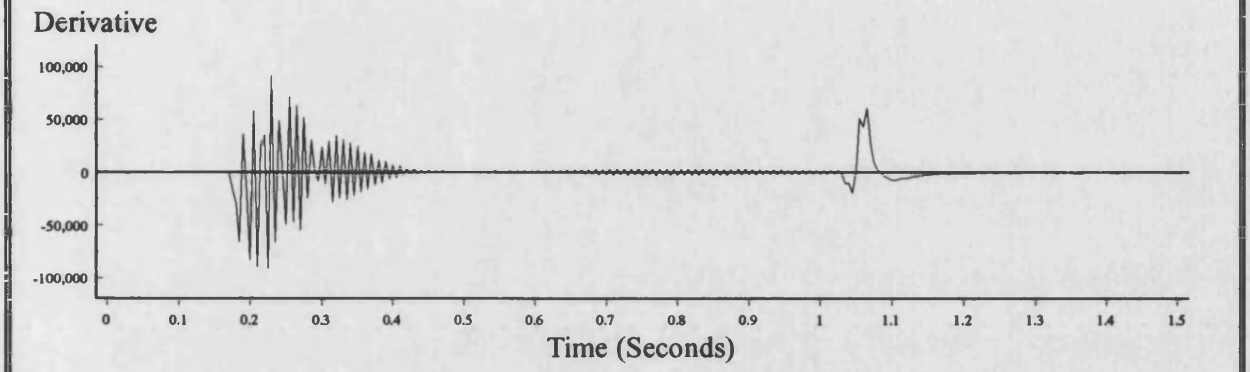

6.13b) Derivative of Filtered Power.

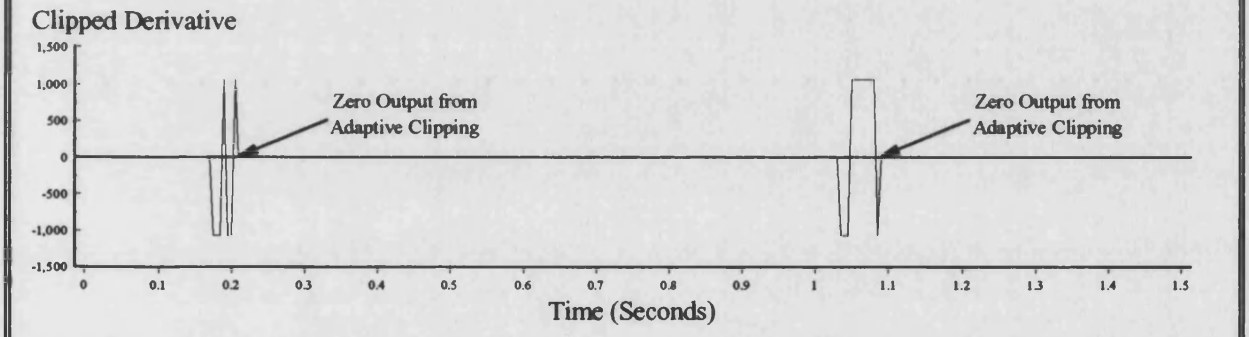

6.13c) Amplitude Limited Derivative.

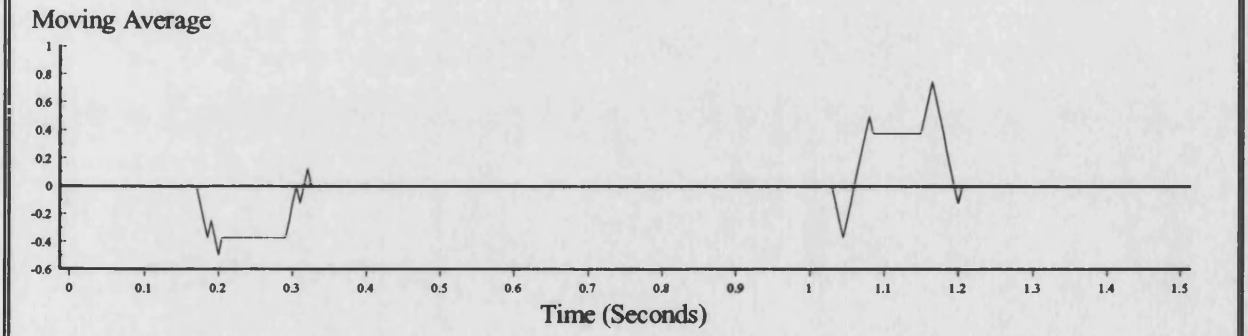

6.13d) Algorithm Output (6 Cycle Moving Average Filter).

Figure 6.13 : A Two Phase to Ground Fault on Local Busbar.
(Laboratory Results)

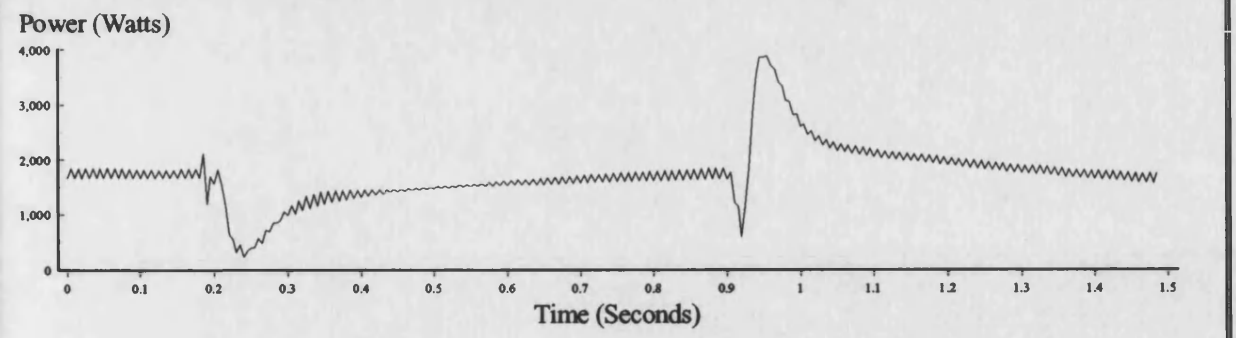

6.14a) Fourier Filtered Power at 4 Samples/Cycle (Input to Algorithm).

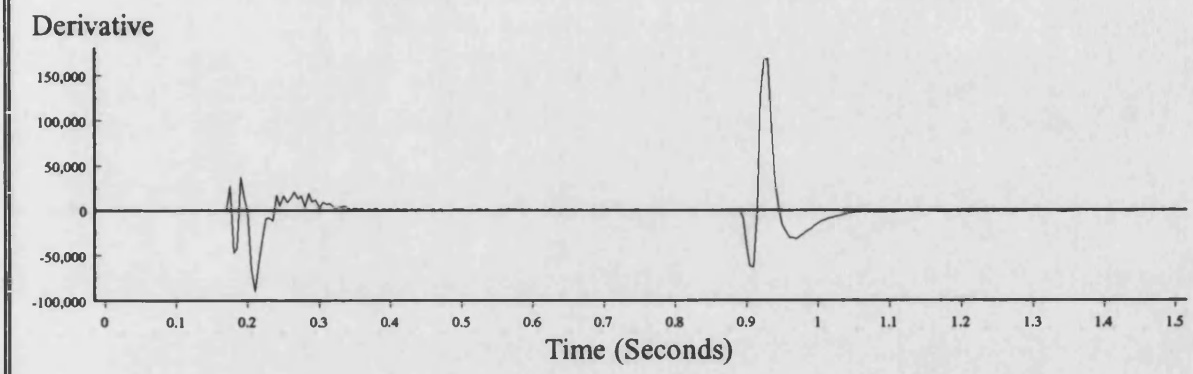

6.14b) Derivative of Filtered Power.

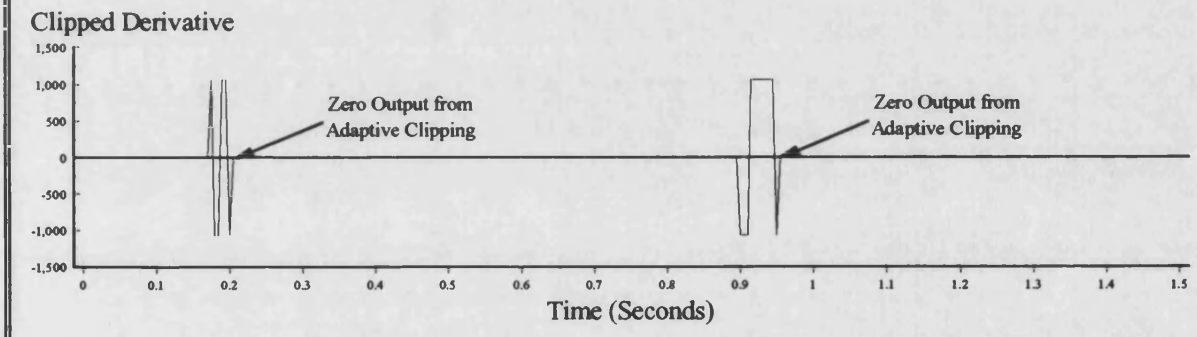

6.14c) Amplitude Limited Derivative.

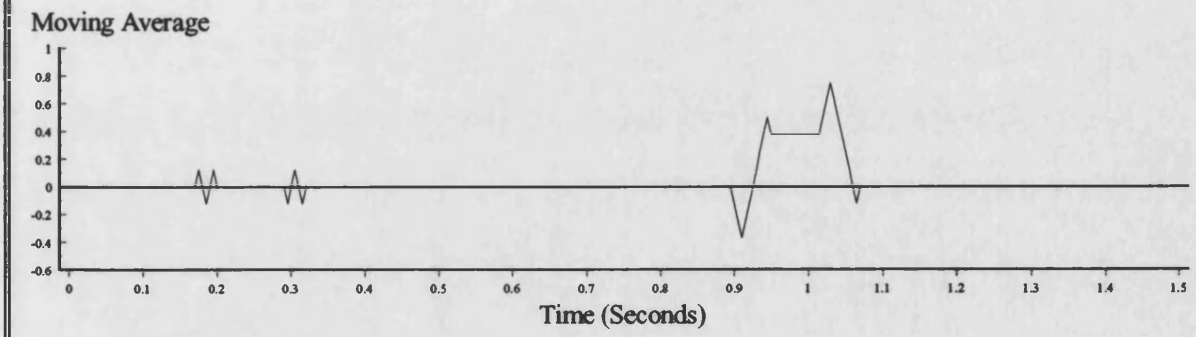

6.14d) Algorithm Output (6 Cycle Moving Average Filter).

Figure 6.14 : Three Phase to Ground Fault on Local Busbar.
(Laboratory Results)

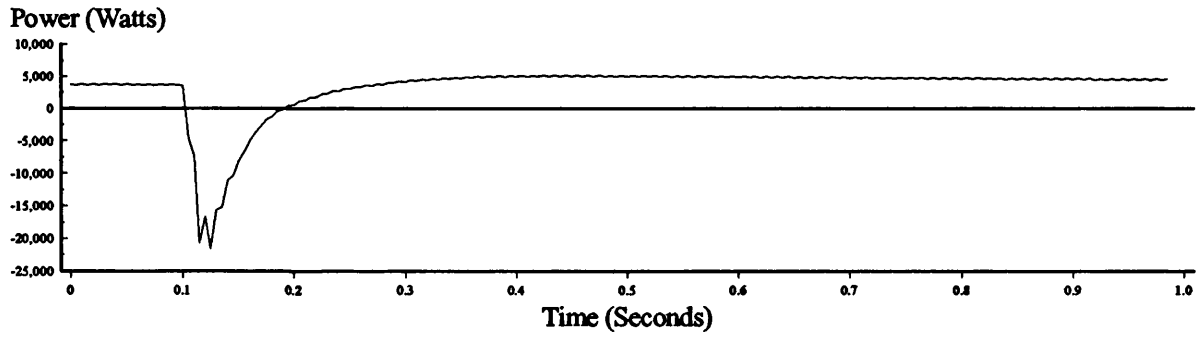

6.15a) Fourier Filtered Power at 4 Samples/Cycle (Input to Algorithm).

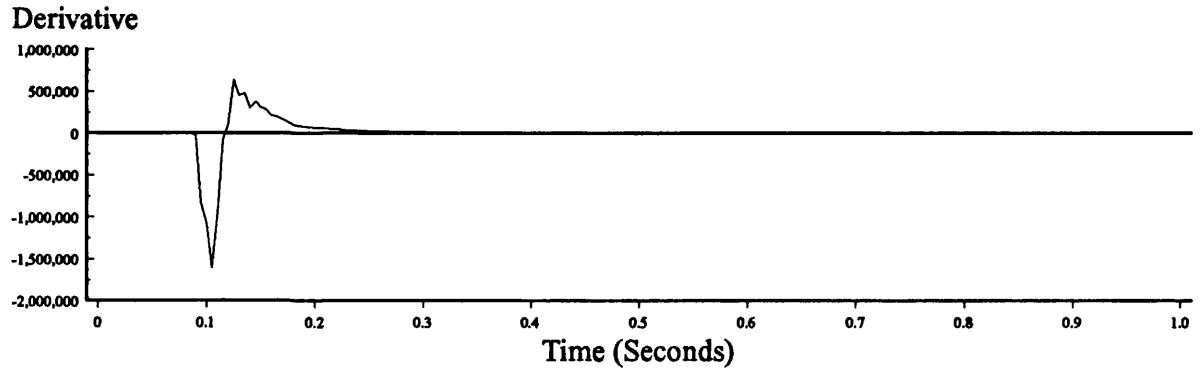

6.15b) Derivative of Filtered Power.

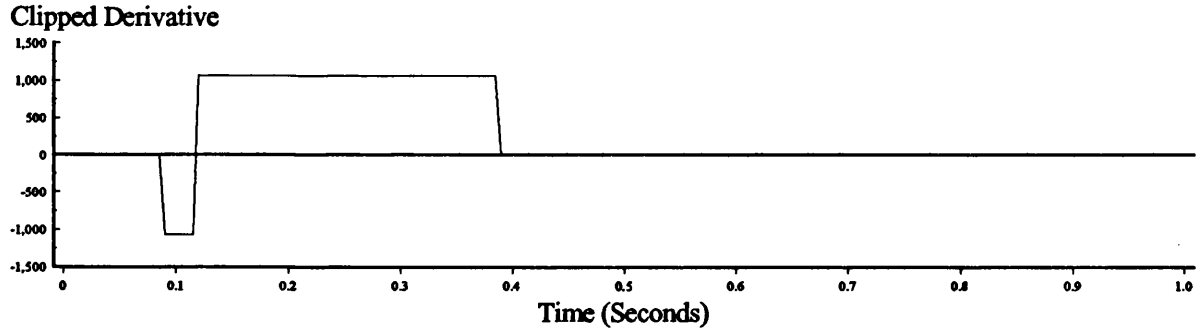

6.15c) Amplitude Limited Derivative.

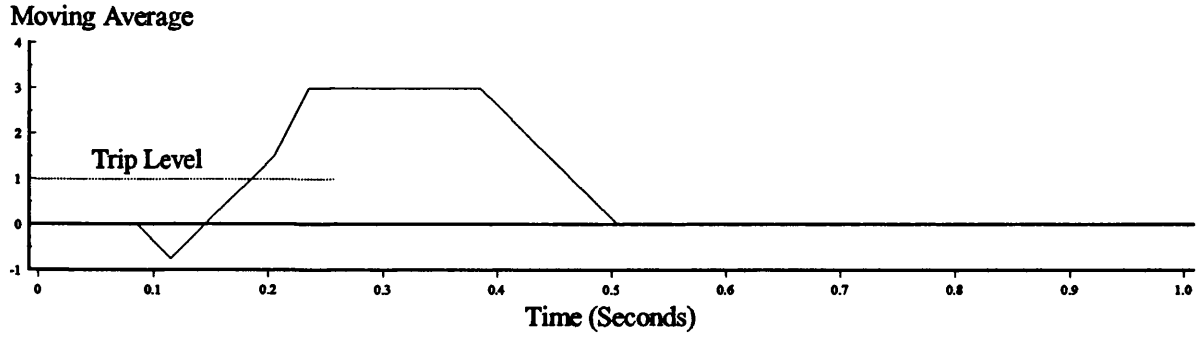

6.15d) Algorithm Output (6 Cycle Moving Average Filter).

Figure 6.15 : A 90 Degree Out of Step Reclosure Between Generator Site and Utility Grid. (Laboratory Results)

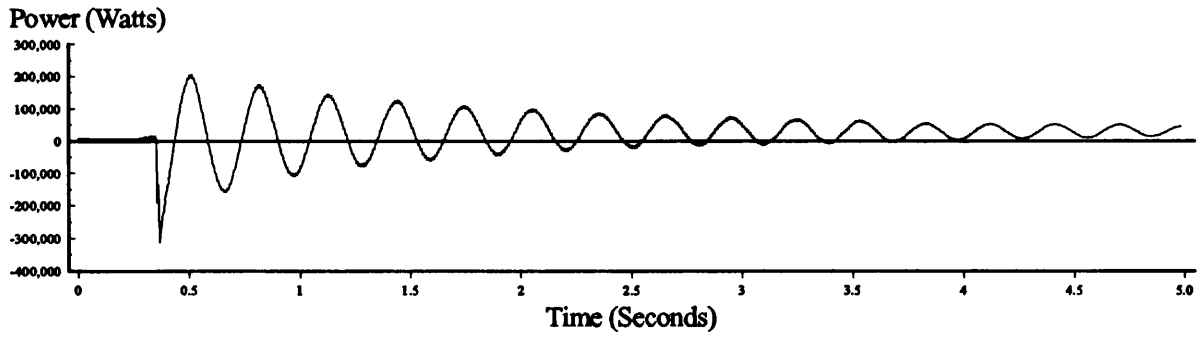

6.16a) Fourier Filtered Power at 4 Samples/Cycle (Input to Algorithm).

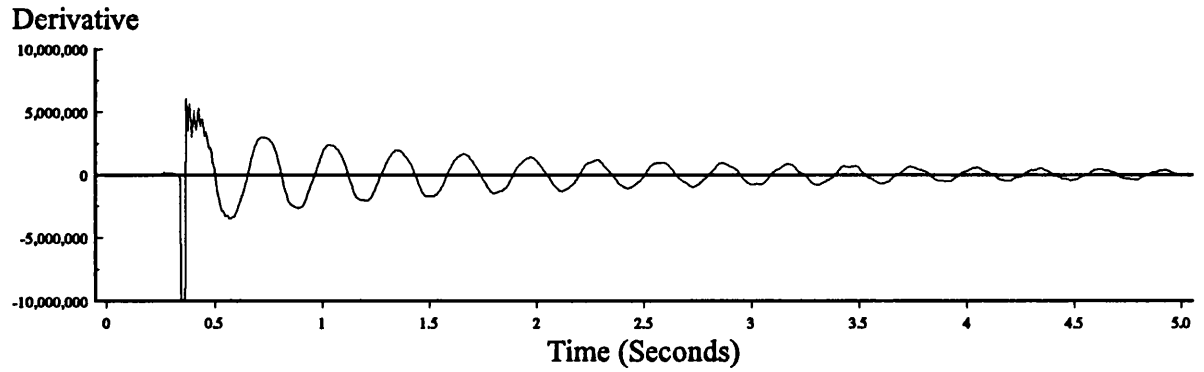

6.16b) Derivative of Filtered Power.

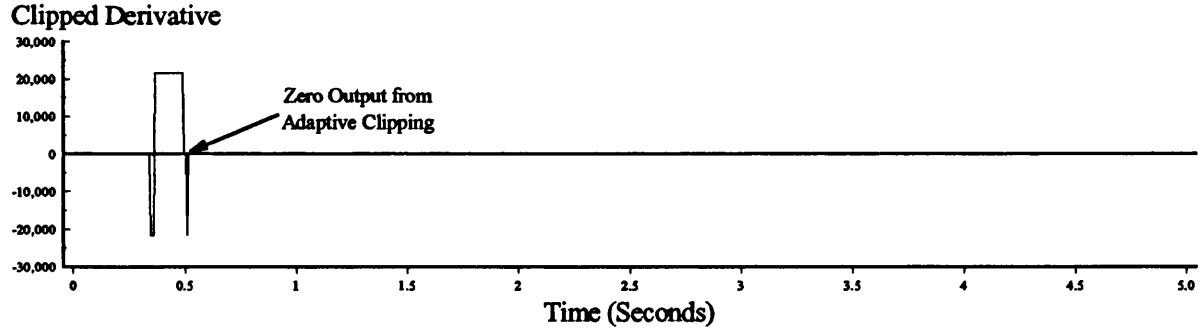

6.16c) Amplitude Limited Derivative.

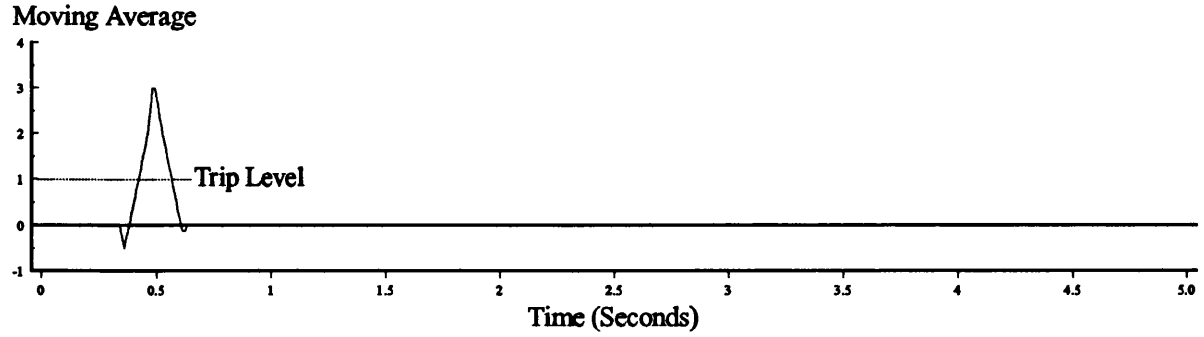

6.16d) Algorithm Output (6 Cycle Moving Average Filter).

Figure 6.16 : Supervised Reclosure Between Generator and Utility Grid.
(Field Trial Results)

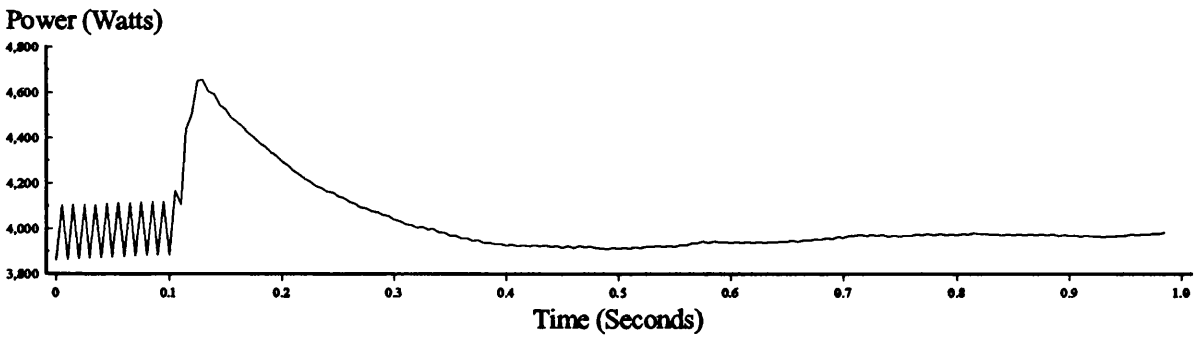

6.17a) Fourier Filtered Power at 4 Samples/Cycle (Input to Algorithm).

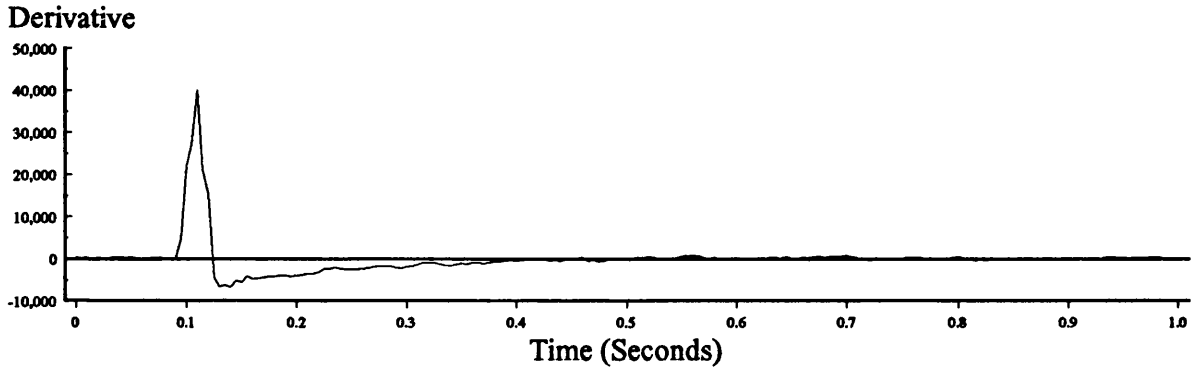

6.17b) Derivative of Filtered Power.

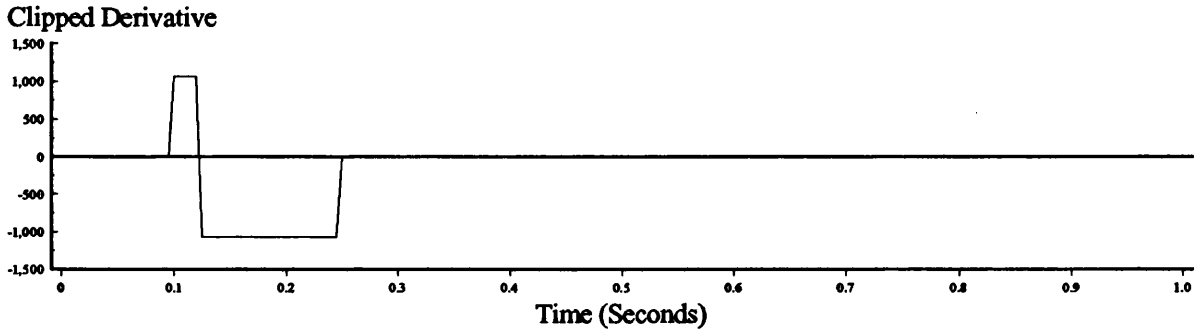

6.17c) Amplitude Limited Derivative.

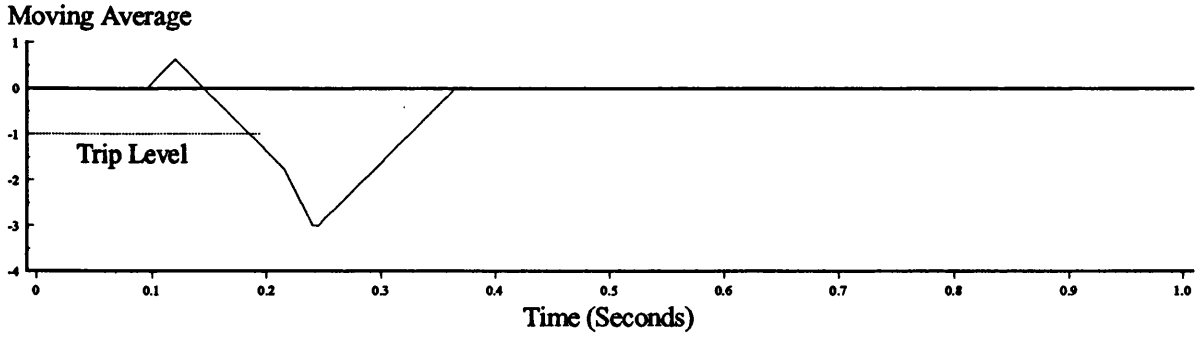

6.17d) Algorithm Output (6 Cycle Moving Average Filter).

Figure 6.17 : Loss of Grid with Two Machines Resulting in a 15% Increase in Loading for each. (Laboratory Results)

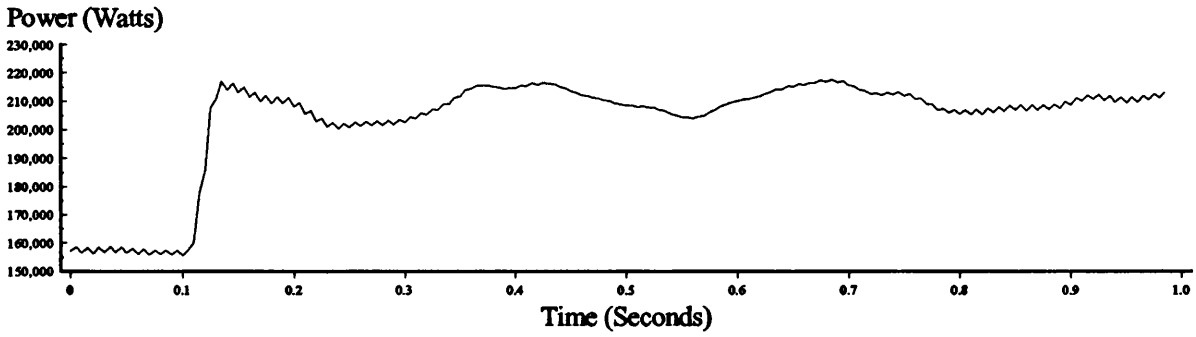

6.18a) Fourier Filtered Power at 4 Samples/Cycle (Input to Algorithm).

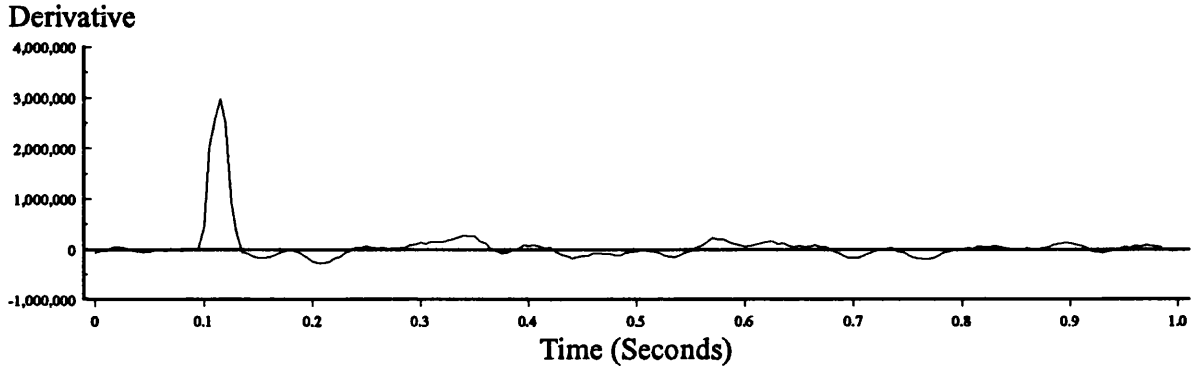

6.18b) Derivative of Filtered Power.

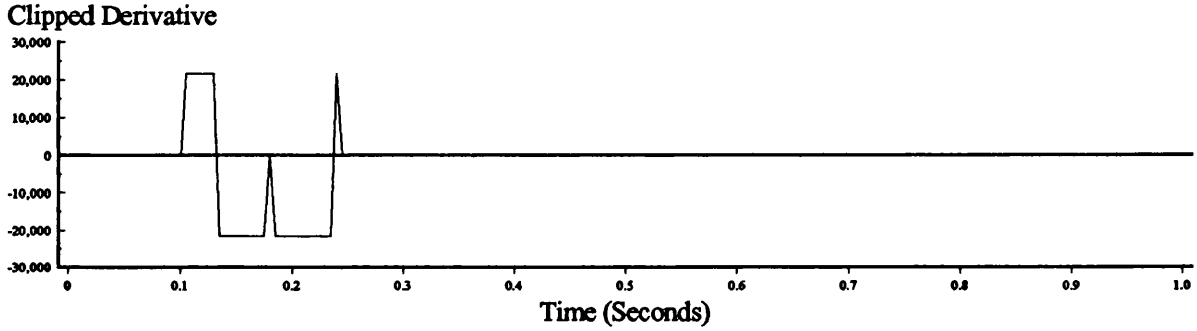

6.18c) Amplitude Limited Derivative.

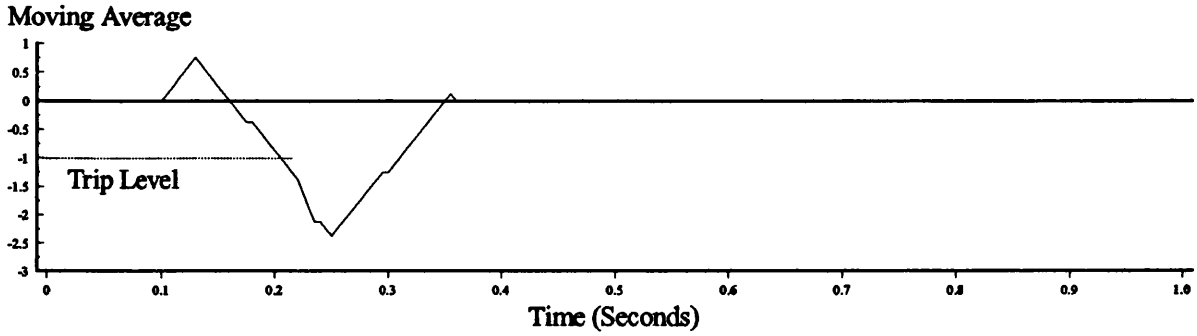

6.18d) Algorithm Output (6 Cycle Moving Average Filter).

Figure 6.18 : Loss of Grid with Two Machines Resulting in a 35% Increase in Loading for each. (Field Trial Results)

Chapter 7

Conclusions and Requirements for Future Work.

Loss of grid protection is a vital part of the protection scheme for an embedded generator which operates in parallel with the utility supply. Since loss of grid is not a conventional fault condition and in itself does not cause any damage, it presents a major challenge to relay and embedded generation scheme designers.

The fundamental criterion for the development of a new loss of grid protection algorithm was that it should be suitable for inclusion in a microprocessor based integrated generator protection package with minimal additional processing or hardware requirements. The resulting protection package will therefore provide high levels of protection in a very cost effective and physically compact unit.

The approach chosen to fit the requirements was a power based algorithm which was conceived after extensive simulation studies. The adaptation of this theoretical algorithm to operate in a practical environment has been presented in this thesis. The final version of the change in power loss of grid algorithm has been shown to trip for both loss of grid and local load change during independent operation. The algorithm remains stable during large local load changes which occur while the utility grid remains connected and also during power system fault conditions.

Laboratory tests in conjunction with field trials have supported the earlier computer simulation results and have demonstrated that the algorithm operates satisfactorily despite the presence of high levels of harmonic interference and system unbalance. These practical test systems have provided the basis for the refinements to the theoretical algorithm which has lead to the implementation of the full algorithm in a microprocessor based protection relay. Throughout this work, the development of the practical algorithm was carried out with a view to its final implementation in an integrated generator

protection relay. This has resulted in an algorithm structure which can be simply included as a single protection task within the relay requiring only additional software.

The fundamental theory on which the algorithm has been based has been proved as far as possible in a research environment but further development is required before its inclusion in a commercially available relay. This development process would include extensive field trials to gain as much information as possible about the response of embedded generation to loss of grid conditions. The result of this would be an algorithm design which would not be scheme specific and could be connected into any configuration of embedded generation system.

The field trials carried out as part of the development process of the new algorithm have highlighted certain areas of future interest with respect to this work and embedded generation projects as a whole. The main area of interest is based around the phenomenon of the low frequency oscillations apparent in the output power of the diesel generator unit. The presence of these oscillations will require further research into their cause and their possible effects on system operation. In particular, a more detailed study of the interface between the generator and the utility is required to provide a better model of the embedded generator scheme and its interface into the utility supply network. The presence of these oscillations at the terminals of a single machine in an embedded generator scheme may not cause any problems, but with the ever-growing interest in embedded generation and the greater penetration of small generators in the utility distribution system, the effects of these oscillations may become more pronounced.

Analysis of the interface between the generator and the utility will provide for a greater understanding of the electrical consequences of increased levels of embedded generation in the network which is particularly pertinent when considering the wider variety of prime mover sources being employed. This further work should also include an investigation into loss of grid events with non-synchronous generators, in particular induction machines, fuel cells and photovoltaic arrays.

Another field for future research can be based around investigating a method for detecting loss of grid at any intertie in a power system network. This is not the same as detecting

a loss of grid at the terminals of a generator which has been the subject of this thesis, but it may be possible to extend some of the theories and techniques devised from this work. Currently, the R.O.C.O.F. relay provides this capability but there is some interest in devising an alternative technique.

A final point about the use of a power based technique to detect a loss of grid is that it allows other protection requirements of a generator to be implemented within the same framework. Work is currently going on into the use of instantaneous power and reactive power to prevent pole slipping of an embedded generator and this technique has been extended to cover loss of excitation. The use of power based algorithms for protecting embedded generators against a number of events is therefore an area for continuing research.

Chapter 8

References

[1] THE ELECTRICITY COUNCIL, 'Engineering Recommendations G59 - Recommendations for the Connection of Private Generating Plant to the Electricity Boards' Distribution Systems.' London, June '85.

[2] ELECTRICITY COUNCIL, 'Notes of Guidance for the Production of Private Generating Sets up to 5MW for Operation in Parallel with Electricity Board's Distribution Networks.' Engineering Technical Reports 113, London, '89.

[3] SOUTH CALIFORNIA EDISON, 'Guide-lines for Operating, Metering and Protection for Co-generators and Small Power Producers.' Los Angeles, June '81.

[4] ANSI/IEEE Standard 1001-1988, 'IEEE Guide for Interfacing Dispersed Storage and Generation Facilities with Electric Utility Systems.' IEEE, New York, '89.

[5] IEEE Special Report, 'Intertie Protection of Consumer-Owned Sources of Generation, 3MVA or Less.' IEEE, 88TH0224-6-PWR, '89.

[6] IEEE Summary Report, 'Intertie Protection of Consumer-Owned Sources of Generation, 3MVA or Less.' IEEE Trans. on Power Delivery, Vol. 5, No. 2, pp 924-929, April '90.

[7] KUNDU, D, 'Technical Requirements to Connect Parallel Generators to the Ontario Hydro Distribution Electricity System.' IEEE Trans. on Energy Conversion, Vol. 7, No. 1, pp 8-13, March '92.

[8] HARLOW, J.H, 'A Multifunction Protective Relay for the Cogeneration Industry.' IEEE Computer Applications in Power, No. 4, pp 25-30, Oct. '90.

[9] GEC ALSTHOM T&D PROTECTION & CONTROL LTD., 'Type LGPG 111 Digital Integrated Generator Protection Relay.' Pub. R4106A.

[10] YIP, H.T, 'An Integrated Approach to Generator Protection.' Canadian Electrical Association Power System Protection Sub-section, Toronto, Mar '94.

[11] YALLA, M.V, 'A Digital Multifunction Protective Relay.' IEEE Trans. on Power Delivery, Vol. 7, No. 1, pp 193-200, Jan. '92.

[12] POWELL, L.J, 'An Industrial View of Utility Cogeneration Protection Requirements.' IEEE Trans. on Industry Applications, Vol. 24, No. 1, pp 75-81, Jan./Feb. '88.

[13] FIELDING, G & BRADLEY, J, 'Local Generation: The Devolution of Power.' IEE Review, Vol. 4, No. 2, pp 117-120, March '90.

[14] 'The Energy Act 1983', Her Majesty's Stationary Office, London.

[15] 'Health and Safety at Work Act 1974', Her Majesty's Stationary Office, London.

[16] 'Electricity Supply Regulations 1937', Her Majesty's Stationary Office, London.

[17] RIZY, D.T, JEWELL, W.T & STOVALL, J.P, 'Operational and Design Considerations for Electric Distribution Systems with Dispersed Storage and Generation (DSG).' IEEE Trans. on Power Apparatus and Systems, Vol. 104, No. 10, pp 2864-2871, Oct. '85.

[18] WOODBURY, F.A, 'Grounding Considerations in Cogeneration.' IEEE Trans. on Industry Applications, Vol. 21, No. 6, pp 1523-1532, Nov./Dec. '85.

[19] M^{C}FADDEN, R.H, 'Grounding of Generators Connected to Industrial Plant Distribution Buses.' IEEE Trans. on Industry Applications, Vol. 17, No. 6, pp 553-556, Nov./Dec. '81.

[20] LOVE, D.J & HASHEMI, N, 'Consideration for Ground Fault Protection in Medium-Voltage Industrial and Cogeneration Systems.' IEEE Trans. on Industry Applications, Vol. 24, No. 4, pp 548-553, July/Aug. '88.

[21] DOUGHTY, R.L, GISE, L, KALKSTEIN, E.W & WILLOUGHBY, R.D, 'Electrical Studies for an Industrial Gas Turbine Cogeneration Facility.' IEEE Trans. on Industry Applications, Vol. 25, No. 4, pp 750-765, July/Aug. '89.

[22] NOBILE, P.A, 'Power System Studies for Cogeneration: What's Really Needed?' IEEE Trans. on Industry Applications, Vol. 23, No. 5, pp 777-785, Sept./Oct. '87.

[23] HOGWOOD, E.E & RICE, D.E, 'The Electrical Aspects of Cogeneration System Design.' IEEE Trans. on Industry Applications, Vol. 23, No. 4, pp 712-722, July/Aug. '87.

[24] NICHOLS, N, 'The Electrical Considerations in Cogeneration.' IEEE Trans. on Industry Applications, Vol. 21, No. 4, pp 754-761, May/June '85.

[25] POPE, J.W, 'Parallel Operation of Customer Generation.' IEEE Trans. on Industry Applications, Vol. 19, No. 1, pp 32-36, Jan./Feb. '83.

[26] PATTON, J.B & CURTICE, D, 'Analysis of Utility Protection Problems Associated with Small Wind-Turbine Interconnection.' IEEE Trans. on Power Apparatus and Systems, Vol. 101, No. 10, pp 3957-3966, Oct. '82.

[27] SIMPSON, R.H, 'Protective Relaying for Multi-Source Generator Buses.' IEEE Trans. on Industry Applications, Vol. 26, No. 2, pp 330-341, March/April '90.

[28] FARDANESH, B & RICHARDS, E.F, 'Distribution System Protection with Decentralised Generation Introduced into the System.' IEEE Trans. on Industry Applications, Vol. 20, No. 1, pp 122-130, Jan./Feb. '84.

[29] DUGAN, R.C & RIZY, D.T, 'Electric Distribution Protection Problems Associated with the Interconnection of Small Dispersed Generation Devices.' IEEE Trans. on Power Apparatus and Systems, Vol. 103, No. 6, pp 1121-1127, June '84.

[30] FEERO, W.E, & GISH, W.B, 'Overvoltages Caused by DSG Operation: Synchronous and Induction Generators.' IEEE Trans. on Power Delivery, Vol. 1, No. 1, pp 258-264, Jan. '86.

[31] WAGNER, C.L, FEERO, W.E, GISH, W.B & JONES, R.H, 'Relay Performance in DSG Islands.' IEEE Trans. on Power Delivery, Vol. 4, No. 1, pp 122-131, Jan. '89.

[32] DALEY, J.M, 'Design Considerations for Operating On-site Generators in Parallel with Utility Service.' IEEE Trans. on Industry Applications, Vol. 21, No. 1, pp 69-80, Jan./Feb. '85

[33] CLARK, H.K & FELTES, J.W, 'Industrial and Cogeneration Protection Problems Requiring Simulation.' IEEE Trans. on Industry Applications, Vol. 25, No. 4, pp 766-775, July/Aug. '89.

[34] ROOK, M.J, GOFF, L.E, POTOCHNEY, G.J & POWELL, L.J, 'Application of Protective Relays on a large Industrial-Utility Tie with Industrial Cogeneration.' IEEE Trans. on Power Apparatus and Systems, Vol. 100, No. 6, pp 2804-2812, June '81.

[35] JONES, R.A, SIMS, T.R & IMECE, A.F, 'Investigation of Potential Islanding of a Self-Commutated Static Power Converter in Photovoltaic Systems.' IEEE Trans. on Energy Conversion, Vol. 5, No. 4, pp 624-631, Dec '90.

[36] WARIN, J.W, 'Loss of Mains Protection.' ERA Conference on 'Circuit Protection for Industrial and Commercial Installations' London '90.

[37] PHADKE, A.G, THORP, J.S & ADAMIAK, M.G, 'A New Measurement Technique for Tracking Voltage Phasors, Local System Frequency and Rate of Change of Frequency.' IEEE Trans. on Power Apparatus and Systems, Vol. 102, No. 5, pp1025-1037, May '83.

[38] MALIK, O.P, HOPE, G.S, HANCOCK, G.C, ZHAOHUI, L, LUQING, Y & SHOUPING, W, 'Frequency Measurement for use with a Microprocessor-Based Water Turbine Governor.' IEEE Trans. on Energy Conversion, Vol. 6, No. 3, pp 361-366, Sept '91.

[39] GIRAY, M.M, & SACHDEV, M.S, 'Off-Nominal Frequency Measurements in Electric Power Systems.' IEEE Trans. on Power Delivery, Vol. 4, No. 3, pp 1573-1578, Jul '89.

[40] MOORE, P.J, CARRANZA, D & JOHNS, A.T, 'Improved Digital Measurement of Power System Frequency.' pp 333-336, 27th UPEC, Bath '92.

[41] SCHALTANLANGEN ELECTRONIK GERATE GMBH & CO., 'Generator / Mains Monitor - GW2.' Pub. GW2/E/810

[42] COOPER, C.B, 'Standby Generation: Problems and Prospective Gains From Parallel Running.' Power System Protection '89, pp 1-6, Singapore '89.

[43] REDFERN, M.A, USTA, O, FENG, B, & FIELDING, G, 'Loss of Mains Protection for Private Generation Operating in Parallel with the Utility Supply.' pp 89-92, 25th UPEC, Aberdeen '90.

[44] REDFERN, M.A, USTA, O, BARRETT, J.I, & FIELDING, G, 'A New Digital Relay For Loss of Grid to Protect Embedded Generation.' 5th IEE International Conference on 'Developments in Power System Protection,' York, March '93.

[45] USTA, O, 'A Power Based Digital Algorithm for the Protection of Embedded Generators.' PhD Thesis, Dec. '92.

[46] ANDERSON, P.M & FOUAD, A.A, 'Power System Control and Stability.' Iowa State Univ. Press, Iowa '77, USA.

[47] REDFERN, M.A, BARRETT, J.I, HEWINGS, D, & USTA, O, 'A Laboratory Facility for Research into Digital Protection Algorithms used for the Protection of Small and Medium Sized Generators.' 26th UPEC, Brighton, '91.

[48] BARRETT, J.I, 'Development of a Laboratory Facility for the Teaching and Research of Digital Protection Algorithms for the Protection of Small Generators.' BEng. Project Report, 1991.

[49] Data Translation 'DT2821 Manual.' MA USA, '91

[50] Data Translation ATLAB Manual.' MA USA, '91

[51] GEC Alsthom Protection and Control Ltd., Stafford, 'B.I.O.S. User Manual'

[52] GEC Alsthom Protection and Control Ltd., Stafford, 'M.T.E. Version 2 User Manual'

[53] HOROWITZ, P, & HILL, W, 'The Art of Electronics.' Cambridge Uni. Press, '80.

[54] SCHWEITZER, E.O & HOU, D, 'Filtering for Protective Relays'

[55] KWONG, W.S, CLAYTON, M.J, & NEWBOULD, A, 'A Microprocessor Based Current Differential Relay for use with Digital Communication Systems.' 3rd IEE International Conference on 'Developments in Power System Protection.' London, April '85.

[56] REDFERN, M.A, USTA, O, BARRETT, J.I, & YIP, T, 'A New Microprocessor Based Loss of Grid Protection for Embedded Generation.' 2nd IEE International Conference on Advances in Power System Control, Operation and Management.' Hong Kong, '93.

[57] REDFERN, M.A, USTA, O, BARRETT, J.I, & FIELDING, G, 'Protection Against Loss of Utility Grid Supply for an Embedded Generator.' 27th UPEC, Bath, '92.

[58] REDFERN, M.A, USTA, O, & BARRETT, J.I, 'Loss of Grid Protection for an Embedded Generator.' IEE Colloquium on 'The Effective Response of a Public Electricity Network to Independent Generators.' Chester, '93.

[59] REDFERN, M.A, USTA, O, & FIELDING, G, 'Protection Against Loss of Utility Grid Supply For a Dispersed Storage and Generation Unit.' IEEE Trans. on Power Delivery, Vol. 8, No. 3, pp948-954, July '93.

Appendix A

Background Theory

A.1 Definition of the Swing Equation.[46]

The swing equation governs the motion of a machine's rotor relating the inertia torque to the resultant mechanical and electrical torques.

$$T_a = J \frac{d^2\theta}{dt^2} \qquad (A.1)$$

Where: J = Moment of Inertia (in Kgm^2),

θ = Mechanical Shaft Angle with respect to a fixed reference (Rads),

T_a = Accelerating Torque acting on the shaft (Nm).

For a generator:

$$T_a = T_m - T_e \qquad (A.2)$$

Where: T_m = Mechanical Driving Torque.

T_e = Electrical Retarding Torque.

Choosing the angular reference relative to a synchronously rotating reference frame moving at constant angular velocity ω_R gives:

$$\theta = (\omega_R t + \alpha) + \delta_m \qquad (rads) \qquad (A.3)$$

Where: α = a constant, δ_m = mechanical torque angle,

ω_R = shaft angular velocity (rad/sec).

Differentiating with respect to time leads to:

$$\frac{d^2\theta}{dt^2} = \frac{d^2\delta_m}{dt^2} = \frac{d\omega_m}{dt} \qquad (A.4)$$

Where: ω_m = Mechanical Angular Velocity (rad/sec).

Therefore:

$$T_a = J\frac{d^2\delta_m}{dt^2} = J\frac{d\omega_m}{dt} \qquad \text{(A.5)}$$

However, the swing equation is best written in terms of an electrical angle that can be conveniently related to the position of the rotor. This is the torque angle δ which is the angle between the field mmf and the resultant mmf in the air gap (i.e. the electrical angle between the generated E.M.F. and the resultant stator voltage phasor). The torque angle δ (equal to the electrical torque angle δ_e) is related to the mechanical angle δ_m by:

$$\delta = \delta_e = (p/2)\,\delta_m \qquad \text{(A.6)}$$

Where: p = Number of Poles.

Returning to the torque equation (A.5) and replacing δ_m with (2/p)δ leads to:

$$T_a = \frac{2J}{p}\cdot\frac{d^2\delta}{dt^2} \qquad \text{(A.7)}$$

This equation can then also be normalised to a per unit torque by dividing by a base quantity equal to the rated torque at rated speed:

$$T_B = \frac{S_B}{\omega_m} = \frac{60S_B}{2\pi n_R} \qquad \text{(A.8)}$$

Giving:

$$T_{a_{p.u.}} = \frac{T_a}{T_B} = \frac{\frac{2J}{p}\cdot\frac{d^2\delta}{dt^2}}{\frac{60S_B}{2\pi n_R}} \qquad \text{(A.9)}$$

By substituting: $p = 120f_R/n_R$, $f_R = \omega_R/2\pi$, $J = 2Wk/\omega_m^2$ and $\omega_m = 2\pi n_R$ gives:

$$T_{a_{p.u.}} = \frac{2W_k}{S_B\omega_R}\cdot\frac{d^2\delta}{dt^2} \qquad \text{(A.10)}$$

Where: W_k = Kinetic energy of rotating mass,

S_B = Common base quantity (MVA)

At this stage an important quantity can be defined as:

$$H = \frac{W_k}{S_B} \qquad (MJ / MVA) \tag{A.11}$$

The swing equation may then be written in one of its most practical forms:

$$T_{a_{p.u.}} = \frac{2H}{\omega_R} \cdot \frac{d^2\delta}{dt^2} \tag{A.12}$$

Where: H is in seconds, ω_R is in rad/sec and T is in per unit.

Note that this form of the swing equation has been adapted for machines with any number of poles, since all machines on the same system synchronize to the same ω_R. A modified and approximate form of the swing equation can be formulated by recognizing that the angular speed ω is nearly constant, and the per unit accelerating power P_a is numerically equal to the accelerating torque. Thus, equation (A.12) becomes:

$$P_{a_{p.u.}} = \frac{2H}{\omega_R} \cdot \frac{d^2\delta}{dt^2} \tag{A.13}$$

The value of the inertia constant H, is usually given for a particular machine, normalized to the base VA rating for that machine. For system studies, the value must be converted to a system base VA such that:

$$H_{sys} = H_{mach} \cdot \left(\frac{S_{B_{mach}}}{S_{B_{sys}}} \right) \qquad (secs) \tag{A.14}$$

A.2 Model of a Single Machine on an Infinite Busbar.

A power system bus of large capacity with respect to the machine under consideration can be considered as an infinite bus since its frequency and voltage are essentially invariable both in magnitude and phase. Consider the classical model of one machine connected to an infinite bus through a transmission line. A schematic representation can be seen in figure A.1).

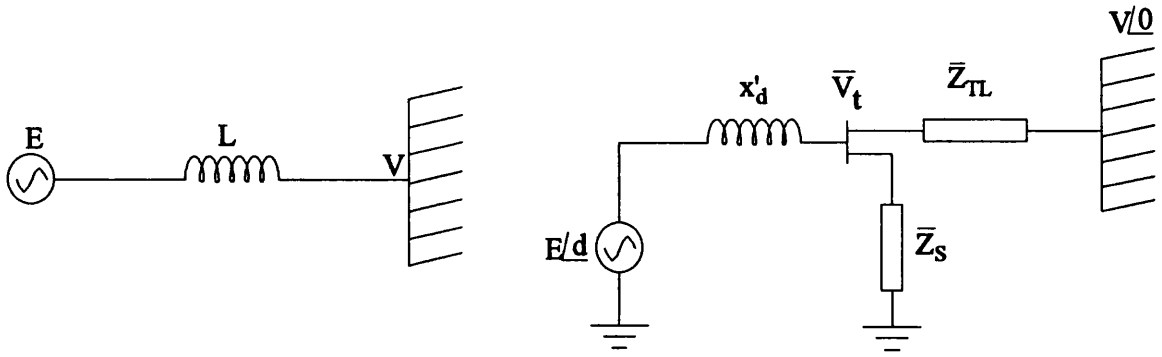

Figure A1) A single machine connected to an infinite busbar through a transmission line: (a) One-line diagram, (b) Equivalent circuit.

Where: V_t = terminal voltage of the synchronous machine,

x'_d = direct axis transient reactance of the machine,

Z_{TL} = series impedance of the transmission network,

Z_s = equivalent shunt impedance at the machine terminal (includes local loads).

This model requires the following assumptions:

1) The mechanical power input remains constant during the period of transient.

2) Damping or asynchronous power is negligible.

3) The synchronous machine is represented (electrically) by a constant voltage source behind a transient reactance.

4) The mechanical angle of the synchronous machine rotor coincides with the electrical phase angle of the voltage behind the transient reactance.

5) If a local load is fed at the terminal voltage of the machine, it can be represented by a constant impedance (or admittance) to neutral.

Using a Y-Δ transformation, the node representing the terminal voltage V_t in figure A.1 can be eliminated leading to the equivalent circuit shown by figure A.2.

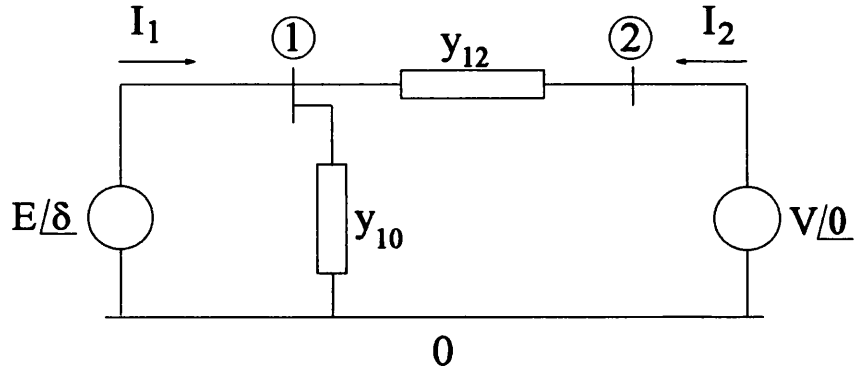

Figure A2) Equivalent circuit for a system of one machine against an infinite busbar.

Note that three admittance elements are obtained (y12, y10 and y20), y20 is omitted since it is not required in the analysis. The two-port network can be described by the equation:

$$\begin{bmatrix} I_1 \\ I_2 \end{bmatrix} = \begin{bmatrix} Y_{11} & Y_{12} \\ Y_{21} & Y_{22} \end{bmatrix} \begin{bmatrix} E \\ V \end{bmatrix} \tag{A.15}$$

Where: $Y_{11} = y_{12} + y_{10}$ and $Y_{12} = -y_{12}$

Network theory shows that power at node 1 is given by $P_1 = \mathcal{R}e\ EI_1^*$ which simplifies to:

$$P_1 = E^2 Y_{11} \cos\theta_{11} + EVY_{12} \cos(\theta_{12} - \delta) \tag{A.16}$$

Now define:

$$\begin{aligned} G_{11} &= Y_{11} \cos\theta_{11} \\ \gamma &= \theta_{12} - \frac{\pi}{2} \end{aligned} \tag{A.17}$$

Then:

$$\begin{aligned} P_1 &= E^2 G_{11} + EVY_{12} \sin(\delta - \gamma) \\ &= P_C + P_M \sin(\delta - \gamma) \end{aligned} \tag{A.18}$$

Where: P_M = Maximum Power (EV/X) and the relationship between P_1 and δ is shown in figure (A.3).

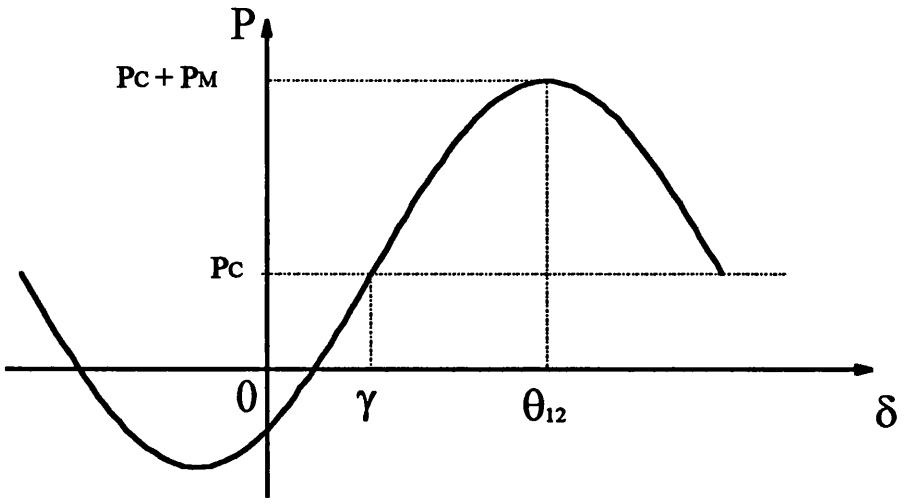

Figure A3) Power output of a synchronous machine connected to an infinite bus.

Where Pc represents the power dissipated in the equivalent network and angle γ is determined by the real component of the transfer admittance Y_{12}.

A.3 Response to Small Disturbances.

When a power impact occurs at some bus in a network, an unbalance between the power input to the system and the power output occurs which results in a transient. After this transient subsides and a steady state condition is reached, the power impact is distributed between the various machines on the system according to the steady state droop characteristics of their governors. However, during the transient period, the power impact is shared according to a different criteria.

A.3.1 The Unregulated Synchronous Machine.

Using the simple model of a voltage behind a transient reactance, from earlier equations (A.13) and (A.18):

$$P_{a_{p.u.}} = P_m - P_e = \frac{2H}{\omega_R} \cdot \frac{d^2\delta}{dt^2} \qquad \text{(A.19)}$$

$$P_e = P_C + P_M \sin(\delta - \gamma) \tag{A.20}$$

Letting $\delta = \delta_0 + \delta_\Delta$; $P_e = P_{e0} + P_\Delta$; $P_m = P_{m0}$ and using the relationship:

$$\sin(\delta - \gamma) = \sin(\delta_0 - \gamma + \delta_\Delta) \approx \sin(\delta_0 - \gamma) + \cos(\delta_0 - \gamma)\delta_\Delta \tag{A.21}$$

the linearized version becomes:

$$\frac{2H}{\omega_R} \cdot \frac{d^2\delta_\Delta}{dt^2} + P_s \delta_\Delta = 0 \tag{A.22}$$

where $P_s = P_M \cos(\delta_0 - \gamma)$ = Synchronizing Power Coefficient.

A.3.2 Modes of Oscillation of an Unregulated Multimachine System.

The electrical power output of the i^{th} machine in an n-machine system is obtained from equations A.16 and A.17:

$$P_{ei} = E_i^2 G_{ii} + \sum_{\substack{j=1 \\ j \neq i}}^{n} E_i V_j Y_{ij} \cos(\theta_{ij} - \delta_{ij}) \tag{A.23}$$

$$P_{ei} = E_i^2 G_{ii} + \sum_{\substack{j=1 \\ j \neq i}}^{n} E_i E_j (B_{ij} \sin\delta_{ij} + G_{ij} \cos\delta_{ij}) \tag{A.24}$$

Where: $\delta_{ij} = \delta_i - \delta_j$,

E_i = constant voltage behind transient reactance for i^{th} machine,

$Y_{ii} = G_{ii} + jB_{ii}$ a diagonal element of the network short circuit admittance matrix,

$Y_{ij} = G_{ij} + jB_{ij}$ an off-diagonal element of the admittance matrix.

Using the incremental model so that $\delta_{ij} = \delta_{ij0} + \delta_{ij\Delta}$ gives:

$$\begin{aligned} \sin\delta_{ij} &= \sin\delta_{ij0} \cos\delta_{ij\Delta} + \cos\delta_{ij0} \sin\delta_{ij\Delta} \approx \sin\delta_{ij0} + \delta_{ij\Delta}\cos\delta_{ij0} \\ \cos\delta_{ij} &\approx \cos\delta_{ij0} - \delta_{ij\Delta}\sin\delta_{ij0} \end{aligned} \tag{A.25}$$

and leads to a final form for $P_{ei\Delta}$,

$$P_{ei\Delta} = \sum_{\substack{j=1 \\ j \neq i}}^{n} E_i E_j (B_{ij} \cos\delta_{ij0} - G_{ij} \sin\delta_{ij0}) \delta_{ij\Delta} \qquad (A.26)$$

For a given initial condition sin δ_{ij0} and cos δ_{ij0} are known and the term in parentheses in equation (A.26) is a constant. Thus:

$$P_{ei\Delta} = \sum_{\substack{j=1 \\ j \neq i}}^{n} P_{sij} \delta_{ij\Delta} \qquad (A.27)$$

P_{sij} is the change in the electrical power of the i^{th} machine due to a change in the angle between machines i and j, with all the other angles held constant. It is a synchronizing power coefficient between nodes i and j and the concept of synchronizing power coefficients can be extended to mean "the change in the electrical power of a given machine due to the change in the angle between its internal E.M.F. and any bus, with all other bus angles held constant.

A.3.3 Distribution of Power Impacts.

The sudden application of a small load $P_{L\Delta}$ at some point in a network creates an unbalance between generation and load and an oscillatory transient occurs before the system settles to a new steady-state condition.

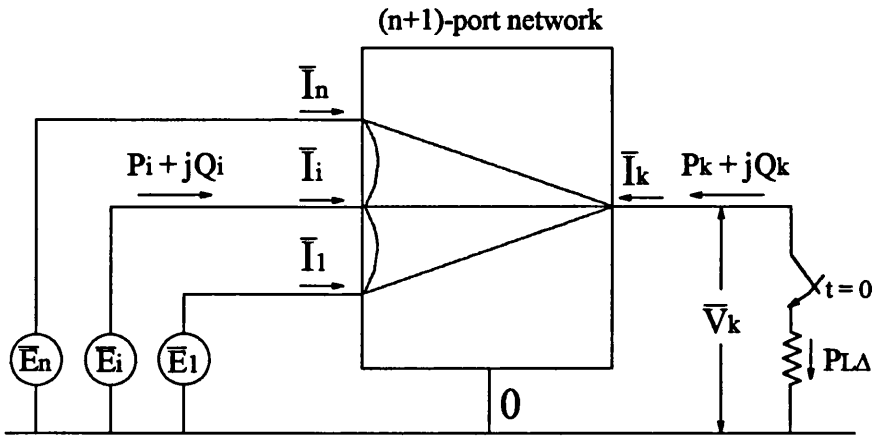

Figure A4: Network with Power Impact at node k.

Referring to the (n+1)-port network in figure A.4, the power into node *i* is obtained from equation A.24 by adding node *k*.

$$P_i = E_i^2 G_{ii} + \sum_{\substack{j=1 \\ j \neq i,k}}^{n} E_i E_j (B_{ij} \sin\delta_{ij} + G_{ij} \cos\delta_{ij}) + E_i V_k (B_{ik} \sin\delta_{ik} + G_{ik} \cos\delta_{ik}) \quad (A.28)$$

For the case of nearly zero conductance (i.e. the network has a very high X/R ratio):

$$P_i \cong \sum_{\substack{j=1 \\ j \neq i,k}}^{n} E_i E_j B_{ij} \sin\delta_{ij} + E_i V_k B_{ik} \sin\delta_{ik} \quad (A.29)$$

and the power into node k (i.e. the load bus) is:

$$P_k = \sum_{\substack{j=1 \\ j \neq k}}^{n} V_k E_j B_{kj} \sin\delta_{kj} \quad (A.30)$$

The immediate effect of the application of $P_{L\Delta}$ is that the angle of bus k is changed while the magnitude of its voltage is unchanged (i.e. $V_k \angle \delta_{k0}$ becomes $V_k \angle \delta_{k0} + \delta_{k\Delta}$). The internal angles of the other machines cannot change instantly due to the inertia of the rotating mass.

These equations are non-linear but since we are only concerned with a small impact $P_{L\Delta}$ we linearize the equations to find:

$$P_i = P_{i0} + P_{i\Delta} \quad ; \quad P_k = P_{k0} + P_{k\Delta} \quad (A.31)$$

and determine only the variables $P_{i\Delta}$ and $P_{k\Delta}$.

These equations are linearized by the relations:

$$\begin{aligned} \sin\delta_{kj} &= \sin(\delta_{kj0} + \delta_{kj\Delta}) \cong \sin\delta_{kj0} + \delta_{kj\Delta} \cos\delta_{kj0} \\ \cos\delta_{kj} &= \cos(\delta_{kj0} + \delta_{kj\Delta}) \cong \cos\delta_{kj0} - \delta_{kj\Delta} \sin\delta_{kj0} \end{aligned} \quad (A.32)$$

Substituting A.32 into equations A.29 and A.30 and eliminating the initial values gives the linearized equations:

$$P_{i\Delta} = \sum_{\substack{j=1 \\ j\neq i,k}}^{n} (E_i E_j B_{ij} \cos\delta_{ij0})\delta_{ij\Delta} + (E_i V_k B_{ik} \cos\delta_{ik0})\delta_{ik\Delta} = \sum_{\substack{j=1 \\ j\neq i,k}}^{n} P_{sij}\delta_{ij\Delta} + P_{sik}\delta_{ik\Delta} \quad \text{(A.33)}$$

$$P_{k\Delta} = \sum_{j=1}^{n} (V_k E_j B_{kj} \cos\delta_{kj0})\delta_{kj\Delta} = \sum_{j=1}^{n} P_{skj}\delta_{kj\Delta}$$

These equations are valid for any time t following the application of the impact.

Immediately following the load impact ($t = 0^+$).

Immediately following the load impact it would be of interest to know exactly how much of the impact $P_{L\Delta}$ is supplied by each generator in the system. At the instant $t = 0^+$ we know that $\delta_{i\Delta} = 0$ for all generators because of the rotor inertias. Thus

$$\begin{aligned} \delta_{ij\Delta} &= 0 \\ \delta_{ik\Delta} &= \delta_{i\Delta} - \delta_{k\Delta} = -\delta_{k\Delta}(0^+) \\ \delta_{kj\Delta} &= \delta_{k\Delta} - \delta_{j\Delta} = \delta_{k\Delta}(0^+) \end{aligned} \quad \text{(A.34)}$$

Including these relationships in equations A.33 leads to:

$$P_{k\Delta}(0^+) = \sum_{j=1}^{n} P_{skj}\delta_{k\Delta}(0^+) \quad \text{(A.35)}$$

$$P_{i\Delta}(0^+) = -P_{sik}\delta_{k\Delta}(0^+) \quad \text{(A.36)}$$

Comparing the above two equations at $t = 0^+$, note at node k:

$$P_{k\Delta}(0^+) = -\sum_{i=1}^{n} P_{i\Delta}(0^+) \quad \text{(A.37)}$$

The change in power at node k is equal to all the power changes of the i machines. At node i, $P_{i\Delta}$ depends upon $B_{ik}\cos\delta_{ik0}$ (equation A.33). In other words, the higher the transfer susceptance B_{ik} and the lower the initial angle δ_{ik0}, the greater the share of the impact "picked up" by machine i. Note also that $P_{k\Delta} = -P_{L\Delta}$ so the previous equations can be written in terms of the load impact as:

$$P_{L\Delta}(0^+) = -\sum_{i=1}^{n} P_{ski}\delta_{k\Delta}(0^+) = \sum_{i=1}^{n} P_{i\Delta}(0^+) \qquad \text{(A.38)}$$

From equations A.37 and A.38 we conclude that:

$$\delta_{k\Delta}(0^+) = -\frac{P_{L\Delta}(0^+)}{\sum_{i=1}^{n} P_{sik}} \qquad \text{(A.39)}$$

$$P_{i\Delta}(0^+) = \left(\frac{P_{sik}}{\sum_{j=1}^{n} P_{sjk}}\right) P_{L\Delta}(0^+) \qquad i = 1, 2, ..., n \qquad \text{(A.40)}$$

At the instant of the load impact ($t = 0^+$) the source of the energy supplied by the generators is the energy stored in their magnetic fields and is distributed according to the synchronizing power coefficients between i and k. As the generator rotor angles cannot change instantly, the energy supplied by the generators cannot come instantly from the energy stored in the rotating masses. $P_{i\Delta}$ depends upon P_{sik} or B_{ik} which depends upon the reactance between generator i and node k.

Equations A.37 and A.38 show that the load impact $P_{L\Delta}$ at network bus k is immediately shared by the synchronous generators according to their synchronizing power coefficients with respect to bus k. Thus the machines *electrically close* (i.e. low reactance line) to the point of impact will pick up the greater share of the load *regardless of their size.*

Consider the deceleration of machine i due to sudden increase in its output power $P_{i\Delta}$. The equation governing the motion of the machine is given by:

$$\frac{2H_i}{\omega_R} \cdot \frac{d\omega_{i\Delta}}{dt} + P_{i\Delta}(t) = 0 \qquad i = 1, 2, ..., n \qquad \text{(A.41)}$$

Using equation A.40 and rearranging gives:

$$\frac{1}{\omega_R} \cdot \frac{d\omega_{i\Delta}}{dt} = -\frac{P_{sik}}{2H_i}\left(\frac{P_{L\Delta}(0^+)}{\sum_{j=1}^{n} P_{sjk}}\right) \qquad i = 1, 2, ..., n \qquad \text{(A.42)}$$

The per unit deceleration of machine i is given by equation A.42 and is dependent on the synchronizing power coefficient P_{sik} and the inertia H_i. This deceleration will be constant until governor action begins.

Behaviour prior to governor action ($t \leq t_g$)

Consider the system behaviour at time t_1 during the period $0 < t < t_g$, where t_g is the time at which governor action begins. Looking at the system as a whole, there will be an overall deceleration of the machines during this period. To obtain a mean deceleration, define an "inertial centre" that has angle $\underline{\delta}$ and angular velocity $\underline{\omega}$, where by definition:

$$\underline{\delta} = \left(\frac{1}{\sum H_i}\right) \sum \delta_i H_i \quad \underline{\omega} = \left(\frac{1}{\sum H_i}\right) \sum \omega_i H_i \tag{A.43}$$

Summing the set (A.42) for all values of i, gives:

$$\frac{2}{\omega_R} \sum \frac{d}{dt}(H_i \omega_{i\delta}) = P_{k\Delta} = - P_{L\Delta}(0^+) \tag{A.44}$$

leading to:

$$\frac{d}{dt} \frac{\underline{\omega}_\Delta}{\omega_R} = - \frac{P_{L\Delta}(0^+)}{\sum_{i=1}^{n} 2H_i} \tag{A.45}$$

Equation A.45 gives the mean acceleration of all the machines in the system defined as the acceleration of a fictitious inertial centre. Each machine in the system follows an oscillatory motion governed by its swing equation. However synchronizing forces tend to pull them towards the mean system retardation and after a transient period they will acquire the same retardation given by equation A.45. When the transient decays, $d\omega_{i\Delta}/dt$ is equal to $d\underline{\omega}_\Delta/dt$ and from equations A.41 and A.45:

$$P_{i\Delta}(t \leq t_g) = \left(\frac{H_i}{\sum_{j=1}^{n} H_j}\right) P_{L\Delta}(0^+) \tag{A.46}$$

Thus at the end of the brief transient ($t = 0^+$) the various machines share the load increase as a function of their inertia constants alone.

In summary, the two modes of operation following a load increase are described by the following equations:

$$P_{i\Delta}(0^+) = \frac{P_{sik}}{\sum_{j=1}^{n} P_{sjk}} P_{L\Delta}(0^+) \tag{A.47}$$

and

$$P_{i\Delta}\ (t \le t_g) = \frac{H_i}{\sum_{j=1}^{n} H_j} P_{L\Delta}(0^+) \tag{A.48}$$

We note that immediately following the impact, the machines share the impact according to their electrical proximity to the point of the impact as expressed by the synchronizing power coefficients. After this brief transient period, the same machines share the same impact according to an entirely different criteria (i.e. their relative inertias).

Appendix B

Power in Polyphase Systems

Instantaneous Power is defined as the product of instantaneous voltage and instantaneous current:

$$p = v * i \tag{B.1}$$

To prove that under balanced conditions:

$$v_a*i_a + v_b*i_b + v_c*i_c = 3\,V\,I\cos\phi \tag{B.2}$$

Where V and I are the RMS voltage and current and ϕ is the phase angle.

Let:

$$v_a = \hat{V}\cos\omega t \qquad i_a = \hat{I}\cos(\omega t + \phi) \tag{B.3}$$

$$v_b = \hat{V}\cos(\omega t + 240°) \qquad i_b = \hat{I}\cos(\omega t + 240° + \phi) \tag{B.4}$$

$$v_c = \hat{V}\cos(\omega t + 120°) \qquad i_c = \hat{I}\cos(\omega t + 120° + \phi) \tag{B.5}$$

The instantaneous power in the A-phase can be found as:

$$P_a = \hat{V}\cos\omega t * \hat{I}\cos(\omega t + \phi) = \hat{V}\hat{I}\cos\omega t\cos(\omega t + \phi) \tag{B.6}$$

Using the identity: 2 CosA CosB = Cos (A+B) + Cos (A-B) gives:

$$P_a = \frac{\hat{V}\hat{I}}{2}\left[\cos(2\omega t + \phi) + \cos\phi\right] \tag{B.7}$$

Similarly for P_b and P_c gives:

$$P_b = \frac{\hat{V}\hat{I}}{2} [\cos(2(\omega t + 240°) + \phi) + \cos\phi] \quad \text{(B.8)}$$

$$P_c = \frac{\hat{V}\hat{I}}{2} [\cos(2(\omega t + 120°) + \phi) + \cos\phi] \quad \text{(B.9)}$$

In terms of R.M.S. quantities these can be simplified to:

$$P_a = VI\cos(2\omega t + \phi) + VI\cos\phi \quad \text{(B.10)}$$

$$P_b = VI\cos(2(\omega t + 240°) + \phi) + VI\cos\phi \quad \text{(B.11)}$$

$$P_c = VI\cos(2(\omega t + 120°) + \phi) + VI\cos\phi \quad \text{(B.12)}$$

Since $P_{Total} = P_a + P_b + P_c$ then:

$$P_{Total} = 3VI\cos\phi + VI[\cos(2\omega t + \phi) + \cos(2(\omega t + 240°) + \phi) + \cos(2(\omega t + 120°) + \phi)] \quad \text{(B.13)}$$

The term in the square bracket is equal to zero giving the final result:

$$P_{Total} = 3VI\cos\phi \quad \text{(B.14)}$$

Which is a constant under balanced conditions.

Appendix C

The Design of the Anti-Aliasing Filters

With a sampling frequency of 1200 Hertz (24 samples per cycle), the anti-aliasing filters must have a cut-off frequency less than 600 Hertz according to Nyquist's theory. For this application, a fourth order Bessel filter was chosen, with the cut-off frequency set to around 550 Hertz. To obtain the fourth order Bessel filter, two VCVS low pass filters were cascaded together. This results in the circuit as shown in figure 4.5. The values of the various components of the first stage were calculated as follows[53]:

$$R_1 C_1 = \frac{1}{2 \pi f_1 f_c} \qquad \text{(C.1)}$$

Where f_c = 3dB cut-off frequency and f_1 = 1.432.

This results in:

$$R_1 C_1 = \frac{1}{2\pi * 1.432 * 550} = 2.021 * 10^{-4} \quad secs \qquad \text{(C.2)}$$

Choosing: C_1 = 3300 pF gives R_1 = 62kΩ

The values of the two feedback resistors can be found by choosing R_3 (k_1 - 1) = 10kΩ where: k_1 = 1.084 leading to R_3= 120kΩ.

The values for the second stage are found in the same way with f_1 replaced by f_2 in equation (C.1) and k_1 by k_2 where: f_2 = 1.606 and k_2 = 1.759.

This leads to the component values: C_2 = 2200pF and R_2 = 82kΩ and R_4 (k_2 - 1) = 91kΩ with R_4 = 120kΩ.

Appendix D

Filter Theory

D.1 The Full-cycle Fourier Filter.[54,55]

The general Fourier series formula for a periodic function y(t) is:-

$$y(t) = \frac{a_0}{2} + \sum_{n=1}^{\infty} [a_n \cos(n\omega t) + b_n \sin(n\omega t)] \quad \text{(D.1)}$$

Where ω is the fundamental angular frequency. The period of the fundamental component is $2\pi/\omega = T$ and

$$a_n = \frac{2}{T} \int_0^T y(t) \cos(n\omega t)\, dt \quad \text{(D.2)}$$

$$b_n = \frac{2}{T} \int_0^T y(t) \sin(nwt)\, dt \quad \text{(D.3)}$$

These are the cosine and sine components at the n^{th} harmonic. For the fundamental frequency they are expressed as:

$$a_1 = \frac{2}{T} \int_0^T y(t) \cos(\omega t)\, dt \quad \text{(D.4)}$$

$$b_1 = \frac{2}{T} \int_0^T y(t) \sin(\omega t)\, dt \quad \text{(D.5)}$$

Let $y(t) = Y \sin(\omega t + \phi)$ then:

$$a_1 = Y \sin \phi \quad \text{(D.6)}$$

$$b_1 = Y \cos \phi \quad \text{(D.7)}$$

Thus, if a_1 and b_1 can be derived from the sampled data, y(t) can be properly defined in its polar form.

The full-cycle Fourier filter algorithm is based upon the above principle to extract the fundamental voltage or current from distorted input data by correlating one cycle of data samples with the stored samples of reference fundamental sine and cosine waves. The general expressions for the cosine and sine components of current at a sample point k are:

$$i_c = \frac{1}{N}\left[i_{k-N} + i_k + 2\sum_{n=1}^{N-1} i_{k-N+n} \cos\left(\frac{2\pi n}{N}\right) \right] \quad \text{(D.8)}$$

$$i_s = \frac{1}{N}\left[2\sum_{n=1}^{N-1} i_{k-N+n} \sin\left(\frac{2\pi n}{N}\right) \right] \quad \text{(D.9)}$$

Where N is the number of samples taken per fundamental cycle. These may be converted to polar form using:

$$I = \frac{1}{\sqrt{2}}\sqrt{i_c^2 + i_s^2} \quad \text{(D.10)}$$

$$\angle I = \tan^{-1}(i_c / i_s) \quad \text{(D.11)}$$

However, for this work only the cosine term (equation D.8) is required as this can be used to extract the in-phase fundamental component from the distorted input data. The frequency response of the resulting One-cycle Cosine filter can be seen in figure D.1 together with the half-cycle and two-cycle cosine filters for comparison. This figure shows that the full-cycle cosine filter frequency response has zero's at d.c. and at each harmonic of the fundamental frequency.

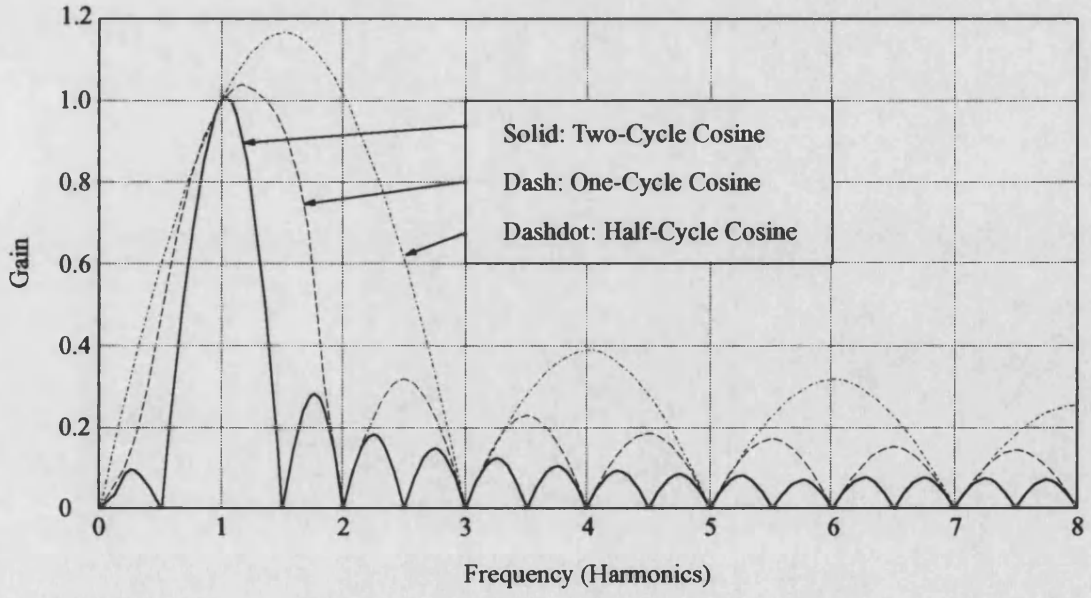

Figure D.1) Frequency Response of Cosine Fourier Filters.

D.2 The Half-cycle Moving Average Filter.

The moving average filter can expressed mathematically as:

$$y_{(n)} = \frac{1}{N}\sum_{r=0}^{N-1} x_{(n-r)} \qquad \text{(D.12)}$$

Where $y_{(n)}$ and $x_{(n)}$ are the n^{th} output and input respectively, and N is the window size.

For the half-cycle moving average filter the window size, N, is equal to half the number of samples taken per fundamental cycle. The resulting impulse response and frequency response for this filter can be seen in figure D.2 (for N=8).

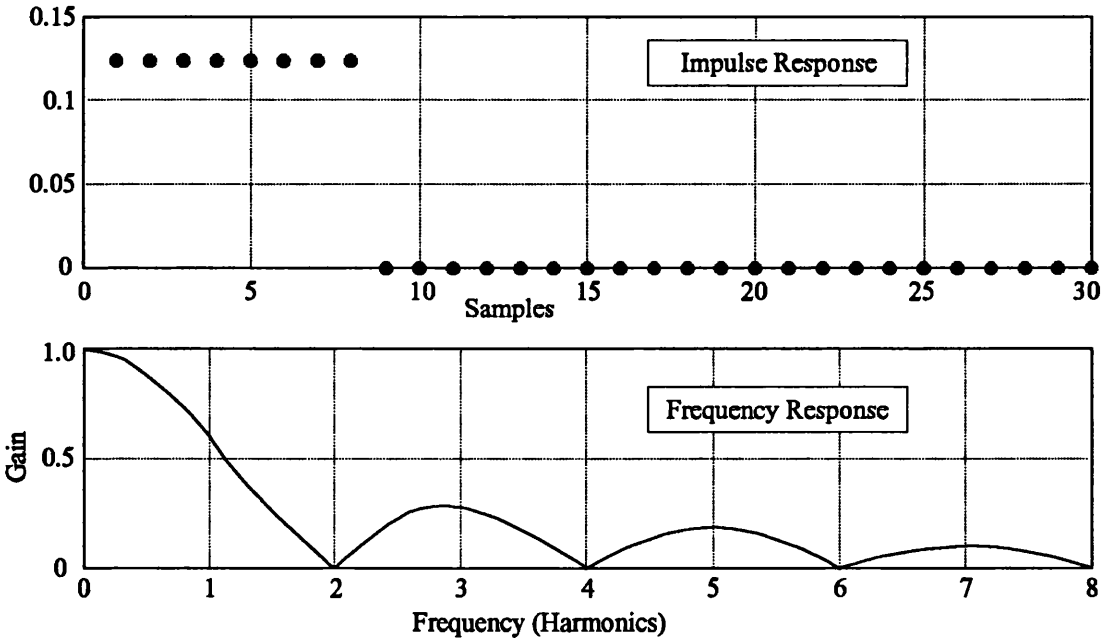

Figure D.2) Impulse Response and Frequency Response of Half-cycle Moving Average Filters.

Published Work

The following papers have been published on the work described in this thesis:

REDFERN, M.A, BARRETT, J.I, HEWINGS, D, & USTA, O, 'A Laboratory Facility for Research into Digital Protection Algorithms used for the Protection of Small and Medium Sized Generators.' 26th UPEC, Brighton, '91.

REDFERN, M.A, USTA, O, BARRETT, J.I, & FIELDING, G, 'Protection Against Loss of Utility Grid Supply for an Embedded Generator.' 27th UPEC, Bath, '92.

REDFERN, M.A, USTA, O, BARRETT, J.I, & FIELDING, G, 'A New Digital Relay For Loss of Grid to Protect Embedded Generation.' 5th IEE International Conference on 'Developments in Power System Protection,' York, March '93.

REDFERN, M.A, USTA, O, & BARRETT, J.I, 'Loss of Grid Protection for an Embedded Generator.' IEE Colloquium on 'The Effective Response of a Public Electricity Network to Independent Generators.' Chester, '93.

REDFERN, M.A, USTA, O, BARRETT, J.I, & YIP, T, 'A New Microprocessor Based Loss of Grid Protection for Embedded Generation.' 2nd IEE International Conference on Advances in Power System Control, Operation and Management.' Hong Kong, '93.

26th Universities Power Engineering Conference, September 1991, Brighton.

A LABORATORY FACILITY FOR RESEARCH INTO DIGITAL PROTECTION ALGORITHMS USED FOR THE PROTECTION OF SMALL AND MEDIUM SIZED SYNCHRONOUS GENERATORS.

M A Redfern, J Barrett, D Hewings and O Usta.

School of Electronic and Electrical Engineering, University of Bath, UK.

INTRODUCTION.

The great potential for the installation of small and medium sized generation operating[1] in parallel with the local utility supply network has led to considerable interest in new digital relaying schemes for protecting embedded generation.

Research into new digital relaying algorithms to be used for protecting embedded generation[2] has led to the development of a laboratory facility for assessing new protection techniques. The facility has been built around a small synchronous machine which is connected to a model power system network containing another machine and inter-ties into the three phase system. The digital relaying environment is provided by either a programmable microprocessor based, general purpose protection relay system or a desk-top computer fitted with the required input and output units to execute real-time protection software.

This facility was initially designed as a teaching system to demonstrate the operation and limitations of differential protection when applied to a three phase generator. The inherent flexibility of the system has made it a powerful teaching aid and invaluable for research into new protection techniques suitable for the integrated generation protection.

The facility provides an intermediate step between the software simulation of new protection algorithms and field trials using relay hardware. It also compliments other evaluation facilities available in the laboratory.

GENERATOR PROTECTION RESEARCH FACILITY.

Power System Model.

The facility uses a 5 kVA synchronous machine, coupled to a dc machine and connected to a model power system network containing a similar machine set and inter-ties into a 200 volt three phase system. Although these machines are intended for generation, they can be used as loads.

The schematic diagram for this model power system is shown in figure 1. The system contains a double bus system similar to that used in a medium range generating station and includes the power system switching systems associated with such an installation. A comprehensive array of current and voltage transformers are installed around the synchronous machine to provide inputs into the protection systems. Other machines and plant can be connected to the system as required for special tests.

To facilitate protection system testing, the machines and breakers are generously rated and the stator windings of the synchronous machines are fitted with accessible taps. Faults can be applied without causing permanent damage.

Digital Generator Protection Relay Research System.

The digital relaying environment is provided by both the desk-top computer system and a programmable microprocessor research relay system. They monitor the behaviour of the synchronous machine using eight primary current transformers and four primary voltage transformers. The laboratory protection systems and their inter-connection to the power system instrument transformers are shown in figure 2.

The desk-top computer based research system uses a COMPAQ 286 microcomputer, containing a third party interface board fitted with 16 analogue inputs and 32 channels of digital input and output, I/O.

The primary transducers are interfaced to the microcomputer using a purpose designed input system. This includes interposing transformers to provide an additional level of isolation for the microelectronic systems from the primary system. The input system also contains the anti-aliasing filters, the sample and hold circuits and the phase-locked loop control circuit to provide the sampling clock frequency generator. The standard generator protection algorithms use twelve samples per 50 Hz cycle, corresponding to 600 samples/sec.

To ensure that there were the least difficulties with the timing between the different input circuit functions, the sample and hold circuits were triggered using the falling edges of the square wave triggering waveform from the phase locked loop and the analogue to digital converters were triggered using the rising edges. The phase locked loop circuit locks onto the power system frequency and outputs a square wave exactly twelve times its frequency.

The trip output from the protection algorithm is provided via the digital I/O port, which with the aid of a driver circuit operates an auxiliary relay, which in turn trips the circuit breaker connecting the synchronous machine to the model power system. The trip circuit includes a ten second delay to enable current and voltage readings to be taken during the fault condition.

The block diagram of the desk-top computer based research system is shown in figure 3.

The programmable microprocessor research relay system uses the INTEL 80186 microprocessor together with the input circuits required to monitor current and voltage transducer secondary signals and output circuits containing the trip and alarm relays. The 80186 is of the same family as the 80286[3] used in the Compaq and with minor modifications programmes developed on this desk-top computer can be used in the programmable relay system.

The relay's input modules contain eight current transformers, four voltage transformers, the input filters, the sampling circuitry and the digital to analogue converters. A RS232 serial communications channel enables the microprocessor relay system to communicate directly to the desk-top computer enabling the operator to measure the currents and voltages monitored by the relay together with trip and flag status information. This communications link has enabled several teaching projects to be automated, dramatically reducing the student's effort in performing the experiments.

Software for the desk-top relaying environment and the microcomputer relay can be developed in either 'C' or Assembly. The close similarity between the two systems

enables research to start on the desk-top computer and then the protection algorithms to be moved to the microprocessor relay for in depth testing. The microprocessor relay is a stand alone system and can therefore be used for field trials or simulator testing.

GENERATOR PROTECTION ALGORITHMS.

Generator Protection Scheme.

The generator protection scheme[3,4] is required to protect the machine from both internal and external faults. A typical protection scheme for a small or medium sized synchronous generator is shown in figure 4. The actual scheme used for a generator depends on the machine being protected and some features shown may be omitted while others may be included.

The IDMT relays, 51V and 51N, provide protection against high current faults on either the generator or the system to which it is connected. The negative sequence relay, 46N, provides protection against unbalanced loads damaging the machine or the loss of a phase connection. The reverse power relay, 32, prevents machine motoring should the prime mover fail.

The over and under voltage relays, 27 and 59, and the over and under frequency relays, 81O and 81U, ensure that the consumer's supply is maintained within defined voltage and frequency limits. Should the supply move outside these for greater than the time period set, the embedded generator is disconnected from the load. The Loss of Mains relay, LOM, detects when the site becomes isolated from the utility's source of generation for whatever cause and opens the inter-tie breaker to the utility resulting in stand alone operation of the site system.

The synchronisation checking relay, 25, ensures that the generator is only connected to the site busbar when the voltages on both sides of the connecting breaker are within tolerable limits of each other and in phase. The operation of the synchronisation checking relay can be inhibited when the generator is being connected to a de-energised busbar.

The main protection for internal faults within the generator's stator winding is provided by the differential protection, 87. Since this is a unit protection, it does not require time grading with other protection systems and can therefore be 'instantaneous'.

Biased Differential Protection.

Arguably, the simplest method of protecting a generator's stator against internal faults is to use current differential protection across the stator windings. Based on the Merz and Price circulating current principles[3], the scheme is enhanced using automatic through-current biasing.

The relay monitors the currents on both sides of the stator winding and determines the differential current which is used as the protection operate measurand. To avoid mal-operation due to current transformer mismatch and high through-currents, the currents measured are used to provide a bias measurand which restrains relay operation. The relay's ideal characteristic curve is shown in figure 5.

For each phase of the generator, the biased differential protection algorithm uses the following trip criterion:-

$$(I_B'-I_A') > K_1 I_N + K_2\frac{(I_A'+I_B')}{2} \qquad (1)$$

Differential current — Setting current — Mean through current

where,

I_N is the relay's nominal current,

I_A' and I_B' are the secondary currents measured at the generator's neutral and line ends.

The values of the constants K_1 and K_2 are the zero current trip setting and the bias setting for the characteristic respectively.

To reduce the effects of noise on the algorithm, a moving window equivalent to one cycle of samples is used to provide inherent filtering. Equation 1 has therefore been modified to provide a running total of the present sample value together with the previous n-1 sample values. The protection algorithm therefore causes trip when:-

$$\sum_{m-(n-1)}^{m}\frac{|I_{Bm}'-I_{Am}'|}{n} > K_1 I_N + K_2\sum_{m-(n-1)}^{m}\frac{|I_{Am}'+I_{Bm}'|}{2n} \qquad (2)$$

Differential current — Setting current — Mean through current

For the differential scheme, after sampling the appropriate two input channels, the values obtained are processed and the results added to a running total for both the operate values and the restraint values as shown below. The operate values are made up of the sum of the differences between the two sample values, and the restraint values, the average of the two sample values. This can be expressed by the following equations:

$$\text{Operate value} = I_{Bm}' - I_{Am}' \qquad (3a)$$

$$\text{Restraint value} = \frac{(I_{Am}' + I_{Bm}')}{2} \qquad (3b)$$

The moving window functions of n samples are obtained by first subtracting the $(m-n)^{th}$ samples from the appropriate running total and then adding the value of the new $(m)^{th}$ samples. The $(m)^{th}$ samples are read into the array in place of the $(m-n)^{th}$ samples, i.e. they overwrite the original values. The summation of the stored samples therefore gives a running total of the n samples which are available for use in the trip calculation.

When the protection algorithm is first energised, i.e. before any samples are taken, it is necessary to restrain the trip function for the first cycle period in order to prevent mal-operation. The values in the array elements are first zeroed and then during this restraint period operational data is collected. Once the program has collected n service samples after energisation, the array has been filled and the restraint is lifted.

To provide three phase protection, the program samples the six input channels corresponding to the six CT's connected on either side of the stator windings. Similar protection algorithms are used on each phase of the machine. The three trip-algorithms provide a common trip output such that whenever a fault is detected on any of the windings, the circuit breaker is tripped, thus disconnecting the machine from the system.

DIFFERENTIAL RELAY PROTECTION PERFORMANCE.

The relay's trip characteristic was determined by applying phase to phase faults between corresponding red and yellow phase taps on the machine. The resulting curve is shown in figure 5 which compares well with the ideal curve. Tripping times were typically 30 msecs, including the delays incurred by the output hinged armature relays.

Further investigations to examine the limitations of the differential protection scheme when an earthing resistor was connected to the machine's star point, produced the relationship shown in figure 6. This shows the percentage of the winding protected by the relay against the maximum fault current that could flow for an internal fault, as a percentage of the rated load current. These results demonstrate an inherent limitation of stator winding differential protection caused by the relay's inability to operate when the fault current is below its trip value.

RESEARCH INTO ENHANCED PROTECTION ALGORITHMS.

This facility provides an environment for further work into new and enhanced protection algorithms for small synchronous motors and generators. Current work is concentrating on both the refinement of new techniques for detecting loss of mains, and new differential protection algorithms to overcome the one cycle dead period following energisation and to extend the percentage of the stator winding protected without the use of injection systems. Several techniques exist for enhanced stator winding protection including monitoring the third harmonic content[7] and monitoring the harmonic content in the machine's rotor[8]. These and other work on generator protection highlight the need for further work in this area.

CONCLUSIONS.

This facility was initially designed as a teaching system to demonstrate the operation and limitations of biased differential protection when applied to a three phase generator.

The inherent flexibility of the system has led to its use for research into new protection techniques suitable for the integrated protection of embedded generation.

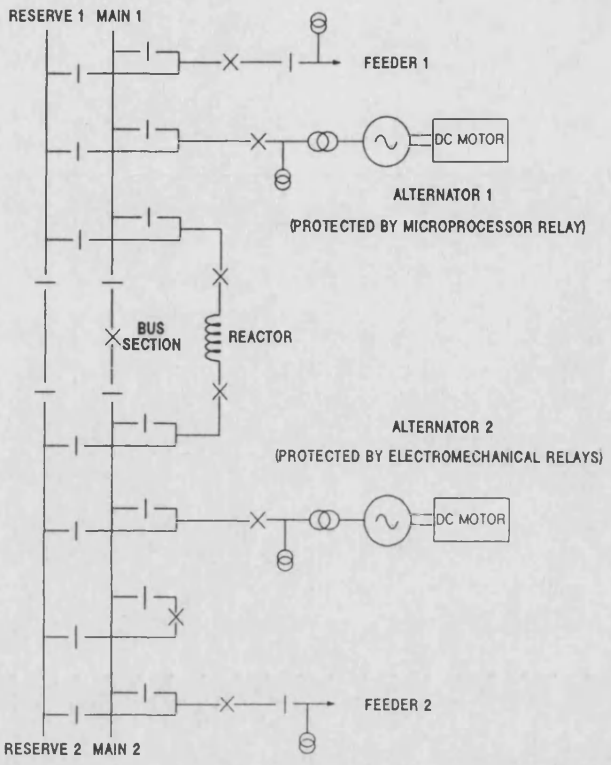

FIGURE 1. SCHEMATIC DIAGRAM FOR THE MODEL POWER SYSTEM.

ACKNOWLEDGEMENTS.

The authors are pleased to acknowledge the help and encouragement provided by the School of Electronic and Electrical Engineering at the University of Bath, South Western Electricity plc, GEC Alsthom Measurements, the SERC and colleagues associated with the research.

REFERENCES.

1. FIELDING G and BRADLEY J. 'Local Generation - The Devolution of Power.' IEE Review, March 1990.

2. REDFERN M A, USTA O, FENG B and FIELDING G. 'Loss of Mains Protection for Private Generation Operating in Parallel with the Utility Supply.' UPEC 1990.

3. 'Protective Relays - Application Guide.' GEC Measurements, 3rd Ed., 1987.

4. 'Recommendations for the Connection of Private Generating Plant to the Electricity Board's Distribution Systems - Engineering Recommendation G59.' The Electricity Council, June 1985.

5. 'Microprocessors.' Intel, 1991, ISBN 1-55512-115-2.

6. KHAN K R and CORY B J. 'Developments in Digital Generator Protection.' Developments in Power System Protection. London 1985, IEE Pub. 249, pp 223-226.

7. DASH P K, MALIK O P, and HOPE G S. 'Fast Generator Protection Against Internal Asymmetrical Faults.' IEEE PAS Vol-96, No 5, Sept/Oct 1977, pp 1498-1506.

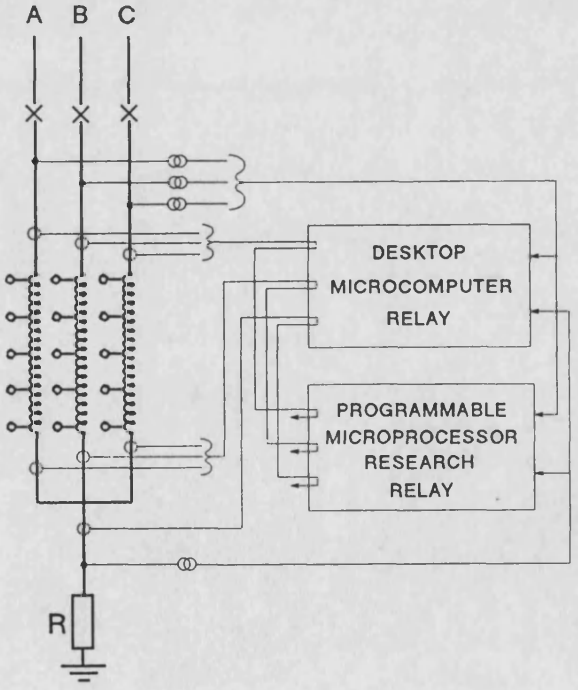

FIGURE 2. LABORATORY PROTECTION SYSTEMS AND THEIR INTERCONNECTION TO THE SYNCHRONOUS MACHINE.

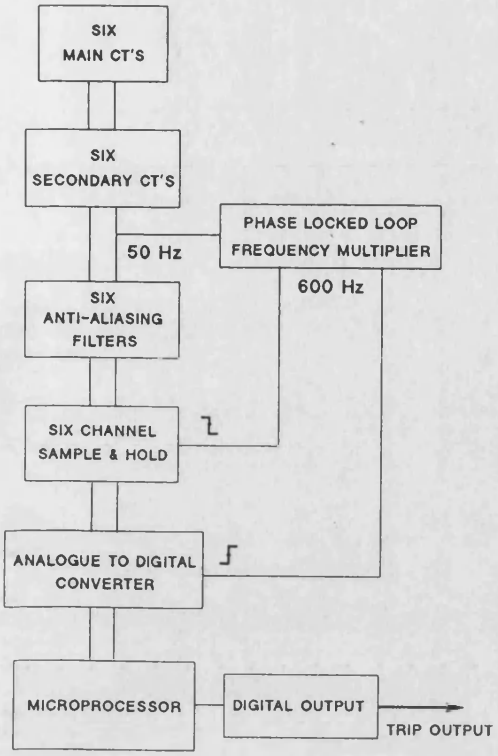

FIGURE 3. DESK-TOP COMPUTER PROTECTION RESEARCH SYSTEM.

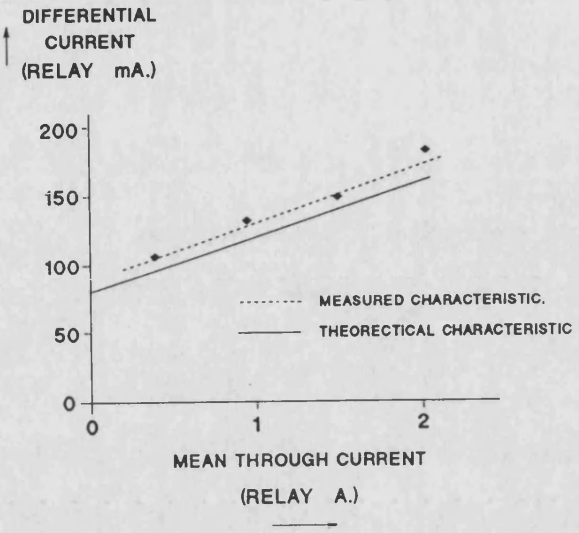

FIGURE 5. BIASED DIFFERENTIAL PROTECTION RELAY CHARACTERISTIC.

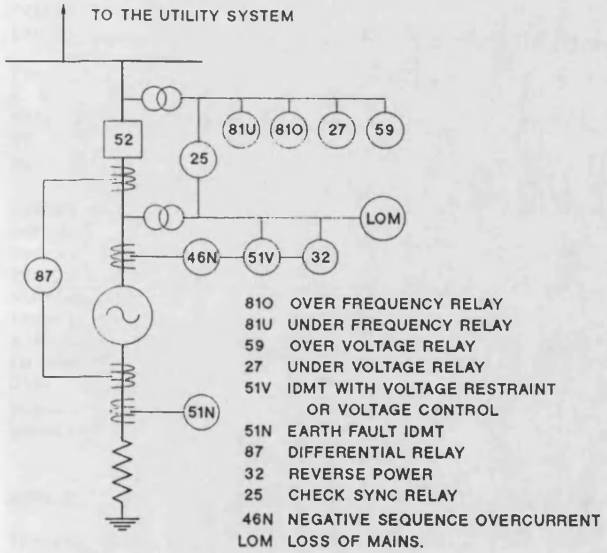

FIGURE 4. TYPICAL PROTECTION SCHEME FOR A SMALL OR MEDIUM SIZED SYNCHRONOUS GENERATOR.

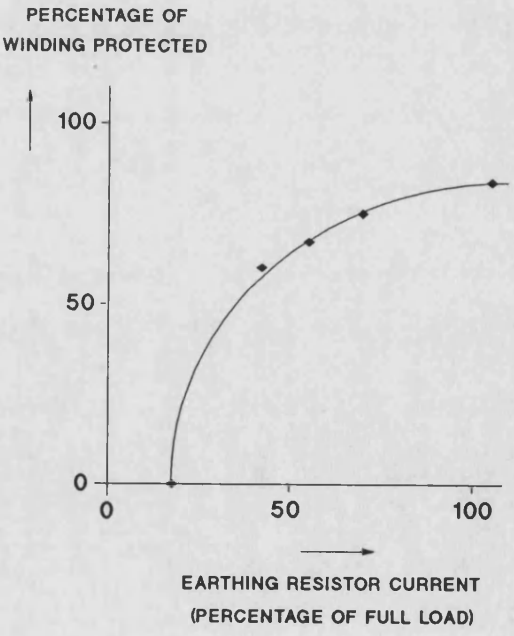

FIGURE 6. PERFORMANCE OF A BIASED DIFFERENTIAL PROTECTION.

27th Universities Power Engineering Conference, September 1992, Bath.

PROTECTION AGAINST LOSS OF UTILITY GRID SUPPLY FOR AN EMBEDDED GENERATOR.

M A Redfern, O Usta, J I Barrett and G Fielding

University of Bath.

GEC Alsthom: Protection and Control Stafford.

INTRODUCTION.

The operation of small or medium sized generation running in parallel with the local utility supply, creates several difficulties for the reliable and safe operation of the power supply system. These difficulties arise from the generator's capacity to supply power to the network and because it operates independently of the network control system.

The protection scheme required by the embedded generator must include functions which provide protection for faults directly affecting the site's generator, protection for the utility from faults on the generator's site, and protection for the generator's site from faults or disturbances on the utility network. An important element in the latter requirement is the need to protect against the accidental isolation of the generator's site from the main source of utility power. In such a situation, the generator's site could be left connected to part of the utility load and operate as an independent power island.

This situation is illustrated in figure 1. Following the opening of the 'loss of grid' circuit breaker, the generator's site is left connected to part of the network load. Ideally the loss of grid protection would trip the inter-tie breaker disconnecting the generator's site from the utility and thereby facilitate the orderly restoration of the utility supply to the network. Unfortunately for the operation of the network, the 'loss of grid' circuit breaker need not be a specific circuit breaker but may potentially be any breaker, switch, or isolator connecting the utility's main source of supply to the generator's site.

Protection designed to detect loss of grid supply is a relatively new area for relaying and is commonly referred to as either loss of grid protection or loss of mains protection. Occasionally it is referred to as islanding protection.

Before a utility will agree to the connection of an embedded generator to its network, they will need to be satisfied that the presence of the embedded generator will not detract from the quality of supply provided to its customers. In the UK, the technical requirements for connecting an embedded generator to a Regional Distribution Company's system are defined in the Electricity Council Engineering Recommendation G59[1]. The protection requirements include the need to provide loss of grid protection as part of the generator's site protection scheme.

LOSS OF GRID PROTECTION.

Several techniques have already been developed for detecting loss of grid[2,3,4,5,6]. The difficulties with this type of relaying have led to considerable interest in exploring new concepts for this function. Quoting from a recent IEEE paper," Providing protection against islanding probably is the single most challenging aspect of designing the electrical system involving cogeneration.[7]". These difficulties arise because loss of grid is not a clearly defined fault condition but is an undesirable and unsafe operating state. For most systems, scenarios exist where the different protection techniques may fail to detect the loss of grid.

The techniques being examined to detect loss of grid are based on monitoring the behaviour of the power system to disturbances and the differences in system characteristics between those experienced when the main utility supply is connected to the embedded generator and those when the embedded generator is operating in isolation. The algorithm uses changes in the power output from the embedded generator to provide an insight into the transfer function of the generating plant feeding the power system. Under normal conditions with the utility supply connected, the transfer function reflects the combination of the main source and the embedded generation. Following loss of grid, or while the embedded generator is operating in isolation, it reflects the characteristics of the embedded generator alone.

Returning to the simplified representation of a power system shown in figure 1, the embedded generator and the main utility supply can be represented by idealised generators of capacity G_g and G_m with inertia constants H_g and H_m respectively. While the utility's source of supply is connected to the network, a change in the system load of DP_s produces a change in the distributed generator's loading of DP_g defined by:-

$$DP_g = DP_s \frac{H_g G_g}{H_g G_g + H_m G_m}$$

However if the distributed generator operates independently from the utility supply, for example following loss of grid, any change of system load will result in the distributed generator's loading of DP_g defined by:-

$$DP_g = DP_s$$

Accepting that the utility has a greater capacity than the embedded generator and that its inertia constant will also be greater, the differences in response to a disturbance provides an immediate basis for determining whether or not the utility supply is connected to the portion of the network containing the embedded generation.

An additional advantage of using the power as the relaying measurement is that it is readily obtained from instantaneous measurements of the generator's terminal voltages and output currents. Providing that the samples are taken at the same instant, they also do not have to be synchronised to the power system frequency. The generator's three phase power output is derived from:-

$$P_g = v_a i_a + v_b i_b + v_c i_c$$

where;

v_a, v_b, v_c are the sampled values of the generator's terminal voltages,

and,

i_a, i_b, i_c are the sampled values of its output currents.

In a typical protection scheme associated with an embedded generator, these measurements are also required for other relaying functions required to protect the machine. The loss of grid protection is therefore suitable for including into an integrated protection package for a small or medium sized embedded generator without dramatically increasing the hardware requirements.

In addition to reliably detecting the occurrence of a loss of grid, the protection algorithm must remain stable during conditions of extreme load unbalance, loss of phase and during load flicker. These conditions have been accommodated by amplitude limiting measurements of changes in power output from the embedded generator and integrating samples over a moving window period. The protection's trip criteria is defined by:-

$$\sum_{n=-t_x}^{n=0} (DPg)n > k_s$$

where;

n is the sampling instant of $(DPg)n$,

k_s is the trip setting,

and,

t_x is the length of the sampling window.

POWER SYSTEM STUDIES.

Extensive simulation studies have been undertaken to study both the effects of loss of grid and of other disturbances to a power system containing an embedded generator. These studies were conducted using both the alternative transients version of the EMTP programme, ATP[8], and programmes developed in-house. Unfortunately, limitations were found in the generation model used in the ATP and hence detailed new models had to be developed.

To illustrate the capabilities of the protection algorithm, an 11 kV network containing a 3.75 MVA embedded generator was modelled. The embedded generator had an inertia constant of 0.91 MW.sec/MVA and the site load was 3 MW. The utility supply was set at 250 MVA with an inertia constant of 10 MW.sec/MVA. The test period considered used a one second window commencing 100 ms before the disturbance.

The length of the sampling window used in the protection algorithm was chosen to give a maximum operating time of six cycles and the amplitude limiting was chosen to provide a minimum tripping time of one cycle. The trip setting was selected such that a one percent load change following loss of grid produced tripping.

The response to a loss of grid producing a 5% increase in generator load is shown in figure 2. For this disturbance, the protection algorithm trips after 26 ms. The traces for the a-phase voltage shows that it dips after the disturbance whereas the a-phase current increases.

The response to a 5% increase in generator load while the generator is operating independently of the utility supply is shown in figure 3. These curves are virtually identical to those of figure 2 and tripping also occurs 26 ms after the disturbance. In a practical situation the loss of grid trip would open the inter-tie breaker if it were closed ensuring that the utility supply could be safely restored to the utility without disturbing the embedded generator. Satisfactory restoration of supply to the adjacent network bus could be followed by a controlled reclosure of the inter-tie breaker. Naturally operation of the loss of grid protection while the inter-tie breaker was open would have no effect.

The restraint of the algorithm to violent load changes while the distributed generator is operating in parallel with the utility supply is shown in figure 4. This shows the response to a 100% change in the local load and the non-operation of the protection algorithm. The auto-scaling feature of the plotting package masks the lack of disturbance to the embedded generator.

Arguably the worst case scenario following a failure to detect loss of grid is an out-of-synchronism reclosure of the loss of grid breaker. An example of this is shown in figure 5 where the phase angle between the two systems is thirty degrees before reclosure. Tripping results 234 ms after the reclosure, disconnecting the embedded generator from the utility before serious damage can result. Although in an ideal world such a reclosure would be unthinkable, in the real world where an embedded generator is connected to an established power network, the distribution switchgear will rarely be equipped with check synchronism or live line/dead bus, dead line/live bus supervision.

In addition to the algorithm's response to switching disturbances, its response to fault conditions is also of interest. A solid three phase fault on the local busbar would produce a condition similar to that for a loss of grid. The fault effectively splits the system into two and would in effect be fed independently by the generation on either side. This type of fault would therefore cause the algorithm to trip the inter-tie breaker. The response to a three phase fault is shown in figure 6, and tripping occurs 340 ms after the fault. The initial violent changes in power output from the distributed generation unit are attenuated by the signal limiting action of the algorithm and hence operation is delayed. Naturally this fault would be seen by other protection functions which would also isolate it from the system. The operating times of the loss of grid protection are suitable to allow proper grading.

A single phase fault on the same busbar, however, need not result in three phase tripping of the inter-tie breaker and hence should be left to other protection relays to clear. The algorithm does not result in tripping for a single phase to ground fault as shown in figure 7. Since in this case, only one phase is effectively lost, the power output oscillates at twice the power system frequency and the integrating nature of the algorithm prevents tripping.

CONCLUSIONS.

The loss of grid protection described in this paper provides an effective technique for detecting this condition and enabling the utility supply to be reconnected in a controlled manner. The algorithm has been shown to remain stable under extreme load fluctuations while the utility supply remains connected to the generator's site, but to operate quickly for small fluctuations when the generator's site is disconnected from the main utility supply.

The algorithm also trips for an out-of-synchronism reclosure of the utility supply onto the generator's site protecting the embedded generator from possible damage. Extreme fault conditions effectively spliting the power system result in tripping, but if the interconnection remains intact, it remains stable.

ACKNOWLEDGEMENTS.

The authors are pleased to acknowledge the help and encouragement provided by the University of Bath, GEC Alsthom Protection and Control, and the Science and Engineering Research Council.

REFERENCES.

1. Electricity Council, 'Recommendations for the Connection of Private Generating Plant to the Electricity Board's Distribution Systems - Engineering Recommendation G59.' The Electricity Council (now the Electricity Association), London, June 1985.
2. Warin J W, 'Loss of Mains Protection.' ERA Conference: Circuit Protection for Industrial and Commercial Installation, London 1990.
3. Cooper C B, 'Standby Generation - Problems and Prospective Gains from Parallel Running.' Power System Protection '89, Singapore 1989.
4. Jones R A, Thomas R S and Imece I F, 'Investigation of Potential Islanding of a Self-Commutated Static Power Converter in Photovoltaic Systems.' IEEE Trans EC 5, No 4 Dec 1990, pp 624-630.
5. Schaltanlagen Electronik Gerate GMBH & Co, 'Generator/Mains Monitor - GW2.' SEG GMBH Publication GW2/E/810.
6. Redfern M A, Usta O, Feng B and Fielding G, 'Loss of Mains Protection for Private Generation Operating in Parallel with the Utility Supply.' pp 89-92, 25th UPEC, Aberdeen 1990.
7. Powell L J, 'An Industrial View of Utility Cogeneration Protection Requirements.' IEEE Trans IA 24, No 1, Jan/Feb 1988, pp 75-81.
8. Leuven EMTP Centre, 'Alternative Transients Program Rule Book.' LEC Belgium, July 1987.

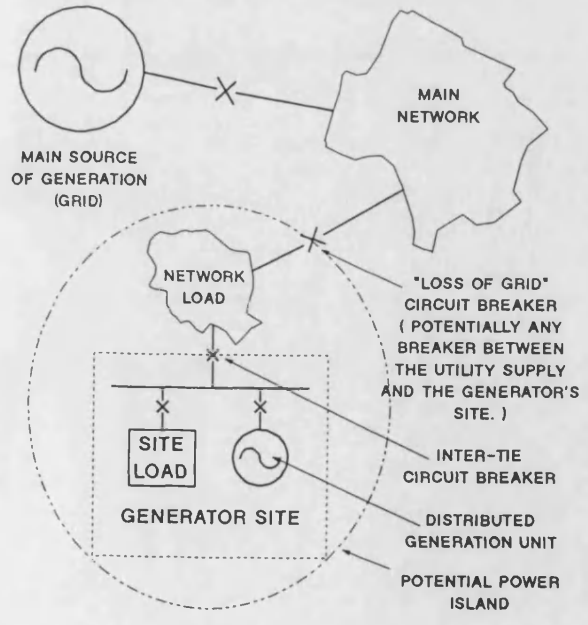

FIGURE 1. NETWORK CONFIGURATION CONTAINING A DISTRIBUTED GENERATION UNIT.

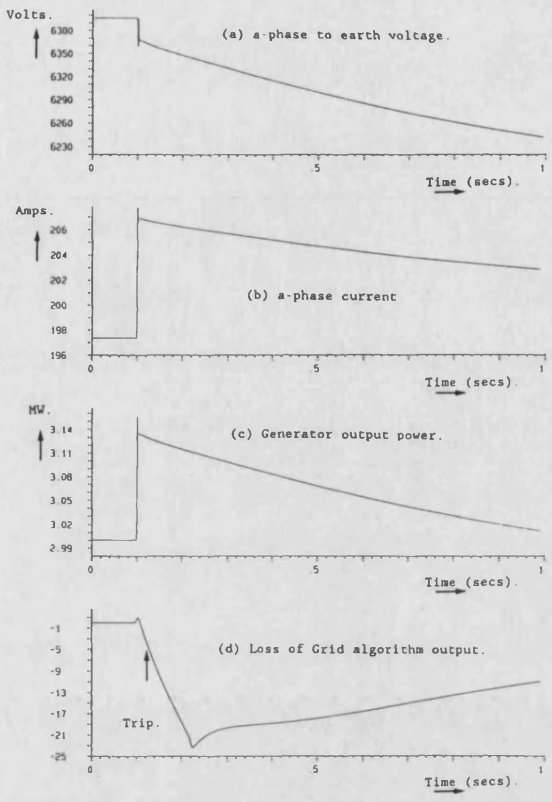

FIGURE 2. RESPONSE TO A LOSS OF GRID PRODUCING A 5% INCREASE IN THE GENERATOR LOADING.

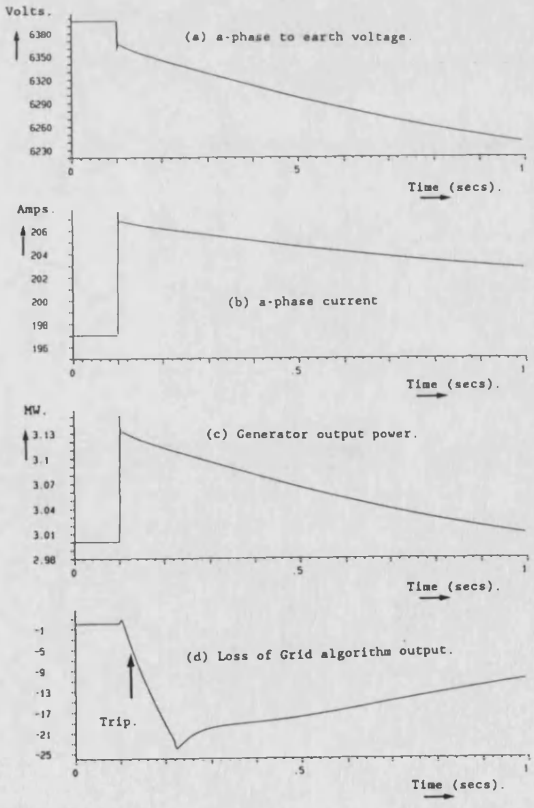

FIGURE 3. RESPONSE TO A DISTURBANCE PRODUCING A 5% INCREASE IN THE GENERATOR LOADING WHILE IT IS OPERATING INDEPENDENTLY OF THE UTILITY SUPPLY.

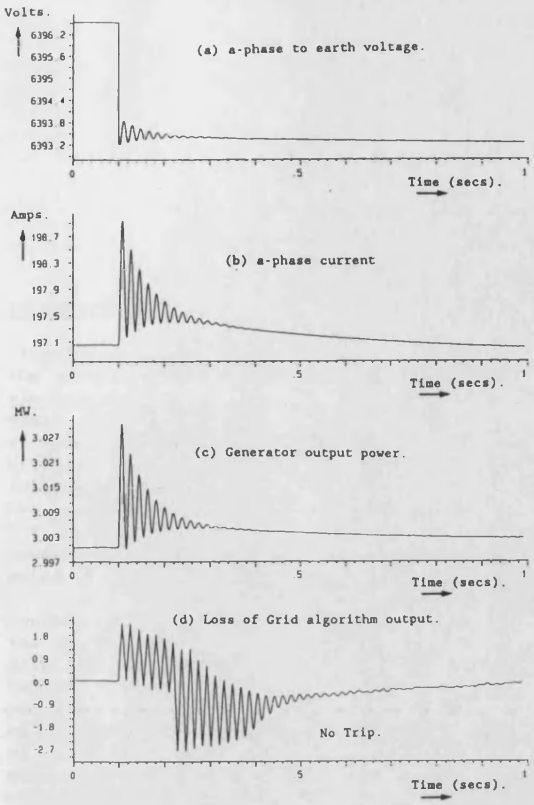

FIGURE 4. RESPONSE TO A DISTURBANCE PRODUCING A 100% INCREASE IN THE LOCAL LOAD WHILE OPERATING IN PARALLEL WITH THE UTILITY SUPPLY.

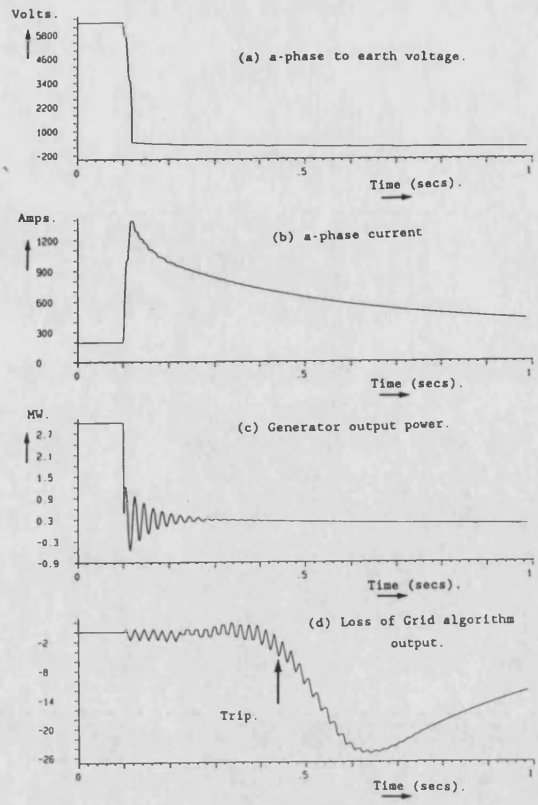

FIGURE 6. RESPONSE TO A THREE PHASE FAULT ON THE LOCAL BUSBAR.

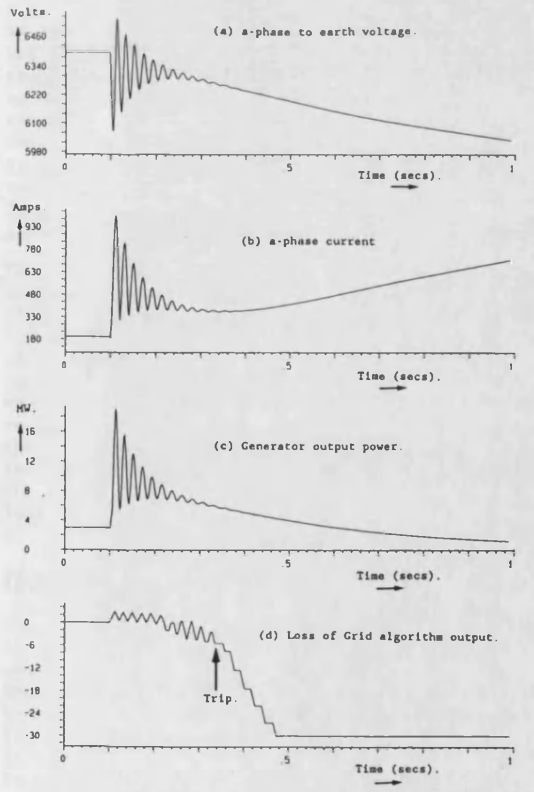

FIGURE 5. RESPONSE TO AN OUT-OF-SYNCHRONISM RECLOSURE BETWEEN THE POWER ISLAND AND THE UTILITY GRID SUPPLY WITH PRE-CLOSURE PHASE SEPARATION OF 30 DEGREES.

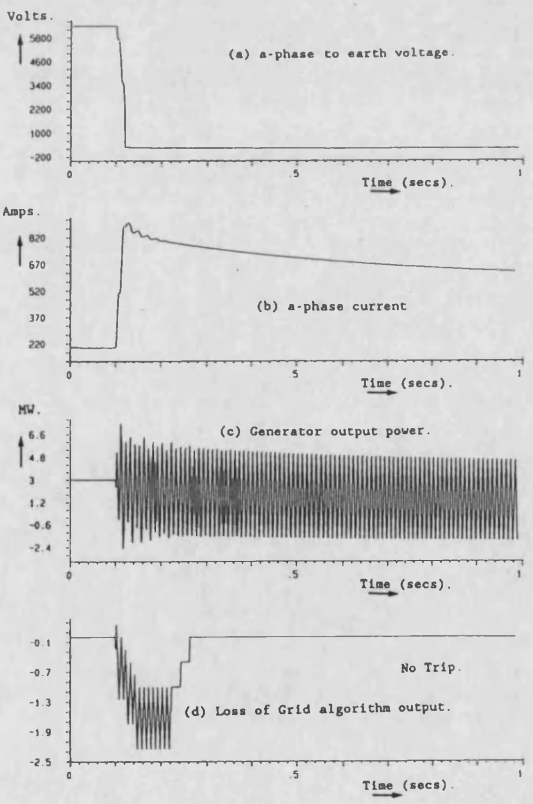

FIGURE 7. RESPONSE TO A SINGLE PHASE FAULT ON THE LOCAL BUSBAR.

IEE 5th International Conference on Developments in Power System Protection, March 1993, York.

A NEW DIGITAL RELAY FOR LOSS OF GRID TO PROTECT EMBEDDED GENERATION.

M A Redfern, O Usta, J I Barrett and G Fielding

University of Bath.

Industrial Consultant. Stafford.

INTRODUCTION.

"Providing protection against islanding probably is the single most challenging aspect of designing the electrical system involved in cogeneration.[1]" For small or medium sized cogenerators, also referred to as embedded generators, operating in parallel with a utility power supply, islanding generally occurs following utility switching operations which leave the generator connected to part of the utility's load but disconnected from the utility's main source of power. The condition is also referred to as loss of mains or more recently as loss of grid.

Considering the simplified system shown in figure 1, the power island is produced by opening the loss of grid breaker. Unfortunately the circuit breaker causing loss of grid could be any of several breakers providing the link between the utility's main source of power and the embedded generator. In itself loss of grid should not damage the power system. However since it produces two separate power networks, it complicates the orderly reconnection of the power supply network. For those utility customers left connected to the embedded generator, it could result in their power supply deviating from required standards. There is also a potential safety hazard to personnel, since following loss of grid part of the utility system remains energised which would normally be expected to be de-energised.

In the UK, Electricity Council Recommendations G59[2] and Engineering Technical Report ET 113[3] describe the requirements of the protection systems which need to be satisfied before the connection of an embedded generator to the utility system can be authorised. These requirements include the need to provide loss of grid protection. Most major utilities in other countries who allow non utility generation to be connected to their system have similar guide-lines[4,5,6].

The requirements of the loss of grid protection as defined by G59[2] are that it should automatically disconnect the generator from the Electricity Board's system in the event of loss of the Board's supply to that installation. The tripping time should be such that the two systems have been successfully separated before automatic reclosing equipment could attempt to reconnect the two systems. On a distribution system the time setting of the recloser could be one second. The protection system is also required to ensure that the embedded generator is properly earthed following loss of grid.

TECHNIQUES FOR DETECTING LOSS OF GRID.

The most direct method for detecting loss of grid is to take advantage of a SCADA system and monitor auxiliary contacts on all circuit breakers on the utility system between the embedded generator and the utility supply[1]. Detection of a loss of grid would be followed by a transfer trip instruction to open the inter-tie breaker connecting the embedded generator to the utility. Although this is the most effective technique available, most distribution systems and the circuit breakers they employ have not been fitted with a suitable supervisory system and the expense involved with a retro-fit is difficult to justify.

Several techniques have been developed for detecting loss of grid using local power system measurements made on the embedded generator's site[7]. These can be divided into active techniques, which have a direct influence on the operation of the power system, and passive techniques, which rely on passive measurements of system parameters. Active techniques include the Reactive Power Export Error Detector[8] and the System Fault Level Monitor[9]. The passive techniques include Under/Over frequency, Under/Over Voltage, Reverse Power, Rate of Change of Frequency[8] and Phase Displacement Monitoring[10]. All of these techniques have limitations and there is considerable interest in investigating new possibilities.

THE NEW LOSS OF GRID PROTECTION ALGORITHM.

The commercial attraction of a loss of grid protection which can be included in an integrated digital protection scheme for an embedded generator led to the formulation of this new algorithm. Unlike previous techniques the algorithm is based on monitoring fluctuations in the generator's power output. The operation of the algorithm depends on the characteristics of these disturbances and the different responses which result when the embedded generator is operating while connected to the utility supply and while it is operating independently.

Considering the simplified system shown in figure 1, both the embedded generator and the utility supply can be modelled by idealised generators of capacity G_g and G_m with inertia constants H_g and H_m respectively. While the utility source of generation remains connected to the utility source of supply, a change in the network loading, ΔP_s, will produce a change in the generator's power output, ΔP_g, defined by:-

$$\Delta P_g = \Delta P_s \frac{H_g G_g}{H_g G_g + H_m G_m}$$

Since the capacity and inertia constant of the utility source is greater than that of the embedded generator, the changes to the generator's power output will be small when compared to the change in the load. However, when the embedded generator is operating independently from the main source of utility supply, a change in the network loading, ΔP_s, will have a direct effect on the generator's power output, ΔP_g, such that:-

$$\Delta P_g = \Delta P_s$$

The measurement of the generator's power output is based on the instantaneous power, P_n, measured in a three phase system:-

$$P_n = v_a i_a + v_b i_b + v_c i_c$$

where v_a, v_b, v_c, i_a, i_b, and i_c represent the sampled values of phase voltages and currents measured at the

generator's terminals at sampling instant n. If the three phase system is balanced, this measurement is divorced from the point-on-wave of the input samples and the system need not be locked onto the power system frequency. A low sampling rate can also be used.

The protection algorithm monitors fluctuations in the power output over a defined sampling window. Fluctuations in the generator's power output are amplitude limited by the function, f_n. This signal is integrated over the sampling window and tripping is initiated when the absolute value of the integrated signal exceeds the trip setting, k_s. The algorithm is defined by:-

$$\left| \sum_{n=-t_x}^{n=0} f_n((\Delta P_s)_n) \right| > k_s$$

where:

n is the sampling instant of ΔP_s

and,

t_x is the length of the sampling window.

Both the use of the sampling window and the amplitude limiting function provide an inherent filtering capability for noise and unbalance. The length of the sampling window is chosen to give a maximum nominal operating time of six cycles of the power system frequency, and provides inherent immunity to mal-operation due to extreme conditions of load unbalance or when an input transducer is lost. This could for example be caused by the loss of one of the voltage transformers. The nominal minimum operating time is defined by the level used for the amplitude limiting function. For the tests illustrated below this has been chosen to be equivalent to one cycle of the power system frequency. The trip setting is chosen such that the relay would just trip whenever a loss of grid or a load disturbance during independent operation produced a pre-defined percentage change in the generator's power output. The choice of setting depends on the application and local conditions. For the algorithm the setting is defined by the sampling interval, the length of the sampling window, the generator's inertia constant and its rated capacity.

MICROPROCESSOR BASED RELAY IMPLEMENTATION.

To complement computer studies of the performance of the loss of grid protection algorithm, initial practical trials have been conducted using a laboratory 200 V, three phase, model power system[11]. The model is based on a double bus generating station and includes two small synchronous generators driven by dc machines. One of these generators has been fitted with a microprocessor protection relay which is supported by a personal computer. This computer is also equipped with input transducers to monitor an array of system voltages and currents, and provides a convenient platform for research into new digital algorithms for generator protection which can be transferred to the relay hardware at a later stage.

The loss of grid protection algorithm was programmed into the personal computer to run in real time alongside other protection functions. Advantage was taken of existing data acquisition and data recording systems. The system used 12 bit A/D converters with a 200% dynamic range for the voltage inputs and a switched range of dynamic ranges for the current inputs. For the following tests a 200% dynamic range was used for the current inputs and the system was run at 16 samples per power system frequency cycle. The personal computer used a 12 MHz 80286 processor together with a 80287 co-processor. The algorithm was coded in assembler using approximately fifty instructions.

PROTECTION PERFORMANCE STUDIES.

The computer studies modelled an 11 kV system similar to that shown in figure 1. The embedded generator was rated at 3.75 MVA with an inertia constant of 0.91 MW-sec/MVA and the utility supply was rated at 250 MW with an inertia constant of 10 MW-sec/MVA. A one second test period was used commencing 100 msec before the switching disturbance. The algorithm's trip setting was set such that it would trip following a loss of grid producing a one percent change in the generator's output loading. A sampling rate of 20 samples per power system frequency cycle was used by the algorithm.

The practical tests used the 5 kVA test machine with a measured inertia constant of 0.35 kW-sec/kVA. The mains supply was rated at 500 KVA with a nominal inertia constant of 10 kW-sec/kVA. To avoid spurious tripping, the relay's trip setting was set such that it would just trip following a loss of grid producing a two and a half percentage change in the generator's output loading. The test system suffered from very high levels of waveform distortion and harmonic interference, particularly in the current waveform which was not fully filtered by the algorithm. The tests and results presented below also demonstrate that the system was sinking noise and harmonics generated by other users of the supply. The filtering capabilities of the algorithm were reinforced by a half cycle digital filter applied to the measured power P_s used by the algorithm.

The responses to a loss of grid producing a 50 percent change in the generator's loading are shown in figure 2. The responses from the computer model, figure 2(a), and test machine, figure 2(b), are very similar apart from the noise and the lower inertia constant seen in the response of the laboratory system. The computer simulation model tripped 28 msec after loss of grid and the microcomputer relay tripped after 50 msec. Part of the difference in these results is the additional filtering used by the laboratory algorithm.

The responses to a loss of grid producing a 5 percent change in the generator's output loading are shown in figure 3. Again the responses from the different tests are similar apart from the noise and lower inertia constant of the laboratory machine. In this case the computer simulation model trips after 30 msec and the microcomputer relay trips after 67.5 msec. This difference is a direct result of the different trip settings used by the two algorithms.

The responses to a 5 percent load change while the generator is operating independently from the utility system are shown in figure 4. The microprocessor relay responses are again similar to those obtained from the computer simulation, with tripping occurring after 87.5 msec and 28 msec respectively. There are many similarities between these responses and those shown in figure 3. The curves from the microcomputer relay reveal a higher level of waveform distortion present while the generator is running in parallel with the mains than when it is operating alone.

The response to a 100 percent load change while the generator is operating in parallel with the utility supply is shown in figure 5. In both cases the algorithms remain stable and do not trip. Although there is a small oscillatory disturbance with the computer simulation this is not apparent with the laboratory test. The laboratory test again demonstrated the effects of waveform distortion and harmonics. The fluctuations in the output of the algorithm's integration however do not cause tripping with the setting chosen.

The response to an out-of-step reclosure is shown in figure 6. For both tests, the phase difference between the two power systems prior to reclosure was 45 degrees. From the computer simulation, the

oscillatory nature of the machine's response and the inherent filtering included in the algorithm slow the protection. Tripping occurred 222 msec after reclosure. The low inertia of the laboratory machine and the capacity of the mains supply produce a more direct response without the subsequent oscillations and tripping occurs after 47.5 msec.

CONCLUSIONS.

A new digital protection algorithm for detecting loss of grid for a small or medium sized embedded generator operating in parallel with a utility supply has been shown to operate correctly for loss of grid conditions, during independent operation, and after an out-of-synchronism reclosure with the utility. It also remains stable during severe load fluctuations while operating in parallel with the utility.

The algorithm has been formulated to be suitable for an integrated digital protection for an embedded generator. The test platform used to demonstrate the practical algorithm's operation was similar to that used by commercially available protection relays.

Laboratory tests have supported results from computer simulation. These tests also demonstrated the successful operation of the algorithm in the presence of high levels of current and voltage waveform distortion and harmonic interference.

ACKNOWLEDGEMENTS.

The authors are pleased to acknowledge the help and encouragement provided by the University of Bath, GEC Alsthom Protection and Control Ltd., South Western Electricity plc., and the SERC.

REFERENCES.

1. POWELL L J, 'An Industrial View of Utility Cogeneration Protection Requirements.' IEEE Trans IA 24, No 1, Jan/Feb '88, pp 75-81.
2. ELECTRICITY COUNCIL, 'Engineering Recommendation G59 - Recommendations for the Connection of Private Generating Plant to the Electricity Board's Distribution Systems.' The Electricity Council, London, '85.
3. ELECTRICITY COUNCIL, 'Engineering Technical Report ET113 - Notes for Guidance for the Protection of Private Generating Sets up to 5MW for Operation in Parallel with Electricity Board's Distribution Networks.' The Electricity Council, London, '89.
4. SOUTH CALIFORNIA EDISON, 'Guide-lines for Operating, Metering and Protection for Co-generators and Small Power Producers.' Los Angeles, June '81.
5. ANSI/IEEE Standard 1001-1988. 'IEEE Guide for Interfacing Dispersed Storage and Generation Facilities with Electric Utility Systems.' IEEE New York, '89.
6. IEEE Special Report, 'Intertie Protection of Consumer-Owned Sources of Generation, 3 MVA or less.' IEEE 88TH0224-6-PWR, '88.
7. M A REDFERN, O USTA and G FIELDING, 'Protection Against Loss of Utility Grid Supply for a Dispersed Storage and Generation Unit.' Paper 92 SM 376-4 PWRD, presented to the IEEE PES Meeting, Seattle, July '92.
8. WARIN J W, 'Loss of Mains Protection.' ERA Conference on Circuit Protection for Industrial and Commercial Installations, London '90.
9. SCHALTANLANGEN ELECTRONIK GERATE GMBH & CO, 'Generator/Mains Monitor - GW2.' Pub. GW2/E/810.
10. COOPER C B, 'Standby Generation - Problems and Prospective Gains from Parallel Running.' Power System Protection '89 Conference, Singapore '89.
11. REDFERN M A, BARRETT J, HEWINGS D, and USTA O, 'A Laboratory Facility for Research into Digital Protection Algorithms used for the Protection of Small and Medium Sized Synchronous Generators.' Proceedings 26th UPEC, September '91, pp 457-460.

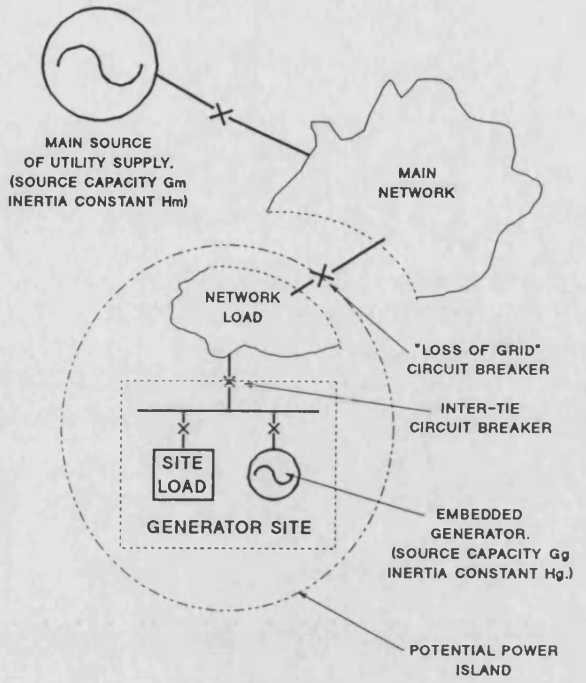

FIGURE 1. TYPICAL NETWORK CONFIGURATION ILLUSTRATING LOSS OF GRID FOR AN EMBEDDED GENERATOR.

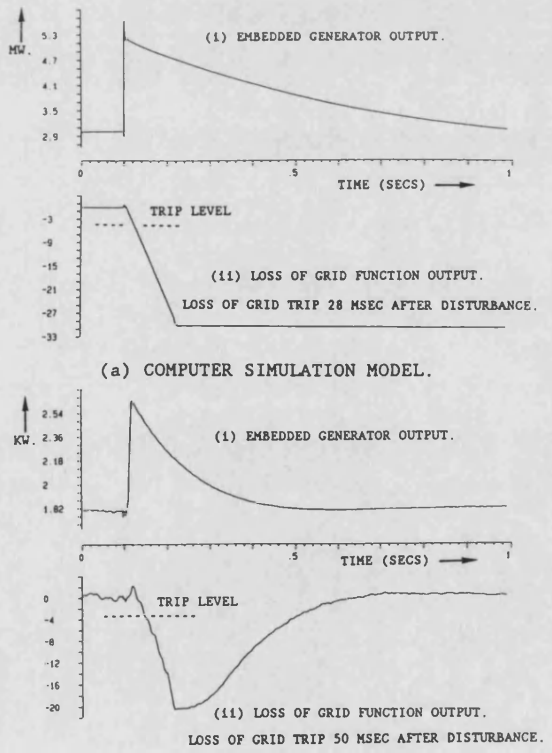

(a) COMPUTER SIMULATION MODEL.

(b) LABORATORY TEST MACHINE.

FIGURE 2. RESPONSE OF LOSS OF GRID ALGORITHM TO A 50% INCREASE IN THE EMBEDDED GENERATOR'S LOAD FOLLOWING LOSS OF GRID.

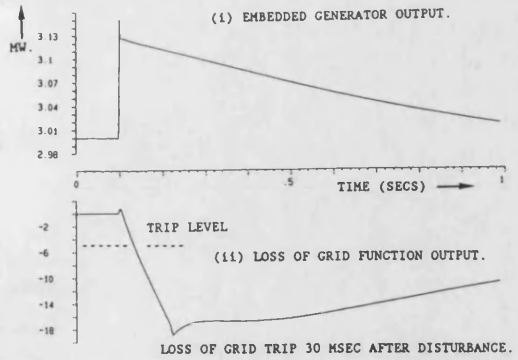

(a) COMPUTER SIMULATION MODEL.

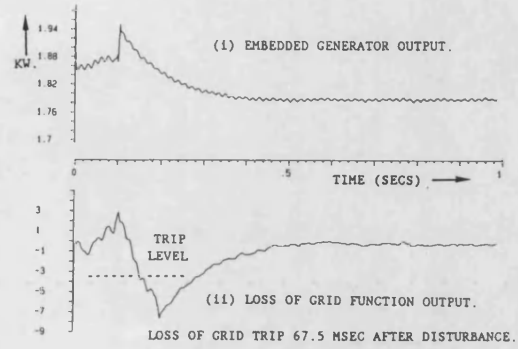

(b) LABORATORY TEST MACHINE.

FIGURE 3. RESPONSE OF LOSS OF GRID ALGORITHM TO A 5% INCREASE IN THE EMBEDDED GENERATOR'S LOAD FOLLOWING LOSS OF GRID.

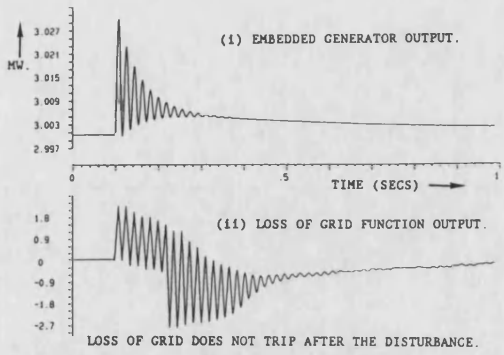

(a) COMPUTER SIMULATION MODEL.

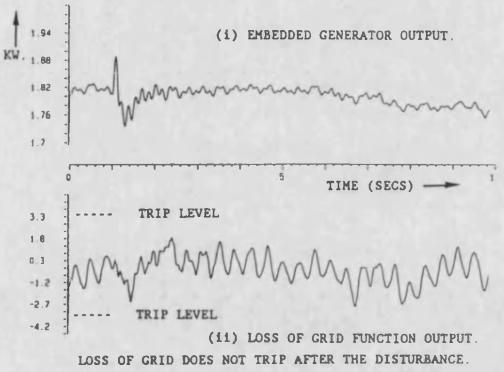

(b) LABORATORY TEST MACHINE.

FIGURE 5. RESPONSE OF LOSS OF GRID ALGORITHM TO A 100% INCREASE IN THE EMBEDDED GENERATOR'S LOAD WHILE OPERATING IN PARALLEL WITH THE UTILITY.

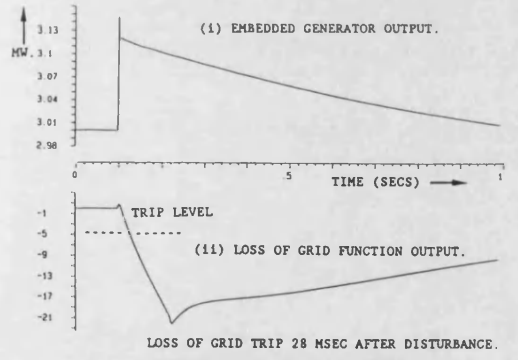

(a) COMPUTER SIMULATION MODEL.

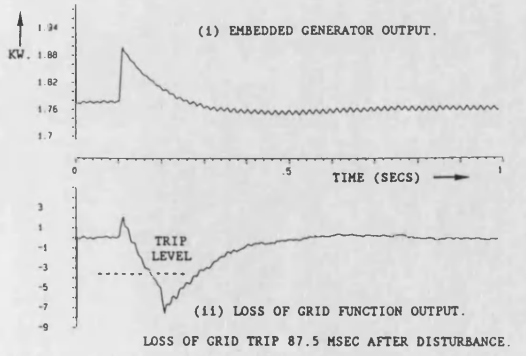

(b) LABORATORY TEST MACHINE.

FIGURE 4. RESPONSE OF LOSS OF GRID ALGORITHM TO A 5% INCREASE IN THE EMBEDDED GENERATOR'S LOAD WHILE OPERATING INDEPENDENTLY FROM THE UTILITY.

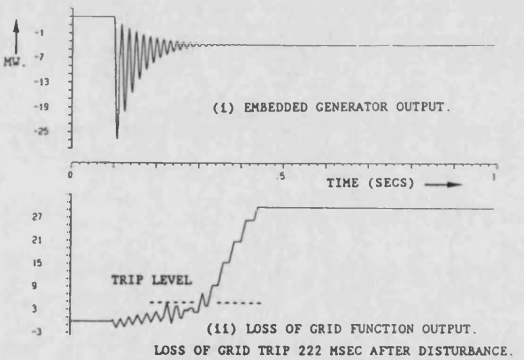

(a) COMPUTER SIMULATION MODEL.

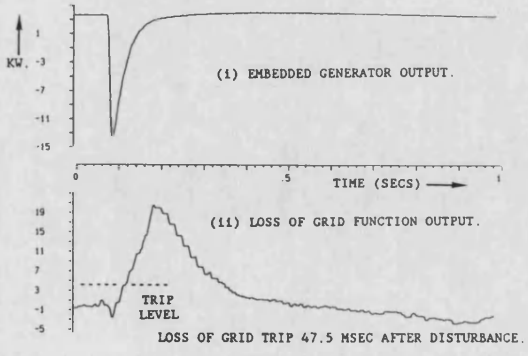

(b) LABORATORY TEST MACHINE.

FIGURE 6. RESPONSE OF LOSS OF GRID ALGORITHM TO A OUT-OF-SYNCHRONISATION RECLOSURE WITH A PHASE DISPLACEMENT OF 45 DEGREES.

IEE Colloquium on The Effective Response of a Public Electricity Network to Independent Generators, April 1993, Chester.

LOSS OF GRID PROTECTION FOR AN EMBEDDED GENERATOR.

M A Redfern, O Usta and J I Barrett.

The operation of small or medium sized generation in parallel with the local utility supply creates several difficulties for the reliable and safe operation of the power system. These difficulties arise from the generator's ability to supply power to the network and since it operates independently of the utility's control system.

The protection scheme required by the embedded generator must include functions to provide protection for faults directly affecting the site's generator, protection for the utility against faults on the generator's site, and protection for the generator's site from faults or disturbances on the utility network. One important element in the latter is the need to protect against the accidental isolation of the generator's site from the main source of utility power, i.e. loss of grid protection.

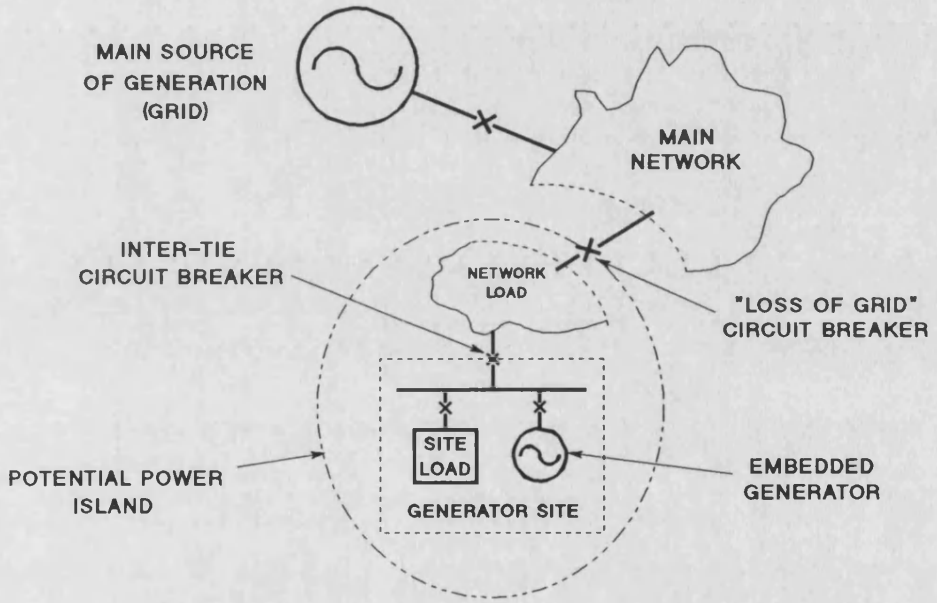

FIGURE 1. A POWER SYSTEM DISTRIBUTION NETWORK CONTAINING AN EMBEDDED GENERATOR.

The loss of grid scenario is illustrated in figure 1. Following the opening of the 'loss of grid' circuit breaker, the generator's site is left connected to part of the network load. Ideally the loss of grid protection would trip the inter-tie breaker disconnecting the generator's site from the utility and thereby facilitating the orderly restoration of the utility supply to the network.

Dr M A Redfern, O Usta and J I Barrett are with the School of Electronic and Electrical Engineering, University of Bath, BATH, BA2 7AY, UK.

Unfortunately, the loss of grid situation is complicated since the circuit breaker which causes the loss of grid need not be a specific circuit breaker in the system, but could be any breaker, switch, or isolator connecting the utility's main source of supply to the generator's site.

Protection designed to detect loss of grid supply is a relatively new area for relaying and is also commonly referred to as loss of mains protection, or islanding protection.

Before a utility will agree to the connection of an embedded generator to its network, they will need to be satisfied that the presence of the embedded generator will not detract from the quality of supply provided to its customers. In the UK, the technical requirements for connecting an embedded generator to a Regional Distribution Company's system are defined in the Electricity Council Engineering Recommendation G59[1]. The protection requirements include the need to provide loss of grid protection in the generator's site protection scheme.

TECHNIQUES FOR DETECTING LOSS OF GRID.

Quoting from a recent IEEE paper, "Providing protection against islanding probably is the single most challenging aspect of designing the electrical system involving cogeneration."[2]. These difficulties arise because loss of grid is not a clearly defined fault condition but is an undesirable and unsafe operating state. For most systems, scenarios exist where the different protection techniques may fail to detect the loss of grid.

The difficulties associated with loss of grid protection have led to considerable interest in exploring new concepts for this function and several techniques have been developed for detecting loss of grid[3,4,5,6]. Work at the University of Bath has concentrated on an alternative technique which monitors fluctuations in the power output of the embedded generator to determine whether or not the connection to the utility's main source of power is intact[6].

Reactive Export Error Detector[3].

The reactive export error detector directly controls the embedded generators excitation current so that it generates a level of reactive current in the utility to generator site inter—tie which cannot be supported unless the utility source is connected. The relay trips when the level of reactive current is not maintained at the required level for greater than a preset period. This time delay prevents maloperation for short lived supply fluctuations. An immediate advantage of this relay is that it can detect loss of grid where the disconnection does not change the generator load.

The time delay is typically set between 2 and 5 seconds and the relay is therefore inherently slow. The approach is also limited when the power factor compensation capacitors remain connected to the island and hence the reactive currents can be maintained. The relay requires both voltage and current inputs, as well as connections to the voltage regulator.

This technique is one of the few techniques suitable for small power supply systems where other relays fail to differentiate between loss of grid and abnormal system fluctuations. It is also used to provide back—up protection to other faster schemes.

Fault Level Monitor[4].

The fault level monitor repeatedly measures the system fault level by monitoring the current flow through a shunt inductor controlled by a point on wave switch triggering an anti—parallel connected thyristor pair together with the resulting changes in the system voltage. Triggering the thyristors just before voltage zero, produces a short pulse of current which reduces system voltage. Measurements enable the source impedance and hence the system fault level to be calculated . The system does not need to be particularly accurate since there is a dramatic change in fault capacity between the embedded generator and the utility supply.

The advantage of this approach is that it responds quickly to loss of grid by measuring the fault level every half cycle. This method has been developed from equipment used to improve static voltage compensator performance, however a commercial unit has not yet been produced.

Rate of Change of Frequency[3].

This protection operates when the rate of change of frequency exceeds a preset limit. The frequency is monitored either at the generator terminals or on the utility to customer inter—tie using a voltage transformer. The relay setting is chosen such that it will operate for the embedded generator load changes associated with the loss of grid, but it will not operate for fluctuations governed by utility time constants. The setting is critical since if it is too sensitive, unnecessary tripping during system disturbances could result and if too high, it could cause failure to detect loss of grid.

Under loss of grid, any changes in the load connected to the embedded generator will result in a dF/dt governed by the inertia constant and rated capacity of the embedded generator. For small and medium sized embedded generation, a trip setting of 0.3 Hz/sec has been found to be optimum. The relay algorithm is designed to ignore slow changes in frequency which could be caused by load changes on the utility network but to respond quickly to rapid changes in frequency when embedded generation becomes isolated. The rate of change of frequency relay is able to operate in from 0.3 to 0.7 seconds, and trips in 80 msecs with large load changes following dramatic disconnections.

An inherent advantage of rate of change of frequency relay, is that when loss of grid does not result in a significant change in the generator loading and the relay initially fails to operate, it will trip when a subsequent load change produces the required dF/dt.

Phase Displacement Monitor[5].

The phase displacement monitor operates when there are sudden changes in the phase displacement in the system voltage waveform. These phase displacements are a direct result of changes in the generator load and its operating frequency. The relay can respond in 50 msec when at the instant of loss of grid, the generator's output power changes by greater than 5% of its rating.

As with the rate of change of frequency relay, the phase displacement monitor will also operate for any subsequent load change which produces the required change in phase displacement, should the loss of grid fail to cause tripping.

Generator Output Power Fluctuations Monitor[6].

This technique detects the loss of grid by monitoring the behaviour of the power system to disturbances to the system and observing the differences in response between those experienced when the main utility supply is connected to the embedded generator and those when the embedded generator is operating in isolation. The algorithm uses changes in the power output from the embedded generator to provide an insight into the transfer function of the generating plant feeding the power system. Under normal conditions with the utility supply connected, the transfer function reflects the combination of the main source and the embedded generation. Following loss of grid, or while the embedded generator is operating in isolation, it reflects the characteristics of the embedded generator alone.

Returning to the simplified representation of a power system shown in figure 1, the embedded generator and the main utility supply can be represented by idealised generators of capacity G_g and G_m with inertia constants H_g and H_m respectively. While the utility's source of supply is connected to the network, a change in the system load of DP_s produces a change in the distributed generator's loading of DP_g defined by:-

$$DP_g = DP_s \frac{H_g G_g}{H_g G_g + H_m G_m}$$

However if the distributed generator operates independently from the utility supply, for example following loss of grid, any change of system load will result in the distributed generator's loading of DP_g defined by:-

$$DP_g = DP_s$$

Accepting that the utility has a greater capacity than the embedded generator and that its inertia constant will also be greater, the differences in response to a disturbance provides an immediate basis for determining whether or not the utility supply is connected to the portion of the network containing the embedded generation.

An additional advantage of using the power as the relaying measurement is that the power measurement is readily obtained from instantaneous measurements of the generator's terminal voltages and output currents. Providing that the samples are taken at the same instant, they also do not have to be synchronised to the power system frequency.

In a typical protection scheme associated with an embedded generator, these measurements are also required for other relaying functions required to protect the machine. This loss of grid protection is therefore suitable for including into an integrated protection package for a small or medium sized embedded generator without dramatically increasing the hardware requirements.

In addition to reliably detecting the occurrence of a loss of grid, the protection algorithm must remain stable during conditions of extreme load unbalance, loss of phase and during load flicker.

These conditions have been accommodated by amplitude limiting measurements of changes in power output from the embedded generator and integrating samples over a moving window period. The protection's trip criteria is defined by:-

$$\left| \sum_{n=-t_x}^{n=0} fn\,(DPg)_n \right| > k_s$$

where;

fn is the amplitude limiting function
n is the sampling instant of $(DPg)_n$,
k_s is the trip setting,

and,

t_x is the length of the sampling window.

Extensive simulation studies have been undertaken to study both the effects of loss of grid and of other disturbances to a power system containing an embedded generator. These studies were conducted using both the alternative transients version of the EMTP programme, ATP[7], and programmes developed in-house.

The amplitude limiting function is used to control the minimum operating time of the protection and the length of the sampling window controls the nominal maximum operating time. For initial studies these were chosen to give a minimum operating time of one cycle and a maximum of six cycles. Simulation studies have shown that the algorithm can reliably trip for loss of grid conditions resulting in a load change at the generator's terminals of greater than one percent of the generator's rating, and that the operating times are as designed.

An attractive feature of this approach is that it responds to out-of-synchronism reclosures of the main source of supply to the embedded generator and can therefore trip the inter-tie breaker to minimise subsequent damage.

Further work on this technique is continuing and the algorithm has been implemented in a laboratory microprocessor based demonstration relay. Opportunities for field trials are being explored.

CONCLUSIONS.

Loss of grid protection is a necessary part of the protection of an embedded generator which operates in parallel with the utility supply. Several techniques have been developed for detecting loss of grid and work is continuing to develop new techniques. Since loss of grid is not a conventional fault condition and in its self does not cause damage, it presents a major challenge to relay designers.

ACKNOWLEDGEMENTS.

The authors are pleased to acknowledge the help and encouragement provided by the University of Bath, GEC Alsthom Protection and Control, and the Science and Engineering Research Council.

REFERENCES.

1. Electricity Council, 'Recommendations for the Connection of Private Generating Plant to the Electricity Board's Distribution Systems - Engineering Recommendation G59.' The Electricity Council (now the Electricity Association), London, June 1985.
2. Powell L J, 'An Industrial View of Utility Cogeneration Protection Requirements.' IEEE Trans IA 24, No 1, Jan/Feb 1988, pp 75-81.2. Warin J W, 'Loss of Mains Protection.' ERA Conference: Circuit Protection for Industrial and Commercial Installation, London 1990.
3. Cooper C B, 'Standby Generation - Problems and Prospective Gains from Parallel Running.' Power System Protection '89, Singapore 1989.
4. Jones R A, Thomas R S and Imece I F, 'Investigation of Potential Islanding of a Self-Commutated Static Power Converter in Photovoltaic Systems.' IEEE Trans EC 5, No 4 Dec 1990, pp 624-630.
5. Schaltanlagen Electronik Gerate GMBH & Co, 'Generator/Mains Monitor - GW2.' SEG GMBH Publication GW2/E/810.
6. Redfern M A, Usta O, Barrett J I and Fielding G, 'A New Digital Relay for Loss of Grid to Protect Embedded Generation.' IEE Conference Developments in Power System Protection, York, 1993.
7. Leuven EMTP Centre, 'Alternative Transients Program Rule Book.' LEC Belgium, July 1987.

IEE 2nd International Conference on Advances in Power System Control, Operation and Management, December 1993, Hong Kong.

A NEW MICROPROCESSOR BASED LOSS OF GRID PROTECTION FOR EMBEDDED GENERATION.

M A Redfern, J I Barrett, O Usta and T Yip.

University of Bath, ENGLAND.

GEC Alsthom Protection and Control, Stafford, ENGLAND.

ABSTRACT.

The installation of small or medium sized embedded generation units operating in parallel with the main utility supply presents several technical complications. This paper describes a new technique for detecting a loss of grid condition by measuring the embedded generator's power output. It also details the implementation of the technique in a microprocessor based multi-function protection relay.

1.0. INTRODUCTION.

Since the early 1980's there have been increased economic, political and environmental pressures on producers of electricity which have greatly increased interest in incorporating embedded generation into public utility networks. Unfortunately, the operation of small or medium sized generation in parallel with the local utility network creates several difficulties for the reliable and safe operation of the power system. These difficulties arise from the embedded generator's ability to supply power to the network from a source that is not under the utility's direct control. Special precautions are therefore required to protect the utility against faults on the generator site and to protect the generator from faults or disturbances on the utility network.

One particularly demanding protection requirement is the need to guard against the accidental isolation of the generator's site from the main source of utility power. In such a situation, the generator's site could be left connected to part of the utility's customer load and operate as an independent power island.

This situation, known as loss of grid, is illustrated in figure 1. Following the opening of the 'loss of grid' circuit breaker, the embedded generator is left connected to its own site load and part of the network load. This produces two separate power networks which complicates the orderly reconnection of the power supply network and presents a potential safety hazard to the public and utility personnel. For those utility customers left connected to the embedded generator, it could result in their power supply deviating from the required quality standards.

In response to the growing interest in the use of embedded generation, several guidelines have been introduced to ensure that the presence of the embedded generator will not detract from the quality of supply to all customers connected to the system. In the U.K., these technical requirements are described in the Electricity Council Recommendations G59[1] and the Engineering Technical Report ET113.[2] These include the need to provide loss of grid protection. Most major utilities in other countries who allow non-utility generation to be connected to their system have similar guidelines.[3,4,5]

2.0. REQUIREMENTS FOR LOSS OF GRID PROTECTION.

The principal objective of loss of grid protection is to detect the condition where the embedded generation unit is left connected to a portion of the utility's load network, but disconnected from the main source of utility power following a switching operation.

There are several possible causes of this condition including; switching operations to clear a fault, load shedding, maintenance outages and equipment failures.

Ideally the loss of grid protection should trip the inter-tie breaker between the generator's site and the utility immediately following the disturbance and hence not impede the orderly restoration of the utility supply to the network. The tripping time should be such that the two systems have been successfully separated before any automatic reclosing equipment can attempt to reconnect the main supply to the power island. This could have potentially disastrous results for the embedded generator should reclosure occur when the two networks are out-of-synchronism.

Unfortunately, the loss of grid situation is further complicated since the circuit breaker that causes the loss of grid need not be a specific breaker in the system, but could be any breaker, switch or isolator which connects the main source of supply to the generator's site. Also, with an established power system, it is unlikely that the status of the circuit breaker is supervised or that it is fitted with synchronism checking or live line/dead bus and live bus/dead line supervision.

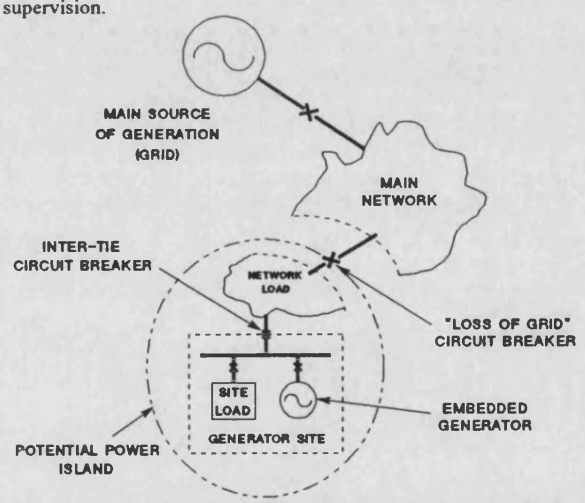

Figure 1: A Typical Distribution Network Containing an Embedded Generator.

The economics of small embedded generator schemes is such that once the desired level of protection is defined, the cost to protect the interconnection does not vary with the generator's capacity.[6] There is a widespread complaint from potential operators of embedded generation that utility grade relays are too expensive for a small embedded generation scheme. In some schemes the protection costs can be comparable to the cost of the generator itself. To make any relatively small embedded generation scheme economically viable, there is obviously a need for low cost, high quality protection packages for the complete protection of the embedded generator system. The use of a single microprocessor based relay with integrated protection functions, including loss of grid, is one solution to this requirement. Such a scheme is shown in figure 2.

3.0. TECHNIQUES FOR DETECTING LOSS OF GRID.

Difficulties arise because loss of grid is not a clearly defined fault condition, but is an undesirable and unsafe operating state. Several techniques[7,8,9,10] have been developed for detecting loss of grid, but as yet an ideal solution has not been found.

The most direct and effective method is to take advantage of a Supervisory Control and Data Acquisition System (SCADA) to monitor auxiliary contacts on all the circuit breakers, switches and isolators in the system between the embedded generator and the main utility supply.[11,12,13,14] A transfer trip signal could then be provided to open the inter-tie circuit breaker. However, most distribution systems, and the circuit breakers they employ, have not been fitted with a suitable supervisory system and the expense involved with a retrofit is difficult to justify.

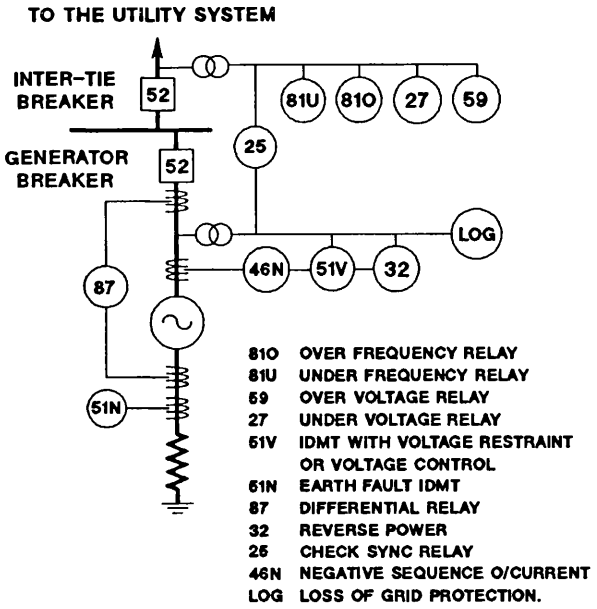

Figure 2: A Typical Microprocessor Based Integrated Generator Protection Scheme.

Several techniques have been devised for detecting loss of grid using local power system measurements made on the embedded generator's site. These can be divided into two categories; active techniques which have a direct influence on the power system, and passive techniques which rely solely on measurement of system parameters.

The most widely used active technique is the Reactive Export Error Detector[7] which forces the generator to generate a level of reactive power flow in the inter-tie that can only be maintained when the main source of utility generation is connected. Another method is the system fault level monitor[8] which measures the power system's source impedance and hence can differentiate between the condition when the grid is connected and when it is not.

The main passive techniques include Under/Over Frequency and Under/Over Voltage relays, Rate of Change of Frequency[7] and Phase Displacement Monitoring.[10]

4.0. THE NEW LOSS OF GRID PROTECTION ALGORITHM.[15]

The commercial attraction of a loss of grid protection technique that can be included in a microprocessor based integrated protection scheme for an embedded generator led to the formulation of this new algorithm.

Unlike previous techniques the algorithm is based on measurements of the generator's power output. The instantaneous three phase power output from the generator is derived from:

$$P_g = v_a i_a + v_b i_b + v_c i_c \qquad (1)$$

where v_a, i_a, v_b, i_b, v_c and i_c represent the simultaneously sampled values of phase voltages and line currents measured at the machine's terminals. If the three phase system is balanced, this measurement is divorced from the point on wave of the input samples and the sampling system does not need to be locked onto the power system frequency.

An advantage of using the output power is that these measurements are required for other relaying functions and therefore algorithms can be added without increasing hardware requirements.

Loss of grid is detected by monitoring the behaviour of the power system to disturbances and observing the differences in response between those experienced when the main utility supply is connected to the embedded generator site and those when the generator site is operating in isolation, which includes the situation following a loss of grid.

Considering the simplified representation of a power system shown in figure 1, the embedded generator and main utility supply can be represented by idealised generators of capacity G_g and G_m with inertia constants H_g and H_m respectively. While the utility source of supply is connected to the network, a change in system load ΔP_L produces a change in the embedded generator's loading of ΔP_g defined by:

$$\Delta P_g = \Delta P_L \frac{H_g G_g}{H_g G_g + H_m G_m} \qquad (2)$$

Accepting that the utility has a greater inertia than the embedded generator, changes in the generator's power output will only be a small fraction of the change in system load as long as the grid is connected.

However, if the embedded generator operates independently from the utility supply, any change of system loading ΔP_L will result in a change in the embedded generator's output power ΔP_g given by:

$$\Delta P_g = \Delta P_L \qquad (3)$$

Since a loss of grid generally produces a system load change, monitoring changes in the power output of the generator provides a direct method for detecting a loss of grid event.

The basic operation of the algorithm therefore depends upon the fact that, in the time frame analysed by the algorithm, following a load impact, the various machines on the system share the impact as a function of their inertia constants and capacity. This is a feature of the system's dynamic response.

In the transient time periods, immediately following a disturbance, the rotor angle of the individual machines cannot change due to the rotor's inertia, so the energy to supply the load change comes from the magnetic field of the generator and is distributed according to the synchronizing power coefficients. These depend upon the reactances from the generator to the load impact point.

For the first few milliseconds after the disturbance the machines 'electrically closest' to the point of load impact will pick up the greater share of the load regardless of size.[16] In the algorithm this phenomenon is overcome by amplitude limiting the change in power ΔP_g by the function f_n. The level of the amplitude limiting function, together with the overall integrating feature also defines the minimum trip time of the algorithm.

The measured fluctuations in the generator's power output ΔP_g are therefore amplitude limited by the function f_n. This signal is then integrated over a moving window of length t_x and tripping is initiated when the absolute value of the integrated signal exceeds the trip setting K_s. The trip criterion for the protection algorithm is defined by:

$$\left| \sum_{n=-t_x}^{n=0} f_n (\Delta P_g)_n \right| \geq K_s \qquad (4)$$

The size of the moving average window t_x allows the nominal maximum trip time of the algorithm to be set. For the studies shown in this paper the moving average window is set to six cycles.

The trip setting K_s is chosen such that the relay will just trip whenever a loss of grid, or a load disturbance during independent operation, produces a predefined percentage change in the generator's loading. The setting, K_s, is defined by the sampling interval, the size of the moving average window, the generator's inertia constant and its rated capacity.

5.0. POWER SYSTEM STUDIES.

The operation of the basic algorithm has been demonstrated using a simulated system containing an embedded generator rated at 3.75 MVA with inertia constant 0.91 MW.sec/MVA connected into an 11kV network.[15] The utility supply was set at 250 MVA with an inertia constant of 10 MW.sec/MVA. The length of the moving average filter window was set to six cycles and the amplitude limiting function was set to give a minimum trip time of one cycle. A sampling rate of 1kHz was used and the setting of the trip level was chosen such that a one percent change in generator loading produced a trip.

To complement computer simulation studies, practical trials have been conducted using a laboratory 200 volt, three phase model power system. The model is based on a double bus generating station and includes two small synchronous generators driven by d.c. machines. One of the generators has been fitted with a microprocessor protection relay which is supported by a personal computer. This computer is also equipped with the necessary input transducers to monitor an array of system voltages and currents and provides a convenient platform for research into new digital algorithms for generator protection which can be transferred to the relay hardware at a later stage.[17] A schematic diagram of the laboratory research facility can be seen in figure 3.

The loss of grid protection algorithm was programmed into the personal computer to run in real time using an existing data acquisition system. The system uses a 12 bit A to D converter with a 200% dynamic range for the voltage inputs and a switch selectable dynamic range for the current inputs. The processing of the algorithm was modified from the above to reduce the computing time required such that several protection algorithms can be operated in a multi-tasking environment. The input data was sampled at 24 samples/cycle and the algorithm was evaluated at four samples per cycle.

The practical laboratory tests used the 5kVA test machines with a measured inertia constant of 0.35 kW.sec/kVA. The mains supply was rated at 500 kVA with a nominal inertia constant of 10 kW.sec/kVA. The settings for the practical tests were similar to those used for the simulation results.

Due to the variety of loads drawn from the laboratory system, the test system was found to suffer from very high levels of waveform distortion and harmonic interference. The effect of these was greatly reduced by using a full-cycle Fourier filter on the sampled values of voltages and currents. This filter however did not remove the double frequency sinusoidal component in the instantaneous power waveform caused by unbalance in the system.

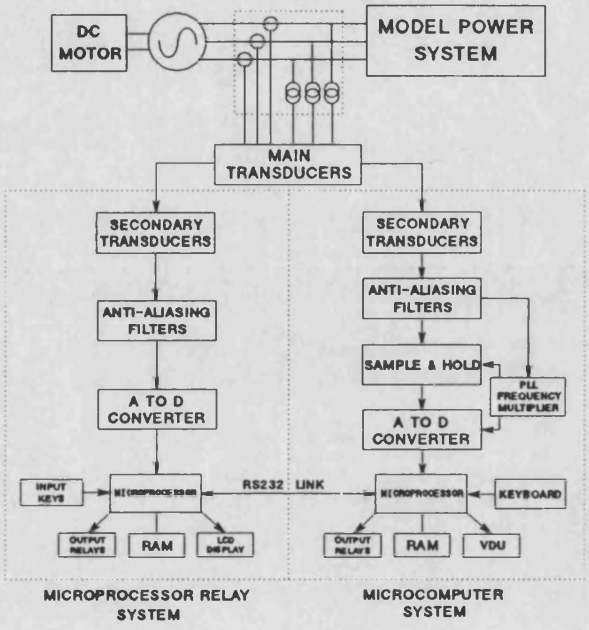

Figure 3: Schematic Diagram of the Laboratory Research Facility.

Unbalance in the power waveform is removed by the algorithm using the effective sampling rate of four samples per cycle with the change in power output ΔP_g calculated using the formula:

$$\Delta P_g = P_n - P_{n-2} \qquad (5)$$

instead of that used in the earlier algorithm [15]:

$$\Delta P_g = P_n - P_{n-1} \qquad (6)$$

(i.e. Using the current power value and the previous but one value).

Using four samples per 50 Hertz cycle has the effect of converting the sinusoidal unbalance term into a triangular waveform. Then by using equation (5), the change in power term ΔP_g consists of only the underlying power changes with the unbalance term removed.

The stability of the algorithm was further improved for the practical test results by adapting the amplitude limiting function f_n from the simple clipping function first used for the simulation results to a function which relies on a simple pattern recognition technique.

The basic operation of the amplitude limiting function is that the change of power ΔP_g is set to zero if the absolute value does not exceed the clip level. If the clip level is exceeded, $f_n(\Delta P_g)$ is written to that level. However, if the sign of the amplitude limited signal changes three times in succession the value of $f_n(\Delta P_g)$ is set to zero. This continues until the value of ΔP_g reduces below the clip level for five consecutive samples at which point the control flag is reset.

The response of the enhanced algorithm to a simulated 10% increase in the generator's loading as a result of a loss of grid can be seen in figure 4.

The effect of the enhancements to the algorithm can be greater appreciated using results from the practical laboratory tests. Figure 5(i) shows the instantaneous power waveform measured at the terminals of the generator for a loss of grid connection which results in a 10% increase in the loading of the embedded generator. The sampling rate for this result was 24 samples/cycle and the effect of the harmonics and unbalance can be clearly seen. The signal shown by figure 5(ii) is from the same test but with the Fourier filter applied to the sampled quantities and the sampling rate reduced to four samples/cycle. The corresponding change in power ΔP_g calculated by the algorithm is, however, free from the effects of the unbalance present in the original signal.

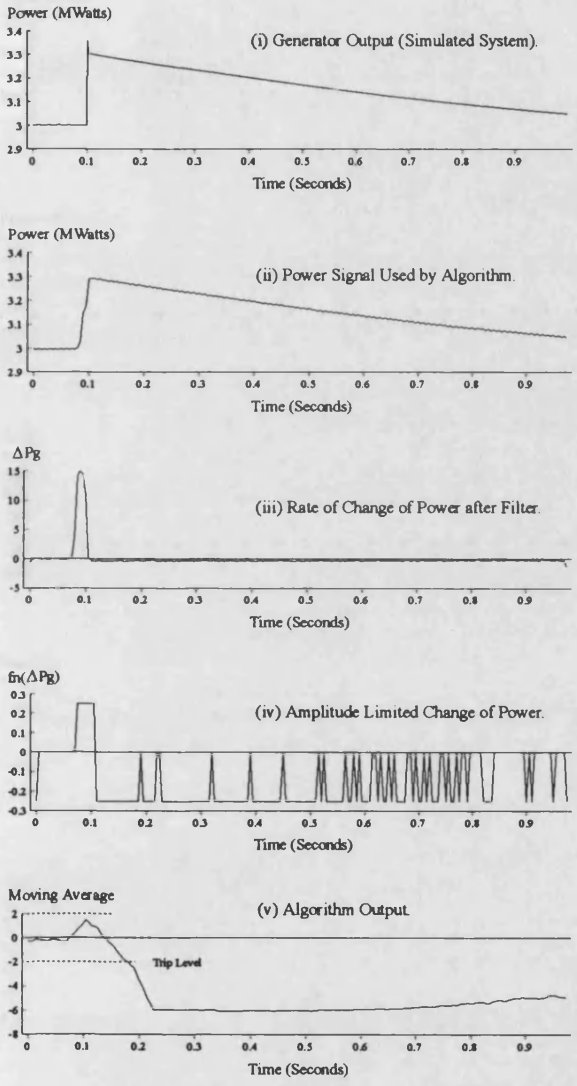

Figure 4: Response of the Loss of Grid Algorithm to a 10% Increase in the Embedded Generator's Load Following a Loss of Grid. (Simulation Results)

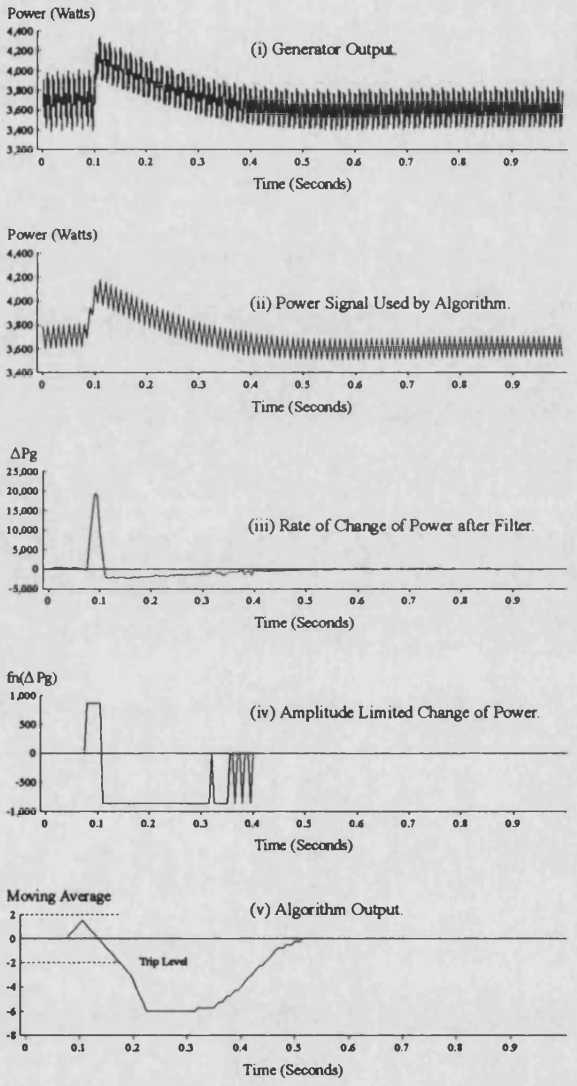

Figure 5: Response of the Loss of Grid Algorithm to a 10% Increase in the Embedded Generator's Load Following a Loss of Grid. (Laboratory Test Results)

Figure 4(i) shows the instantaneous power output from the simulated embedded generator following the 10% load increase. At the instant of the load impact, t=0.1 seconds, the source of energy supplied by the generator is the energy stored in its magnetic field[16]. Following this period the characteristics of the generator's power output are governed by the inertia constant of the embedded generation unit alone. The response of the algorithm is a trip after 80 milliseconds.

After the application of the amplitude limiting function f_n the resulting waveform $f_n(\Delta P_g)$ is as shown in figure 5(iv). The algorithm output produces a trip decision after 80 milliseconds. This result can be compared to that obtained for the simulated system shown in Figure 4. The dramatic reduction of the noise in the waveform allows a low trip setting to be used without the risk of nuisance tripping.

The operation of the algorithm when the generator operates in isolation from the main supply is also important should the loss of grid fail to produce the disturbance required to cause relay operation. Although this was initially considered to be an academic scenario, recent experiences have shown that it is not as rare as anticipated. Such a situation is shown in figure 6 which considers a 10% change in local load with the generator operating in isolation from the utility system. The results are almost identical to those obtained for the loss of grid condition because the characteristics of the embedded generator dictates the response in both cases. The algorithm again produces a trip decision after 80 milliseconds.

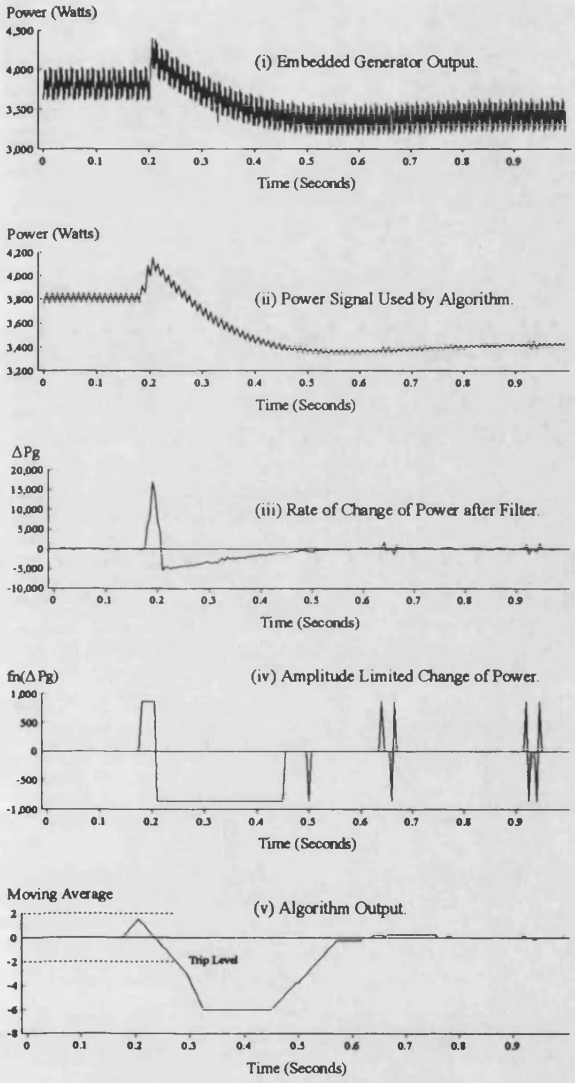

Figure 6: Response of the Loss of Grid Algorithm to a 10% Increase in the Embedded Generator's Load While Operating Independently from the Utility System.

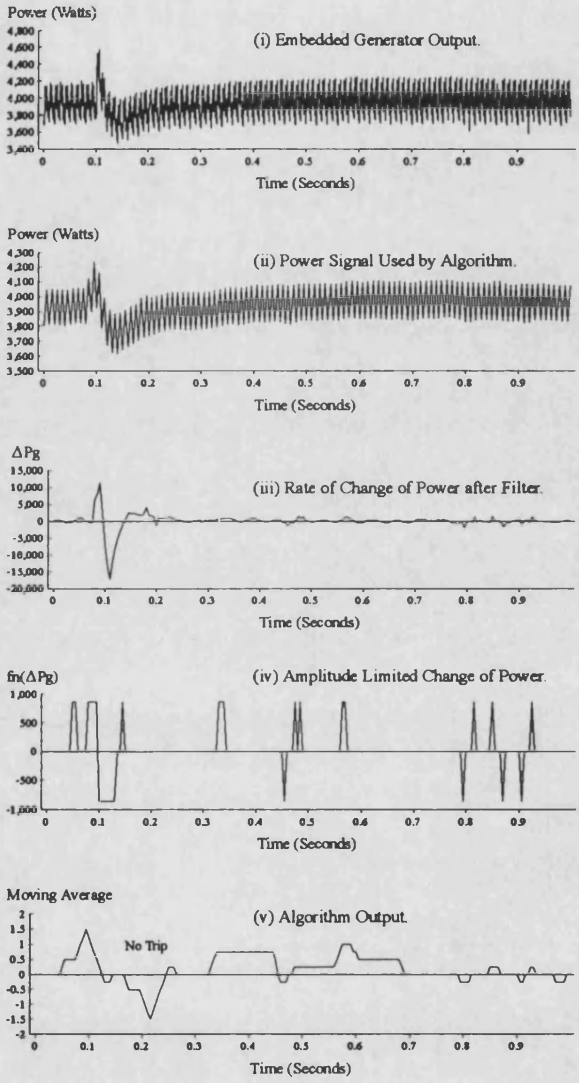

Figure 7: Response of the Loss of Grid Algorithm to a 100% Change in the Local Load While the Generator Operates in Parallel with the Utility Supply.

The stability of the algorithm to severe load changes which occur while the embedded generator is operating in parallel with the main source of supply is also of very great importance. The algorithm must not trip under these conditions and figure 7 shows the response of the algorithm to a local load change of 100% of the generator's rating. The operation of the amplitude limiting function f_n can be seen in figure 7(iv) where the output $f_n(\Delta P_g)$ is set to zero after the third successive change of sign. The algorithm output, figure 7(v), does not produce a trip decision. Further tests have shown that there is no indication that a trip would occur even for larger local load changes.

Finally, the stability of the algorithm in the presence of short circuit fault conditions has also been tested. The result of a single phase to ground fault on the local busbar can be seen in figure 8. The high levels of unbalance due to this type of fault leads to a large double frequency term present in the instantaneous power waveform. This oscillation, does not permeate through to the change in power ΔP_g term due to the filtering introduced by the 4 times per cycle processing rate. The ΔP_g waveform includes the fault-on and fault-off sections of the waveform, but since the amplitude limiting function f_n produces a zero output signal after the third successive change in the sign of the ΔP_g signal, mal-operation does not result.

6.0. CONCLUSION.

Quoting from a recent IEEE paper[13], "Providing protection against islanding probably is the single most challenging aspect of designing the electrical power system involving cogeneration." This loss of grid protection reduces the complication of installing embedded generation.

The new digital protection algorithm for detecting loss of grid has been shown to trip for both loss of grid and local load changes during independent operation. The algorithm remains stable during large local load changes while the utility grid remains connected and also during local power system fault conditions.

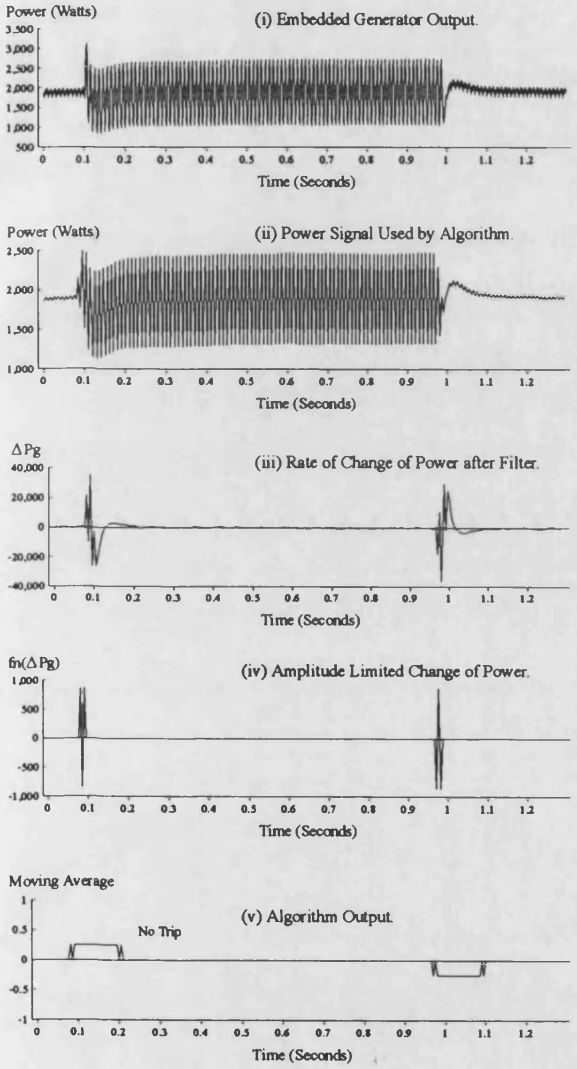

Figure 8: Response of the Loss of Grid Algorithm to a Single Phase to Ground Fault on the Local Busbar.

Laboratory tests have supported earlier computer simulation results and have demonstrated the satisfactory operation of the algorithm despite the presence of high levels of harmonic interference and system unbalance.

The technique has been specially formulated to be suitable for inclusion in an integrated generator protection package for embedded generation requiring additional software only. This enables an economically attractive protection package to be produced.

7.0. ACKNOWLEDGEMENTS.

The authors are pleased to acknowledge the help and encouragement provided by the University of Bath, GEC Alsthom Protection and Control Ltd., South Western Electricity plc., and the Science and Engineering Research Council.

8.0. REFERENCES.

[1] THE ELECTRICITY COUNCIL, 'Engineering Recommendations G59 - Recommendations for the Connection of Private Generating Plant to the Electricity Boards' Distribution Systems.' London, June '85.

[2] THE ELECTRICITY COUNCIL, 'Engineering Technical Report ET113 - Notes for Guidance for the Protection of Private Generating Sets up to 5MW for Operation in Parallel with Electricity Board's Distribution Networks.' London, '89.

[3] SOUTH CALIFORNIA EDISON, 'Guidelines for Operating, Metering and Protection for Co-generators and Small Power Producers.' Los Angeles, June '81.

[4] ANSI/IEEE Standard 1001-1988, 'Guide for Interfacing Dispersed Storage and Generation Facilities with Electric Utility Systems.' IEEE, New York, April '89.

[5] IEEE Special Report, 'Inter-tie Protection of Consumer-Owned Sources of Generation, 3MVA or Less.' IEEE 88TH0224-6-PWR, '88.

[6] HARLOW J H, 'A Multifunction Protective Relay for the Cogeneration Industry.' IEEE Comp App in Power, No 4, pp 25-30, Oct. '90.

[7] WARIN J W, 'Loss of Mains Protection.' ERA Conference on 'Circuit Protection for Industrial and Commercial Installations.' London '90.

[8] COOPER C B, 'Standby Generation: Problems and Prospective Gains From Parallel Running.' Power System Protection '89 Conference, pp 1-6, Singapore '89.

[9] JONES R A, SIMS T R & IMECE A, 'Investigation of Potential Islanding of a Self-Commutated Static Power Converter in Photovoltaic Systems.' IEEE Trans on EC, Vol 5, No 4, pp 624-631.

[10] SCHALTANLANGEN ELECTRONIK GERATE GMBH & CO, 'Generator/Mains Monitor - GW2.' Pub. GW2/E/810

[11] DUGAN R, RIZY D, 'Electric Distribution Protection Problems Associated with the Interconnection of Small Dispersed Generation Devices.' IEEE Trans on PAS, Vol 103, No 6, pp 1121-1127.

[12] ROOK M, GOFF M, POTOCHNEY G, & POWELL L, 'Application of Protective Relays on a large Industrial-Utility Tie with Industrial Cogeneration.' IEEE Trans on PAS, Vol 100, No 6, pp 2804-2812, June '81.

[13] POWELL L J, 'An Industrial View of Utility Cogeneration Protection Requirements.' IEEE Trans on Ind App, Vol 24, No 1, pp 75-81, Jan/Feb '88.

[14] CLARK H & FELTES J, 'Industrial and Cogeneration Protection Problems Requiring Simulation.' IEEE Trans on Ind App, Vol 25, No 4, pp 766-775, July/Aug '89.

[15] REDFERN M A , USTA O, & FIELDING G, 'Protection Against Loss of Utility Grid Supply for a Dispersed Storage and Generation Unit.' IEEE Paper 92 SM 376-4 PWRD Presented to the PES Summer Meeting, Seattle, '92

[16] ANDERSON P M & FOUAD A A, 'Power System Control and Stability.' Iowa State Univ. Press, Iowa '77, USA.

[17] REDFERN M A, BARRETT J I, HEWINGS D, & USTA O, 'A Laboratory Facility for Research into Digital Protection Algorithms used for the Protection of Small and Medium Sized Generators.' Proc. 26th UPEC, pp 16-19, Brighton, '91.